UNIVERSIDADE FEDERAL DE GOIÁS (UFG)
INSTITUTO DE QUÍMICA (IQ)
PROGRAMA DE PÓS GRADUAÇÃO EM QUÍMICA

GEOVANA DE MELO MENDES

Development of disposable microfluidic devices for bioanalytical applications

Desenvolvimento de dispositivos microfluídicos descartáveis para aplicações bioanalíticas

GOIÂNIA
2025

UNIVERSIDADE FEDERAL DE GOIÁS
INSTITUTO DE QUÍMICA

TERMO DE CIÊNCIA E DE AUTORIZAÇÃO (TECA) PARA DISPONIBILIZAR VERSÕES ELETRÔNICAS DE TESES

E DISSERTAÇÕES NA BIBLIOTECA DIGITAL DA UFG

Na qualidade de titular dos direitos de autor, autorizo a Universidade Federal de Goiás (UFG) a disponibilizar, gratuitamente, por meio da Biblioteca Digital de Teses e Dissertações (BDTD/UFG), regulamentada pela Resolução CEPEC nº 832/2007, sem ressarcimento dos direitos autorais, de acordo com a Lei 9.610/98, o documento conforme permissões assinaladas abaixo, para fins de leitura, impressão e/ou download, a título de divulgação da produção científica brasileira, a partir desta data.

O conteúdo das Teses e Dissertações disponibilizado na BDTD/UFG é de responsabilidade exclusiva do autor. Ao encaminhar o produto final, o autor(a) e o(a) orientador(a) firmam o compromisso de que o trabalho não contém nenhuma violação de quaisquer direitos autorais ou outro direito de terceiros.

1. Identificação do material bibliográfico

[ ] Dissertação [X] Tese [ ] Outro*:_____

*No caso de mestrado/doutorado profissional, indique o formato do Trabalho de Conclusão de Curso, permitido no documento de área, correspondente ao programa de pós-graduação, orientado pela legislação vigente da CAPES.

Exemplos: Estudo de caso ou Revisão sistemática ou outros formatos.

2. Nome completo do autor

Geovana de Melo Mendes

3. Título do trabalho

Development of disposable microfluidic devices for bioanalytical applications

4. Informações de acesso ao documento (este campo deve ser preenchido pelo orientador)

Concorda com a liberação total do documento [X] SIM [ ] NÃO[1]

[1] Neste caso o documento será embargado por até um ano a partir da data de defesa. Após esse período, a possível disponibilização ocorrerá apenas mediante:
a) consulta ao(à) autor(a) e ao(à) orientador(a);
b) novo Termo de Ciência e de Autorização (TECA) assinado e inserido no arquivo da tese ou dissertação.
O documento não será disponibilizado durante o período de embargo.
Casos de embargo:
- Solicitação de registro de patente;
- Submissão de artigo em revista científica;
- Publicação como capítulo de livro;
- Publicação da dissertação/tese em livro.

Obs. Este termo deverá ser assinado no SEI pelo orientador e pelo autor.

Documento assinado eletronicamente por **Gabriela Rodrigues Mendes Duarte**, **Professor do Magistério Superior**, em 05/11/2024, às 11:01, conforme horário oficial de Brasília, com fundamento no § 3º do art. 4º do Decreto nº 10.543, de 13 de novembro de 2020 .

Documento assinado eletronicamente por **Geovana De Melo Mendes**, **Discente**, em 22/11/2024, às 09:18, conforme horário oficial de Brasília, com fundamento no § 3º do art. 4º do Decreto nº 10.543, de 13 de novembro de 2020.

A autenticidade deste documento pode ser conferida no site https://sei.ufg.br/sei/controlador_externo.php?acao=documento_conferir&id_orgao_acesso_externo=0, informando o código verificador **4945813** e o código CRC **6E5D5F47**.

GEOVANA DE MELO MENDES

Development of disposable microfluidic devices for bioanalytical applications

Desenvolvimento de dispositivos microfluídicos descartáveis para aplicações bioanalíticas

Tese apresentada ao Programa de Pós-Graduação em Química, do Instituto de Química (IQ) da Universidade Federal de Goiás (UFG), como requisito para obtenção do título de Doutora em Química.
Área de concentração: Química
Linha de pesquisa: Química Analítica

Orientadoras: Profa. Dra. Gabriela Rodrigues Mendes Duarte e
Profa. Dra. Anne Varenne

GOIÂNIA
2025

Ficha de identificação da obra elaborada pelo autor, através do
Programa de Geração Automática do Sistema de Bibliotecas da UFG.

Mendes, Geovana de Melo
Development of disposable microfluidic devices for bioanalytical applications [manuscrito] : Desenvolvimento de dispositivos microfluídicos descartáveis para aplicações bioanalíticas / Geovana de Melo Mendes. - 2025.
CCLXXXVII, 287 f.: il.

Orientador: Profa. Dra. Gabriela Rodrigues Mendes Duarte; co orientadora Dra. Anne Varenne.
Tese (Doutorado) - Universidade Federal de Goiás, Instituto de Química (IQ), Programa de Pós-Graduação em Química, Goiânia, 2025.
Bibliografia.
Inclui siglas, fotografias, abreviaturas, símbolos, gráfico, tabelas, lista de figuras, lista de tabelas.

1. Microfluídica. 2. Biomoléculas. 3. Proteômica. 4. Diagnóstico Molecular. 5. Point-of-care. I. Duarte, Gabriela Rodrigues Mendes, orient. II. Título.

CDU 54

UNIVERSIDADE FEDERAL DE GOIÁS

INSTITUTO DE QUÍMICA

ATA DE DEFESA DE TESE

Ata Nº **191** da sessão de Defesa de Tese de **Geovana de Melo Mendes** que confere o título de **Doutora em Química**, na área de concentração em **Química.**

Aos **vinte e um dias do mês de novembro de dois mil e vinte e quatro**, a partir das **10h:00m**, **por Videoconferência**, realizou-se a sessão pública de Defesa de Tese intitulada ***"Development of disposable microfluidic devices for bioanalytical applications"***. Os trabalhos foram instalados pela Orientadora, Professora Doutora Gabriela Rodrigues Mendes Duarte **(IQ-UFG)** com a participação dos demais membros da Banca Examinadora: Professor Doutor **Wendell Karlos Tomazelli Coltro (IQ – UFG)**; Professor Doutor **José Alberto Fracassi da Silva (IQ-Unicamp)**, Professora Doutora **Anne Varenne (Chimie ParisTech PSL)**, Professora Doutora **Susan Lunte (Universidade do Kansas)** e Professor Doutor **Yann Verdier (ESPCI Paris PSL)**. Durante a arguição, os membros da banca **não/fizeram** sugestão de alteração do título do **trabalho**. A Banca Examinadora reuniu-se em sessão secreta a fim de concluir o julgamento da Tese, tendo sida a candidata **aprovada** pelos seus membros. Proclamados os resultados pela Professora Doutora **Gabriela Rodrigues Mendes Duarte**, **Presidente da Banca Examinadora**, foram encerrados os trabalhos e, para constar, lavrou-se a presente ata que é assinada pelos Membros da Banca Examinadora, aos **vinte e um dias do mês de novembro de dois mil e vinte e quatro.**

Minutes No. **191** of the Thesis Defense Session of **Geovana de Melo Mendes**, which confers the title of Doctor of **Chemistry**, in the area of concentration in **Chemistry**.

On the **twenty-first day of November, two thousand and twenty-four**, starting at **11:00 a.m., via Videoconference**, the public Thesis Defense session entitled "Development of disposable microfluidic devices for bioanalytical applications" was held. The works were installed by the Advisor, Professor **Gabriela Rodrigues Mendes Duarte (IQ-UFG)** with the participation of the other members of the Examining Board: Professor **Wendell Karlos Tomazelli Coltro (IQ – UFG)**; Professor **José Alberto Fracassi da Silva (IQ-Unicamp)**, Professor **Anne Varenne (Chimie ParisTech PSL)**, Professor **Susan Lunte (University of Kansas)** and Professor **Yann Verdier (ESPCI Paris PSL)**. During the argument, the members of the board **did not make any** suggestions to change the title of the work. The Examining Board met in secret session in order to conclude the judgment of the Thesis, having the candidate was **approved** by its members. The results were announced by Professor **Gabriela Rodrigues Mendes Duarte, President of the Examining Board**, and the proceedings were concluded and, for the record, these minutes were drawn up and signed by the Members of the Examining Board, on the **twenty-first day of November, two thousand and twenty-four**.

TÍTULO SUGERIDO PELA BANCA

Documento assinado eletronicamente por **Gabriela Rodrigues Mendes Duarte**, **Professor do Magistério Superior**, em 21/11/2024, às 13:15, conforme horário oficial de Brasília, com fundamento no § 3º do art. 4º do Decreto nº 10.543, de 13 de novembro de 2020 .

Documento assinado eletronicamente por **Wendell Karlos Tomazelli Coltro**, **Professor do Magistério Superior**, em 21/11/2024, às 14:16, conforme horário oficial de Brasília, com fundamento no § 3º do art. 4º do Decreto nº 10.543, de 13 de novembro de 2020 .

Documento assinado eletronicamente por **José Alberto Fracassi da Silva**, **Usuário Externo**, em 21/11/2024, às 15:27, conforme horário oficial de Brasília, com fundamento no § 3º do art. 4º do Decreto nº 10.543, de 13 de novembro de 2020 .

A autenticidade deste documento pode ser conferida no site https://sei.ufg.br/sei/controlador_externo.php?acao=documento_conferir&id_orgao_acesso_externo=0, informando o código verificador **4939521** e o código CRC **8368741D**.

Referência: Processo nº 23070.056142/2024-89 SEI nº 4939521

I wish to express my gratitude to Professors Susan Lunte and José Alberto Fracassi for agreeing to report on this thesis. I also thank professors Yann Verdier and Wendell Coltro for agreeing to be the examiners of this thesis. I am immensely grateful to Professor Gabriela Duarte, who has been my mentor for nearly ten years. I have learned a great deal from her—thank you for the advice, patience, life lessons, and constant care.

I also extend my thanks to *Coordenação de Aperfeiçoamento de Pessoal de Nível Superior – Brasil* (CAPES) for providing my scholarship and to the CAPES-COFECUB project (grant number: 88887.192880/2018-00; Ph C 952/19) for funding my research and supporting my 1 year and 8-month stay in Paris.

I wish to express my gratitude and admiration to Professor Anne Varenne, who has welcomed and supervised me since my arrival in Paris. Thank you for your kindness, humanity, scientific guidance, and good mood. I am also grateful to my co-supervisor, Fanny d'Orlye, for her assistance with the experiments, insightful advice, and all the shared knowledge. A special thanks to Laura Trapiella for her support and patience throughout my journey.

I would like to thank all the Associate Professors and Research Scholars of the Synthesis Electrochemistry, Imaging, and Analytical Systems for the Diagnosis team for receiving me so warmly: Bich-Thuy Doan, Sophie Griveau, Camille Lescot, Fethi Bedioui, and Cyrine Slim.

I was fortunate to have the greatest luck during my stay in Paris. I thank all the friends who welcomed me, helped me, and made me feel at home and loved, even being more than 5,000 miles away from my hometown. With all my heart, I thank Alice, Sun Jie (Solecito), Amina, Elahe, Rafael, Géssica Maria, Lucas, Marta, Tahani, Amal, Cris, Fernando, Karen, Yiqian, Zhang, Ximena, Samuele, and Karl.

To my dear friends who provided unwavering support and love, making my journey lighter and guiding me to the end of this PhD: thank you, Sarah, Ana, Paulo, Kezia, Janaina, Larissa, Renato, and Gerson. I also wish to acknowledge the wonderful people I have met in the Biomicrofluidica laboratory: Laura, Márcio, Leonardo, Charliane, Giovanna, Gabriela, Carlos, and Lívia.

My heartfelt thanks go to my parents, Sônia and Geraldo, for their unconditional love and the opportunities they provided me—opportunities they never had themselves. I love you infinitely. I am also deeply grateful to my entire family for their support, with special thanks to Joaquim, Mychelle, Hermann, Marta, Vera, and Walter. A warm thank you to Mychell for his indescribable help, love, support, and attentive ear; for his kind words; and for sharing the burdens, making them lighter.

RESUMO

Esta tese foi desenvolvida no contexto de uma cotutela entre a Universidade Federal de Goiás (Goiânia, Brasil) e a Chimie ParisTech-PSL (Paris, França). O trabalho teve início no Brasil, no auge da pandemia, com foco no desenvolvimento de metodologias baseadas em amplificação isotérmica mediada por loop (LAMP) para o diagnóstico da COVID-19. A LAMP foi empregada para criar um teste simples e de baixo custo, viabilizando sua implementação no point-of-care em um hospital onde os testes convencionais não eram acessíveis. Esse método permitiu diagnósticos rápidos e precisos, contribuindo para a triagem de pacientes em condições críticas. Além disso, propusemos um método não invasivo de monitoramento baseado na detecção de RNA viral em saliva, voltado para o rastreamento frequente de trabalhadores essenciais durante a pandemia. Essa abordagem demonstrou ser prática e eficaz para testes frequentes. A transposição preliminar dessa metodologia para uma plataforma microfluídica de papel apresentou resultados promissores, sugerindo seu potencial para o monitoramento em tempo real de infecções, com destaque para o SARS-CoV-2, diretamente no ponto de necessidade. Já os trabalhos conduzidos no laboratório francês concentraram-se no desenvolvimento e na otimização de uma plataforma baseada em papel para a focalização isoelétrica de proteínas. O objetivo foi integrar etapas da análise proteômica em um microdispositivo, avançando na miniaturização de técnicas analíticas para diagnósticos de biomoléculas. A focalização isoelétrica em papel demonstrou se precisa e reprodutível para a separação de proteínas, incluindo para análise de amostras biológicas reais, com resolução e eficiência satisfatórias. Os avanços apresentados nesta tese representam um passo significativo em direção à integração de todas as etapas da análise proteômica em um único dispositivo, com potencial aplicação em contextos de baixo custo e recursos limitados. O desenvolvimento de sistemas diagnósticos voltados para biomoléculas, priorizando acessibilidade, rapidez e simplicidade, reforça a viabilidade do papel como substrato para testes analíticos. Os dispositivos a base de papel desenvolvidos neste trabalho se mostraram uma alternativa viável e eficaz para a detecção de biomoléculas em aplicações no point-of-care.

Palavras-chaves: Microfluídica, biomoléculas, focalização isoelétrica, proteômica, diagnóstico molecular, point-of-care.

This doctoral manuscript details the project: development of disposable microfluidic devices for bioanalytical applications. The thesis opens with a summary written in both French and Portuguese, followed by the main chapters written in English. Chapter I presents the state of the art, while Chapters II, III, and V consist of articles produced during the course of this thesis. Chapter IV presents preliminary results that extend the studies developed in Chapters II and III.

- **Chapter I** – State of the Art.
- **Chapter II** – Can a Field Molecular Diagnosis Be Accurate? A Performance Evaluation of Colorimetric RT-LAMP for the Detection of SARS-CoV-2 in a Hospital Setting.
- **Chapter III** – Detection of SARS-CoV-2 in Saliva by RT-LAMP During a Screening of Workers in Brazil, Including Pre-Symptomatic Carriers.
- **Chapter IV** – Study of the Application of RT-LAMP pH-Based Detection Methodology on a Paper Platform for Real-Time Monitoring.
- **Chapter V** – Streamlined Integrated Protein Isoelectric Focusing Using a Microfluidic Paper-Based Device.

Introduction

Au cours des trois dernières décennies, les dispositifs analytiques microfluidiques sont apparus comme une alternative prometteuse aux méthodes traditionnelles pour des tests rapides au chevet du patient. (Ríos et al., 2012) Initialement développés à partir de matériaux à base de silicium et de plastique, ces dispositifs ont par la suite intégré le papier comme alternative viable. (Terry et al., 1979) L'utilisation de papier hydrophile confiné par une barrière de cire hydrophobe pour l'analyse chimique, introduite dès 1937, (Yagoda, 1937) a reçu une reconnaissance importante à la suite d'une publication clé du groupe du Professeur Whitesides en 2007. (Martinez et al., 2007) La communauté scientifique reconnaît que les dispositifs analytiques microfluidiques à base de papier (µPAD) offrent des avantages substantiels par rapport aux dispositifs microfluidiques à base de plastique en raison de leurs caractéristiques uniques.(Trinh et al., 2022)

Les µPAD (dispositifs analytiques microfluidiques à base de papier) offrent des avantages considérables grâce à leurs structures poreuses et à leur inertie chimique, qui facilitent l'immobilisation et le stockage efficaces des réactifs. De plus, leur légèreté et leur souplesse favorisent le transport. L'action capillaire dans ces dispositifs élimine le besoin de pompes externes pour déplacer les liquides, un avantage significatif pour les applications sur le lieu de soins. Ces propriétés permettent aux µPAD de répondre aux critères ASSURED (abordables, sensibles, spécifiques, conviviaux, rapides et robustes, sans équipement et livrables), ce qui en fait des outils idéaux pour

diagnostiquer les maladies transmissibles dans les environnements où les ressources sont limitées. Trinh et al., 2022)

Cette thèse porte sur deux classes de molécules biologiques : les protéines et l'ARN viral, toutes deux essentielles au diagnostic clinique et à la gestion de maladies. Les protéines permettent de comprendre les mécanismes moléculaires impliqués dans des pathologies, en raison de leurs structures complexes et de leurs fonctions cellulaires essentielles. (Farmerie et al., 2021) Quant à l'ARN viral, en particulier celui des virus hautement infectieux, il est essentiel pour la détection et la surveillance des maladies infectieuses. (Cassedy et al., 2021 ; Domingo, 2020)

La menace des maladies infectieuses s'est accrue ces dernières années, principalement en raison des bactéries résistantes aux antibiotiques et de la propagation de virus hautement contagieux. Bien que les progrès de la science et de la technologie médicales aient amélioré la précision et l'efficacité des traitements cliniques, le coût élevé et la complexité de ces technologies limitent leur accessibilité dans les régions moins développées. (Han et al., 2020) Chaque épidémie de maladie infectieuse met en évidence la nécessité de tests évolutifs pouvant être réalisés en dehors des laboratoires centralisés, sur les lieux des épidémies, afin de prévenir, de suivre et de surveiller les menaces endémiques et pandémiques. Les méthodes actuelles de détection des agents pathogènes, telles que la réaction en chaîne par polymérase (PCR), l'essai immuno-enzymatique (ELISA) et la culture cellulaire, prennent beaucoup de temps et nécessitent un personnel qualifié, ce qui entrave la réaction rapide aux nouveaux agents pathogènes. Il est donc essentiel de développer

des techniques rapides, précises, sensibles, portables, conviviales et adaptées aux utilisateurs non formés. (Trinh et al., 2022)

L'amplification isotherme induite par boucles (Loop-mediated isothermal amplification, LAMP) est un test d'amplification des acides nucléiques (NAAT- *nucleic acid amplification techniques*) qui s'est imposé comme une alternative rentable aux méthodes conventionnelles pour le diagnostic via l'ADN. La méthode LAMP fournit des résultats en 30 à 60 minutes sans équipement sophistiqué, ce qui permet de l'utiliser en cas de crise sanitaire et sur des plates-formes microfluidiques. Cette combinaison exploite les avantages des techniques isothermes et microfluidiques, améliorant à la fois l'efficacité et l'accessibilité. (Han et al., 2020 ; Notomi et al., 2000 ; Tomita et al., 2008)

La caractérisation des protéines est essentielle pour comprendre les mécanismes des maladies et développer des diagnostics. En général, le processus analytique nécessite des procédures complexes. La stratégie "top-down" analyse directement les protéines intactes à l'aide de la spectrométrie de masse (MS), tandis que la stratégie "bottom-up" consiste à digérer les protéines en peptides avant de les séparer et de les détecter par MS. La protéomique "middle-down", qui implique la digestion en fragments peptidiques plus importants, fait le lien entre ces approches. (Lenčo et al, 2022 ; Maráková et al, 2023 ; Miller & Smith, 2022 ; Moradian et al, 2014). Diverses méthodologies de séparation des protéines, telles que la chromatographie et l'électrophorèse, (S. Liu et al., 2020) ont été développées. En particulier, la focalisation isoélectrique (IEF) est un mode de séparation électrocinétique

particulièrement puissante pour séparer et concentrer les protéines en fonction de leur point isoélectrique (pI) par établissement d'un gradient de pH sous champ électrique, en présence d'un mélange d'ampholytes porteurs (carrier ampholytes, CA). L'IEF peut ensuite être couplée à des méthodes de détection efficaces. (Farmerie et al., 2021; Lecoeur et al., 2010; Maurer, 2011; Mokaddem et al., 2009)

Les progrès technologiques ont permis l'intégration de méthodes de séparation dans des formats microfluidiques, promettant de rationaliser le processus analytique en automatisant les étapes successives. Cette intégration permet de réduire le temps d'analyse, d'éviter les erreurs manuelles et la contamination croisée, de diminuer les coûts et d'étendre les applications aux environnements à faibles ressources. L'application de méthodes telles que LAMP ou IEF dans le cadre de la microfluidique est particulièrement prometteuse. Les plateformes microfluidiques offrent plusieurs avantages, notamment l'intégration, un faible coût, des volumes d'échantillons minimes, l'utilisation de matériaux simples et jetables et la possibilité d'applications sur le lieu de soins. (Akyazi et al., 2018 ; Boobphahom et al., 2020 ; Dinh & Lee, 2022 ; Lim et al., 2019 ; Nge et al., 2013)

Cette thèse a été effectuée dans le contexte d'une co-tutelle entre l'Université Fédérale de Goias (Goiania, Brésil) et Chimie ParisTech PSL. Elle a débuté au Brésil, au début de la pandémie, ce qui a très fortement orienté le travail dans le laboratoire brésilien. Ainsi, ce travail de thèse présente des résultats obtenus dans la lutte contre le COVID-19 pendant la pandémie. La méthode LAMP a été développée, optimisée et validée pour des applications de terrain dans ce contexte. Après la publication des

données de la pandémie, la méthode développée et validée a été appliquée à un stade préliminaire sur des plateformes papier. Les premiers résultats démontrent le potentiel combiné de la technique et les avantages de la miniaturisation. Dans le cadre de la co-tutelle, des travaux ont été effectués ensuite dans le laboratoire français pour le développement et l'optimisation d'une plateforme papier pour la focalisation isoélectrique des protéines, en vue d'intégrer toutes les étapes de l'analyse protéomique dans un microdispositif. Après une présentation de l'état de l'art dans ces deux domaines, le manuscrit présente les évancées scientifiques développées durant cette thèse, avec les deux méthodes (LAMP et IEF) pour le diagnostic médical.

Un diagnostic moléculaire sur le terrain peut-il être précis ? Évaluation des performances de la RT-LAMP colorimétrique pour la détection du SARS-CoV-2 en milieu hospitalier

Lívia do Carmo Silva†, Carlos Abelardo dos Santos†, Geovana de Melo Mendes†, Kézia Gomes de Oliveira† et al. Can a field molecular diagnosis be accurate? A performance evaluation of colorimetric RT-LAMP for the detection of SARS-CoV-2 in a hospital setting. Analytical Methods : Advancing Methods and Applications. 2021 Jul;13(26):2898-2907. DOI: 10.1039/d1ay00481f. PMID: 34109949.

† Les auteurs ont contribué de manière égale à ce travail.

Nous avons effectué le test RT-LAMP colorimétrique en milieu hospitalier et la méthodologie (Figure 1) s'est avérée être un outil puissant pour détecter le SARS-CoV-2 avec un excellent rapport coût-bénéfice dans le contexte du soin auprès du

patient. Elle a également permis de détecter l'acide nucléique du SARS-CoV-2 directement dans des échantillons d'écouvillons non extraits. Les résultats ont montré que la méthode pouvait fournir des résultats fiables et précis, tant sur le terrain qu'en laboratoire. En outre, la RT-LAMP utilisée à l'hôpital a présenté des performances diagnostiques comparables à celles de la RT-qPCR (please indicate the full name) et du test effectué dans le laboratoire de référence, avec une sensibilité (88,89 %) et une spécificité (94,20 %) élevées. D'après ces données, la limite de la RT-LAMP, par rapport la méthode de référence est la sensibilité. Toutefois, la technique directe de RT-LAMP est plus facile à mettre en œuvre, ce qui élimine la nécessité d'un équipement complexe et peut contribuer à augmenter la fréquence des tests. Notre test RT-LAMP a un grand potentiel pour faciliter le dépistage du SRAS-CoV-2 sur le terrain et permettre un traitement rapide et précis des patients infectés.

*****

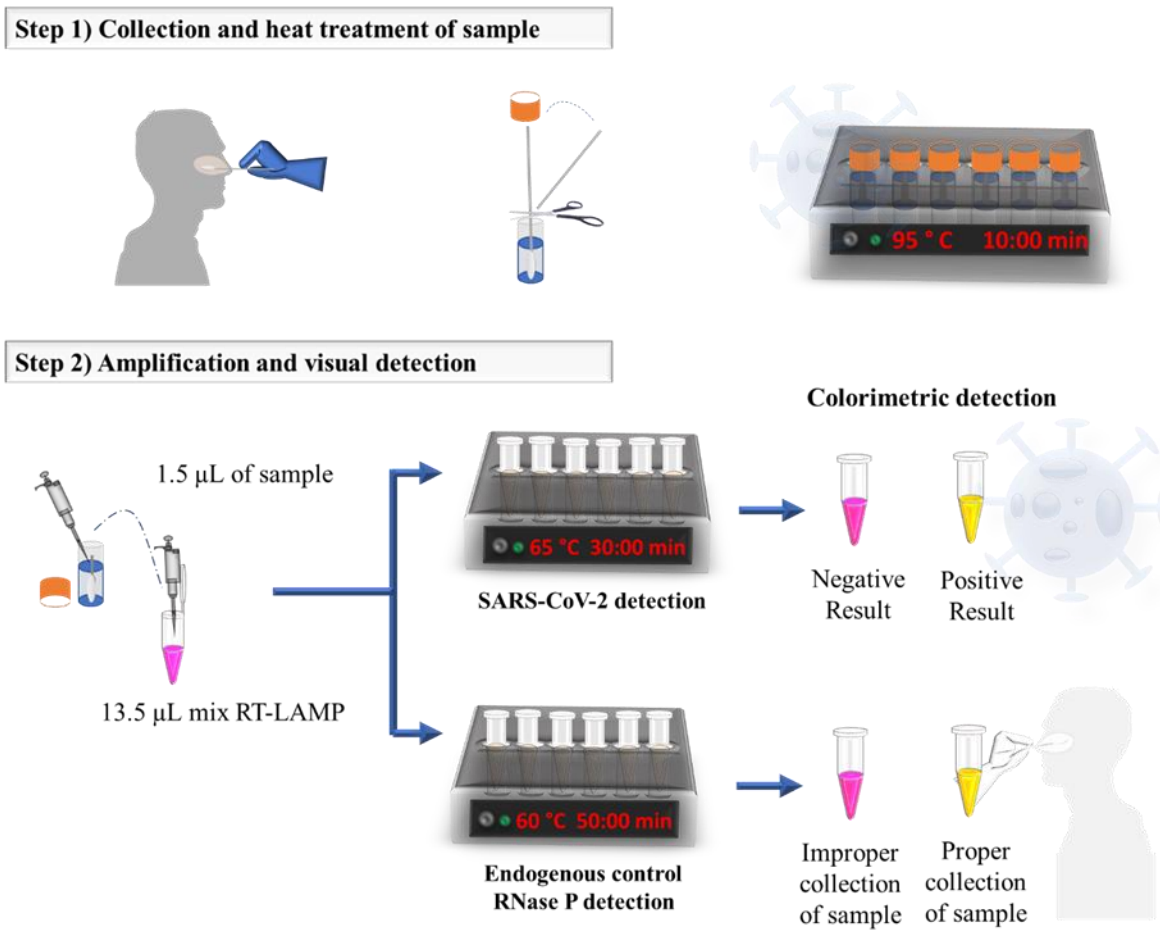

Figure 1: Vue d'ensemble schématique de la procédure RT-LAMP. Étape 1 : Collecte par écouvillonnage et traitement thermique des échantillons. L'échantillon nasopharyngé a été collecté à l'aide d'un écouvillon et conservé dans une cryotube contenant 1 mL de solution saline à 0,9 %. Les échantillons ont été soumis à une extraction thermique à 95 °C pendant 10 minutes pour l'extraction thermique et l'inactivation virale. Étape 2 : Amplification et détection visuelle ; 1,5 µL d'échantillon a été ajouté à deux mélanges, chacun contenant soit les amorces du SARS-CoV-2, soit celles de l'ARNse P, de l'eau, et du WarmStart Colorimetric LAMP 2X Master Mix, puis incubé dans deux thermoblocs ; l'un pendant 30 minutes à 65 °C pour la détection du SARS-CoV-2, et l'autre pendant 50 minutes à 60 °C pour la détection deu contrôle engodègne par l'ARNse P dans les échantillons collectés. La positivité des échantillons a été déterminée en observant le changement de couleur de rose (échantillon négatif) à jaune (échantillon positif). Des modifications des températures d'incubation pour la détection de l'ARNse P et du SARS-CoV-2 peuvent entraîner une faible efficacité d'amplification, elles doivent donc être maintenues comme décrit précédemment.

Dans les lieux où les ressources sont limitées, plusieurs défis ont été associés aux diagnostics basés sur la PCR, notamment le manque d'infrastructures, de personnel formé et d'équipements coûteux. Dans ce contexte, la demande de tests instrumentalement plus simples ("tests rapides"), généralement basés sur la détection par flux latéral (lateral flow essay, LFA), a rapidement émergé. Actuellement, des tests à flux latéral sont disponibles pour la détection des anticorps et des antigènes.

Notre manuscrit apporte des avantages évidents, en réalisant la détection du SARS-CoV-2 dans 100% des échantillons avec Ct < 30 (Ct: «cycle threshold», brièvement il s'agit du point où le signal généré par l'amplification de l'ADN atteint un niveau détectable) sur le terrain directement dans les échantillons d'écouvillons nasopharyngés en utilisant seulement le traitement thermique (Figure 2). Le traitement thermique de l'échantillon, tel qu'il est décrit dans notre article, est avantageux car, en plus d'être rapide, il ne nécessite pas d'étapes d'ouverture des tubes d'échantillon, ce qui corrobore la biosécurité dans la réalisation des tests. En plus du processus de préparation de l'échantillon, un contrôle endogène (RP- Rnase P) est utilisé, qui détermine la viabilité de l'échantillon, ce qui confère une plus grande fiabilité au test. En outre, dans cette étude, les limites de "l'application potentielle de la méthode" sont dépassées, pour une application efficace en environnement hospitalier, avec de bons résultats en termes de diagnostic rapide, précis et sensible, ce qui peut contribuer au contrôle de la pandémie, en particulier dans les environnements où les ressources sont limitées.

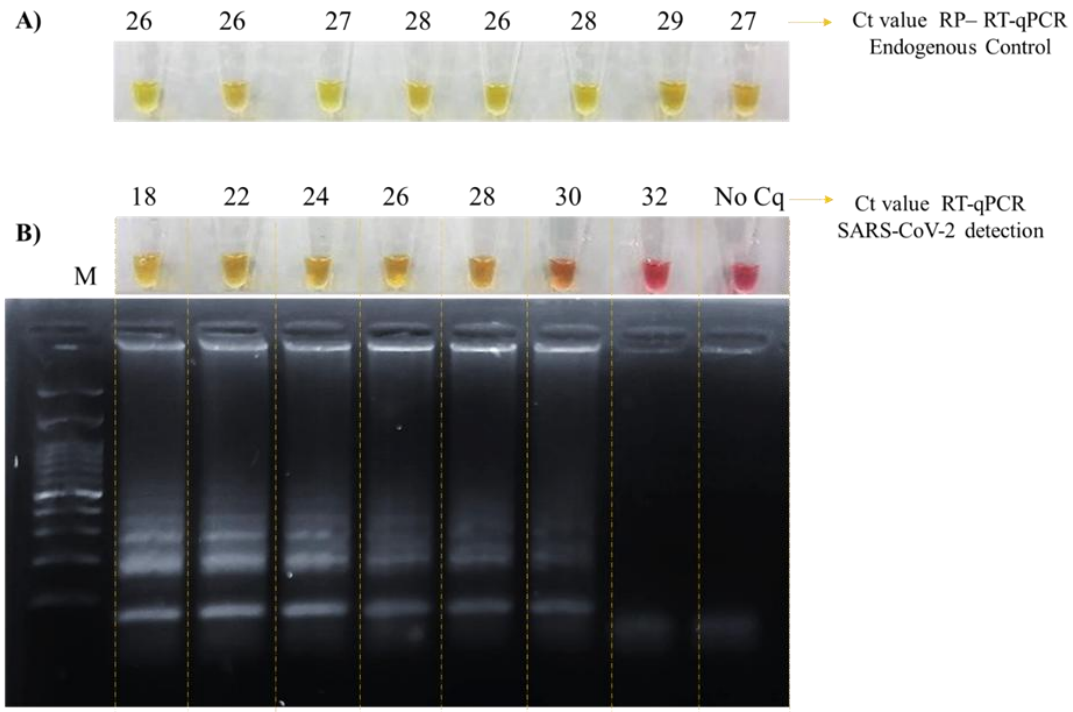

Figure 2: Détection du produit amplifié par RT-LAMP. (A) Évaluation de la qualité du contrôle endogène RNase P (RP) humain dans des échantillons d'écouvillonnage ; huit (8) échantillons positifs par RT-qPCR. (B) Détection du SARS-CoV-2 par RT-LAMP dans huit (8) échantillons avec différentes charges virales, visualisée par détection visuelle et séparation électrophorétique. No Cq : pas de cycle de quantification.

Étant donné que l'utilisation de réactifs chimiques, tels que les tampons de lyse, modifie considérablement le pH des échantillons, cette condition rend impossible une analyse colorimétrique basée sur la variation du pH. Outre qu'il favorise le processus d'inactivation en dénaturant les protéines essentielles à l'attachement et à la réplication du virus dans une cellule hôte, le protocole de préchauffage (Hasan et al.,

2020 ; Lista et al., 2021 ; Patterson et al., 2020) s'est avéré être un prétraitement idéal des écouvillons nasopharyngés pour libérer l'ARN à l'aide de la chaleur, sans qu'il soit nécessaire d'extraire l'acide nucléique. Cette approche de préchauffage des échantillons a également été utilisée comme stratégie pour exposer le génome viral et dénaturer les éventuels inhibiteurs de la réaction PCR. (Nawattanapaiboon et al., 2021)

En ce qui concerne la limite de détection, nos résultats pour le SARS-CoV-2 concordent avec ceux d'autres études qui décrivent la diminution de la sensibilité due à la présence d'une matrice biologique. Les performances de la RT-LAMP rapportées dans ce travail concordent également avec celles décrites précédemment dans la littérature. (Chow et al., 2020 ; Klein et al., 2020 ; Nawattanapaiboon et al., 2021)

Les valeurs de Ct de la réaction RT-qPCR sont inversement corrélées à la charge virale (Tom & Mina, 2020) et certaines études ont établi une corrélation entre le potentiel d'infectivité et les valeurs de Ct. (Bullard et al., 2020). Magleby et al. ont établi une corrélation entre le Ct des patients et la gravité de la maladie, et un Ct > 30 est lié à une mortalité plus faible. (Magleby et al., 2021) Ainsi, compte tenu de la limite de détection trouvée dans nos analyses conforme à la limite rapportée dans d'autres études, (Loan Dao Thi et al., 2020) le test proposé ici peut être utile pour le dépistage des patients au début de l'infection avec une charge virale élevée et, par conséquent, avec un plus grand potentiel de propagation virale et de progression vers des conditions cliniques graves dues à l'infection par le SRAS-CoV-2. Par conséquent, bien que le test RT-LAMP décrit ici ait une sensibilité plus faible que la RT-PCR, la

détection d'un Ct < 30 est suffisante pour détecter les individus susceptibles d'être contagieux et faciliter la mise en œuvre de mesures d'isolement.

Ainsi, compte tenu de la simplicité de l'exécution du test, de la rapidité des résultats (moins de 2h), du coût global le plus faible, de l'analyse du scénario d'engorgement des salles d'urgence pendant la pandémie et de la nécessité d'isoler les patients infectés, les résultats présentés ici démontrent que la méthode RT-LAMP a une application clinique cruciale, principalement dans le secteur du dépistage hospitalier, pour tenter de minimiser le problème de l'engorgement, en permettant une prise en charge immédiate des patients les plus urgents.

Détection du SARS-CoV-2 dans la salive par RT-LAMP lors d'un dépistage des travailleurs au Brésil, y compris des porteurs pré-symptomatiques

Santos CA dos†, Oliveira KG de†, Mendes GM†, Silva LC, Souza Jr. MN de, Estrela PFN, et al.. Detection of SARS-CoV-2 in Saliva by RT-LAMP During a Screening of Workers in Brazil, Including Pre-Symptomatic Carriers. J Braz Chem Soc [Internet]. 2021Nov;32(11):2071–7. Available from: https://doi.org/10.21577/0103-5053.20210098

† Les auteurs ont contribué de manière égale à ce travail.

La pandémie de coronavirus a causé des dégâts dans de nombreux pays, les systèmes de santé publics et privés. Certains patients infectés étaient contaminés par un coronavirus-2 du syndrome respiratoire aigu sévère (SARS-CoV-2) même s'ils ne présentaient aucun symptôme, et étaient donc probablement capables de le transmettre. Au cours des premiers mois très critiques de la pandémie de coronavirus,

le fait de diagnostiquer et d'isoler correctement les patients infectés a constitué une étape importante dans la prévention de nouvelles infections (Falahi & Kenarkoo). (Falahi & Kenarkoohi, 2020 ; Fierabracci et al., 2020 ; Y. C. Liu et al., 2020 ; See et al., 2021) L'amplification isotherme à médiation en boucle (RT-LAMP) s'est imposée comme une alternative viable, car elle est plus rapide et nécessite moins d'infrastructures, ce qui permet de l'appliquer dans des scénarios à faibles ressources et même au chevet du patient.

Nous présentons ici un test RT-LAMP colorimétrique capable de détecter le SARS-CoV-2 à partir de l'acide ribonucléique (ARN) dans des échantillons de salive afin de dépister les travailleurs symptomatiques et asymptomatiques. Nous avons obtenu des données sur les symptômes liés au COVID-19 à l'aide d'un questionnaire et avons établi une corrélation entre l'apparition des symptômes et la positivité, ce qui montre l'efficacité du test pour séparer les cas positifs des cas négatifs.

Bien que les écouvillons nasopharyngés aient été proposés comme les échantillons idéaux pour détecter le SARS-CoV-2, il s'agit d'une méthode invasive qui peut présenter un certain risque pour les professionnels de la santé qui collectent les échantillons ou un prélèvement aléatoire de la part des patients. Nous avons donc décidé d'utiliser des échantillons de salive pour réaliser la RT-LAMP, car il s'agit d'un test moins invasif. En outre, certaines études ont démontré la fiabilité de la salive en tant qu'échantillon adéquat pour détecter le SARS-CoV-2. (Sohn et al., 2020 ; Teo et al., 2021 ; Zhu et al., 2020) Les échantillons de salive non traités ne sont pas idéaux pour travailler directement avec la RT-LAMP colorimétrique, étant donné la large

gamme naturelle de pH dans laquelle la salive peut être collectée. Les échantillons de salive acides feraient jaunir l'indicateur de pH dans la réaction, avant même l'étape d'amplification, ce qui entraînerait une interprétation erronée des résultats. (Uribe-Alvarez et al., 2021)

Nous avons développé un test colorimétrique RT-LAMP qui peut détecter le SARS-CoV-2 dans l'ARN d'échantillons de salive de travailleurs à différents stades de l'infection (Figure 3), y compris les porteurs pré-symptomatiques, avec une spécificité globale de 100 %, une sensibilité de 80 % et une précision de 99,59 %, et un kappa de Cohen de 0,887. En outre, la méthode prend moins de temps que la méthode de référence (RT-qPCR). Nos résultats montrent que notre test colorimétrique RT-LAMP est adapté au dépistage de groupes importants, car la grande majorité des travailleurs ont été correctement diagnostiqués sur la base de ce test d'amplification simple, rapide et peu coûteux.

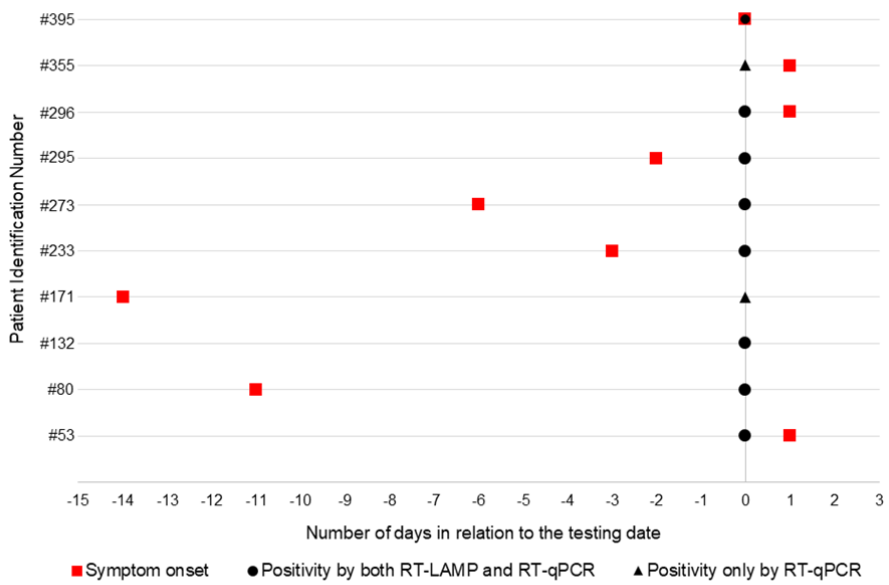

Figure 3: Relation entre le nombre de jours depuis l'apparition des symptômes et la date du résultat positif dans un test moléculaire. Chaque ligne représente l'évolution de la maladie chez un patient. Le jour 0 est considéré comme la date du test. Les nombres négatifs représentent le nombre de jours avant le test, tandis que les nombres positifs représentent le nombre de jours après la réalisation du test. La plupart des patients ont présenté des symptômes avant le test, tandis que trois patients (53, 296 et 355) ont obtenu un résultat positif avant l'apparition des symptômes. Le patient 395 a signalé l'apparition des symptômes le même jour que le test, et le patient 132 a affirmé n'avoir jamais présenté de symptômes.

La possibilité de diagnostiquer correctement les personnes porteuses du SRAS-CoV-2 transmissible et de les isoler rapidement est un avantage important qui contribue à prévenir la propagation du virus, car le contact avec d'autres personnes est fortement réduit. En raison de son faible coût et de sa simplicité par rapport à la RT-qPCR, la RT-LAMP pourrait être utilisée dans les pays qui ne disposent pas des ressources nécessaires pour effectuer la RT-qPCR à grande échelle, ce qui permettrait d'augmenter la capacité de test sans nécessairement accroître les coûts.

Étude d'application de la méthodologie de détection basée sur le pH par RT-LAMP sur une plateforme en papier, en vue d'un suivi en temps réel.

Compte tenu des avantages apportés par notre méthodologie LAMP, des études préliminaires ont été initiées pour réaliser le test sur une plateforme papier. L'utilisation de cette méthodologie sur une plateforme microfluidique pourrait offrir des avantages tels que le contrôle en temps réel sans nécessiter d'équipement sophistiqué. L'objectif est de mettre en œuvre le test RT-LAMP sur un système à base de papier, en contrôlant l'amplification à l'aide d'un microscope numérique portable (USB) qui peut être connecté à un ordinateur ou à un smartphone. La première étape consiste à déterminer une plateforme de support (pour faciliter le transport et la manipulation) pour le papier pour la RT-LAMP, en se concentrant sur des matériaux simples, jetables et peu coûteux adaptés aux environnements à faibles ressources.

Le premier support évalué était un système à base de toner polystyrène construit comme proposé par (Duarte et al., 2011). Pour produire ce support, les deux faces d'un film polystyrène ont été enduites de couches de toner, puis découpées de manière sélective selon le motif souhaité à l'aide d'une machine à découper (Silhouette Cameo 4). Ces films polystyrène-toner intermédiaires ont ensuite été alignés sur une base en polystyrène (couche inférieure) où le cercle de papier prédécoupé a été placé, et sur une couche supérieure en polystyrène. La couche supérieure contenait des trous pour permettre l'accès aux réactifs. Une fois alignés, les films ont été laminés, créant ainsi un dispositif microfluidique prêt à l'emploi.

Malgré la simplicité du support polystyrène-toner, certains inconvénients ont été identifiés. Tout d'abord, la composition du support a affecté le pH de la solution RT-LAMP, provoquant le jaunissement du mélange avant le processus d'amplification. Deuxièmement, le film de polystyrène utilisé pour la couche supérieure n'était pas suffisamment transparent, ce qui rendait difficile l'observation du changement de couleur dans le mélange RT-LAMP.

Le deuxième matériau de support évalué était le film d'étanchéité utilisé pour les tests PCR (ruban adhésifs), généralement fabriqué en polyéthylène. Dans cette étude, le film d'étanchéité PCR s'est avéré très approprié comme matériau de base pour les dispositifs microfluidiques en raison de son excellente biocompatibilité, d'une large gamme de températures de travail, de son faible coût, de ses propriétés auto-adhésives et de sa transmittance optique dans le domaine visible. (Fan et al., 2018) Nous avons utilisé un traceur Silhouette Cameo 4 pour découper les films d'étanchéité PCR dans la configuration souhaitée. Le papier a simplement été placé sur le film adhésif sans la couche protectrice, puis la couche supérieure (avec des trous découpés pour permettre l'accès au papier) a été placée sur le papier. Les couches ont finalement été collées par une légère pression du doigt en utilisant leurs propres propriétés adhésives (Figure 4).

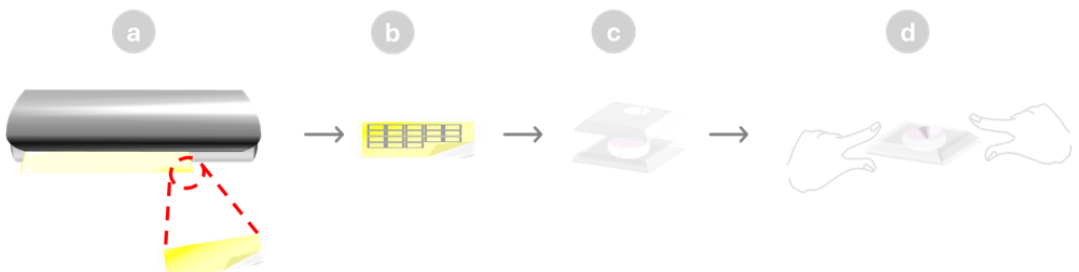

Figure 4: Illustration schématique du processus de fabrication du support du dispositif microfluidique en papier à l'aide d'un film de scellement pour PCR : (a) découpe du film adhésif avec un traceur de découpe ; (b) retrait du film protecteur des films adhésif; (c) alignement des films adhésifs avec le papier ; et (d) assemblage du dispositif final en appliquant une légère pression pour lier les couches. Créé par l'auteur.

Le format du papier a été optimisé pour minimiser l'évaporation tout au long du processus de réchauffement. Nous avons optimisé les points d'accès en mettant en place deux "branches" s'étendant vers la chambre. Ainsi, les films protecteurs adhésifs sont situés aux extrémités des branches, préservant ainsi l'adhésion et réduisant le risque d'évaporation. La Figure 5 présente une série d'images capturées toutes les 10 minutes pendant la réaction RT-LAMP sur des dispositifs avec deux formats de papier différents : un avec un simple cercle et l'autre avec des extensions jusqu'à la chambre de réaction. Ces images mettent en évidence l'efficacité de ce dispositif pour réduire l'évaporation dans le système, améliorant ainsi la cohérence de la réaction au fil du temps et minimisant la possibilité de contamination croisée. En plus de réduire l'évaporation, ce design de papier a considérablement amélioré l'homogénéité de la couleur de la réaction, un facteur crucial pour une quantification colorimétrique précise. Obtenir une homogénéité de couleur constante est essentiel pour les lectures colorimétriques dans les µPADs, car cela permet des mesures plus précises et améliore les performances globales de la méthode analytique. (Morbioli et al., 2017)

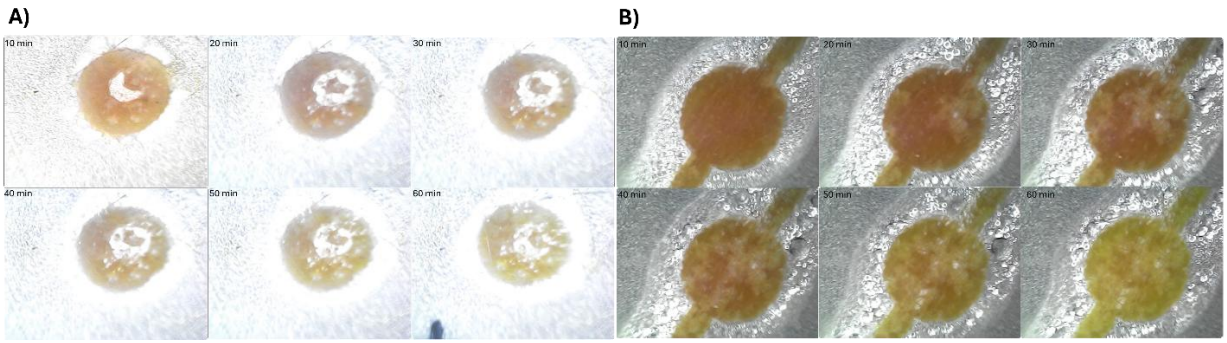

Figure 5: Images capturées à intervalles de 10 minutes pendant la réaction RT-LAMP en utilisant A) le format avec un cercle et B) le design de papier avec les branches prolongées.

Les prochaines étapes de cette étude incluent la détermination des figures de mérite, l'évaluation et la comparaison du temps d'amplification avec les valeurs Ct, et l'application de la méthode à des échantillons réels. Les résultats préliminaires de cette étude exploratoire indiquent le potentiel de combiner l'essai RT-LAMP avec des dispositifs analytiques microfluidiques basés sur le papier (μPADs) pour la détection en temps réel. Nous avons conçu un dispositif simple utilisant du papier découpé et des films adhésifs comme support. Ce dispositif est faisable et rentable, ne nécessitant aucun équipement sophistiqué ni formation spécialisée. Il peut être produit manuellement, ce qui le rend adapté à une utilisation dans des environnements éloignés ou à ressources limitées. En optimisant la conception du papier pour réduire l'évaporation et améliorer l'homogénéité de la couleur, nous avons amélioré la fiabilité de la quantification colorimétrique. .

Nos résultats suggèrent que cette méthode pourrait être une alternative viable aux systèmes de diagnostic plus complexes et coûteux, en particulier pour les soins

de santé sur le terrain. La nature exploratoire de notre étude nécessite de recherches supplémentaires pour exploiter pleinement son potentiel. Ce travail pose les bases de l'avancement de notre essai RT-LAMP en le transposant à une plateforme basée sur le papier. Cela fournira un outil économique, accessible et fiable pour le suivi et la gestion des maladies en temps réel.

Focalisation isoélectrique intégrée et rationalisée des protéines à l'aide d'un dispositif microfluidique à base de papier

Geovana M. Mendes, Fanny d'Orlye, Laura Trapiella-Alfonso, Gabriela R.M. Duarte, Anne Varenne.Streamlined integrated protein isoelectric focusing using microfluidic paper-based device. Journal of Chromatography A, Volume 1732, 2024, 465222, ISSN 0021-9673,https://doi.org/10.1016/j.chroma.2024.465222.

L'objectif principal de cette étude était de développer et d'optimiser un dispositif de séparation et préconcentration de protéines basé sur la focalisation isoélectrique, en vue de son couplage avec une digestion ultérieure des protéines en peptides et la détection par spectrométrie de masse des peptides générés. Comme l'ont expliqué Tata Rao et al. en 2020, (Tata Rao et al., 2020) un microdispositif analytique doit posséder plusieurs attributs clés en plus de ses performances élevées, notamment la portabilité, l'automatisation, le haut débit, la versatilité et le rapport coût-efficacité. Dans ce contexte, une plateforme de focalisation isoélectrique (IEF) sur papier a été conçue en développant un un support imprimé en 3D avec des électrodes en platine intégrées, des réservoirs d'électrolyte et un canal de séparation sur papier. La géométrie de la plateforme a été optimisée pour permettre des séparations efficaces, robustes et précises des protéines. Le canal de séparation IEF est composé d'une

bandelette de papier (50 mm x 4,5 mm) placée dans la partie inférieure de la plate-forme, tandis que les réservoirs composés d'éponges de cellulose/coton 70/30 % (m/m) sont placés dans la partie supérieure (Figure 6). Le canal de papier et les réservoirs sont connectés efficacement dans le support imprimé en 3D par fermeture efficace avec la partie supérieure dans laquelle les électrodes en platine sont placées, assurant une stabilité du champ électrique et un robustesse de la focalisation isoélectrique.

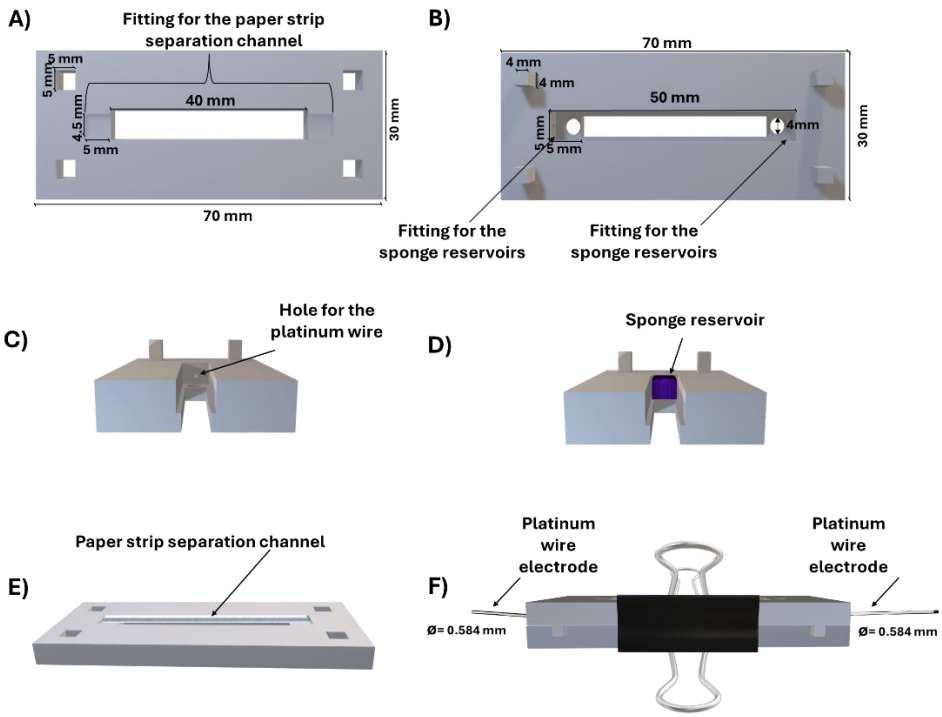

Figure 6: Schéma du support conçu et imprimé en 3D : A) Pièce inférieure ; B) Pièce supérieure ; C) Coupe transversale de la pièce supérieure montrant l'orifice pour les électrodes en fil de platine ; D) Coupe transversale de la pièce supérieure montrant le reservoir à éponge ; E) Pièce inférieure montrant l'ajustement du canal de séparation de la bande de papier ; F) Support assemblé avec un trombone.

Pour déterminer l'efficacité du microdispositif IEF sur papier, une série d'étapes procédurales ont été définies pour chaque résultat expérimental (Figure 7). Tout d'abord, en ce qui concerne les paramètres expérimentaux à optimiser, la séparation IEF a été suivie par l'évolution du courant sous champ électrique. Ensuite, le gradient de pH sur la bande de papier a été visualisé grâce à des portions de papier pH positionnées sur une autre bande. Par imprégnation par capillarité à partir de la bande de papier, la valeur du pH en fonction de la distance sur la bande de papier a été déterminée, permettant d'établir une relation linéaire pH/ position sur la bandelette de papier, permettant de déterminer l'efficacité et la précision du gradient de pH ainsi que sa largeur sur la bande de papier.

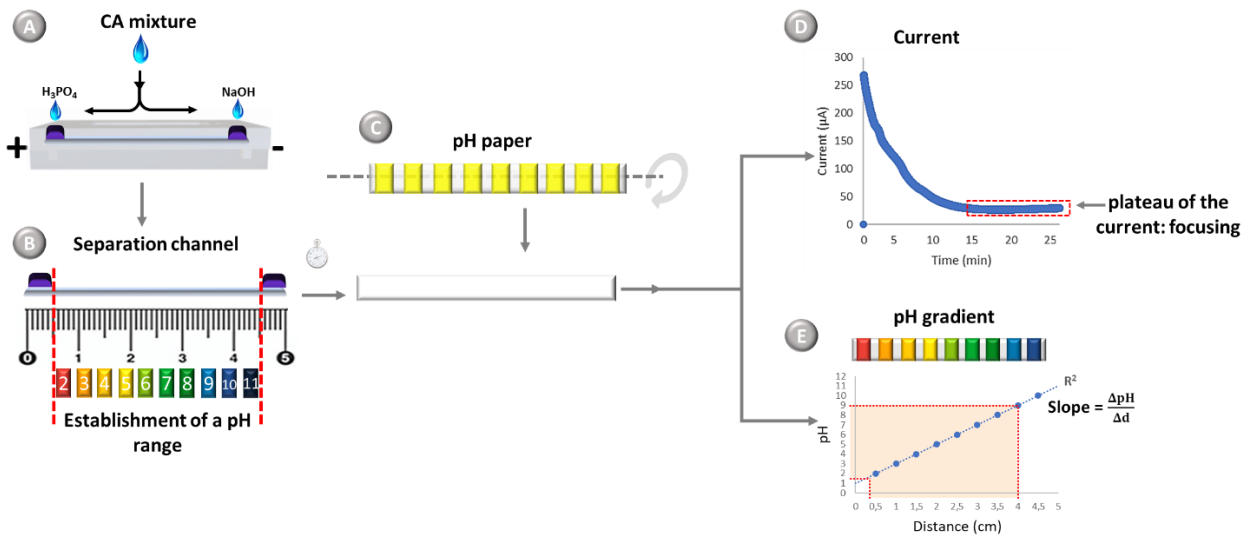

Figure 7: Schéma complet pour le traitement d'image et l'analyse des résultats. A : Chargement du mélange d'ampholytes porteurs (carrier ampholytes, CA). dans le système ; B : Établissement du gradient de pH le long de la bande de papier ; C : Placement du papier pH sur le canal de séparation de la bande de papier ; C : Placement du papier pH sur le canal de séparation de la bande de papier pour évaluer le gradient de pH ; D : Evolution du courant au fil du temps obtenu par l'alimentation électrique ; E : Tracé des valeurs de pH (basé sur le profil de papier pH obtenu) en fonction de la distance sur la bande de papier.

Des protéines chromophores modèles ont ensuite été séparées, d'abord pour permettre une coloration visuelle des différentes parties de la bande de papier, puis pour un traitement des données de la photographie de la bandelette de papier afin de générer des électrophérogrammes à l'aide du logiciel ImageJ. Les électrophérogrammes ont été dessinés avant et après la coupure de la tension de séparation pour mettre en évidence toute dispersion des bandes de protéines ; dans ce dernier cas, la détermination du gradient de pH a été effectuée après la photographie.

Le milieu de séparation était composé d'eau/glycérol (85/15, v/v) car ce milieu évite l'ajout de tout gel qui pourrait gêner ensuite le couplage à la spectrométrie de masse pour la caractérisation des protéines. De plus, le glycerol permet la solubilisation de la majorité des protéines hydrophobes et hydrophiles (Busnel et al., 2005 ; Lecoeur et al., 2010 ; Mokaddem et al., 2009)et est donc compatible avec la mise en œuvre d'une analyse protéomique intégrée sur puce. Enfin, l'emploi de glycérol permet de réduire l'évaporation prématurée des solutions sur le papier. Le mélange d'ampholytes porteurs a été optimisé en combinant trois gammes de pH (pH 3-5 à 0,5%, pH 3-10 à 1%, et pH 9-11 à 0,5%), conduisant à un total de 2% de mélange d'ampholytes porteurs dans le milieu de séparation. L'anolyte et le catholyte étaient composés respectivement de $H_3 PO_4$ (pH 2) et de NaOH (pH 13).

La littérature existant au début de ces travaux (Gaspar et al., 2016; Niu et al., 2018; Xie et al., 2018; Yu et al., 2019) concernant le développement de l'IEF sur papier a montré les défis à relever quant à la robustesse du système analytique. Pour pallier

cela, une plateforme de microdispositif de focalisation isoélectrique (IEF) sur bandelette de papier a été conçu avec l'aide d'une impression 3D. En concevant et en développant un support efficace imprimé en 3D, tous les composants de la procédure IEF ont été intégrés pour gagner en robustesse analytique. Cette plateforme polyvalente peut s'adapter à différentes configurations, en termes de volumes de réservoirs d'électrolyte et de canaux fluidiques à base de papier, et pourrait être utilisée pour d'autres processus analytiques. Construite comme un «hub», elle permet d'établir un gradient de pH robuste, une corrélation linéaire entre le pH et la distance de focalisation isoélectrique des protéines sur la bandelette de papier, et un traitement simplifié des données. L'optimisation de la conception du support imprimé en 3D a contribué à maintenir l'intégrité du système, offrant des avantages tels qu'une précision accrue, une manipulation simplifiée, une réduction des erreurs de manipulation, et donc un potentiel pour les applications de diagnostic au chevet du patient. Alors que plusieurs études ont exploré l'utilisation d'agents chimiques tels que la polyvinylpyrrolidone (PVP) (S. Yu et al., 2019) pour préparer les substrats de papier pour l'IEF, la plate-forme microfluidique à base de papier développée dans cette étude a démontré une séparation efficace des protéines sans traitement préalable de la bandelette de papier. De plus, à notre connaissance, il s'agit de la première preuve de concept d'emploi d'un mélange de glycérol et d'eau comme milieu de séparation dans un dispositif analytique à base de papier. Après avoir optimisé différents paramètres du système analytique, dont le pourcentage en glycérol, le temps de focalisation, l'influence de la conservation ou la coupure de la tension de séparation pendant la détection, la preuve de concept a été réalisée par dopage de protéines modèles dans

une matrice de salive (Figure 8), montrant un très faible impact de la matrice sur la séparation de trois protéines chromophores, soulignant la viabilité pratique de la plateforme.

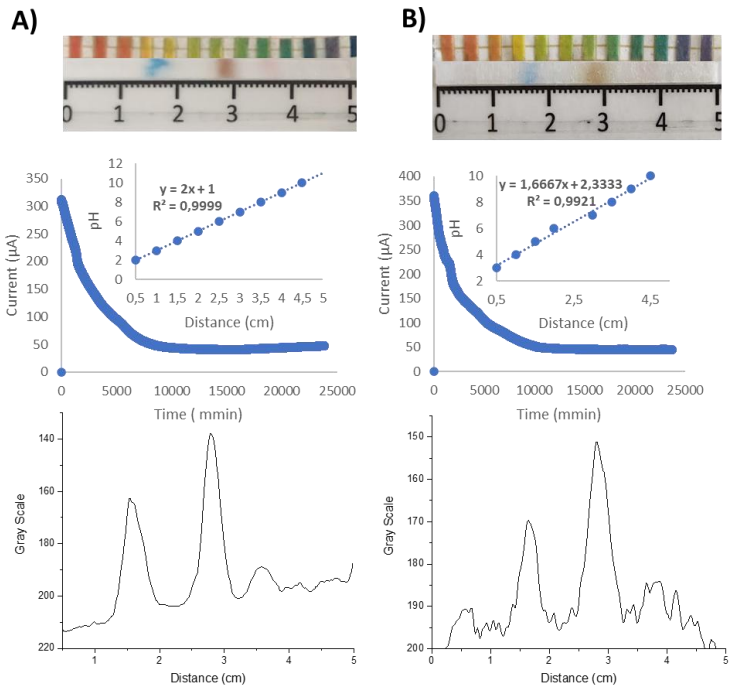

Figure 8: Focalisation isoélectrique (IEF) d'un mélange de phycocyanine, de myoglobine et de cytochrome C, A) dissous dans le milieu IEF et B) ajouté à un échantillon de salive (2,0 $mgmL^{-1}$). Conditions expérimentales : tension appliquée : 200 V ; milieu de séparation : 2 % de C.A. (intervalle de pH 3-11) dans un mélange de glycérol/eau (85/15, v:v) ; anolyte : H_3PO_4 (pH 2) ; catholyte : NaOH (pH 13) ; temps de focalisation : 25 minutes.

Cette étude représente un pas en avant dans l'intégration d'une analyse protéomique dans un dispositif microfluidique à base de papier. La plateforme IEF sur papier esquissée offre une solution économiquement réalisable et polyvalente pour le prétraitement et la séparation de protéines sur papier, en tirant parti de la miniaturisation et d'une approche simplifiée. Elle ouvre la voie à son intégration

ultérieure dans une analyse protéomique sur puce en trois étapes, avec digestion ultérieure des protéines focalisées par IEF et caractérisation des peptides générés par spectrométrie de masse.

Conclusions

Dans ce travail, nous avons développé des systèmes de diagnostic pour les biomolécules appliqués ou applicables au chevet du patient. La méthode LAMP (Loop mediated isothermal amplification) a été utilisée pour créer un test simple et économique pendant la pandémie de COVID-19. Nous avons mis en œuvre ce test au point de soins dans un hôpital submergé par le nombre de patients, où les tests standards n'étaient pas réalisables. Notre test a fourni des diagnostics rapides et précis. De plus, nous avons proposé une méthode de dépistage non invasive basée sur l'ARN extrait de la salive des travailleurs essentiels durant la pandémie, qui s'est révélée à la fois pratique et efficace pour des tests fréquents. La transposition préliminaire de cette méthodologie à une plateforme en papier a montré des résultats prometteurs pour le suivi en temps réel des infections, en particulier celles du SARS-CoV-2, au point-of-care.

Nous avons développé la focalisation isoélectrique sur une plateforme à base de papier, obtenant une séparation des protéines précise et reproductible, y compris dans des échantillons réels, avec une résolution et une efficacité acceptables. Ce système représente une étape supplémentaire dans un projet plus vaste visant à intégrer toutes les étapes protéomiques sur une seule puce. Nos avancées ont permis

de passer à la phase suivante, à savoir l'intégration de la digestion, tout en maintenant une résolution et une efficacité de séparation suffisantes. Grâce à la capillarité, les protéines séparées peuvent être transposées au sein du même dispositif à base de papier pour la digestion, avant d'être dirigées vers la détection par spectrométrie de masse (MS).

Le développement réussi de méthodes d'analyse des biomolécules, privilégiant l'économie, la rapidité et la simplicité, met en lumière le potentiel du papier en tant que plateforme pour ces tests diagnostiques. Le papier s'est avéré être une plateforme adaptée et accessible pour la réalisation de ces tests, soulignant son potentiel dans des contextes à ressources limitées.

Références

Akyazi, T., Basabe-Desmonts, L., & Benito-Lopez, F. (2018). Review on microfluidic paper-based analytical devices towards commercialisation. In Analytica Chimica Acta (Vol. 1001, pp. 1–17). Elsevier B.V. https://doi.org/10.1016/j.aca.2017.11.010

Boobphahom, S., Ly, M. N., Soum, V., Pyun, N., Kwon, O. S., Rodthongkum, N., & Shin, K. (2020). Recent advances in microfluidic paper-based analytical devices toward high-throughput screening. In Molecules (Vol. 25, Issue 13). MDPI AG. https://doi.org/10.3390/molecules25132970

Bullard, J., Dust, K., Funk, D., Strong, J. E., Alexander, D., Garnett, L., Boodman, C., Bello, A., Hedley, A., Schiffman, Z., Doan, K., Bastien, N., Li, Y., van Caeseele, P. G., & Poliquin, G. (2020). Predicting infectious severe acute respiratory syndrome coronavirus 2 from diagnostic samples. Clinical Infectious Diseases, 71(10), 2663–2666. https://doi.org/10.1093/cid/ciaa638

Busnel, J. M., Varenne, A., Descroix, S., Peltre, G., Gohon, Y., & Gareil, P. (2005). Evaluation of capillary isoelectric focusing in glycerol-water media with a view to hydrophobic protein applications. Electrophoresis, 26(17), 3369–3379. https://doi.org/10.1002/elps.200500252

Cassedy, A., Parle-McDermott, A., & O'Kennedy, R. (2021). Virus Detection: A Review of the Current and Emerging Molecular and Immunological Methods. In Frontiers in Molecular Biosciences (Vol. 8). Frontiers Media S.A. https://doi.org/10.3389/fmolb.2021.637559

Chow, F. W. N., Chan, T. T. Y., Tam, A. R., Zhao, S., Yao, W., Fung, J., Cheng, F. K. K., Lo, G. C. S., Chu, S., Aw-Yong, K. L., Tang, J. Y. M., Tsang, C. C., Luk, H. K. H., Wong, A. C. P., Li, K. S. M., Zhu, L., He, Z., Tam, E. W. T., Chung, T. W. H., … Lau, S. K. P. (2020). A rapid, simple, inexpensive, and mobile colorimetric assay covid-19-lamp for mass on-site screening of covid-19. International Journal of Molecular Sciences, 21(15), 1–10. https://doi.org/10.3390/ijms21155380

Dinh, V. P., & Lee, N. Y. (2022). Fabrication of a fully integrated paper microdevice for point-of-care testing of infectious disease using Safranin O dye coupled with loop-mediated isothermal amplification. Biosensors and Bioelectronics, 204. https://doi.org/10.1016/j.bios.2022.114080

Domingo, E. (2020). Introduction to virus origins and their role in biological evolution. In Virus as Populations (pp. 1–33). Elsevier. https://doi.org/10.1016/b978-0-12-816331-3.00001-5

Duarte, G. R. M., Price, C. W., Augustine, B. H., Carrilho, E., & Landers, J. P. (2011). Dynamic solid phase DNA extraction and PCR amplification in polyester-toner based microchip. Analytical Chemistry, 83(13), 5182–5189. https://doi.org/10.1021/ac200292m

Falahi, S., & Kenarkoohi, A. (2020). Transmission routes for SARS-CoV-2 infection: review of evidence. In New Microbes and New Infections (Vol. 38). Elsevier Ltd. https://doi.org/10.1016/j.nmni.2020.100778

Fan, Y., Liu, S., He, J., Gao, K., & Zhang, Y. (2018). Rapid prototyping of flexible multilayer microfluidic devices using polyester sealing film. Microsystem Technologies, 24(6), 2847–2852. https://doi.org/10.1007/s00542-017-3630-3

Farmerie, L., Rustandi, R. R., Loughney, J. W., & Dawod, M. (2021). Recent advances in isoelectric focusing of proteins and peptides. In Journal of Chromatography A (Vol. 1651). Elsevier B.V. https://doi.org/10.1016/j.chroma.2021.462274

Fierabracci, A., Arena, A., & Rossi, P. (2020). COVID-19: A review on diagnosis, treatment, and prophylaxis. In International Journal of Molecular Sciences (Vol. 21, Issue 14, pp. 1–16). MDPI AG. https://doi.org/10.3390/ijms21145145

Gaspar, C., Sikanen, T., Franssila, S., & Jokinen, V. (2016). Inkjet printed silver electrodes on macroporous paper for a paper-based isoelectric focusing device. Biomicrofluidics, 10(6). https://doi.org/10.1063/1.4973246

Han, T., Jin, Y., Geng, C., Aziz, A. ur R., Zhang, Y., Deng, S., Ren, H., & Liu, B. (2020). Microfluidic Paper-based Analytical Devices in Clinical Applications. In Chromatographia (Vol. 83, Issue 6, pp. 693–701). Springer. https://doi.org/10.1007/s10337-020-03892-1

Hasan, M. R., Mirza, F., Al-Hail, H., Sundararaju, S., Xaba, T., Iqbal, M., Alhussain, H., Yassine, H. M., Perez-Lopez, A., & Tang, P. (2020). Detection of SARS-CoV-2 RNA by direct RT-qPCR on nasopharyngeal specimens without extraction of viral RNA. PLoS ONE, 15(7 July). https://doi.org/10.1371/journal.pone.0236564

Klein, S., Müller, T. G., Khalid, D., Sonntag-Buck, V., Heuser, A. M., Glass, B., Meurer, M., Morales, I., Schillak, A., Freistaedter, A., Ambiel, I., Winter, S. L., Zimmermann, L., Naumoska, T., Bubeck, F., Kirrmaier, D., Ullrich, S., Miranda, I. B., Anders, S., … Chlanda, P. (2020). SARS-CoV-2 RNA extraction using magnetic beads for rapid large-scale testing by RT-qPCR and RT-LAMP. Viruses, 12(8). https://doi.org/10.3390/v12080863

Lecoeur, M., Gareil, P., & Varenne, A. (2010). Separation and quantitation of milk whey proteins of close isoelectric points by on-line capillary isoelectric focusing-Electrospray ionization mass spectrometry in glycerol-water media. Journal of Chromatography A, 1217(46), 7293–7301. https://doi.org/10.1016/j.chroma.2010.09.043

Lenčo, J., Jadeja, S., Naplekov, D. K., Krokhin, O. V., Khalikova, M. A., Chocholouš, P., Urban, J., Broeckhoven, K., Nováková, L., & Švec, F. (2022). Reversed-Phase Liquid Chromatography of Peptides for Bottom-Up Proteomics: A Tutorial. Journal of Proteome Research, 21(12), 2846–2892. https://doi.org/10.1021/acs.jproteome.2c00407

Lim, H., Jafry, A. T., & Lee, J. (2019). Fabrication, flow control, and applications of microfluidic paper-based analytical devices. In Molecules (Vol. 24, Issue 16). MDPI AG. https://doi.org/10.3390/molecules24162869

Lista, M. J., Matos, P. M., Maguire, T. J. A., Poulton, K., Ortiz-Zapater, E., Page, R., Sertkaya, H., Ortega-Prieto, A. M., Scourfield, E., O'Byrne, A. M., Bouton, C., Dickenson, R. E., Ficarelli, M., Jimenez-Guardeño, J. M., Howard, M., Betancor, G., Galao, R. P., Pickering, S., Signell, A. W., … Martinez-Nunez, R. T. (2021). Resilient SARS-CoV-2 diagnostics workflows including viral heat inactivation. PLoS ONE, 16(9 September). https://doi.org/10.1371/journal.pone.0256813

Liu, S., Li, Z., Yu, B., Wang, S., Shen, Y., & Cong, H. (2020). Recent advances on protein separation and purification methods. Advances in Colloid and Interface Science, 284(102254), 1–23. https://doi.org/10.1016/j.cis.2020.102254

Liu, Y. C., Kuo, R. L., & Shih, S. R. (2020). COVID-19: The first documented coronavirus pandemic in history. In Biomedical Journal (Vol. 43, Issue 4, pp. 328–333). Elsevier B.V. https://doi.org/10.1016/j.bj.2020.04.007

Loan Dao Thi, V., Herbst, K., Boerner, K., Meurer, M., Kremer, L. P., Kirrmaier, D., Freistaedter, A., Papagiannidis, D., Galmozzi, C., Stanifer, M. L., Boulant, S., Klein, S., Chlanda, P., Khalid, D., Barreto Miranda, I., Schnitzler, P., Kräusslich, H.-G., Knop, M., & Anders, S. (2020). A colorimetric RT-LAMP assay and LAMP-sequencing for detecting SARS-CoV-2 RNA in clinical samples. In Sci. Transl. Med (Vol. 12). https://www.science.org

Magleby, R., Westblade, L. F., Trzebucki, A., Simon, M. S., Rajan, M., Park, J., Goyal, P., Safford, M. M., & Satlin, M. J. (2021). Impact of Severe Acute Respiratory Syndrome Coronavirus 2 Viral Load on Risk of Intubation and Mortality among Hospitalized Patients with Coronavirus Disease 2019. Clinical Infectious Diseases, 73(11), E4197–E4205. https://doi.org/10.1093/cid/ciaa851

Maráková, K., Opetová, M., & Tomašovský, R. (2023). Capillary electrophoresis-mass spectrometry for intact protein analysis: Pharmaceutical and biomedical applications

(2018–March 2023). In Journal of Separation Science (Vol. 46, Issue 15). John Wiley and Sons Inc. https://doi.org/10.1002/jssc.202300244

Martinez, A. W., Phillips, S. T., Butte, M. J., & Whitesides, G. M. (2007). Patterned Paper as a Platform for Inexpensive, Low-Volume, Portable Bioassays. Angewandte Chemie, 119(8), 1340–1342. https://doi.org/10.1002/ange.200603817

Maurer, M. H. (2011). Proteomic definitions of mesenchymal stem cells. In Stem Cells International. https://doi.org/10.4061/2011/704256

Miller, R. M., & Smith, L. M. (2022). Overview and considerations in bottom-up proteomics. In Analyst (Vol. 148, Issue 3, pp. 475–486). Royal Society of Chemistry. https://doi.org/10.1039/d2an01246d

Mokaddem, M., Gareil, P., & Varenne, A. (2009). Online CIEF-ESI-MS in glycerol-water media with a view to hydrophobic protein applications. Electrophoresis, 30(23), 4040–4048. https://doi.org/10.1002/elps.200900091

Moradian, A., Kalli, A., Sweredoski, M. J., & Hess, S. (2014). The top-down, middle-down, and bottom-up mass spectrometry approaches for characterization of histone variants and their post-translational modifications. In Proteomics (Vol. 14, Issues 4–5, pp. 489–497). Wiley-VCH Verlag. https://doi.org/10.1002/pmic.201300256

Nawattanapaiboon, K., Pasomsub, E., Prombun, P., Wongbunmak, A., Jenjitwanich, A., Mahasupachai, P., Vetcho, P., Chayrach, C., Manatjaroenlap, N., Samphaongern, C., Watthanachockchai, T., Leedorkmai, P., Manopwisedjaroen, S., Akkarawongsapat, R., Thitithanyanont, A., Phanchana, M., Panbangred, W., Chauvatcharin, S., & Srikhirin, T. (2021). Colorimetric reverse transcription loop-mediated isothermal amplification (RT-LAMP) as a visual diagnostic platform for the detection of the emerging coronavirus SARS-CoV-2. Analyst, 146(2), 471–477. https://doi.org/10.1039/d0an01775b

Nge, P. N., Rogers, C. I., & Woolley, A. T. (2013). Advances in microfluidic materials, functions, integration, and applications. In Chemical Reviews (Vol. 113, Issue 4, pp. 2550–2583). https://doi.org/10.1021/cr300337x

Niu, J. C., Zhou, T., Niu, L. L., Xie, Z. S., Fang, F., Yang, F. Q., & Wu, Z. Y. (2018). Simultaneous pre-concentration and separation on simple paper-based analytical device for protein analysis. Analytical and Bioanalytical Chemistry, 410(6), 1689–1695. https://doi.org/10.1007/s00216-017-0809-5

Notomi, T., Okayama, H., Masubuchi, H., Yonekawa, T., Watanabe, K., Amino, N., & Hase, T. (2000). Loop-mediated isothermal amplification of DNA. In Nucleic Acids Research (Vol. 28, Issue 12).

Patterson, E. I., Prince, T., Anderson, E. R., Casas-Sanchez, A., Smith, S. L., Cansado-Utrilla, C., Solomon, T., Griffiths, M. J., Acosta-Serrano, Á., Turtle, L., &

Hughes, G. L. (2020). Methods of Inactivation of SARS-CoV-2 for Downstream Biological Assays. Journal of Infectious Diseases, 222(9), 1462–1467. https://doi.org/10.1093/infdis/jiaa507

Ríos, Á., Zougagh, M., & Avila, M. (2012). Miniaturization through lab-on-a-chip: Utopia or reality for routine laboratories? A review. In Analytica Chimica Acta (Vol. 740, pp. 1–11). https://doi.org/10.1016/j.aca.2012.06.024

See, I., Paul, P., Slayton, R. B., Steele, M. K., Stuckey, M. J., Duca, L., Srinivasan, A., Stone, N., Jernigan, J. A., & Reddy, S. C. (2021). Modeling Effectiveness of Testing Strategies to Prevent Coronavirus Disease 2019 (COVID-19) in Nursing Homes - United States, 2020. Clinical Infectious Diseases, 73(3), E792–E798. https://doi.org/10.1093/cid/ciab110

Sohn, Y., Jeong, S. J., Chung, W. S., Hyun, J. H., Baek, Y. J., Cho, Y., Kim, J. H., Ahn, J. Y., Choi, J. Y., & Yeom, J. S. (2020). Assessing viral shedding and infectivity of asymptomatic or mildly symptomatic patients with COVID-19 in a later phase. Journal of Clinical Medicine, 9(9), 1–9. https://doi.org/10.3390/jcm9092924

Tata Rao, L., Rewatkar, P., Dubey, S. K., Javed, A., & Goel, S. (2020). Performance optimization of microfluidic paper fuel-cell with varying cellulose fiber papers as absorbent pad. International Journal of Energy Research, 44(5), 3893–3904. https://doi.org/10.1002/er.5188

Teo, A. K. J., Choudhury, Y., Tan, I. B., Cher, C. Y., Chew, S. H., Wan, Z. Y., Cheng, L. T. E., Oon, L. L. E., Tan, M. H., Chan, K. S., & Hsu, L. Y. (2021). Saliva is more sensitive than nasopharyngeal or nasal swabs for diagnosis of asymptomatic and mild COVID-19 infection. Scientific Reports, 11(1). https://doi.org/10.1038/s41598-021-82787-z

Terry, S. C., Jerman, J. H., & Angell, J. B. (1979). A Gas Chromatographic Air Analyzer Fabricated on a Silicon Wafer. IEEE Trans. Electron Dev., 26(12), 1880–1886.

Tom, M. R., & Mina, M. J. (2020). To Interpret the SARS-CoV-2 Test, Consider the Cycle Threshold Value. In Clinical Infectious Diseases (Vol. 71, Issue 16, pp. 2252–2254). Oxford University Press. https://doi.org/10.1093/cid/ciaa619

Tomita, N., Mori, Y., Kanda, H., & Notomi, T. (2008). Loop-mediated isothermal amplification (LAMP) of gene sequences and simple visual detection of products. Nature Protocols, 3(5), 877–882. https://doi.org/10.1038/nprot.2008.57

Trinh, K. T. L., Chae, W. R., & Lee, N. Y. (2022). Recent advances in the fabrication strategies of paper-based microfluidic devices for rapid detection of bacteria and viruses. In Microchemical Journal (Vol. 180). Elsevier Inc. https://doi.org/10.1016/j.microc.2022.107548

Uribe-Alvarez, C., Lam, Q., Baldwin, D. A., & Chernoff, J. (2021). Low saliva pH can yield false positives results in simple RT-LAMP-based SARS-CoV-2 diagnostic tests. PLoS ONE, 16(5 May). https://doi.org/10.1371/journal.pone.0250202

Xie, S. F., Gao, H., Niu, L. L., Xie, Z. S., Fang, F., Wu, Z. Y., & Yang, F. Q. (2018). Carrier ampholyte-free isoelectric focusing on a paper-based analytical device for the fractionation of proteins. Journal of Separation Science, 41(9), 2085–2091. https://doi.org/10.1002/jssc.201701438

Yu, S., Yan, C., Hu, X., He, B., Jiang, Y., & He, Q. (2019). Isoelectric focusing on microfluidic paper-based chips. Analytical and Bioanalytical Chemistry, 411(21), 5415–5422. https://doi.org/10.1007/s00216-019-02008-5

Zhu, J., Guo, J., Xu, Y., & Chen, X. (2020). Viral dynamics of SARS-CoV-2 in saliva from infected patients. In Journal of Infection (Vol. 81, Issue 3, pp. e48–e50). W.B. Saunders Ltd. https://doi.org/10.1016/j.jinf.2020.06.059

Introdução

Nas últimas três décadas, os dispositivos analíticos microfluídicos surgiram como uma alternativa promissora aos métodos tradicionais para testes rápidos aplicáveis no *point-of-care*. (Ríos et al., 2012) Inicialmente desenvolvidos a partir de materiais à base de silício e plástico, posteriormente esses dispositivos incorporaram o papel como uma alternativa viável. (Terry et al., 1979)O uso de papel hidrofílico confinado em uma barreira de cera hidrofóbica para análise química, introduzido em 1937, (Yagoda, 1937) recebeu reconhecimento significativo após uma publicação do grupo do professor Whitesides em 2007. (Martinez et al., 2007) Já consolidado pela comunidade científica, os dispositivos analíticos microfluídicos à base de papel (μPAD) oferecem vantagens substanciais em comparação aos dispositivos microfluídicos à base de plástico devido às suas características. (Trinh et al., 2022)

Os μPADs (dispositivos analíticos microfluídicos à base de papel) oferecem vantagens consideráveis devido às suas estruturas porosas e à sua inércia química, que facilitam a imobilização e o armazenamento eficaz de reagentes. Além disso, a leveza e flexibilidade favorecem o manuseio, a ação capilar nesses dispositivos elimina a necessidade de bombas externas para mover os líquidos, um benefício para aplicações no local de atendimento. Essas propriedades permitem que os μPADs atendam aos critérios ASSURED (do inglês affordable, sensitive, specific, user-friendly, fast and robust, equipment-free, and deliverable,): acessíveis, sensíveis, específicos, de fácil uso, rápidos e robustos, sem necessidade de equipamentos e de fácil distribuição, o que torna esses dispositivos ferramentas ideais para o diagnóstico

e controle de doenças transmissíveis em ambientes com recursos limitados. (Trinh et al., 2022)

Esta tese aborda duas classes de moléculas biológicas: proteínas e RNA viral, ambas essenciais para o diagnóstico clínico e o gerenciamento de doenças. As proteínas permitem entender os mecanismos moleculares envolvidos em patologias, devido às suas estruturas complexas e funções celulares essenciais. (Farmerie et al., 2021) Quanto ao RNA viral, em particular o de vírus altamente infecciosos, ele é crucial para a detecção e monitoramento de diversas doenças infecciosas. (Cassedy et al., 2021; Domingo, 2020)

A ameaça das doenças infecciosas aumentou nos últimos anos, principalmente devido a bactérias resistentes a antibióticos e à propagação de vírus altamente contagiosos. Embora os avanços da ciência e da tecnologia tenham melhorado a precisão e a eficácia dos diagnósticos clínicos, o alto custo e a complexidade dessas tecnologias limitam sua acessibilidade em regiões com recursos limitados. (T. Han et al., 2020) Cada surto de doença infecciosa evidencia a necessidade de testes adaptáveis que possam ser realizados fora de laboratórios centralizados, nos locais dos surtos, para prevenir, acompanhar e monitorar ameaças endêmicas e pandêmicas. Os métodos atuais de detecção de patógenos, como a reação em cadeia da polimerase (PCR), o ensaio imunenzimático (ELISA) e a cultura celular, demandam muito tempo e requerem pessoal qualificado, o que dificulta a resposta rápida a novos patógenos. Portanto, é essencial desenvolver técnicas rápidas, precisas, sensíveis, portáteis, de fácil uso e adequadas a usuários não treinados. (Trinh et al., 2022)

A amplificação isotérmica mediada por loop (LAMP) é um teste de amplificação de ácidos nucleicos (NAAT - nucleic acid amplification techniques) que se consolidou como uma alternativa viável aos métodos convencionais. A técnica LAMP fornece resultados de 30 a 60 minutos sem necessidade de equipamentos sofisticados, permitindo sua aplicação em crises sanitárias e sua adaptação em plataformas microfluídicas. Técnicas isotérmicas de amplificação de DNA facilitam a adaptação da técnica a plataformas microfluídicas, melhorando tanto a eficiência quanto a acessibilidade. (T. Han et al., 2020; Notomi et al., 2000; Tomita et al., 2008a)

A caracterização de proteínas é essencial para compreender os mecanismos das doenças e desenvolver diagnósticos. Em geral, o processo analítico requer procedimentos complexos. A estratégia "top-down" analisa diretamente proteínas intactas por espectrometria de massa (MS), enquanto a estratégia "bottom-up" envolve a digestão das proteínas em peptídeos antes de separá-los e detectá-los por MS. A proteômica "middle-down", que envolve a digestão em fragmentos peptídicos maiores, estabelece a ponte entre essas abordagens. (Lenčo et al., 2022a; Maráková et al., 2023; Miller & Smith, 2022; Moradian et al., 2014) Diversas metodologias de separação de proteínas, como cromatografia e eletroforese, foram desenvolvidas. (Y. C. Liu et al., 2020) Em particular, a focalização isoelétrica (IEF) é um método de separação eletrocinético poderoso para separar e concentrar proteínas baseado em seus pontos isoelétricos (pI), gerando um gradiente de pH sob campo elétrico na presença de uma mistura de anfólitos carreadores (carrier ampholytes, CA). A IEF pode ser acoplada a métodos de detecção. (Farmerie et al., 2021; Lecoeur et al., 2010; Maurer, 2011; Mokaddem et al., 2009)

Os avanços tecnológicos permitiram a integração de métodos de separação em escalas microfluídicas, propondo otimizar o processo analítico ao automatizar etapas sucessivas. Essa integração permite reduzir o tempo de análise, evitar erros manuais e contaminação cruzada, diminuir custos e expandir as aplicações para ambientes com poucos recursos. A aplicação de métodos como a LAMP ou a IEF no contexto da microfluídica é especialmente promissora. As plataformas microfluídicas oferecem várias vantagens, incluindo integração, baixo custo, volumes mínimos de amostras, uso de materiais simples e descartáveis e a possibilidade de aplicações no local de necessidade. (Akyazi et al., 2018; Boobphahom et al., 2020; Dinh & Lee, 2022; H. Lim et al., 2019; Nge et al., 2013)

Esta tese foi realizada no contexto de uma co-tutela entre a Universidade Federal de Goiás (Goiânia, Brasil) e a Chimie ParisTech PSL. Iniciado no Brasil, no começo da pandemia, o trabalho desenvolvido durante o doutorado na instituição brasileira se concentrou em desenvolver metodologias baseadas em LAMP com detecção colorimétrica com indicador de pH para diagnóstico da COVID-19. Assim, este trabalho de tese apresenta resultados obtidos no combate à COVID-19 durante a pandemia. A metodologia LAMP foi desenvolvida, otimizada e validada para aplicações em campo. Após a publicação dos dados da pandemia, o método desenvolvido e validado foi adaptado para plataformas de papel. No âmbito da co-tutela, os trabalhos foram então realizados no laboratório francês para o desenvolvimento e otimização de uma plataforma de papel para a focalização isoelétrica de proteínas, com o objetivo de integrar as etapas da análise proteômica

em um microdispositivo. Após uma apresentação do estado da arte nesses dois domínios, as duas metodologias (LAMP e IEF) são apresentadas.

Um diagnóstico molecular em campo pode ser preciso? Avaliação do desempenho da RT-LAMP colorimétrica para a detecção do SARS-CoV-2 em ambiente hospitalar

Lívia do Carmo Silva†, Carlos Abelardo dos Santos†, Geovana de Melo Mendes†, Kézia Gomes de Oliveira† et al. Can a field molecular diagnosis be accurate? A performance evaluation of colorimetric RT-LAMP for the detection of SARS-CoV-2 in a hospital setting. Analytical Methods : Advancing Methods and Applications. 2021 Jul;13(26):2898-2907. DOI: 10.1039/d1ay00481f. PMID: 34109949.

† Os autores contribuiram igualmente para este trabalho.

Neste trabalho realizamos o teste RT-LAMP colorimétrico em um ambiente hospitalar, e a metodologia (Figura 1) demonstrou ser uma ferramenta valiosa para detectar o SARS-CoV-2 com excelente custo-benefício em situações de *point-of-care*. Foi possível detectar o ácido nucleico do SARS-CoV-2 diretamente em amostras de swabs sem necessidade de extração do RNA. Os resultados mostraram que o método oferece resultados confiáveis e precisos, tanto no campo (hospital) quanto no laboratório. Além disso, a RT-LAMP usada no hospital apresentou desempenhos diagnósticos comparáveis aos da RT-qPCR e ao teste realizado no ambiente laboratorial, com alta sensibilidade (88,89%) e especificidade (94,20%). De acordo com os dados, a limitação da RT-LAMP, em comparação com o método de referência, é a sensibilidade. No entanto, a RT-LAMP é mais fácil de implementar, o que elimina a necessidade de equipamentos sofisticados e pode contribuir para aumentar a frequência dos testes. Nosso teste RT-LAMP possui um grande potencial facilitador

do rastreamento do SARS-CoV-2 no campo, permitindo um gerenciamento rápido e preciso dos pacientes infectados.

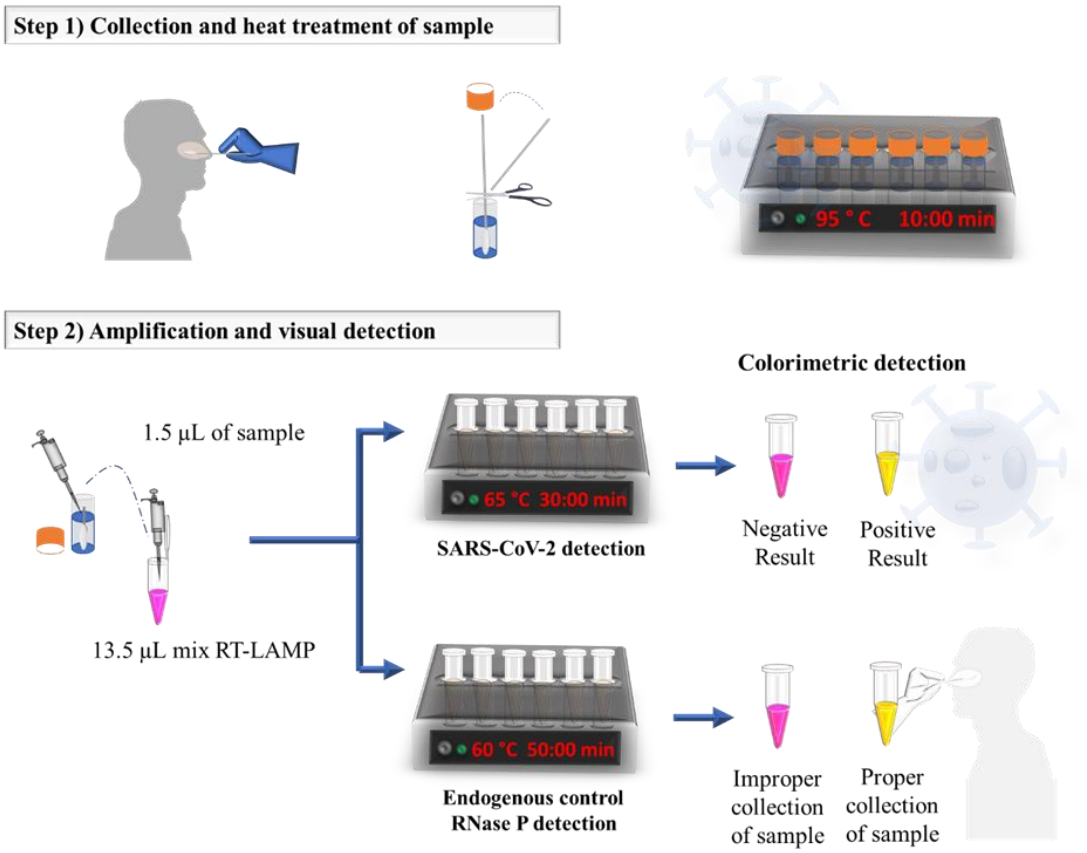

Figure 1: Visão geral do procedimento RT-LAMP. Etapa 1: Coleta por swab e tratamento térmico das amostras. A amostra nasofaríngea foi coletada com um swab e armazenada em tubo criogênico contendo 1 mL de solução salina a 0,9%. As amostras foram submetidas a tratamento térmico a 95 °C por 10 minutos para extração térmica e inativação viral. Etapa 2: Amplificação e detecção visual; 1,5 µL da amostra foi adicionado a dois misturas, cada uma contendo primers para SARS-CoV-2 ou RNase P, água e o WarmStart Colorimetric LAMP 2X Master Mix, e incubado em dois termoblocos; um por 30 minutos a 65 °C para a detecção do SARS-CoV-2 e o outro por 50 minutos a 60 °C para a detecção da RNase P nas amostras coletadas. A positividade das amostras foi determinada observando a mudança de cor de rosa (amostra negativa) para amarelo (amostra positiva). Alterações nas temperaturas de incubação para a detecção da RNase P e do SARS-CoV-2 podem resultar em baixa eficiência de amplificação e, portanto, devem ser mantidas conforme descrito anteriormente.

Em locais com recursos limitados, vários desafios foram associados aos diagnósticos baseados em PCR, incluindo a falta de infraestrutura, pessoal treinado e equipamentos caros. Nesse contexto, a demanda por testes instrumentalmente mais simples ("testes rápidos"), geralmente baseados na detecção por fluxo lateral (lateral flow assay, LFA), emergiu rapidamente. Atualmente, testes de fluxo lateral estão disponíveis para a detecção de anticorpos e antígenos. Nosso teste oferece vantagens evidentes, realizando a detecção no *point-of-care* do SARS-CoV-2 em 100% das amostras com Ct < 30 (Ct - ciclo threshold, é o ponto onde o sinal gerado pela amplificação do DNA atinge um nível detectável) diretamente em amostras de swabs nasofaríngeos usando apenas o tratamento térmico (Figura 2). O tratamento térmico da amostra, como descrito em nosso artigo, é vantajoso porque, além de ser rápido, não requer etapas de abertura dos tubos de amostra, o que reforça a biossegurança na realização dos testes. Além do processo de preparação da amostra, um controle endógeno (RP-RNase P) foi utilizado, o que determinou a viabilidade da amostra, conferindo maior confiabilidade ao teste. Além disso, neste estudo, os limites da "potencial aplicação do método" foram superados, para uma real aplicação em um ambiente hospitalar, com bons resultados em termos de diagnóstico rápido, preciso e sensível, o que contribiu para o controle da pandemia, especialmente em ambientes onde os recursos são limitados.

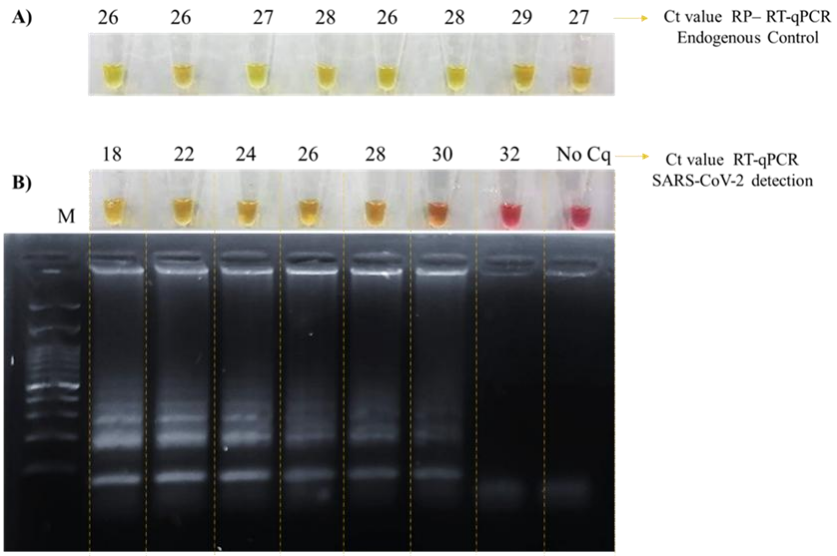

Figure 2: Detecção dos produtos de amplificação por RT-LAMP. (A) Avaliação da qualidade do controle endógeno RNase P (RP) humano em amostras de swab; oito (8) amostras positivas por RT-qPCR. (B) Detecção do SARS-CoV-2 por RT-LAMP em oito (8) amostras com diferentes cargas virais visualizadas por detecção visual e separação eletroforética. No. Cq: nenhum ciclo de quantificação.

Dado que o uso de reagentes químicos, como tampões de lise, altera significativamente o pH das amostras, essa abordagem dificulta uma análise colorimétrica baseada na variação do pH. Além de promover a inativação ao desnaturar as proteínas essenciais para a adesão e replicação do vírus em uma célula hospedeira, o protocolo de pré-aquecimento (Hasan et al., 2020; Lista et al., 2021; Patterson et al., 2020b) provou ser um pré-tratamento ideal para swabs nasofaríngeos para liberar o RNA usando calor, sem a necessidade de extrair o ácido nucleico. Essa abordagem de pré-aquecimento das amostras também já foi utilizada como estratégia para expor o genoma viral e desnaturar os possíveis inibidores da reação PCR. (Nawattanapaiboon et al., 2021)

Quanto ao limite de detecção, nossos resultados para detecção do SARS-CoV-2 concordam com os de outros estudos que descrevem a diminuição da sensibilidade devido à presença de uma matriz biológica. O desempenho da RT-LAMP relatado neste trabalho também está alinhado com os descritos por outros trabalhos na literatura. (Chow et al., 2020; Klein et al., 2020; Nawattanapaiboon et al., 2021) Os valores de Ct da reação RT-qPCR estão inversamente correlacionados com a carga viral (Tom & Mina, 2020) e alguns estudos estabeleceram uma correlação entre o potencial de infectividade e os valores de Ct. (Bullard et al., 2020). Magleby et al. estabeleceram uma correlação entre o Ct dos pacientes e a gravidade da doença, e um Ct > 30 está relacionado a uma mortalidade mais baixa. (Magleby et al., 2021) Assim, considerando o limite de detecção encontrado em nossas análises, que está em conformidade com o limite relatado em outros estudos, (Loan Dao Thi et al., 2020b) o teste proposto aqui pode ser útil para o rastreamento de pacientes no início da infecção com uma carga viral alta e, portanto, com maior potencial de propagação viral e progressão para condições clínicas graves devido à infecção pelo SARS-CoV-2. Portanto, embora o teste RT-LAMP descrito aqui tenha uma sensibilidade menor do que a RT-PCR, a detecção de um Ct < 30 é suficiente para identificar indivíduos que podem ser contagiosos e facilitar a implementação de medidas de isolamento.

Assim, considerando a simplicidade de execução do teste, a rapidez dos resultados (menos de 2h), o custo global mais baixo, a análise do cenário de sobrecarga das salas de emergência durante a pandemia e a necessidade de isolar os pacientes infectados, os resultados apresentados aqui demonstram que a metodologia RT-LAMP tem uma aplicação clínica essencial, principalmente no setor

de rastreamento hospitalar, para tentar minimizar o problema da sobrecarga, permitindo um atendimento imediato dos pacientes mais urgentes.

Detecção de SARS-CoV-2 em saliva por RT-LAMP, para triagem no Brasil, incluindo pacientes pré-sintomáticos

Santos CA dos†, Oliveira KG de†, Mendes GM†, Silva LC, Souza Jr. MN de, Estrela PFN, et al.. Detection of SARS-CoV-2 in Saliva by RT-LAMP During a Screening of Workers in Brazil, Including Pre-Symptomatic Carriers. J Braz Chem Soc [Internet]. 2021Nov;32(11):2071–7. Available from: https://doi.org/10.21577/0103-5053.20210098

† Os autores contribuiram igualmente para este trabalho.

A pandemia de coronavírus causou danos em muitos países e sistemas de saúde públicos e privados. Alguns pacientes infectados com coronavírus-2 da síndrome respiratória aguda severa (SARS-CoV-2) não apresentam sintomas, mas provavelmente são capazes de transmiti-lo. Nos primeiros meses críticos da pandemia de coronavírus, diagnosticar e isolar corretamente os pacientes infectados foi uma etapa importante na prevenção de novas infecções (Falahi & Kenarkoohi, 2020; Fierabracci et al., 2020; Y. C. Liu et al., 2020; See et al., 2021) A amplificação isotérmica mediada por loop (RT-LAMP) se estabeleceu como uma alternativa viável, pois é mais rápida e requer menos infraestrutura, permitindo sua aplicação em cenários de poucos recursos e no *point-of-care*.

Apresentamos aqui um teste colorimétrico RT-LAMP capaz de detectar o SARS-CoV-2 a partir do ácido ribonucleico (RNA) em amostras de saliva para rastrear indivíduos sintomáticos e assintomáticos. Obtivemos dados sobre os sintomas relacionados ao COVID-19 por meio de um questionário e estabelecemos uma correlação entre o surgimento dos sintomas e a positividade, o que demonstra a eficácia do teste para separar casos positivos de casos negativos, independente dos sintomas.

Embora os swabs nasofaríngeos tenham sido propostos inicialmente como a forma de coletar as amostras biológicas para detectar o SARS-CoV-2, é um método invasivo que pode apresentar algum risco para os profissionais de saúde e pode ser desconfortável para os pacientes, especialmente crianças. Portanto, este trabalho propõe usar amostras de saliva para realizar a RT-LAMP, já que é um coleta menos invasiva. Além disso, alguns estudos demonstraram a confiabilidade da saliva como amostra adequada para detectar o SARS-CoV-2. (Sohn et al., 2020; Teo et al., 2021; Zhu et al., 2020) Amostras de saliva não tratadas não são ideais para trabalhar diretamente com a RT-LAMP colorimétrica, dado o amplo intervalo de pH natural em que a saliva pode ser coletada. Amostras de saliva ácidas fariam com que o indicador de pH mudasse para amarelo na reação, mesmo antes da etapa de amplificação, levando a uma interpretação incorreta dos resultados. (Uribe-Alvarez et al., 2021)

Desenvolvemos um teste colorimétrico RT-LAMP que pode detectar o SARS-CoV-2 no RNA extraído de amostras de saliva em diferentes estágios da infecção (Figura 3), incluindo portadores pré-sintomáticos, com uma especificidade geral de

100%, sensibilidade de 80% e precisão de 99,59%, e um kappa de Cohen de 0,887. Além disso, o método leva menos tempo do que o método de referência (RT-qPCR). Nossos resultados mostram que nosso teste colorimétrico RT-LAMP é adequado para o rastreamento de grandes grupos, pois a grande maioria dos trabalhadores foi corretamente diagnosticada (quando comparado com o RT-qPCR) através de um teste de amplificação simples, rápido e de baixo custo.

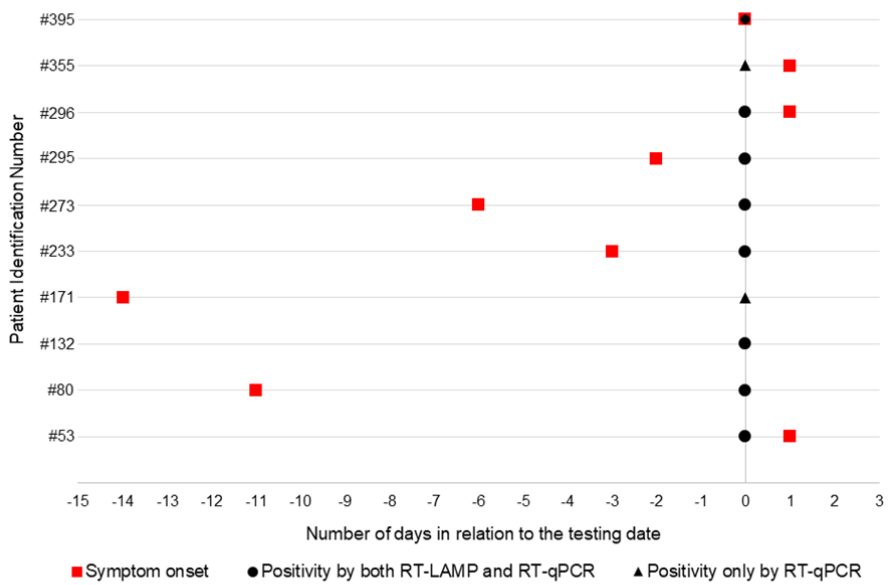

Figure 3: Relação entre o número de dias desde o surgimento dos sintomas e a data do resultado positivo no teste molecular. Cada linha representa a evolução da doença em um paciente. O dia 0 é considerado a data do teste. Os números negativos representam o número de dias antes do teste, enquanto os números positivos representam o número de dias após o teste. A maioria dos pacientes apresentou sintomas antes do teste, enquanto três pacientes (53, 296 e 355) obtiveram um resultado positivo antes do surgimento dos sintomas. O paciente 395 relatou o surgimento dos sintomas no mesmo dia do teste, e o paciente 132 afirmou nunca ter apresentado sintomas.

A possibilidade de diagnosticar corretamente as pessoas infectadas com SARS-CoV-2 transmissível e isolá-las rapidamente é uma vantagem importante que

contribui para prevenir a propagação do vírus, já que o contato com outras pessoas é fortemente reduzido. Devido ao seu baixo custo e simplicidade em comparação com a RT-qPCR, a RT-LAMP poderia ser utilizada em países que não dispõem dos recursos necessários para realizar a RT-qPCR em larga escala, permitindo aumentar a capacidade de teste sem necessariamente aumentar os custos.

Estudo da Aplicação da RT-LAMP Colorimétrica em uma Plataforma de Papel para Detecção em Tempo Real

Considerando as vantagens trazidas pela nossa metodologia LAMP, foram iniciados estudos preliminares para realizar o teste em uma plataforma de papel. O uso dessa metodologia em uma plataforma microfluídica pode oferecer benefícios, como controle em tempo real sem a necessidade de equipamentos sofisticados. O objetivo é implementar o teste RT-LAMP em um sistema baseado em papel, controlando a amplificação com o auxílio de um microscópio digital portátil (USB) que pode ser conectado a um computador ou smartphone. O primeiro passo foi determinar uma plataforma de suporte (para facilitar o transporte e a manipulação) para o papel para a RT-LAMP, focando em materiais simples, descartáveis e de baixo custo adequados para ambientes com poucos recursos.

O primeiro suporte avaliado foi um sistema baseado em poliéster-toner, construído conforme proposto por (Duarte et al., 2011). Para produzir esse suporte, ambas as faces de um filme de poliéster foram revestidas com camadas de toner e, em seguida, recortadas seletivamente de acordo com o padrão desejado com o uso

de uma máquina de corte (Silhouette Cameo 4). Esses filmes intermediários de poliéster-toner foram então alinhados sobre uma base de poliéster (camada inferior), onde o círculo de papel pré-cortado foi colocado, e sobre uma camada superior de poliéster. A camada superior contém uma abertura circular pequena para permitir o acesso aos reagentes. Uma vez alinhados, os filmes foram laminados, criando um dispositivo pronto para uso.

Apesar da simplicidade do suporte de poliéster -toner, alguns inconvenientes foram identificados. Primeiro, a composição do suporte afetou o pH da solução RT-LAMP, provocando o amarelamento da mistura antes do processo de amplificação. Em segundo lugar, o filme de poliéster usado para a camada superior não era suficientemente transparente para visualizar a mudança de cor na mistura RT-LAMP.

O segundo material de suporte avaliado foi o filme usado para selar as palcas de PCR (fitas adesivas), geralmente feito de polietileno. Neste estudo, o filme de selagem de placas da PCR mostrou-se apropriado como material base para dispositivos microfluídicos devido à sua excelente biocompatibilidade, ampla faixa de temperaturas de trabalho, baixo custo, propriedades auto-adesivas e transmitância óptica na faixa visível. (Y. Fan et al., 2018) Usamos uma máquina cortadora Silhouette Cameo 4 para cortar os filmes de selagem de placas de PCR na configuração desejada. O papel foi simplesmente colocado sobre o filme adesivo sem a camada protetora da fase adesiva, e a camada superior (com reservatórios recortados para permitir o acesso ao papel) foi colocada sobre o papel. As camadas foram finalmente

coladas com uma leve pressão dos dedos, usando suas próprias propriedades adesivas (Figura 4).

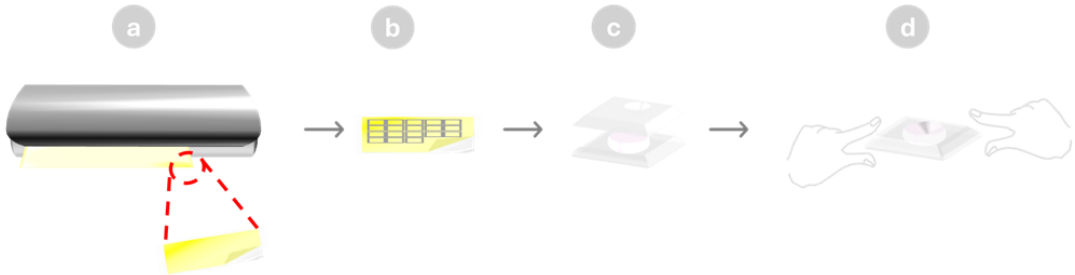

Figure 4: Ilustração esquemática do processo de fabricação do suporte do dispositivo a base de papel usando um filme de selagem para PCR: (a) corte do filme adesivo com um cortador; (b) remoção do filme protetor dos filmes adesivos; (c) alinhamento dos filmes adesivos com o papel; e (d) montagem do dispositivo final aplicando uma leve pressão para unir as camadas. Criado pelo autor.

O formato do papel foi otimizado para minimizar a evaporação da solução ao longo do processo de aquecimento. Otimizamos os pontos de acesso criando extensões a partir da câmara onde fica o papel. Assim, os filmes protetores adesivos estão localizados nas extremidades das extensões, preservando a adesão e reduzindo o risco de evaporação. A Figura 5 apresenta uma série de imagens capturadas a cada 10 minutos durante a reação RT-LAMP em dispositivos com dois formatos de papel diferentes: um com um círculo simples e outro com extensões até a câmara reacional. Essas imagens destacam a eficácia desse dispositivo em reduzir a evaporação no sistema, melhorando a consistência da reação ao longo do tempo e minimizando a possibilidade de contaminação cruzada. Além de reduzir a evaporação, esse *design* do papel melhorou consideravelmente a homogeneidade da cor da reação, um fator crucial para uma quantificação colorimétrica precisa. Obter

uma homogeneidade de cor constante é essencial para leituras colorimétricas em µPADs, pois permite medições mais precisas e melhora o desempenho geral do método analítico. (Morbioli et al., 2017)

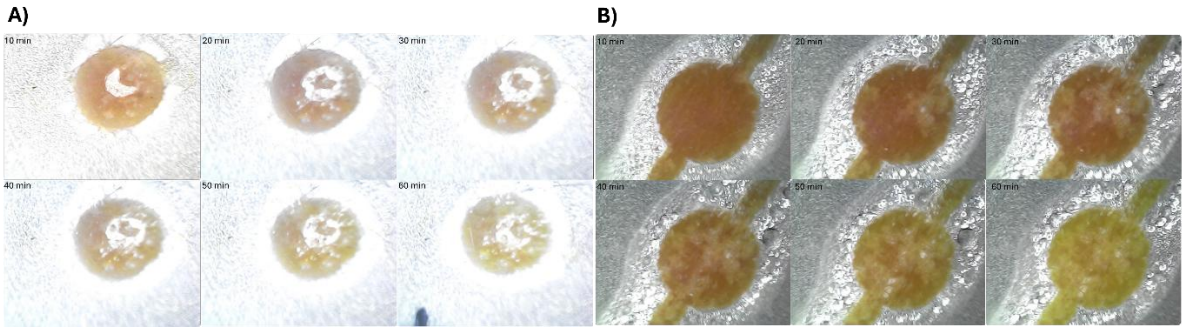

Figure 5: Imagens capturadas em intervalos de 10 minutos durante a reação RT-LAMP usando A) o formato de círculo e B) o desenho do papel com a extensão.

Os próximos passos deste trabalho incluem a determinação das figuras de mérito, a avaliação e comparação do tempo de amplificação com os valores de Ct e a aplicação do método a amostras reais. Os resultados preliminares deste estudo exploratório indicam o potencial de combinar o teste RT-LAMP com dispositivos analíticos microfluídicos baseados em papel (µPADs) para a detecção em tempo real. Projetamos um dispositivo simples usando papel recortado e filmes adesivos como suporte. Este dispositivo é viável e de baixo custo, não requerendo equipamentos sofisticados nem treinamento especializado. Pode ser produzido manualmente, o que o torna adequado para uso em ambientes remotos ou com recursos limitados. Ao otimizar o *design* do papel para reduzir a evaporação e melhorar a homogeneidade da cor, melhoramos a confiabilidade da quantificação colorimétrica.

Nossos resultados sugerem que este método pode ser uma alternativa viável aos sistemas de diagnóstico mais complexos e caros, especialmente para cuidados de saúde no campo. Este estudo apresenta resultados preliminares sendo ainda necessário mais pesquisas para explorar completamente seu potencial. Este trabalho estabelece as bases para o avanço de nosso teste RT-LAMP ao transpor para uma plataforma baseada em papel, fornecendo uma ferramenta econômica, acessível e confiável para monitoramento e gerenciamento de doenças em tempo real.

Focalização Isoelétrica Integrada e Otimizada para Proteínas Utilizando um Dispositivo Microfluídico Baseado em Papel

Geovana M. Mendes, Fanny d'Orlye, Laura Trapiella-Alfonso, Gabriela R.M. Duarte, Anne Varenne.Streamlined integrated protein isoelectric focusing using microfluidic paper-based device. Journal of Chromatography A, Volume 1732, 2024, 465222, ISSN 0021-9673,https://doi.org/10.1016/j.chroma.2024.465222.

O objetivo principal deste estudo foi desenvolver e otimizar um dispositivo de separação e pré-concentração de proteínas baseado na focalização isoelétrica, visando seu acoplamento posterior com a digestão das proteínas em peptídeos e a detecção por espectrometria de massas dos peptídeos gerados. Conforme descrito por Tata Rao et al. em 2020 (Tata Rao et al., 2020), um microdispositivo analítico deve possuir vários atributos além de alto desempenho, como portabilidade, automação, alta taxa de processamento, versatilidade e custo-benefício. Nesse contexto, uma plataforma de focalização isoelétrica (IEF) em papel foi projetada utilizando um

suporte impresso em uma impressora 3D com eletrodos de platina integrados, reservatórios de eletrólitos e um canal de separação em papel. A geometria da plataforma foi otimizada para permitir separações eficientes, robustas e precisas de proteínas. O canal de separação IEF é composto por uma tira de papel (50 mm x 4,5 mm) posicionada na parte inferior da plataforma, enquanto os reservatórios, feitos de esponjas de celulose/algodão (70/30%, m/m), são colocados na parte superior (Figura 6). O canal de papel e os reservatórios estão conectados de forma eficiente no suporte impresso em 3D, garantindo a estabilidade do campo elétrico e a robustez da focalização isoelétrica.

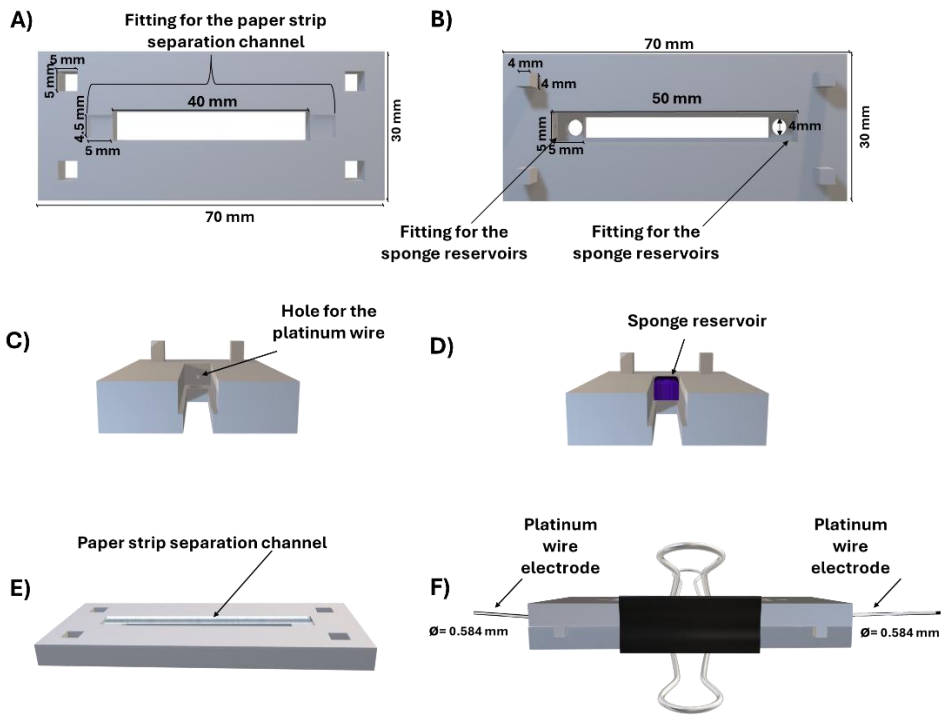

Figura 6: Aqui está a tradução para o português: Ilustração do suporte impresso em 3D: A) Peça inferior; B) Peça superior; C) Corte transversal da peça superior mostrando o orifício para os eletrodos de fio de platina; D) Corte transversal da peça superior mostrando o reservatório para esponja; E) Peça inferior mostrando o encaixe para o canal de separação/tira de papel; F) Suporte montado com um clipe de papel.

Para avaliar a eficiência do microdispositivo IEF em papel, foram definidas etapas experimentais específicas para cada resultado experimental (Figura 7). Primeiramente, a separação IEF foi monitorada pelo desenvolvimento da corrente sob o campo elétrico. Em seguida, o gradiente de pH na tira de papel foi visualizado por meio de pedaços de papel indicador de pH posicionadas em uma outra tira. Por capilaridade, a transferência dos líquidos do papel/canal de separação para a tira de papel indicador permitiu determinar o valor de pH em função da distância, estabelecendo uma relação linear entre o pH e a posição na tira, o que permitiu avaliar a precisão e a eficiência do gradiente de pH.

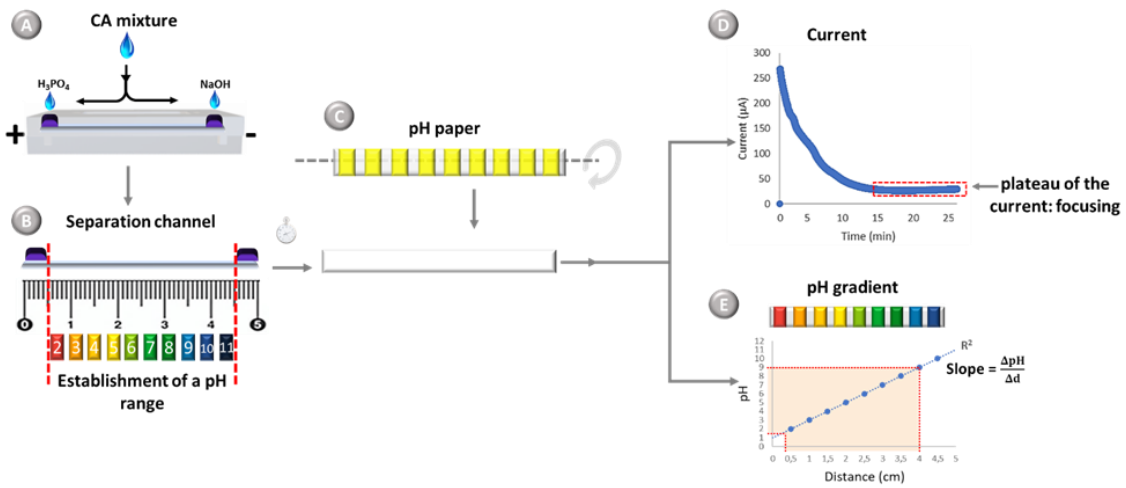

Figure 7: Esquema completo para o processamento de imagem e análise. Criado pelo autor.

Proteínas cromóforas modelo foram separadas, sendo visualizadas através de diferentes cores na tira de papel e, em seguida, para o processamento de dados da fotografia da tira de papel foi usado o software ImageJ para gerar eletroferogramas.

Esses eletroferogramas foram analisados antes e após a interrupção da tensão de separação para observar qualquer dispersão das bandas de proteínas. A determinação do gradiente de pH foi realizada após a fotografia.

O meio de separação consistiu em uma mistura de água/glicerol (85/15, v/v), eliminando o uso de géis que poderiam interferir na espectrometria de massas para a caracterização das proteínas. O glicerol, além de compatível com a análise proteômica integrada em chip, facilita a solubilização de proteínas hidrofóbicas e hidrofílicas. O sistema foi otimizado com uma combinação de três faixas de pH (pH 3-5 a 0,5%, pH 3-10 a 1% e pH 9-11 a 0,5%), resultando em 2% de mistura de anfólitos carreadores no meio de separação. O anólito e o católito foram respectivamente H_3PO_4 (pH 2) e NaOH (pH 13).

Estudos prévios (Gaspar et al., 2016; J. C. Niu et al., 2018; Xie et al., 2018; P. Yu et al., 2020) destacaram os desafios na robustez do sistema analítico para IEF em papel. Para resolver essas questões, uma plataforma microfluídica de focalização isoelétrica em tira de papel foi projetada com suporte impresso em 3D. Essa plataforma adaptável pode acomodar diferentes volumes de reservatórios de eletrólitos e canais fluídicos, sendo potencialmente útil para outras análises. Desenvolvida como um "hub", a plataforma garante um gradiente de pH robusto, uma correlação linear entre o pH e a focalização das proteínas e um tratamento simplificado dos dados.

Enquanto estudos anteriores (S. Yu et al., 2019) utilizaram agentes químicos como a polivinilpirrolidona (PVP) para preparar substratos de papel para IEF, a

plataforma desenvolvida aqui demonstrou a separação eficiente de proteínas sem tratamento prévio do papel. Além disso, este é o primeiro relato do uso de uma mistura de glicerol e água como meio de separação em um dispositivo analítico baseado em papel. Após a otimização dos parâmetros do sistema, uma prova de conceito foi realizada com proteínas modelo em uma matriz de saliva (Figura 8), mostrando baixo impacto da matriz na separação de três proteínas cromóforas e destacando a viabilidade prática da plataforma.

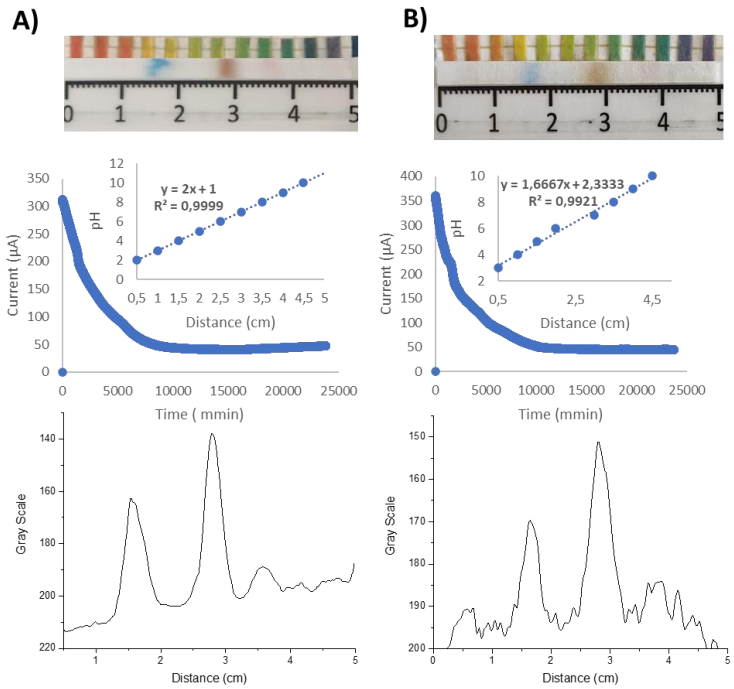

Figure 8: Focalização isoelétrica (IEF) de uma mistura de ficocianina, mioglobina e citocromo C, A) dissolvida no meio IEF e B) adicionada a uma amostra de saliva (2,0 mg/mL). Condições experimentais: tensão aplicada: 200 V; meio de separação: 2% de C.A. (intervalo de pH 3-11) em uma mistura de glicerol/água (85/15, v:v); anólito: H_3PO_4 (pH 2); católito: NaOH (pH 13); tempo de focalização: 25 minutos.

Este estudo avança na integração da análise proteômica em um dispositivo microfluídico baseado em papel. A plataforma IEF proposta oferece uma solução

econômica e versátil para a separação de proteínas, aproveitando a miniaturização e uma abordagem simplificada. Essa abordagem possibilita sua futura integração em uma análise proteômica em três etapas, com digestão das proteínas focalizadas e caracterização dos peptídeos gerados por espectrometria de massas.

Conclusões

Neste trabalho, desenvolvemos sistemas de diagnóstico para biomoléculas aplicadas ou aplicáveis no ponto de cuidado. A amplificação isoterma mediada por loop (RT-LAMP) foi usada para criar um teste simples e e de baixo custo durante a pandemia de COVID-19. Implementamos este teste no ponto de cuidado em um hospital sobrecarregado com o número de pacientes, onde os testes padrão não eram viáveis. Nosso teste trouxe diagnósticos rápidos e precisos. Além disso, propusemos um método de rastreamento não invasivo baseado no RNA extraído da saliva de trabalhadores essenciais durante a pandemia, que se mostrou prático e eficaz para testes frequentes. A transposição preliminar dessa metodologia para uma plataforma de papel mostrou resultados promissores para monitoramento em tempo real de infecções, especialmente do SARS-CoV-2, no ponto de cuidado.

Para a análise de proteínas, a focalização isoelétrica em uma plataforma de papel permitiu a separação precisa e reprodutível de proteínas, incluindo em amostras reais, com resolução e eficiência aceitáveis. Este sistema representa um avanço em um projeto mais amplo que visa integrar todas as etapas proteômicas em um único

chip. Nossos avanços permitiram passar para a fase seguinte, que é a integração da digestão, mantendo uma resolução e eficiência de separação suficientes. Graças à capilaridade, as proteínas separadas podem ser transpostas dentro do mesmo dispositivo baseado em papel para a digestão, antes de serem direcionadas para a detecção por espectrometria de massa (MS).

O desenvolvimento bem-sucedido de métodos de análise de biomoléculas, priorizando custo-benefício, rapidez e simplicidade, destaca o potencial do papel como uma plataforma para esses testes diagnósticos. O papel mostrou-se uma plataforma adequada e acessível para a realização desses testes, ressaltando seu potencial em contextos com recursos limitados.

Bibliografia

Akyazi, T., Basabe-Desmonts, L., & Benito-Lopez, F. (2018). Review on microfluidic paper-based analytical devices towards commercialisation. In Analytica Chimica Acta (Vol. 1001, pp. 1–17). Elsevier B.V. https://doi.org/10.1016/j.aca.2017.11.010

Boobphahom, S., Ly, M. N., Soum, V., Pyun, N., Kwon, O. S., Rodthongkum, N., & Shin, K. (2020). Recent advances in microfluidic paper-based analytical devices toward high-throughput screening. In Molecules (Vol. 25, Issue 13). MDPI AG. https://doi.org/10.3390/molecules25132970

Bullard, J., Dust, K., Funk, D., Strong, J. E., Alexander, D., Garnett, L., Boodman, C., Bello, A., Hedley, A., Schiffman, Z., Doan, K., Bastien, N., Li, Y., van Caeseele, P. G., & Poliquin, G. (2020). Predicting infectious severe acute respiratory syndrome coronavirus 2 from diagnostic samples. Clinical Infectious Diseases, 71(10), 2663–2666. https://doi.org/10.1093/cid/ciaa638

Busnel, J. M., Varenne, A., Descroix, S., Peltre, G., Gohon, Y., & Gareil, P. (2005). Evaluation of capillary isoelectric focusing in glycerol-water media with a view to hydrophobic protein applications. Electrophoresis, 26(17), 3369–3379. https://doi.org/10.1002/elps.200500252

Cassedy, A., Parle-McDermott, A., & O'Kennedy, R. (2021). Virus Detection: A Review of the Current and Emerging Molecular and Immunological Methods. In Frontiers in Molecular Biosciences (Vol. 8). Frontiers Media S.A. https://doi.org/10.3389/fmolb.2021.637559

Chow, F. W. N., Chan, T. T. Y., Tam, A. R., Zhao, S., Yao, W., Fung, J., Cheng, F. K. K., Lo, G. C. S., Chu, S., Aw-Yong, K. L., Tang, J. Y. M., Tsang, C. C., Luk, H. K. H., Wong, A. C. P., Li, K. S. M., Zhu, L., He, Z., Tam, E. W. T., Chung, T. W. H., … Lau, S. K. P. (2020). A rapid, simple, inexpensive, and mobile colorimetric assay covid-19-lamp for mass on-site screening of covid-19. International Journal of Molecular Sciences, 21(15), 1–10. https://doi.org/10.3390/ijms21155380

Dinh, V. P., & Lee, N. Y. (2022). Fabrication of a fully integrated paper microdevice for point-of-care testing of infectious disease using Safranin O dye coupled with loop-mediated isothermal amplification. Biosensors and Bioelectronics, 204. https://doi.org/10.1016/j.bios.2022.114080

Domingo, E. (2020). Introduction to virus origins and their role in biological evolution. In Virus as Populations (pp. 1–33). Elsevier. https://doi.org/10.1016/b978-0-12-816331-3.00001-5

Duarte, G. R. M., Price, C. W., Augustine, B. H., Carrilho, E., & Landers, J. P. (2011). Dynamic solid phase DNA extraction and PCR amplification in polyester-toner based

microchip. Analytical Chemistry, 83(13), 5182–5189. https://doi.org/10.1021/ac200292m

Falahi, S., & Kenarkoohi, A. (2020). Transmission routes for SARS-CoV-2 infection: review of evidence. In New Microbes and New Infections (Vol. 38). Elsevier Ltd. https://doi.org/10.1016/j.nmni.2020.100778

Fan, Y., Liu, S., He, J., Gao, K., & Zhang, Y. (2018). Rapid prototyping of flexible multilayer microfluidic devices using polyester sealing film. Microsystem Technologies, 24(6), 2847–2852. https://doi.org/10.1007/s00542-017-3630-3

Farmerie, L., Rustandi, R. R., Loughney, J. W., & Dawod, M. (2021). Recent advances in isoelectric focusing of proteins and peptides. In Journal of Chromatography A (Vol. 1651). Elsevier B.V. https://doi.org/10.1016/j.chroma.2021.462274

Fierabracci, A., Arena, A., & Rossi, P. (2020). COVID-19: A review on diagnosis, treatment, and prophylaxis. In International Journal of Molecular Sciences (Vol. 21, Issue 14, pp. 1–16). MDPI AG. https://doi.org/10.3390/ijms21145145

Gaspar, C., Sikanen, T., Franssila, S., & Jokinen, V. (2016). Inkjet printed silver electrodes on macroporous paper for a paper-based isoelectric focusing device. Biomicrofluidics, 10(6). https://doi.org/10.1063/1.4973246

Han, T., Jin, Y., Geng, C., Aziz, A. ur R., Zhang, Y., Deng, S., Ren, H., & Liu, B. (2020). Microfluidic Paper-based Analytical Devices in Clinical Applications. In Chromatographia (Vol. 83, Issue 6, pp. 693–701). Springer. https://doi.org/10.1007/s10337-020-03892-1

Hasan, M. R., Mirza, F., Al-Hail, H., Sundararaju, S., Xaba, T., Iqbal, M., Alhussain, H., Yassine, H. M., Perez-Lopez, A., & Tang, P. (2020). Detection of SARS-CoV-2 RNA by direct RT-qPCR on nasopharyngeal specimens without extraction of viral RNA. PLoS ONE, 15(7 July). https://doi.org/10.1371/journal.pone.0236564

Klein, S., Müller, T. G., Khalid, D., Sonntag-Buck, V., Heuser, A. M., Glass, B., Meurer, M., Morales, I., Schillak, A., Freistaedter, A., Ambiel, I., Winter, S. L., Zimmermann, L., Naumoska, T., Bubeck, F., Kirrmaier, D., Ullrich, S., Miranda, I. B., Anders, S., … Chlanda, P. (2020). SARS-CoV-2 RNA extraction using magnetic beads for rapid large-scale testing by RT-qPCR and RT-LAMP. Viruses, 12(8). https://doi.org/10.3390/v12080863

Lecoeur, M., Gareil, P., & Varenne, A. (2010). Separation and quantitation of milk whey proteins of close isoelectric points by on-line capillary isoelectric focusing-Electrospray ionization mass spectrometry in glycerol-water media. Journal of Chromatography A, 1217(46), 7293–7301. https://doi.org/10.1016/j.chroma.2010.09.043

Lenčo, J., Jadeja, S., Naplekov, D. K., Krokhin, O. V., Khalikova, M. A., Chocholouš, P., Urban, J., Broeckhoven, K., Nováková, L., & Švec, F. (2022). Reversed-Phase

Liquid Chromatography of Peptides for Bottom-Up Proteomics: A Tutorial. Journal of Proteome Research, 21(12), 2846–2892. https://doi.org/10.1021/acs.jproteome.2c00407

Lim, H., Jafry, A. T., & Lee, J. (2019). Fabrication, flow control, and applications of microfluidic paper-based analytical devices. In Molecules (Vol. 24, Issue 16). MDPI AG. https://doi.org/10.3390/molecules24162869

Lista, M. J., Matos, P. M., Maguire, T. J. A., Poulton, K., Ortiz-Zapater, E., Page, R., Sertkaya, H., Ortega-Prieto, A. M., Scourfield, E., O'Byrne, A. M., Bouton, C., Dickenson, R. E., Ficarelli, M., Jimenez-Guardeño, J. M., Howard, M., Betancor, G., Galao, R. P., Pickering, S., Signell, A. W., … Martinez-Nunez, R. T. (2021). Resilient SARS-CoV-2 diagnostics workflows including viral heat inactivation. PLoS ONE, 16(9 September). https://doi.org/10.1371/journal.pone.0256813

Liu, S., Li, Z., Yu, B., Wang, S., Shen, Y., & Cong, H. (2020). Recent advances on protein separation and purification methods. Advances in Colloid and Interface Science, 284(102254), 1–23. https://doi.org/10.1016/j.cis.2020.102254

Liu, Y. C., Kuo, R. L., & Shih, S. R. (2020). COVID-19: The first documented coronavirus pandemic in history. In Biomedical Journal (Vol. 43, Issue 4, pp. 328–333). Elsevier B.V. https://doi.org/10.1016/j.bj.2020.04.007

Loan Dao Thi, V., Herbst, K., Boerner, K., Meurer, M., Kremer, L. P., Kirrmaier, D., Freistaedter, A., Papagiannidis, D., Galmozzi, C., Stanifer, M. L., Boulant, S., Klein, S., Chlanda, P., Khalid, D., Barreto Miranda, I., Schnitzler, P., Kräusslich, H.-G., Knop, M., & Anders, S. (2020). A colorimetric RT-LAMP assay and LAMP-sequencing for detecting SARS-CoV-2 RNA in clinical samples. In Sci. Transl. Med (Vol. 12). https://www.science.org

Magleby, R., Westblade, L. F., Trzebucki, A., Simon, M. S., Rajan, M., Park, J., Goyal, P., Safford, M. M., & Satlin, M. J. (2021). Impact of Severe Acute Respiratory Syndrome Coronavirus 2 Viral Load on Risk of Intubation and Mortality among Hospitalized Patients with Coronavirus Disease 2019. Clinical Infectious Diseases, 73(11), E4197–E4205. https://doi.org/10.1093/cid/ciaa851

Maráková, K., Opetová, M., & Tomašovský, R. (2023). Capillary electrophoresis-mass spectrometry for intact protein analysis: Pharmaceutical and biomedical applications (2018–March 2023). In Journal of Separation Science (Vol. 46, Issue 15). John Wiley and Sons Inc. https://doi.org/10.1002/jssc.202300244

Martinez, A. W., Phillips, S. T., Butte, M. J., & Whitesides, G. M. (2007). Patterned Paper as a Platform for Inexpensive, Low-Volume, Portable Bioassays. Angewandte Chemie, 119(8), 1340–1342. https://doi.org/10.1002/ange.200603817

Maurer, M. H. (2011). Proteomic definitions of mesenchymal stem cells. In Stem Cells International. https://doi.org/10.4061/2011/704256

Miller, R. M., & Smith, L. M. (2022). Overview and considerations in bottom-up proteomics. In Analyst (Vol. 148, Issue 3, pp. 475–486). Royal Society of Chemistry. https://doi.org/10.1039/d2an01246d

Mokaddem, M., Gareil, P., & Varenne, A. (2009). Online CIEF-ESI-MS in glycerol-water media with a view to hydrophobic protein applications. Electrophoresis, 30(23), 4040–4048. https://doi.org/10.1002/elps.200900091

Moradian, A., Kalli, A., Sweredoski, M. J., & Hess, S. (2014). The top-down, middle-down, and bottom-up mass spectrometry approaches for characterization of histone variants and their post-translational modifications. In Proteomics (Vol. 14, Issues 4–5, pp. 489–497). Wiley-VCH Verlag. https://doi.org/10.1002/pmic.201300256

Nawattanapaiboon, K., Pasomsub, E., Prombun, P., Wongbunmak, A., Jenjitwanich, A., Mahasupachai, P., Vetcho, P., Chayrach, C., Manatjaroenlap, N., Samphaongern, C., Watthanachockchai, T., Leedorkmai, P., Manopwisedjaroen, S., Akkarawongsapat, R., Thitithanyanont, A., Phanchana, M., Panbangred, W., Chauvatcharin, S., & Srikhirin, T. (2021). Colorimetric reverse transcription loop-mediated isothermal amplification (RT-LAMP) as a visual diagnostic platform for the detection of the emerging coronavirus SARS-CoV-2. Analyst, 146(2), 471–477. https://doi.org/10.1039/d0an01775b

Nge, P. N., Rogers, C. I., & Woolley, A. T. (2013). Advances in microfluidic materials, functions, integration, and applications. In Chemical Reviews (Vol. 113, Issue 4, pp. 2550–2583). https://doi.org/10.1021/cr300337x

Niu, J. C., Zhou, T., Niu, L. L., Xie, Z. S., Fang, F., Yang, F. Q., & Wu, Z. Y. (2018). Simultaneous pre-concentration and separation on simple paper-based analytical device for protein analysis. Analytical and Bioanalytical Chemistry, 410(6), 1689–1695. https://doi.org/10.1007/s00216-017-0809-5

Notomi, T., Okayama, H., Masubuchi, H., Yonekawa, T., Watanabe, K., Amino, N., & Hase, T. (2000). Loop-mediated isothermal amplification of DNA. In Nucleic Acids Research (Vol. 28, Issue 12).

Patterson, E. I., Prince, T., Anderson, E. R., Casas-Sanchez, A., Smith, S. L., Cansado-Utrilla, C., Solomon, T., Griffiths, M. J., Acosta-Serrano, Á., Turtle, L., & Hughes, G. L. (2020). Methods of Inactivation of SARS-CoV-2 for Downstream Biological Assays. Journal of Infectious Diseases, 222(9), 1462–1467. https://doi.org/10.1093/infdis/jiaa507

Ríos, Á., Zougagh, M., & Avila, M. (2012). Miniaturization through lab-on-a-chip: Utopia or reality for routine laboratories? A review. In Analytica Chimica Acta (Vol. 740, pp. 1–11). https://doi.org/10.1016/j.aca.2012.06.024

See, I., Paul, P., Slayton, R. B., Steele, M. K., Stuckey, M. J., Duca, L., Srinivasan, A., Stone, N., Jernigan, J. A., & Reddy, S. C. (2021). Modeling Effectiveness of Testing Strategies to Prevent Coronavirus Disease 2019 (COVID-19) in Nursing Homes - United States, 2020. Clinical Infectious Diseases, 73(3), E792–E798. https://doi.org/10.1093/cid/ciab110

Sohn, Y., Jeong, S. J., Chung, W. S., Hyun, J. H., Baek, Y. J., Cho, Y., Kim, J. H., Ahn, J. Y., Choi, J. Y., & Yeom, J. S. (2020). Assessing viral shedding and infectivity of asymptomatic or mildly symptomatic patients with COVID-19 in a later phase. Journal of Clinical Medicine, 9(9), 1–9. https://doi.org/10.3390/jcm9092924

Tata Rao, L., Rewatkar, P., Dubey, S. K., Javed, A., & Goel, S. (2020). Performance optimization of microfluidic paper fuel-cell with varying cellulose fiber papers as absorbent pad. International Journal of Energy Research, 44(5), 3893–3904. https://doi.org/10.1002/er.5188

Teo, A. K. J., Choudhury, Y., Tan, I. B., Cher, C. Y., Chew, S. H., Wan, Z. Y., Cheng, L. T. E., Oon, L. L. E., Tan, M. H., Chan, K. S., & Hsu, L. Y. (2021). Saliva is more sensitive than nasopharyngeal or nasal swabs for diagnosis of asymptomatic and mild COVID-19 infection. Scientific Reports, 11(1). https://doi.org/10.1038/s41598-021-82787-z

Terry, S. C., Jerman, J. H., & Angell, J. B. (1979). A Gas Chromatographic Air Analyzer Fabricated on a Silicon Wafer. IEEE Trans. Electron Dev., 26(12), 1880–1886.

Tom, M. R., & Mina, M. J. (2020). To Interpret the SARS-CoV-2 Test, Consider the Cycle Threshold Value. In Clinical Infectious Diseases (Vol. 71, Issue 16, pp. 2252–2254). Oxford University Press. https://doi.org/10.1093/cid/ciaa619

Tomita, N., Mori, Y., Kanda, H., & Notomi, T. (2008). Loop-mediated isothermal amplification (LAMP) of gene sequences and simple visual detection of products. Nature Protocols, 3(5), 877–882. https://doi.org/10.1038/nprot.2008.57

Trinh, K. T. L., Chae, W. R., & Lee, N. Y. (2022). Recent advances in the fabrication strategies of paper-based microfluidic devices for rapid detection of bacteria and viruses. In Microchemical Journal (Vol. 180). Elsevier Inc. https://doi.org/10.1016/j.microc.2022.107548

Uribe-Alvarez, C., Lam, Q., Baldwin, D. A., & Chernoff, J. (2021). Low saliva pH can yield false positives results in simple RT-LAMP-based SARS-CoV-2 diagnostic tests. PLoS ONE, 16(5 May). https://doi.org/10.1371/journal.pone.0250202

Xie, S. F., Gao, H., Niu, L. L., Xie, Z. S., Fang, F., Wu, Z. Y., & Yang, F. Q. (2018). Carrier ampholyte-free isoelectric focusing on a paper-based analytical device for the

fractionation of proteins. Journal of Separation Science, 41(9), 2085–2091. https://doi.org/10.1002/jssc.201701438

Yu, S., Yan, C., Hu, X., He, B., Jiang, Y., & He, Q. (2019). Isoelectric focusing on microfluidic paper-based chips. Analytical and Bioanalytical Chemistry, 411(21), 5415–5422. https://doi.org/10.1007/s00216-019-02008-5

Zhu, J., Guo, J., Xu, Y., & Chen, X. (2020). Viral dynamics of SARS-CoV-2 in saliva from infected patients. In Journal of Infection (Vol. 81, Issue 3, pp. e48–e50). W.B. Saunders Ltd. https://doi.org/10.1016/j.jinf.2020.06.059

SUMMARY

List of Figures

Abbreviations

μPADs: ..... Microfluidic paper-based analytical devices

μTAS: ..... Micro total analysis system

2D:..... Two-dimensional

2D PAGE:..... Two-dimensional polyacrylamide gel electrophoresis

3D:..... Three-dimensional

BIP: ..... Backward inner primer

CA: .....Carrier ampholytes

CA II: ..... Carbonic anhydrase II

cDNA:..... Complementary DNA

CI:..... Confidence Interval

CIEF:..... Capillary Isoelectric Focusing

CPE:..... Cytopathic effects

Cq:..... Quantification cycle

CytC: ..... Cytochrome C

DNA:..... Deoxyribonucleic acid

dNTPs: ..... Triphosphate deoxyribonucleotides

EKS:..... Electrokinetic stacking

ELISA:..... Enzyme-linked immunosorbent assay

EOF:..... Electroosmotic flow

ESI: ..... Electrospray ionization

ESI-MS:.....Electrospray ionization mass spectrometry

FIP:.....Forward inner primer

FTICR:.....Fourier transform ion cyclotron resonance

ICP: ..... Ion concentration polarization

IEF:.....Isoelectric focusing

IgG: ..... Immunoglobulin G

IgM: .....Immunoglobulin M

IPG:.....Immobilized pH gradient

ITP:..... Isotachophoresis

LAMP: .....Loop-mediated isothermal amplification

LFA:..... Lateral flow assay

LOC:..... Lab-on-chip

LOD:.....Limit of detection

LOQ:.....Limit of quantification

MERS:.....Middle East Respiratory Syndrome

MERS-CoV:..... MERS coronavirus

Mr: .....Relative molar mass

MS:..... Mass spectrometry

Myo: .....Myoglobin

NMR: .....Nuclear magnetic resonance

NPIs: .....Non-pharmaceutical intervention

NTC:..... No template control

NAAT:..... Nucleic Acid Amplification Testing

OTS:..... Octadecyltrichlorosilane

PCR: Polymerase chain reaction

PDMS: Polydimethylsiloxane

PeT: Polyester-toner

pI: Isoelectric point

PLA: Polylactic acid

PMMA: Poly(methylmethacrylate)

POCT: Point-of-care testing

PTMs: Post-translational modifications

PVP: Polyvinylpyrrolidone

qPCR: Quantitative PCR

RNA: Ribonucleic acid

Rnase: Ribonuclease

RT-LAMP: Reverse transcription LAMP

RT-PCR: Reverse transcription polymerase chain reaction

RT-qPCR: Reverse Transcription quantitative Polymerase Chain Reaction

SARS-CoV: Severe acute respiratory syndrome coronavirus

SDS: Sodium dodecyl sulfate

TAS: Total analysis system

TI: Trypsin inhibitor

TRIS: Trihydroxymethylaminomethane

UV: Ultraviolet

WCID: Whole Column Imaging Detection

WHO: World Health Organization

α-Tryp: ..... α-chymotrypsinogen

βCoV: ..... Beta coronavirus

β-Lac: ..... β-lactoglobulin

1. General Introduction

For the past three decades, microfluidic analytical devices have been considered a promising alternative to traditional methods for achieving rapid point-of-care testing. (Ríos et al., 2012) Initially developed using silicon-based materials and plastics, these devices incorporated paper as an alternative material. (Terry et al., 1979) Using hydrophilic paper confined with a hydrophobic wax barrier for chemical analysis was introduced in 1937. Yagoda conducted spot tests using a paraffin wax barrier embedded in the fibers of the filter paper to measure the metal content of pure nickel and copper salts with an accuracy of 1 to 3 percent. (Yagoda, 1937) However, paper-based analytical devices became widely recognized after a significant publication by the Whitesides group in 2007. (Martinez et al., 2007) The scientific community agrees that microfluidic paper-based analytical devices (μPADs) are excellent alternatives to plastic-based microfluidics due to their beneficial features. Their porous structures and chemical inertness facilitate effective immobilization and storage of reagents, while their lightweight and flexibility make transportation easier. Capillary action removes the need for external pumps to move liquids, a significant advantage of these devices. These properties help μPADs meet the ASSURED criteria (affordable, sensitive, specific, user-friendly, rapid and robust, equipment-free, and deliverable), making them ideal for low-resource settings to diagnose transmissible diseases. (Trinh et al., 2022)

In this context, proteins and viral RNA (ribonucleic acid) play key roles in medical diagnostics and infectious disease management. Proteins are crucial to understanding the molecular mechanisms of health and disease, with their intricate structures and essential functions within cells. Conversely, viral RNA, particularly from highly infectious viruses, is central to detecting and tracking emerging infectious diseases.

The risk of infectious diseases has increased in recent years due to the emergence of antibiotic-resistant bacteria and the spread of highly contagious viruses. Although advances in medical science and technology have improved the accuracy and efficiency of clinical treatments, these technologies' high cost and complexity limit their accessibility in less developed regions. (T. Han et al., 2020)

Each new infectious disease outbreak highlights the need for scalable testing that can be performed outside centralized laboratory settings at the point-of-care (POC) to prevent, track, and monitor endemic and pandemic threats. Current pathogen detection methods, including polymerase chain reaction (PCR), , enzyme-linked immunosorbent assay (ELISA), and cell culture, are time-consuming and require trained personnel, hindering rapid response to emerging pathogens. Therefore, there is a critical need to develop rapid, accurate, sensitive, portable techniques that are easy for untrained users to use. (Trinh et al., 2022)

Isothermal techniques, such as loop-mediated isothermal amplification (LAMP), have emerged as alternatives to conventional methods. The isothermal mechanism of LAMP allows for more cost-effective nucleic acid detection, providing results within 30-

60 minutes. Additionally, LAMP does not require sophisticated equipment, making it both economical and suitable for use in microfluidic platforms. This combination leverages the advantages of isothermal techniques and microfluidics, keeping efficiency and enhancing accessibility. (Lanciotti et al., 1992; Notomi et al., 2000; Tomita et al., 2008a; Wang et al., 2011)

Simultaneously, protein characterization, which is essential for understanding disease mechanisms and developing diagnostics, typically requires complex procedures. Proteomic analysis is a complex process, requiring many individual steps, and it is often laborious and time-consuming, as outlined in Figure 1. The top-down strategy directly analyzes intact proteins using mass spectrometry (MS). The bottom-up strategy involves first digesting proteins into peptides before separating and detecting them by MS. Middle-down proteomics is a digestion-based approach to the proteins, but the digested peptides are composed of more than 30 amino acids. (Lenčo et al., 2022a; Maráková et al., 2023; Miller & Smith, 2022; Moradian et al., 2014)

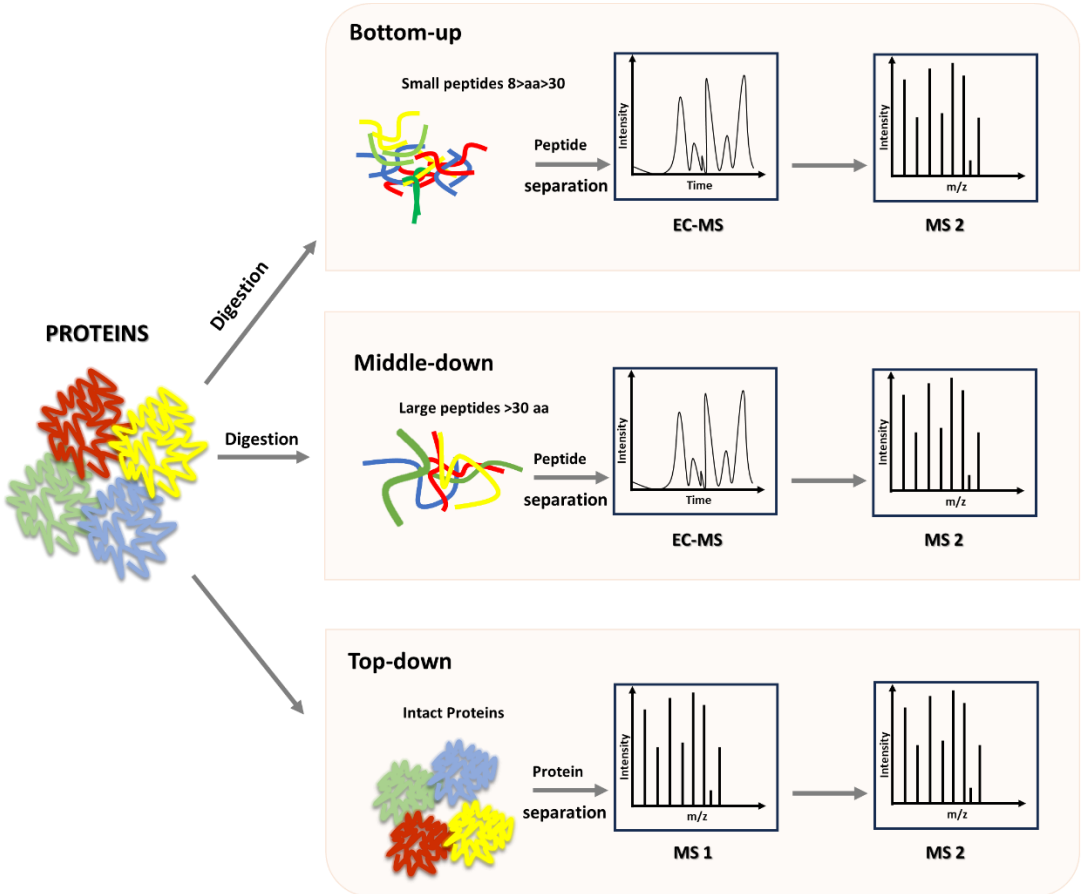

Figure 1: Schematic illustration of bottom-up, middle-down, and top-down strategies. Adapted from (El Kennani et al., 2018).

Technological advancements have led to the development of various methodologies for protein separation, including isoelectric precipitation, organic solvent precipitation, dialysis, ultrafiltration, chromatography, electrophoresis, molecular imprinting, magnetic separation, reverse micelles, and crystallization. (S. Liu et al., 2020) Among electrokinetic separations, isoelectric focusing (IEF) is a powerful method for separating and enriching proteins and peptides by establishing a pH gradient with a carrier ampholyte (CA) mixture, allowing proteins to be separated

under an electric field according to their isoelectric point (pI), and then coupling with detection methods. (Farmerie et al., 2021; Maurer, 2011)

Developing proteomics in a microfluidic format is promising. Microfluidics offers the potential to integrate the different required steps into an automated process, reducing analysis time, preventing manual errors and cross-contamination, lowering analysis costs, and extending applications to low-resource settings. This integration of microfluidic technology with proteomics advances disease diagnostics and enhances the ability to respond to infectious disease outbreaks with greater efficiency and precision.

The development of this PhD started in March 2020 in Goiânia-GO, Brazil, when the World Health Organization (WHO) classified the coronavirus outbreak as a pandemic and implemented social distancing measures worldwide. To date, the Brazilian research group Biomicrofluidics Laboratory has already published several studies on the molecular diagnosis of viruses in disposable microdevices. Given the urgent need for a rapid, simple, and accessible diagnostic test for COVID-19, the research group focused on developing a test that could be used for community testing, in order to contribute to society in managing the pandemic. Therefore, this thesis describes the intensive efforts made during 2020 and 2021 to study, develop, and apply a rapid and inexpensive molecular test for COVID-19. As a result of the tests described in this thesis, over 4,000 individuals were tested, and the technology (more details in chapters II and III) was transferred free of charge to private laboratories. The research team also trained these companies to implement the methodology, enabling

them to provide testing at a significantly reduced cost compared to traditional PCR methods. During the cotutelle exchange period at Chimie ParisTech-PSL in the SEISAD group in 2022 and 2023, a study on isoelectric focusing on paper-based devices was developed and subsequently published in a scientific paper.

Consequently, this manuscript is organized into five chapters: the first chapter presents the state of the art in the context of diagnostics for proteins and RNA ; the second chapter details the work developed for proteins separation in a paper-based microdevice (in article format); chapters three and four describe the studies conducted during the pandemic employing LAMP for efficient detection of COVID-19 (also in article format); and the final chapter discusses preliminary results on the transposition of the developed LAMP method on a paper platform.

Chapter I: State of the art

2. Miniaturized Systems

Over approximately the last three decades, the need for continuous and rapid analyses of samples with reduced volumes and low-concentration has propelled research in diverse domains of analytical chemistry. The total analysis system (TAS) approach emerged to address this need. Ideally, a TAS executes all stages of a comprehensive analysis in an integrated and automated manner. These stages encompass sampling, sample pretreatment, chemical reactions, analytical separations, analyte detection, product isolation, and data analysis. The tenets of TAS have facilitated advancements in online chemical analyses; however, substantial drawbacks persist, such as sluggish sample transport, elevated reagent consumption, unsatisfactory separation efficiencies, and the necessity to engineer interfaces between distinct components. (Ríos et al., 2012)

The inception of microfluidic technology dates back to the early 1950s, when endeavors were made to dispense reduced quantities of liquids, laying the foundation for inkjet technology. In 1979, the silicon-based miniaturized system emerged as a novel microfluidic integrated device, inaugurating a veritable "microfluidics revolution" and the significant evolution of miniaturized analytical systems. (Terry et al., 1979) Manz et al. introduced the micro total analysis system (μTAS) concept, which aimed to fabricate an automated, integrated device within a miniaturized system. (Manz et al., 1990) μTAS has grown exponentially, transforming into a broader research domain that encompasses diverse microfabricated systems. These systems include chemical,

biochemical, and biological processes, collectively known as lab-on-a-chip (LOC).These microfluidic analysis systems aim to automate conventional laboratory processes and execute chemical and biochemical analyses in a scaled-down format. The advantages include speed, cost-efficiency, minimal reagent consumption, and reduced waste generation. Furthermore, research outcomes can be obtained within seconds rather than hours or days. (Manz et al., 1990; Ríos et al., 2012)

Overall, the expected or recently identified behaviors of fluids at the micrometer scale, the continual emergence of novel analytical devices with escalating complexity and capabilities to physically or chemically harness microfluidics in finely controlled manners, and the enticing prospective applications of these devices in chemistry, biology, physics, and material sciences have spurred yet another global "gold rush" among scientists across diverse scientific disciplines. (Reyes et al., 2002; Ríos et al., 2012; Vilkner et al., 2004) LOC benefits from substantial contributions across a spectrum of scientific and engineering disciplines and equally span a remarkably diverse array of analytical chemistry applications, encompassing clinical diagnostics (Kline et al., 2008; Nie & Fung, 2008; Obubuafo et al., 2008; Qin et al., 2009), nucleic acids (Beer et al., 2007; Hashimoto et al., 2006; Neuzil et al., 2006), proteins (Emrich et al., 2007; Lönnberg & Carlsson, 2006) etc.

Firstly, as already mentioned, microfluidic devices used silicon and glass-based substrates. As the field progressed, the exploration of alternative materials intensified. These materials can be categorized into three overarching groups: inorganic, polymeric, and paper. Inorganic materials have expanded beyond traditional glass and silicon substrates to encompass materials like low-temperature cofired ceramics and vitroceramics. Polymeric materials, on the other hand, can be further classified into elastomers and thermoplastics. Notably, paper-based microfluidics has emerged as a

distinctive and innovative technology, presenting a significant departure from devices constructed with either polymeric or inorganic materials. (Nge et al., 2013)

Paper as an analytical substrate dates back to the 1940s and 1950s when it was initially employed for chromatography and electrophoresis. Notably in 2007, Professor George Whitesides' group introduced the paper-based microfluidic analysis device (μPAD) shown in Figure 2, marking a significant moment in the field. (Martinez et al., 2007) The adoption of paper as a substrate gained momentum due to its cost-effectiveness, biocompatibility, ubiquity, and ability to absorb fluids through capillary action without external pump sources (see Figure 3). Moreover, paper can be easily modified, allowing for stacking, folding, cutting, and chemical treatment. (Akyazi et al., 2018)

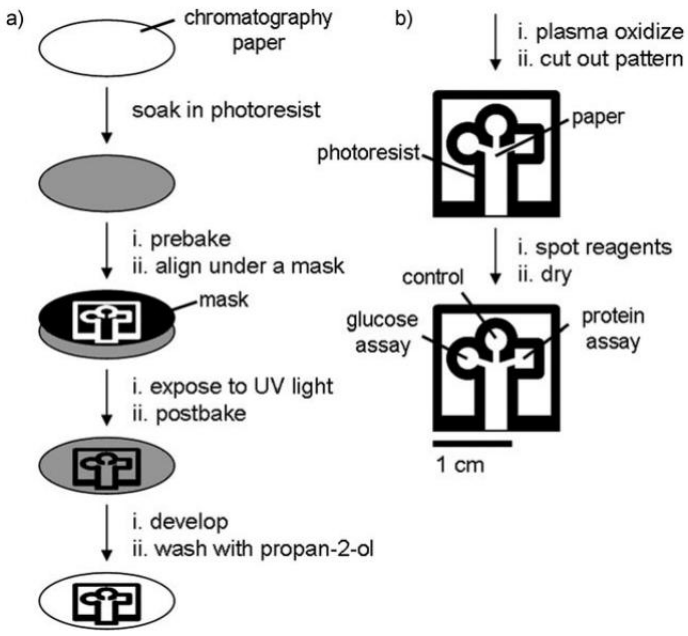

Figure 2: Illustration of the method proposed by Martinez et al. for patterning paper into millimeter-sized channels. (Martinez et al., 2007)

Paper-based devices are a notably promising approach for point-of-care testing (POCT) at low-resource settings not only due to their cost-effectiveness, reliability, and

simplicity but also their efficiency for clinical diagnosis (Fu et al., 2019; Snyder et al., 2020) and potential integration with other techniques, such as isotachophoresis (ITP), (Rosenfeld & Bercovici, 2018; Schaumburg et al., 2020) ion concentration polarization (ICP), (S. Il Han et al., 2019; Perera et al., 2020) and electrokinetic stacking (EKS). (Zhai et al., 2020; Zhang et al., 2019) Lab-on-paper devices have thus attracted significant attention in the literature in recent years. (Lee et al., 2021)

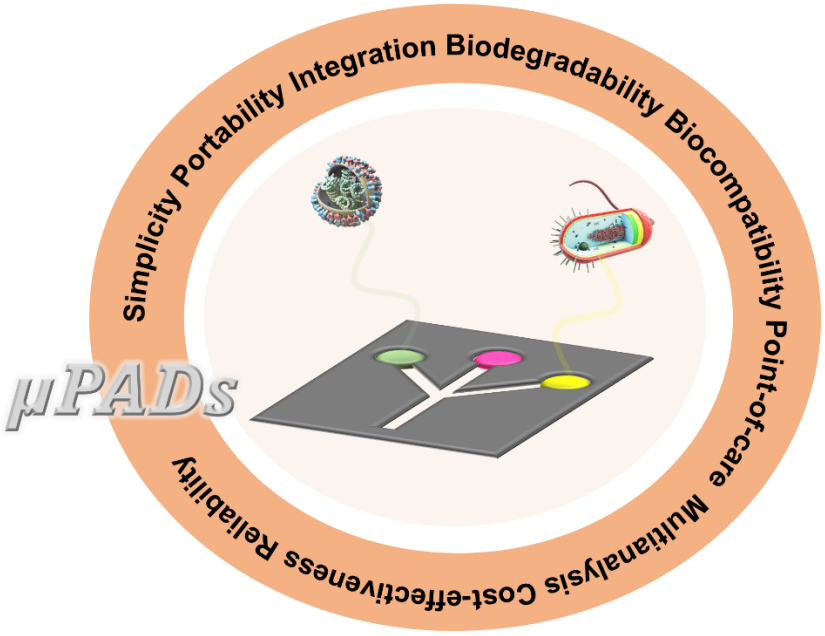

Figure 3: Schematic illustration of a paper-based microdevice designed for hypothetical colorimetric detection of bacteria and viruses. Created by the author.

The literature has recently witnessed significant attention devoted to lab-on-paper devices. These devices are crafted through chemical or physical patterning methods. Chemical methods involve utilizing hydrophobic materials to fill paper pores, forming impermeable barriers and microchannels. Techniques such as wax printing(Dias et al., 2023), inkjet printing (J. H. Yu et al., 2015), laser printing (Ghosh et al., 2019), and various other methods fall under this category. (H. Lim et al., 2019;

M. Yang et al., 2017) On the other hand, physical patterning methods employ cutting or embossing techniques to create defined microchannels and shapes on the paper substrate, encompassing techniques like laser cutting (Mahmud et al., 2016), knife plotting (Fenton et al., 2009), and embossing (Juang et al., 2019). The choice between these methods depends on the device's intended use, considering factors such as compatibility with test samples containing organic solvents. (Boobphahom et al., 2020; H. Lim et al., 2019)

Lab-on-paper platforms exhibit two-dimensional (2D) or three-dimensional (3D) structures (see Figure 4), enabling the analysis of simple plane and lateral flows and complex separation, mixing, multi-stage reactions, and multi-analysis operations. (Lee et al., 2021) Devices with a 2D structure are relatively straightforward to manufacture and offer efficient transference reaction and detection on a single plane. (Guzman et al., 2018; C. C. Liu et al., 2017; Shrivas et al., 2020) In contrast, 3D devices, though more complex, facilitate sample and reagent transfer in both horizontal and vertical directions, enabling more intricate procedures. (Mora et al., 2019; Walgama et al., 2020; P. Yu et al., 2020)

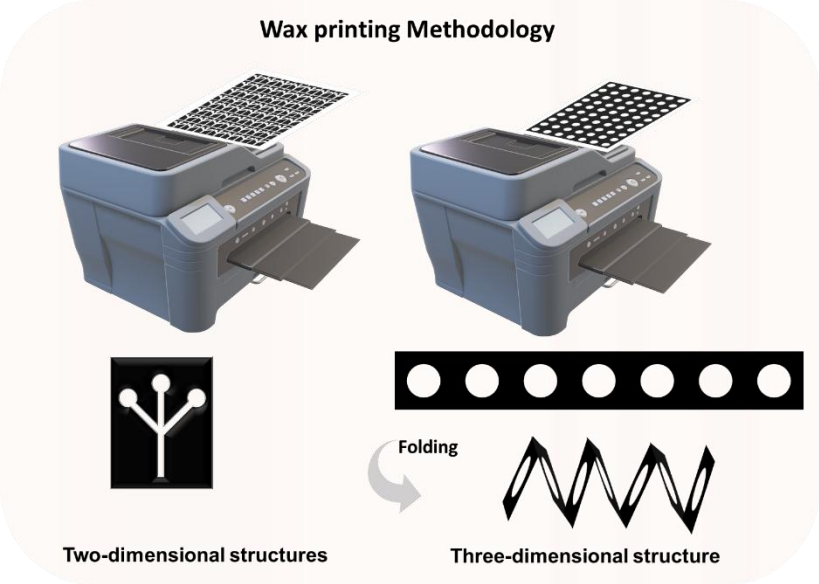

Figure 4: Schematic illustration of a two-dimensional (2D) and three-dimensional (3D) paper-based microfluidic platform. Created by the author.

Lab-on-paper devices with a 3D structure can be single-sheet 3D, stacked 3D, folding-based 3D, or slip-based 3D, depending on the method employed for creating the 3D structure and performing the detection operation. The ultimate goal of these platforms is to provide end users with portable diagnostic tools that are user-friendly, rapid, and cost-effective. Consequently, the seamless integration of the paper platform with the detection system is imperative for the practical feasibility of the device. (Lee et al., 2021)

Various detection systems have been proposed in recent years, ranging from read-by-eye quantification to colorimetric, electrochemical, chemiluminescence, fluorescence, and spectrometry detection. Each technology has merits and drawbacks but provides reliable, simple, miniaturized, easy-to-integrate, cost-effective inspection procedures for diverse detection and analysis applications. (Lee et al., 2021; Luo et al., 2014; J. Niu et al., 2021)

Human biological samples are challenging due to their variety and complex composition, such as enzymes, electrolytes, acids, organic compounds etc, (Fatima

et al., 2020; Tainturierd D. et al., 1984) requiring sample pre-treatment processes. These processes include sample collection and storage, separation, extraction, concentration/amplification and detection. With rapid advances in paper chip modification and manufacturing technologies, lab-on-paper platforms can perform even complex sample pretreatment steps. (Lee et al., 2021)

3. Virology

Viruses are entities that request a host to replicate. They can infect many life forms, from bacteria to plants and animals. Structurally, viruses consist of a nucleic acid genome and a capsid. The capsid is a highly symmetrical structure composed of multiple copies of a limited number of proteins encoded by the viral genome. Viral nucleic acid packaging offers protection and various roles, such as cell entry, genome uncoating, or intracellular trafficking. Some viruses may have an additional layer of protection called an envelope, usually consisting of lipids or glycoproteins. Lipid envelopes are derived from the infected host's cell membrane, while the viral genome encodes glycoprotein envelopes. The viral genome encodes proteins that facilitate virus particle replication and assembly. (Cassedy et al., 2021; Domingo, 2020)

Although viruses share structural features, their genetic diversity makes it challenging to comprehensively understand the viruses in our environment. Despite their prevalence, their genome remains unexplored. Furthermore, there is still a need to fully understand the interactions between viruses and their hosts. (Paez-Espino et al., 2016) Although some viruses can cause harm to their hosts, in other cases, the relationship may be mutually beneficial. Many interactions between viruses and hosts

may go unnoticed because the host remains unaffected, and symptoms are not recognizable. (Cassedy et al., 2021)

Defining a virus's host range and the number of species it can infect can be challenging as it is often unclear. Factors such as climate change, global transport, centralized agriculture, and high densities of crops, animals, and humans can also contribute to viral emergence. The role of viral genomes in expanding viral host ranges and environmental tolerances is significant due to their flexibility and diversity. Some viruses can mutate rapidly, with RNA viruses exhibiting mutation rates up to a million times higher than their hosts and DNA (deoxyribonucleic acid) viruses mutating at slower rates. Detecting current and emergent viral strains requires dynamic methods due to the rapid mutation and transmission of viruses between hosts. (McLeish et al., 2019; Reddy & Saier, 2020; Sanjuán & Domingo-Calap, 2016; L. Zhao et al., 2019)

3.1 Coronaviruses

Coronaviruses (order Nidovirales, family Coronaviridae, and subfamily Coronavirinae) are a diverse group of positive-sense single-stranded RNA viruses with genome sizes ranging from 26 Kb to 32 Kb. These viruses originate from zoonotic sources and often migrate from animals to humans, with several animal species serving as potential intermediate hosts, facilitating cross-species transmission. The Middle East Respiratory Syndrome (MERS) is a zoonotic transmission attributed to the MERS coronavirus (MERS-CoV). This virus circulated between bats and camels before infecting humans, leading to respiratory complications associated with MERS-CoV infection. (Fierabracci et al., 2020; Y. C. Liu et al., 2020)

Human coronavirus infections primarily affect the upper respiratory tract, with about six strains capable of causing mild cold-like respiratory illness. However, certain

strains, such as Severe acute respiratory syndrome coronavirus (SARS-CoV) and MERS-CoV, are notorious for their aggressive nature, targeting the lower respiratory tract and causing severe, often fatal, symptoms. The emergence of the novel coronavirus SARS-CoV-2 has resulted in a spectrum of clinical manifestations ranging from mild respiratory infections similar to the common cold to severe and fatal outcomes. Fatal cases are often attributed to acute lower respiratory tract infections leading to hypoxemia and acute respiratory failure, requiring interventions such as orotracheal intubation and mechanical ventilation to prevent clinical deterioration and mortality. (Hasöksüz et al., 2020; Maier et al., 2015)

SARS-CoV-2, a lineage B beta coronavirus (βCoV), is characterized by its single-stranded RNA genome and four structural proteins: spike (S), envelope (E), membrane (M), and nucleocapsid (N) proteins (see Figure 5). These proteins play a crucial role in the virus's structure and replication, contributing to its pathogenicity and potential for transmission.(Y. C. Liu et al., 2020)

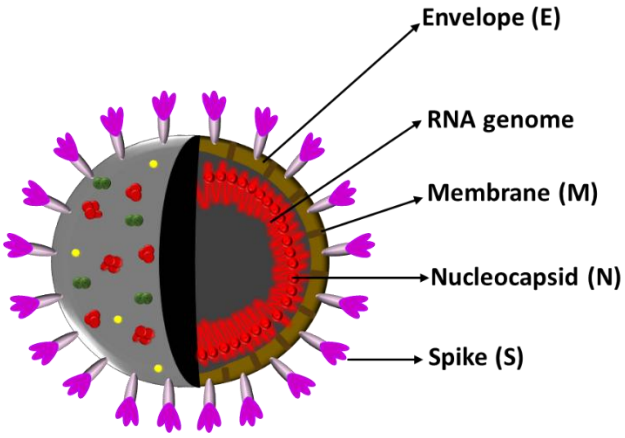

Figure 5: Illustration of the SARS-CoV-2 structure. Image credit: Created by the author.

The onset of the COVID-19 pandemic dates to 31 December 2019, when an outbreak of pneumonia cases of unknown etiology occurred in Wuhan Province, China, leading to heightened concern among public health authorities. Subsequent

isolation, sequencing, and phylogenetic analysis led to the identification of the causative agent as severe acute respiratory syndrome coronavirus 2 (SARS-CoV-2), subsequently named COVID-19. On 30 January 2020, due to its rapid global spread and profound impact, COVID-19 was declared a public health emergency of international concern, reflecting its elevated risk to the worldwide population. Within a short time, the epidemic affected 266 countries across all continents, prompting the World Health Organization to declare COVID-19 a pandemic on 11 March 2020. (Candido et al., 2020; Jiang et al., 2020; Maier et al., 2015)

The transmission of COVID-19 primarily revolves around respiratory routes facilitated by person-to-person interactions. Aerosolized particles, respiratory droplets, and contaminated surfaces serve as vehicles for virus spread, with viable virus particles able to survive on surfaces for prolonged periods, facilitating disease transmission. In addition, the potential for transmission from asymptomatic or pre-symptomatic individuals further complicates disease surveillance and control efforts, underscoring the challenges of containing the spread of SARS-CoV-2. (Rabaan et al., 2021)

3.2 Diagnostic Methods for Virus Identification

Diagnosing viral infections typically involves techniques such as virus isolation, nucleic acid detection, identification of viral antigens, and serology (antibody detection). Nonetheless, additional methods may sometimes be employed. (Cassedy et al., 2021)

Virus isolation involves the propagation of virus particles by introducing them into a suitable host cell line. This method remains central as it cultivates existing and emerging viruses for further investigation and characterization. Although traditional

viral cell culture was considered a slow diagnostic method, modernized methods have significantly reduced the overall time. For decades, virus isolation in cell culture has been the gold standard for virus detection. In recent years, however, significant technological advances, from the development of monoclonal antibodies to the advent of molecular diagnostics, have provided tremendous resources for endeavors to identify viral infections. (Leland & Ginocchio, 2007)

Another approach to diagnosing viruses is evaluating the changes in cell morphology when infected by a virus, which is called cytopathic effects (CPE). Common CPE includes rounding infected cells, merging with neighboring cells to create syncytia (polykaryocytes), and the emergence of nuclear or cytoplasmic inclusion bodies. (Albrecht, 1996)These morphological cell changes can be detected by microscopy. The schematic workflow of a CPE-based diagnostic is outlined in Figure 6. Unfortunately, the development of CPE can take days to weeks, making rapid results difficult. (Fenner et al., 1974) In addition, as a presumptive diagnosis tool, CPE diagnosis poses challenges in the identification of the causative virus, as it only applies to CPE-inducing viruses. (Cassedy et al., 2021)

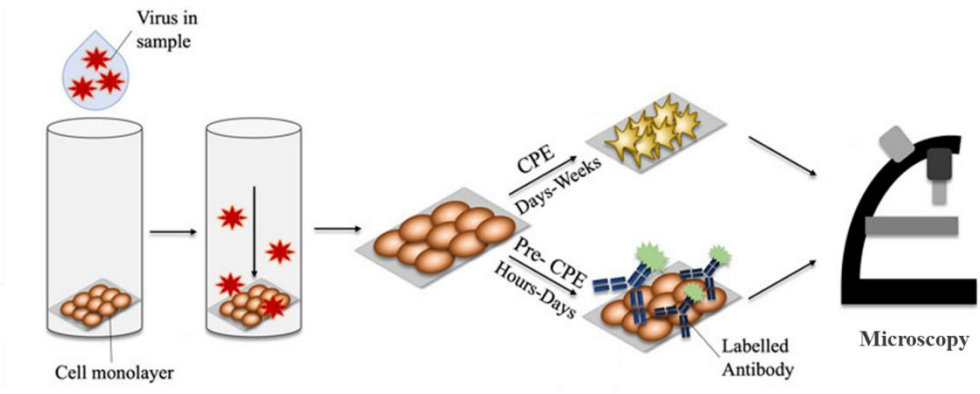

Figure 6: Schematic illustration of the workflow of CPE and Pre-CPE based diagnostic. Adapted from(Cassedy et al., 2021)

Overcoming the limitations of CPE-based diagnosis, the pre-CPE techniques bring faster results because before the cells exhibit CPE, they identify the coverslips from shell vial cultures. Usually, coverslip detection is achieved by staining it with a highly sensitive and specific agent, like an antibody that targets a virus-associated protein (see Figure 6). An enzyme- or fluorescent-labeled antibody is applied to the cell monolayer on the coverslip. The coverslip is subsequently inspected for a positive signal from the labeled antibody, confirming a specific virus's presence. The pre-CPE methods benefit from using virus-specific antibodies, allowing for the accurate confirmation of a specific virus or strain. (Leland & Ginocchio, 2007) Although pre-CPE diagnostics reduce times compared to traditional cell culture, the final result can still take days in some cases. (Cassedy et al., 2021) Because of that, the pre-CPE methods are still inadequate for emergencies, such as a pandemic.

As mentioned, virus culture methods, including sampling, transport to secure laboratories, and growth do not meet the requirements of rapid testing. As a result, there has been a move towards molecular techniques that allow direct sampling from the source, rapid results, and adaptability to emerging viruses. Techniques of virus detection without propagation, known as direct detection, including nucleic acid and immunological detection, have gained interest in the quest for fast diagnostics. as they do not require the virus to multiply. In this case, the virus is detected directly in the suspected sample. These methods traditionally use sophisticated and expensive techniques. (Cassedy et al., 2021)

Another potential diagnostic method is immunoassays, which use antibodies to detect viruses in samples. Polyclonal antibodies, which originate from multiple B cell clones, bind to various structures or epitopes on the target organism or molecule. These antibodies are advantageous for the unbiased detection of all viral strains or for

capturing all strains of a particular virus present in a sample. On the other hand, monoclonal antibodies (derived from a single B cell clone) and some recombinant antibodies are specific to a single epitope. Specific antibodies are highly valued in diagnostics because they enable targeted detection of distinct regions on the target molecule. In virus diagnostics, this specificity helps distinguish between different isolates or genotypes of a single virus or similar viral species within a genus. (Cassedy et al., 2021)

Isolating specific antibodies can be challenging, particularly for similar targets. To address the challenge, antibodies can be selected based on their ability to recognize short peptide sequences corresponding to distinct regions on the target protein. This approach enables the detection of specific regions unique to particular strains. (Mario Geysen et al., 1985). However, selecting the appropriate target peptide requires consideration of potential conformational changes, and a key step in this process is validating the peptide's binding capability to the native epitope. (Conroy et al., 2009; O'Kennedy et al., 2017)

Therefore, DNA amplification methods have proven to be a viable alternative in developing diagnostic tests for infectious diseases caused by viruses, offering several advantages such as reliability, fast results, and cost-effectiveness.

3.2.1 Nucleic Acid-Based Detection Methods

Nucleic acid amplification is an enzymatic process that induces a significant multiplication, varying from thousands to millions, of copies of the targeted DNA of interest. The first method for nucleic acid amplification, the Polymerase Chain Reaction (PCR), was pioneered in the 1980s by the biochemist Kary Mullis and stands

as the predominant form of amplification in research and clinical analysis laboratories. (Ali et al., 2018; Mullis, 1990)

3.2.1.1 Polymerase Chain Reaction- PCR

The Polymerase Chain Reaction (PCR) is an enzymatic technique for in vitro nucleic acid amplification, relying on thermal cycles. A pair of primers specifically designed to hybridize with the target DNA is employed for PCR amplification. The process involves the DNA polymerase *taq* polymerase (derived from *Thermus aquaticus bacterium*) and triphosphate deoxyribonucleotides (dNTPs) and occurs in a partially buffered environment. Amplification occurs through specific thermal variations over a period promoted by thermocycling equipment. Each thermal cycle includes denaturation of the target DNA, hybridization of oligonucleotides (primers), and extension of the complementary strand. After one cycle, the initial amount of DNA is doubled. Typically, 35 to 45 cycles are required to produce detectable quantities of amplicons. (Mullis, 1990; Rahman et al., 2013)

Quantitative PCR or real-time PCR (qPCR), introduced in 2003, differentiates itself from conventional PCR by constantly monitoring and quantifying the amplification process. Many strategies are applied to perform qPCR, such as adding low concentrations of DNA intercalating reagents or using labeled probes to monitor the reaction by promoting fluorescence upon amplification (see Figure 7). An essential parameter in qPCR is the quantification cycle (Cq), which represents the thermal cycle where the fluorescence signal statistically differs from the non-target reaction (baseline), marking the exponential phase threshold. Consequently, a lower Cq value correlates with a higher target concentration within the sample. Quantification, in terms

of copy numbers and target concentration, relies on known target amounts in reactions emitting fluorescence. (Cassedy et al., 2021; Marin et al., 2017)

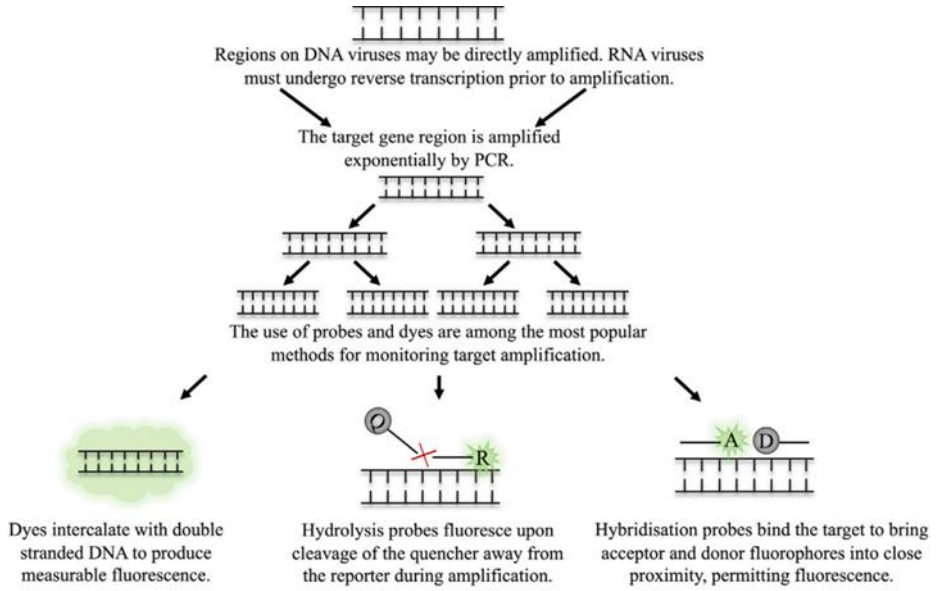

Figure 7: Schematic illustration of the polymerase chain reaction (PCR) mechanism and its real-time monitoring techniques. (Cassedy et al., 2021)

While PCR-based molecular diagnosis ensures high specificity, sensitivity, and reliability, it demands significant time, cost, skilled professionals, and laboratory infrastructure. Consequently, there is a pursuit of alternative methodologies to simplify molecular diagnosis instruments, with Loop-Mediated Isothermal Amplification (LAMP) based on Nucleic Acid Amplification Testing (NAAT) emerging as a remarkable solution (Notomi et al., 2015)

3.2.1.2 Loop-Mediated Isothermal Amplification- LAMP

Loop-Mediated Isothermal Amplification (LAMP) was developed in 2000 by Notomi and collaborators. Currently, it is a primary isothermal technique for nucleic acid amplification, particularly in molecular diagnostic methodologies for pathogen detection. In recent years, there has been an exponential increase in publications

related to LAMP, reaching a high record during the COVID-19 pandemic. (Lanciotti et al., 1992; Notomi et al., 2000; Tomita et al., 2008a; Wang et al., 2011)

Nucleic acid amplification in LAMP utilizes *Bacillus stearothermophilus* (Bst) DNA polymerase and three pairs of primers (FIP, BIP, F3, B3, LBP, and LFP) designed to recognize six distinct regions of a target gene. Bst DNA Polymerase, derived from *Bacillus stearothermophilus*, has 5' → 3' polymerase activity without 5' → 3' (Figure 8) exonuclease activity. LAMP unfolds in two stages: the non-cyclic stage and the cyclic stage.

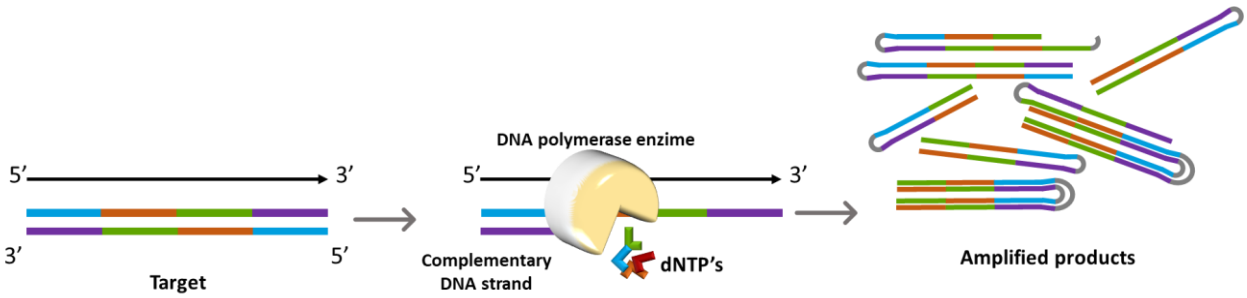

Figure 8: Bst DNA Polymerase 5' → 3' polymerase activity. Created by the author.

The amplification process (see Figure 9a) begins with the approximation and hybridization of the F2 part of the FIP primer to the 3' end of the target DNA. The FIP (forward inner primer) primer comprises F2 and F1c, with F2 complementary to the target DNA and F1c to the synthesized F1. After this, the enzyme Bst DNA Polymerase is directed to synthesize the complementary strand. After the enzyme extends the strand, the external primer F3 recognizes and hybridizes to its complementary region at the 3' end, displacing the previously synthesized single strand. Due to the complementarity of the F1 and F1c regions at the end of the same synthesized strand, a loop is generated. Then, at the opposite end to the generated loop (5' end), the B2 part of the internal primer BIP (backward inner primer) approaches the previously synthesized strand, already containing a loop at the 3' end, hybridizes and directs the

enzyme to the extension. Subsequently, hybridization of the external primer B3 occurs, extension of the strand by the enzyme, and displacement of the previously synthesized strand. Due to the proximity and complementarity of the B1 and B1c regions in the strand, a loop is generated. (Notomi et al., 2000; Tomita et al., 2008a)

The final structure of the acyclic step is a single strand of DNA with loops at the ends. The product of the acyclic step, the single strand with loops at the ends, serves as the starting material for the cyclic amplification step. (Notomi et al., 2000; Tomita et al., 2008a)

In the cyclic stage(see Figure 9b), the internal primer FIP initially hybridizes to the loop at the 3' end , directing the enzyme to the extension of the stem-loop structure. The loop present in the starting structure of the cyclic step promotes self-activation (self-primed), directing the enzyme for synthesis. At this stage, the displacement of the synthesized strand does not occur through the action of the external primer F3 but through the loops generated at the ends of the strand. (Notomi et al., 2000) After self-activation of the synthesis promoted by the loop, the strand previously synthesized by the FIP initiator is released. The released single strand is an inverted repeat of the starting structure, with loops at each end. In the single-stranded structure with loops at the ends, the BIP initiator recognizes its complementary region located in the loop and, also through the self-primed action, extension occurs to a stem-loop structure through the action of the enzyme (Bst DNA Polymerase), which ultimately generates the single-stranded structure again with loops at the ends, in a cyclic process. (Notomi et al., 2000; Tomita et al., 2008a) The action of internal primers to the stem structures -loop, generates multiple structures of different molecular sizes as shown in Figure 9c. At this stage, exponential amplification of loop-shaped structures occurs through the action of internal primers, promoting the production of approximately 109 copies of the

target gene in less than an hour. In the cyclic step, the loop primers, LF and LB, are also used, which are optional in the reaction and hybridize only in loops where the internal primers, FIP and BIP, are absent. The use of 2 loop primers promotes the acceleration of the amplification reaction, as they cause an increase in the number of reactive regions in which the internal primers can act, reducing the reaction time from 1/3 to 1/2 of the time required. LAMP has been used extensively in diverse methodologies for molecular diagnosis. (Notomi et al., 2000; Tomita et al., 2008a)

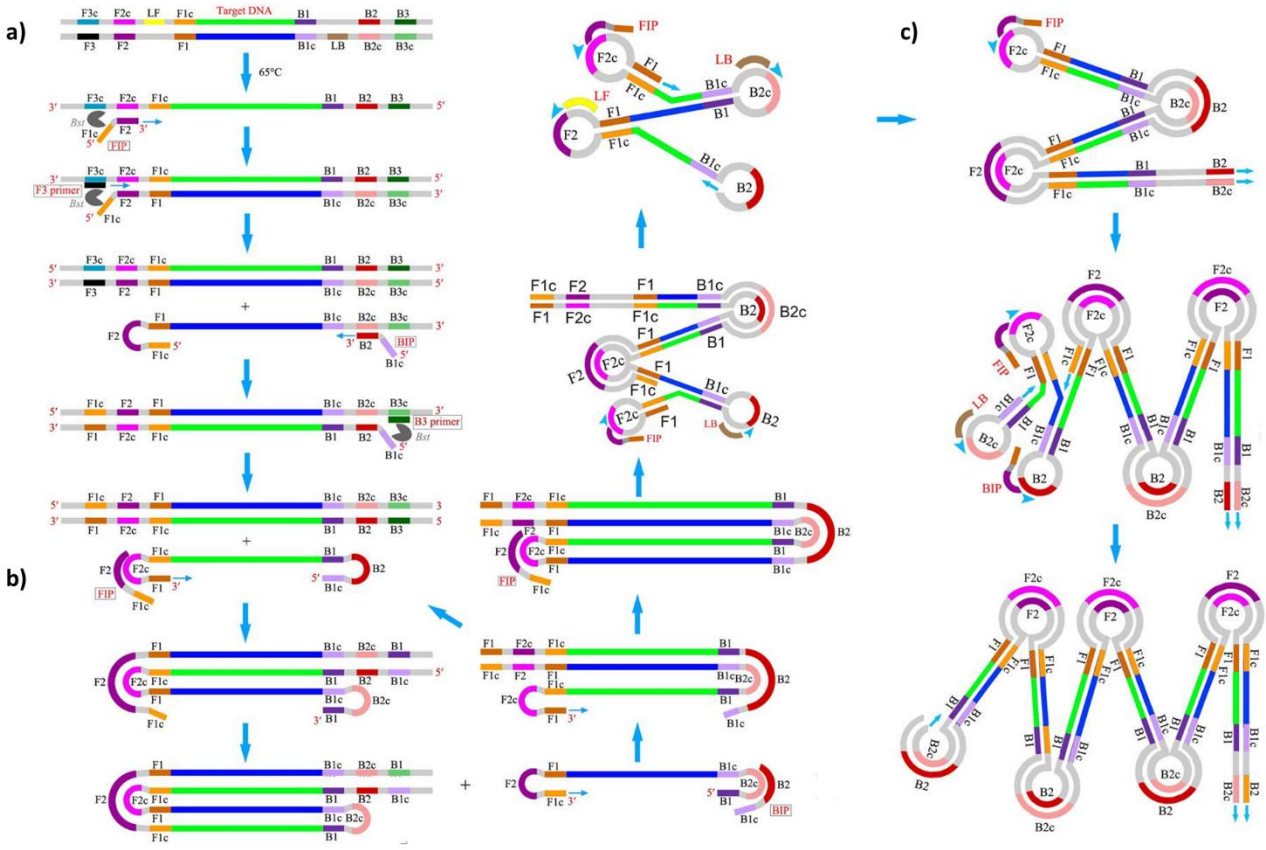

Figure 9: Loop-mediated isothermal amplification (LAMP) mechanism. (Li et al., 2016)

LAMP, by promoting alternately inverted repetition of the target sequence through cyclic and non-cyclic steps, results in amplified DNA fragments of varying sizes, producing a distinctive pattern on agarose gel compared to PCR, which yields a single amplicon size. (Notomi et al., 2000) Moreover, LAMP exhibits robust performance in the presence of inhibitors found in complex samples, allowing direct

application to diverse sample types, such as serum (Mora-Cárdenas & Marcello, 2017), whole blood (Mansuy et al., 2018), urine (Calvert et al., 2017), oral fluid (Singh et al., 2013), and semen (Musso et al., 2015). These advantages, coupled with high sensitivity, specificity, and visual detection through turbidity, (Mori et al., 2001; Wastling et al., 2010) lateral flow, (Chowdry et al., 2014; Nurul Najian et al., 2016), fluorescence, (Iwamoto et al., 2003; Le et al., 2012; Tomita et al., 2008a), and metal indicator (Goto et al., 2009), and pH indicator (Li et al., 2023) contribute to the utility of LAMP in molecular diagnosis.

Visual detection is among the most used methods for identifying LAMP amplicons. End-point colorimetric detection usually involves detecting reaction byproducts (directly or indirectly), such as protons or pyrophosphates, using pH-sensitive dyes or metal ion indicators, respectively, or detecting amplicons with intercalating dyes. (G. Choi et al., 2023)

During DNA synthesis, the Bst DNA polymerase enzyme incorporates each nucleotide (dNTP) into the DNA strand, releasing a proton and lowering the pH of the LAMP mixture from about 8.5 to 6.0–6.5. This pH change is easily detectable with widely available pH-sensitive dyes. The most commonly used dye in LAMP reactions, phenol red, changes from pink to yellow as the pH falls below 6.8 during amplification. The significant advantage of pH-based LAMP detection is the clear color change, which allows results to be observed with the naked eye, eliminating the need for specialized equipment beyond possibly a simple camera/smartphone for documentation.(Tanner et al., 2015)

Studies have shown that phenol red exhibits the most apparent color change among various tested pH dyes, making it particularly easy to interpret visually. These

pH-sensitive dyes do not interfere with the amplification process, allowing for a one-pot, closed-tube reaction. This is crucial as it minimizes the risk of cross-contamination often observed when tubes are opened for post-incubation analysis. The pH-based colorimetric approach requires minimal or no specialized equipment, making them well-suited for point-of-care applications. (Scott et al., 2020; Tanner et al., 2015; Tomita et al., 2008b)

However, if the target nucleic acid in the study is RNA rather than DNA, as it is for SARS-CoV-2, the original LAMP protocol needs to be modified to enable amplification and detection, resulting in the development of reverse transcription LAMP (RT-LAMP). In RT-LAMP, RNA sequences are targeted instead of DNA. Including reverse transcriptase in the LAMP reaction enables the conversion of viral RNA into complementary DNA (cDNA), which then acts as the template for amplification. This method has proven highly effective in diagnosing numerous RNA viruses. (Thompson & Lei, 2020)

Therefore, with the global demand for tests during the COVID-19 pandemic, the RT-LAMP with pH-based colorimetric detection has proven to be an invaluable tool for the molecular diagnosis of SARS-CoV-2, showcasing its high potential for application in straightforward methodologies. (Baek et al., 2020; Lalli et al., 2021; Lu et al., 2020)

3.3 Paper-based Colorimetric LAMP systems for SARS-CoV-2

Early identification of SARS-CoV-2 is essential to reducing mortality and exacerbations and improving prognosis. Several laboratory techniques are used to do this, including cell culture, polymerase chain reaction, and immunoassays. However,

these methods are hampered by their time-consuming nature and the need for trained personnel, limiting their immediate applicability in critical situations. (Chu et al., 2020)

To address this need, developing microfluidic devices for point-of-care testing has emerged as a viable solution. Among these innovations, paper-based microfluidic analytical devices have received considerable attention. Paper as a substrate has promising properties for POCT due to its cost-effectiveness, ease of fabrication, ease of disposal, and ability to operate pump-free, facilitated by capillary action. (Chowdury & Khalid, 2021) However, only a few reports in the scientific literature document assays that use paper substrates for loop-mediated isothermal amplification (LAMP) reactions.

Garneret et al. developed a portable assay for the extraction and isothermal amplification of SARS-CoV-2 RNA, followed by detection by intercalating dyes or fluorescent probes. The dubbed "COVIDISC" device (see Figure 10) was 3D printed using polylactic acid (PLA) resin. The device comprises two sheets of black polypropylene coated on one side with PCR tape. The design incorporates pretreated laser-cut membranes: one for nucleic acid extraction and two for RT-LAMP reactions. These membranes are made of binder-free glass fiber. Detection times vary from twenty minutes to one hour, depending on the tested samples' viral load. In experiments with 16 pools of nasopharyngeal swab eluates, the estimated detection limit was found to be comparable to real-time RT-PCR (reverse transcription polymerase chain reaction). (Garneret et al., 2021)

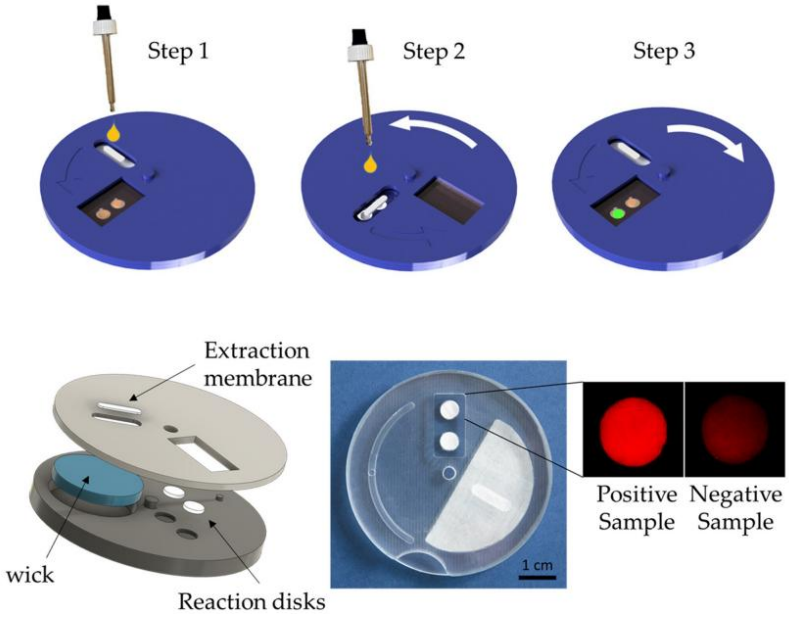

Figure 10: Schematic illustration of the COVIDISC workflow. (Garneret et al., 2021)

Davidson et al. presented the development of a paper-based pathogen nucleic acid detection device (see Figure 11) using LAMP and providing a colorimetric response. The device, optimized for detecting SARS-CoV-2 in human saliva without pre-processing, demonstrated a sensitivity of 97% and a specificity of 100% with a detection limit of 200 genomic copies/µL using image analysis. The device was constructed from grade 222 chromatography paper and polystyrene spacers on a Melinex® base and features configurable reaction zones. (Davidson et al., 2021)

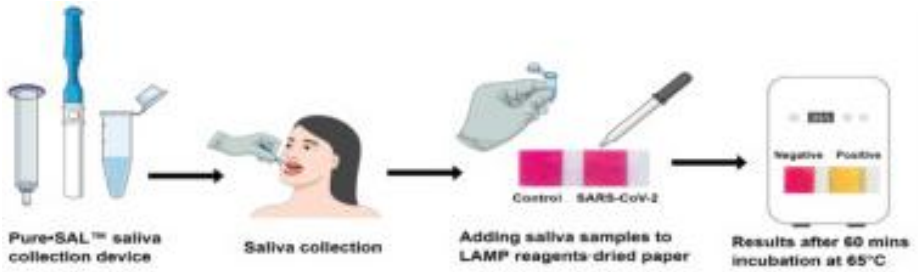

Figure 11: Schematic illustration of the workflow for the device proposed by Davidson and co-workers. (Davidson et al., 2021)

Dinh et al. introduced a paper microdevice that integrates DNA extraction, loop-mediated isothermal amplification (LAMP), and Safranin O-based colorimetric detection for identifying SARS-CoV-2 and Enterococcus faecium (see Figure 12). The paper microdevice consists of two distinct components: sample and reaction chambers. A sealing film, which serves as the base layer, facilitates the folding motion, enabling the transfer of DNA from the sample chamber to the reaction chamber. An FTA card was used in the sample chamber to extract and purify DNA from bacterially contaminated milk samples. Following the LAMP reaction, a breakthrough in aggregation-based DNA detection was achieved by polymerizing Safranin O within the reaction chamber. Using the Safranin O-based detection method, SARS-CoV-2 and E. faecium were successfully detected by the naked eye within 60 minutes. (Dinh & Lee, 2022)

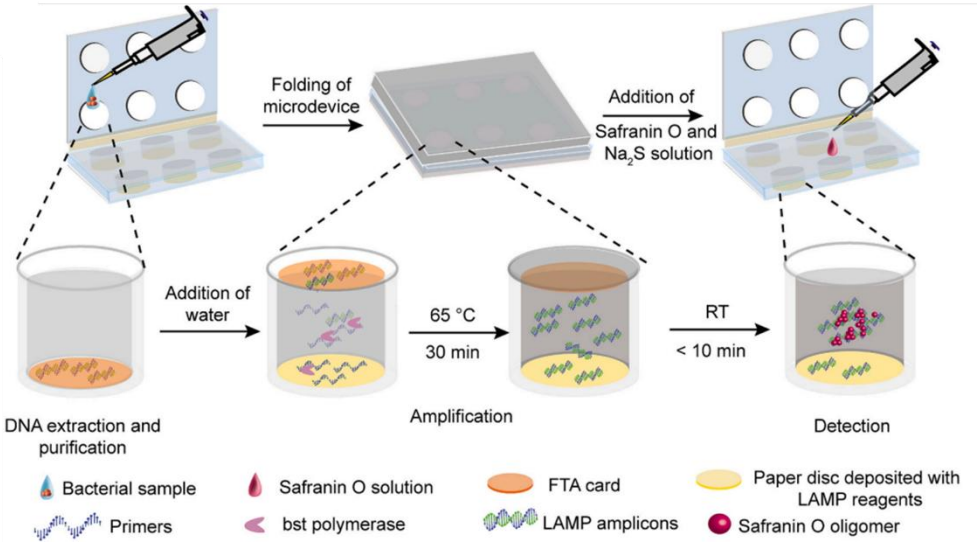

Figure 12: Illustration of the DNA extraction, purification, amplification, and detection of LAMP amplicons within the integrated paper-based device proposed by Dinh and coworkers.(Dinh & Lee, 2022)

3.4 Conclusion

The advancement of diagnostic tools for viruses has been driven by the need for more accurate, efficient, and rapid methods. While classical techniques like PCR and immunoassays have played vital roles in diagnostics, emerging alternatives such as LAMP offer promise for rapid, point-of-care testing. The shift towards miniaturized methods represents a significant leap forward in the field, aiming to overcome existing challenges. Despite the promise of paper-based microdevices, their presence in scientific literature remains sparse. Addressing these challenges is crucial for advancing the field and improving global health outcomes, making diagnostics more accessible, especially in low-resource settings.

4. Proteome

Proteins, the building blocks of life, are the final products of the decoding process that begins with the information in cellular DNA. They are responsible for many functions, from molecular motors to signaling. Proteins catalyze reactions, transport molecules, form the building blocks of viral capsids, create regulated channels across membranes, and transmit information from DNA to RNA. They are involved in the synthesis and degradation of new molecules and play important roles in the immune response and viral entry into cells. (Keskin et al., 2008)

Proteins are composed of amino acids, organic molecules consisting of a central alpha carbon atom linked to an amino group, a carboxyl group, a hydrogen atom, and a variable side chain. Within a protein, multiple amino acids are connected by peptide bonds, forming a long chain. This linear sequence of amino acids is known as the protein's primary structure (see Figure 13-I) (David Whitford, 2005). Charged amino acid side chains can form ionic bonds, while polar amino acids can create

hydrogen bonds. Hydrophobic side chains interact through weak van der Waals interactions, with most bonds formed by these side chains being noncovalent. (David Whitford, 2005; Gimpelev et al., 2004)

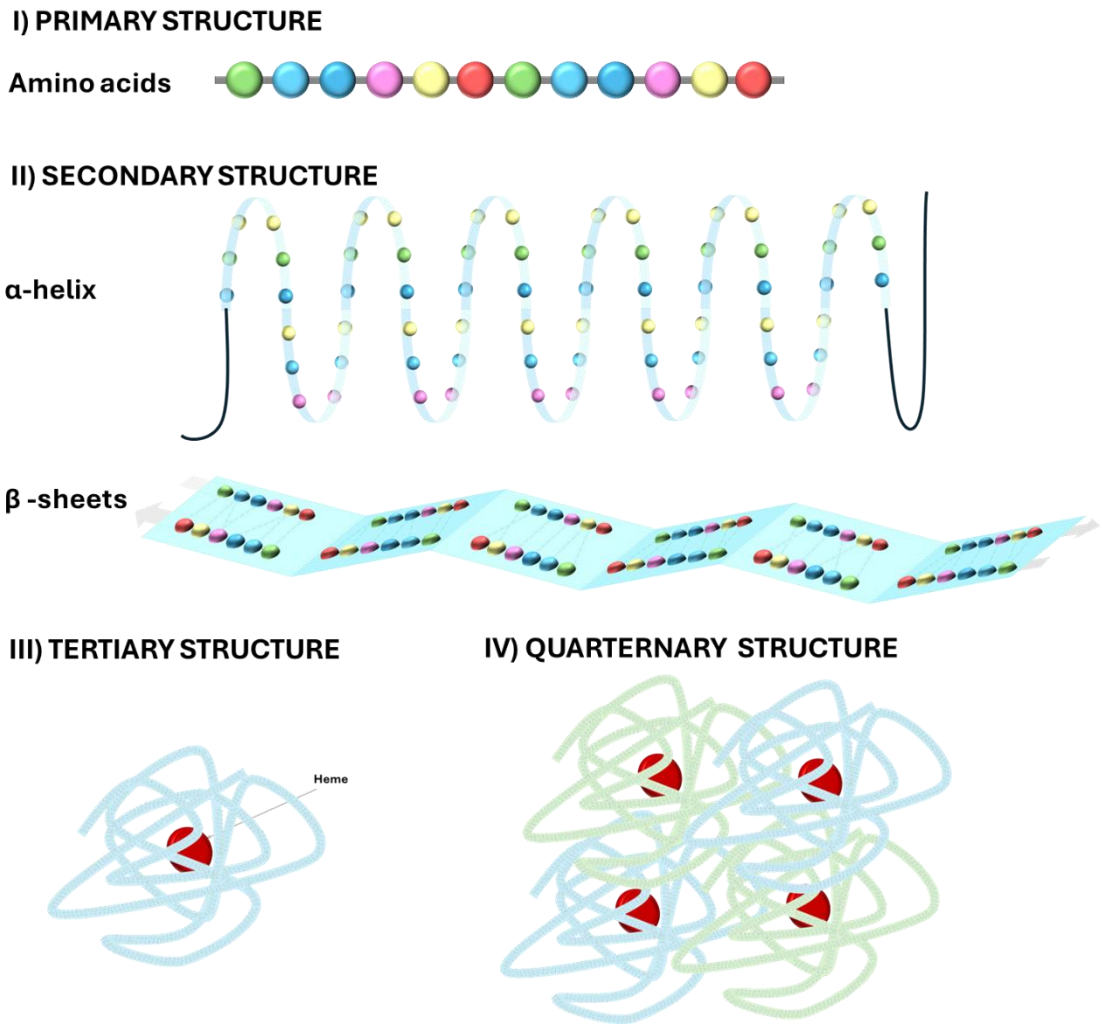

Figure 13: Schematic illustration of a protein structure, highlighting the primary (I), secondary (II), tertiary (III), and quaternary (IV) structures.Created by the author.

Hydrogen bonding between amino groups and carboxyl groups in neighboring regions of the protein chain can lead to specific folding patterns. The alpha helices and beta sheets are stable folding patterns, collectively referred to as a protein's secondary structure (see Figure 13-II). The overall arrangement of these formations and folds in a single amino acid chain, also known as a polypeptide, constitutes the protein's

tertiary structure (Figure 13-III). Finally, the quaternary structure of a protein (Figure 13-IV) refers to macromolecules composed of multiple polypeptide chains or subunits. As a newly synthesized protein folds, it explores various conformations before settling into its most energetically favorable shape. This final form is unique and compact, maintained by thousands of noncovalent bonds between amino acids. Additionally, the chemical interactions between a protein and its immediate environment contribute to its shape and stability. (David Whitford, 2005)

The unique distribution of amino acids within the protein molecule is a key determinant of protein behavior. Amino acids, with their dual acidic and basic groups, also function as electrolytes. The ions that form from the amino acid groups are essential in the transport of electricity. (Cohn & Mistry, 1925)

The isoelectric point (pI) concept is a physicochemical parameter that provides valuable information for protein identification. The pI corresponds to the pH at which the net surface charge and, consequently, the mobility of a protein equals zero. For a protein in a random coil state, the pI depends solely on its amino acid composition and can be calculated from analytical or sequence data. However, in a protein's native structure, where interactions among amino acid stretches can occur within the 3D structure, the experimental pI may be subtly altered. (Cohn & Mistry, 1925; Righetti, 2004)

In terms of structure, proteins can be categorized as water-soluble or membrane proteins, i.e., hydrophilic or hydrophobic, respectively. The properties of these two types of proteins differ fundamentally, as the surfaces of soluble proteins are much more polar than the lipid-interacting regions of membrane proteins. The lipid phase causes membrane proteins to form intramolecular hydrogen bonds. This

characteristic most probably results in the helices-dominant structural element in this class of proteins. (Gimpelev et al., 2004)

The term proteome, conceived by Wilkins in 1996 (Wilkins1 et al., 1996) due to the development of two-dimensional electrophoresis, states the collection of all the distinct proteins expressed by a genome of a single species. The proteome can change due to the different conditions of the protein environment or even due to the tissues of a single living organism. (Wilkins et al., 1996)

Another fundamental term, proteomics, indicates proteins' characterization and relative quantification under a defined set of conditions. Thus, proteomics focuses on describing, characterizing, and analytically quantifying and assembling large bodies of experimental observations in numerical databases.(Anderson & Anderson, 1998)

4.1 Classical Methodologies in Proteomics

The field of diagnostics has been greatly enriched by the advent of high-throughput technologies, which are now widely used to uncover molecular pathways and identify biomarkers for various diseases. Quantification techniques allow simultaneously studying the collective changes in protein expression induced by environmental or anthropogenic stresses. Advanced techniques such as nuclear magnetic resonance (NMR) and mass spectrometry-based characterization methods facilitate the study of the proteome. As a result, these methods generate vast amounts of molecular data that hold great promise for advancing molecular biomarker identification. Data analysis and statistical methods tailored to integrated proteomics analyses are essential to realize this potential. (Mali, 2015; Ramalingam et al., 2015; Shen et al., 2014)

Classically, protein characterization involves complex procedures. Two prominent strategies, bottom-up and top-down, are employed to analyze proteins. Additionally, a middle-down approach combines elements of both (see Figure 1). Each proteomics strategy—bottom-up, top-down, and middle-down—has its own unique advantages and challenges.

Bottom-up proteomics involves the digestion of proteins into shorts peptides (see Figure 14) through enzymatic(Schräder et al., 2017), chemical (A. Li et al., 2001), or electrochemical methods (Permentier & Bruins, 2004). These peptides are then separated and analyzed using tandem mass spectrometry. This method is widely adopted due to the simplicity of peptide separation, predictable fragmentation patterns, and commercial hardware and software availability that allow for the re-construction of the whole initial protein thanks to a database. However, challenges include abundant common peptides that complicate accurate protein identification and the risk of missing crucial information when sequences are incomplete, novel, or modified. (El Kennani et al., 2018; Sidoli et al., 2016)

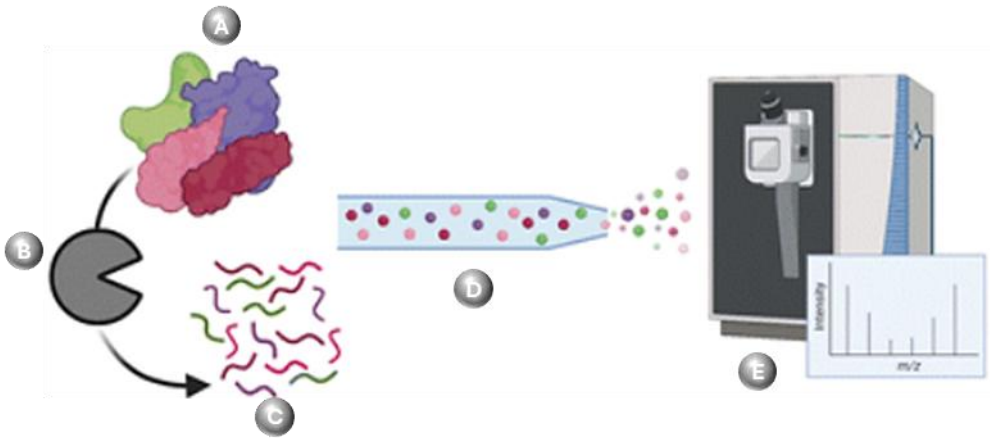

Figure 14: Schematic illustration of the bottom-up approach: A) Protein mixture; B) Enzymatic digestion of proteins into peptides; C) Resulting peptides; D) Peptide separation; E) Detection and analysis using MS. Adapted from *(Millera & Smith, 2023)*

In contrast, top-down proteomics directly analyzes intact proteins using MS without prior digestion (see Figure 15). (Capriotti et al., 2011) This approach enables the examination of protein isoforms and modifications, offering a comprehensive view of proteins and addressing some limitations of bottom-up proteomics. Despite its advantages in identifying post-translational modifications and protein isoforms, it is less commonly employed due to its complexity and demanding technical requirements. It requires high-accuracy mass measurement analyzers such as Fourier transform ion cyclotron resonance (FTICR, and hybrid ion trap-FTICR instruments capable of separating the multi-charged isotopic cluster of proteins as large as 229 kDa. Also, there is a challenge in determining product ion masses from multiply charged productions (with the potential of misinterpretation of top-down MS/MS spectra) and the need for suitable software for reconstructing protein identity. (Capriotti et al., 2011; El Kennani et al., 2018; Toby et al., 2016)

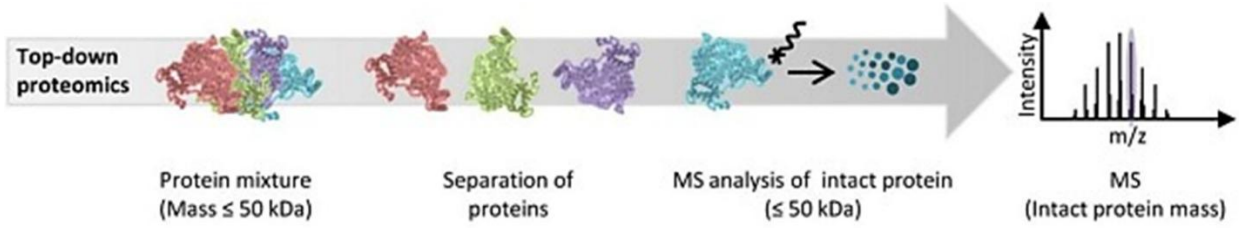

Figure 15: Schematic illustration of the top-down approach.(Jin et al., 2022)

Middle-down proteomics has emerged as a high-throughput method for investigating the coexistence of post-translational modifications (PTMs). This approach, which examines large protein fragments exceeding 30 amino acids, bridges bottom-up and top-down techniques (see Figure 16). It enhances protein sequence coverage and is particularly effective for PTM profiling, offering valuable insights into the patterns and frequency of PTM coexistence. (El Kennani et al., 2018; Sidoli & Garcia, 2017) Therefore, the middle-down strategy combines the strengths of both bottom-up and top-down methods, making a unique contribution to protein characterization. (El Kennani et al., 2018; Sidoli et al., 2016; Sidoli & Garcia, 2017; Toby et al., 2016)

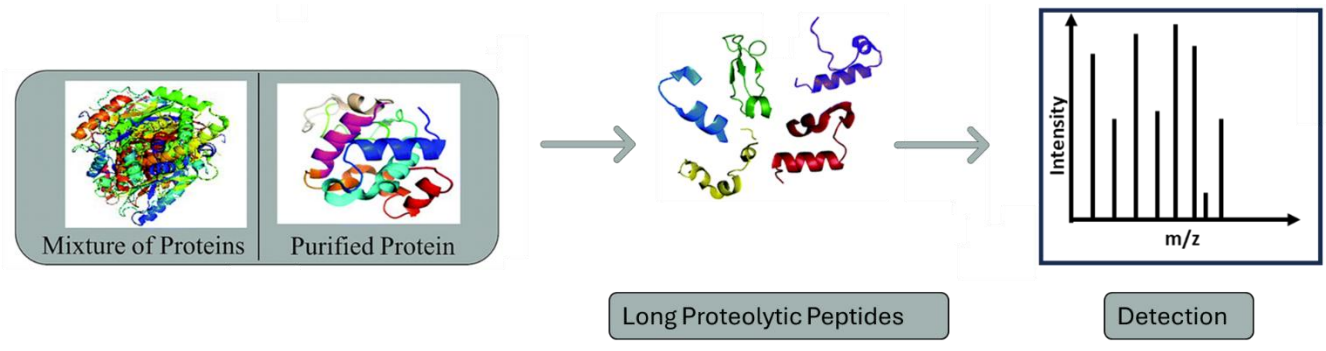

Figure 16: Schematic Illustration of the middle-down approach. Adapted from *(Pandeswari & Sabareesh, 2019)*

4.1.1. Isoelectric Focusing

Isoelectric focusing (IEF) is a separation technique for amphoteric compounds based on their isoelectric point (pI). The advancement of Isoelectric Focusing is often attributed to Arne Tiselius, a Nobel Prize laureate in 1948. Tiselius's pivotal contribution lies in recognizing the importance of maintaining a stationary concentration distribution of electrolytes and achieving equilibrium between electromigration and diffusion through electrolysis. Tiselius introduced a concept by establishing distinct pH values at the cathodic and anodic ends of the separation platform, a methodology termed the "moving boundary method." This innovation represented a departure from conventional techniques, facilitating the separation of samples, including biological species like sera, once considered entirely pure. (Arne Tiselius, 1937)

While Tiselius's Isoelectric Focusing technology demonstrated significant advancements for its time, it took several years for it to mature into a reliable analytical technique. His pioneering work laid the groundwork for subsequent advances in the field, underscoring the potential to separate complex samples and challenging prevailing assumptions regarding the purity of biological substances.(Hjertén S., 2003)

The emergence of Isoelectric Focusing in the 1950s, spearheaded by Alexander Kolin, marked an innovative method for protein separation and yielded numerous novel discoveries. Kolin's contributions facilitated the resolution of protein mixtures into distinct zones within an isoelectric spectrum. (Kolin, 1954) In recent years, substantial enhancements to the IEF method have amplified its significance across diverse research and biomedical laboratories. IEF is celebrated for its resolving

power during fractionation and sample concentration. (Mayer et al., 2021; Xu et al., 2022; Zha et al., 2023)

Isoelectric focusing is an electrophoretic mode that segregates amphoteric compounds by their isoelectric point, employing a pH gradient that ascends along a channel from the anode (lower pH value) to the cathode (higher pH value). A fundamental operational distinction between isoelectric focusing and traditional electrophoresis lies in the predetermined endpoint of the former, wherein analytes organize into distinct zones based on their isoelectric point.(Farmerie et al., 2021) Diverse IEF modes offer versatile approaches, including liquid state IEF, Immobilized/free pH gradient IEF, Capillary IEF (cIEF), and Microchip IEF. (Farmerie et al., 2021)

The principle of immobilized pH gradient (IPG) IEF is to generate the pH gradient before the IEF runs itself by copolymerizing and thus insolubilizing the pH gradient within the fibers of a polyacrylamide matrix. (Righetti, 1984; Righetti & Bossi, 1997) Liquid isoelectric focusing uses an immobilized pH gradient within a tray, which has a frame containing 12 or 24 wells over the strips. Proteins are compelled to migrate through the IPG strips. Focusing occurs within the strips, where each protein migrates until it reaches the well corresponding to its isoelectric point (see Figure 17). (Beldarrain et al., 2018) Capillary IEF and Microchip IEF will be discussed more deeply in the following sections of this thesis.

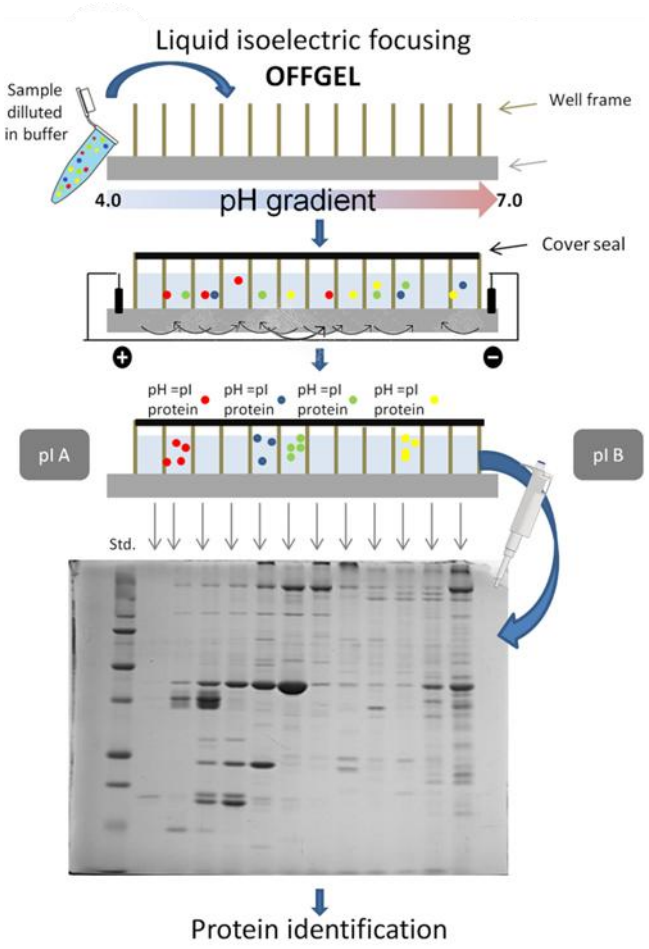

Figure 17: Schematic illustration of immobilized pH gradient isoelectric focusing. Adapted from (Beldarrain et al., 2018).

Some of these modes can be integrated with detection techniques, such as MS, UV, and fluorescent detection, effectively enabling the separation and profiling of various species. (Silvertand et al., 2008) Nevertheless, the proper comprehension of isoelectric focusing is based on understanding the electrophoresis principle.

The pH gradient is established by applying an electric field in a solution of carrier ampholytes (CA) in a suitable anticonvective medium. (Silvertand et al., 2008) During the electrophoretic process, heat is expected to be generated due to the electric current. So, the system's temperature will rise if the heat is not dissipated at the same rate it is produced. Thermal gradients can lead to convection, and to mitigate

the convection effects, an anti-convective support media (gels, capillaries, or paper) must be used. (Rudge & Monnig, 2000)

The ampholyte molecules have scattered pI values across a specific pH range. These carrier ampholytes consist of a mixture of aliphatic poly-amino-polycarboxylic acids. Due to the application of an electric field, the carrier ampholytes stack based on their pI. The pKa of the ionic forms of the ampholyte molecules allows the generation of pH gradients in liquid media, typically spanning pH units 4 to 9, when an electric field is applied. Reaching the steady state, the linearity of the pH gradient can be evaluated by analyzing a mixture of known pI markers or peptides. (Farmerie et al., 2021; Landers, 1997; Silvertand et al., 2008)

Thus, when the analyte is introduced into the pH gradient, it migrates according to its net charge influenced by the applied electric field. Acidic species move toward the anode, while basic ones move toward the cathode. When reaching a pH matching its pI, an analyte acquires a neutral charge and stops the migration; at this moment, the analyte is focused (see Figure 18). At this point, species can be subjected to staining or imaging along the channel. Another process consists of mobilizing the focused zones till a detector at the end of the channel, either by pressure application (hydrodynamic mobilization), anolyte or catholyte composition modification so as to change the pH gradient (chemical mobilization), or both combined together. Following mobilization and detection, the relative mobility of individual proteins is computed and graphically represented in relation to the compiled isoelectric point data. The linear regression analysis is applied for discerning unidentified molecules by using their isoelectric point or migration time. (Farmerie et al., 2021; Landers, 1997; Silvertand et al., 2008)

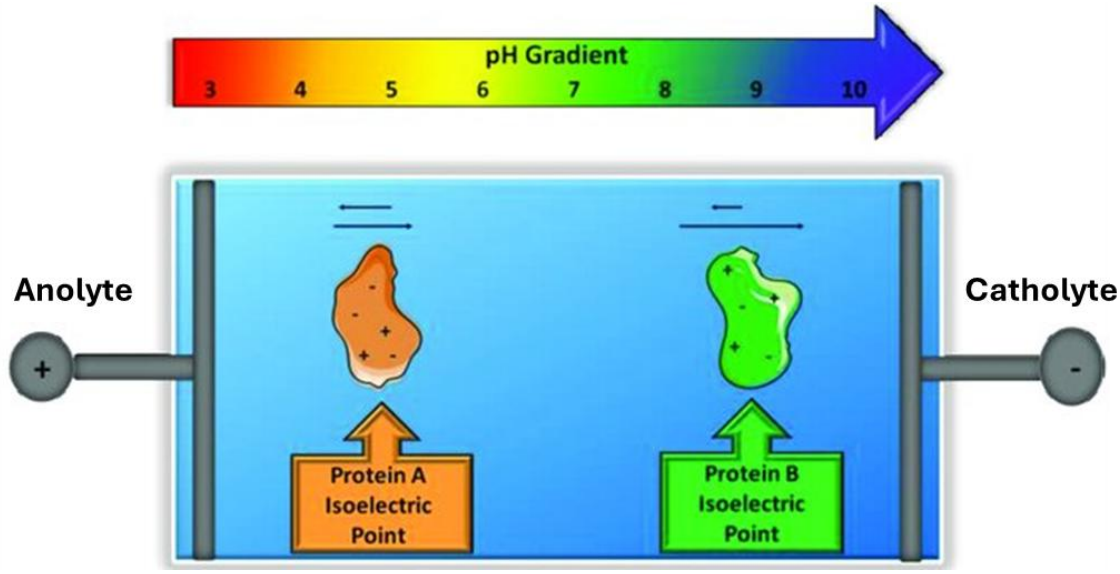

Figure 18: Principle of isoelectric focusing: When exposed to a pH gradient and an electric field, two proteins with different isoelectric points will move until each protein reaches a point where its net charge is zero. At this point, the protein stops migrating: focusing. (Pergande & Cologna, 2017)

4.1.2. Protein separation in 2D-polycarylamide gel electrophoresis (2D-PAGE)

In 1975, Patrick O'Farrells published a scientific paper describing a protein separation technique with a two-dimensional polyacrylamide gel electrophoresis (2D PAGE). This liquid-phase technique concentrates and separates proteins in two dimensions. (O'farrells, 1975)

The first-dimension separation is based on the isoelectric point of the proteins, that is, by isoelectric focusing. At the end of the focalization, the gel undergoes separation in a polyacrylamide gel (PAGE) in the presence of sodium dodecyl sulfate (SDS) in a transverse direction (see Figure 19). This second dimension, named gel electrophoresis, is based on a separation due to the molecular weight of the proteins; the larger the proteins, the slower their movement. So, in this second dimension, the movement of proteins is inversely proportional to their size. The molecular weight of each protein is determined by comparing it with denatured proteins of a known

molecular weight. (Dorri, 2019; Macgillivray & Wood, 1974; O'farrells, 1975; Rabilloud et al., 2010)

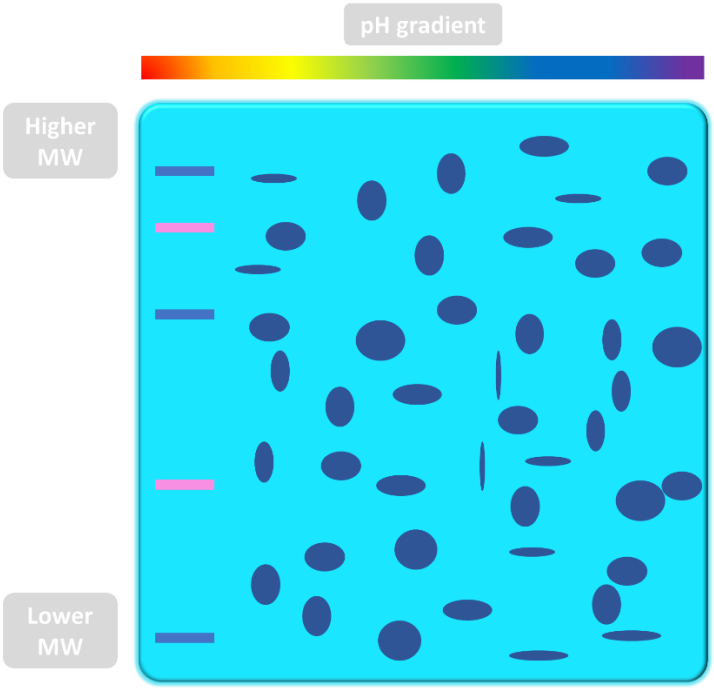

Figure 19: Schematic illustration of a two-dimensional polyacrylamide gel electrophoresis (2D PAGE). The first-dimension separation is based on protein IEF, and in the second dimension, the movement of proteins is based on the molecular weight. Created by the author.

Even though conventional two-dimensional gel electrophoresis proved effective in elucidating constituents of complex systems, it has some drawbacks. One of the most evident drawbacks is the separation speed, ultimately constrained by the Joule effect. The temperature can rise significantly depending on the system voltage, affecting viscosity, electrolyte permittivity, and zeta potential. As temperature increases, electrolyte viscosity decreases while the zeta potential increases. Viscosity is temperature-dependent, and the migration speed of molecules shows an inverse correlation with fluid viscosity. Additionally, electrolyte conductivity and the diffusion coefficients of the species are impacted. Consequently, these variations in conductivity due to temperature changes generate a consistent heat source within the system,

leading to band broadening in the sample plug. The poor dissipation of Joule heat in slab systems confines their applicability to electric fields of low potential. (Landers, 1997)

Additionally, the analytical procedure for SDS gels involves a series of laborious, time-intensive activities, encompassing the gel casting, preparation and loading of samples, electrophoretic resolution of ionic/molecular species, all the way to the concluding stage where the gel is stained, and the outcomes are acquired. Besides low reproducibility, especially in two-dimensional analysis, variations in staining based on the analyte, complicating the achievement of quantitative accuracy (e.g., glycosylated proteins exhibit distinct dye-binding properties compared to their unglycosylated counterparts), and the complex methodology, making the entire process unfeasible of automation. (Albar & Monteoliva, n.d.; Landers, 1997; Sanchez et al., 2004)

4.1.3. Capillary Isoelectric Focusing

Isoelectric Focusing (IEF), initially employing the conventional slab gel format, was transposed to capillaries (Capillary Isoelectric Focusing-CIEF) due to issues with gel reproducibility. Capillary Isoelectric Focusing has emerged as the predominant mode of IEF, offering enhanced reliability. CIEF incorporates an anticonvective medium, such as gels, co-polymers, or additives in the electrolyte solution. (Landers, 1997; Silvertand et al., 2008)

The pH gradient is established inside the capillary by employing a mixture of carrier ampholytes with a broad range of pI under an electric field. After introducing the sample-ampholyte solution into the capillary, focusing is initiated by placing one

end of the capillary in an anolyte solution (anode) and the other in a catholyte solution (cathode) and applying an electric field. During the focusing process, distinct sample bands form at both ends of the sample-ampholyte segment. Once a steady state is achieved, these duplicate bands merge into a single zone at one end of the capillary at the protein's isoelectric point (see Figure 20). (Rodriguez-Diaz et al., 1997) Subsequently, the focused compounds are detected based on their pI order at the detection window after a hydrodynamic or chemical mobilization step.(Farmerie et al., 2021; Silvertand et al., 2008) .

Figure 20 illustrates that when an analyte's pH aligns with its isoelectric point (pI), it attains a neutral charge and stops migration. At this point, species can undergo staining or imaging for analysis or be mobilized to a detection window for further scrutiny. The resulting data can be visualized in an electropherogram, showcasing the separation and detection of proteins (Figure 16).

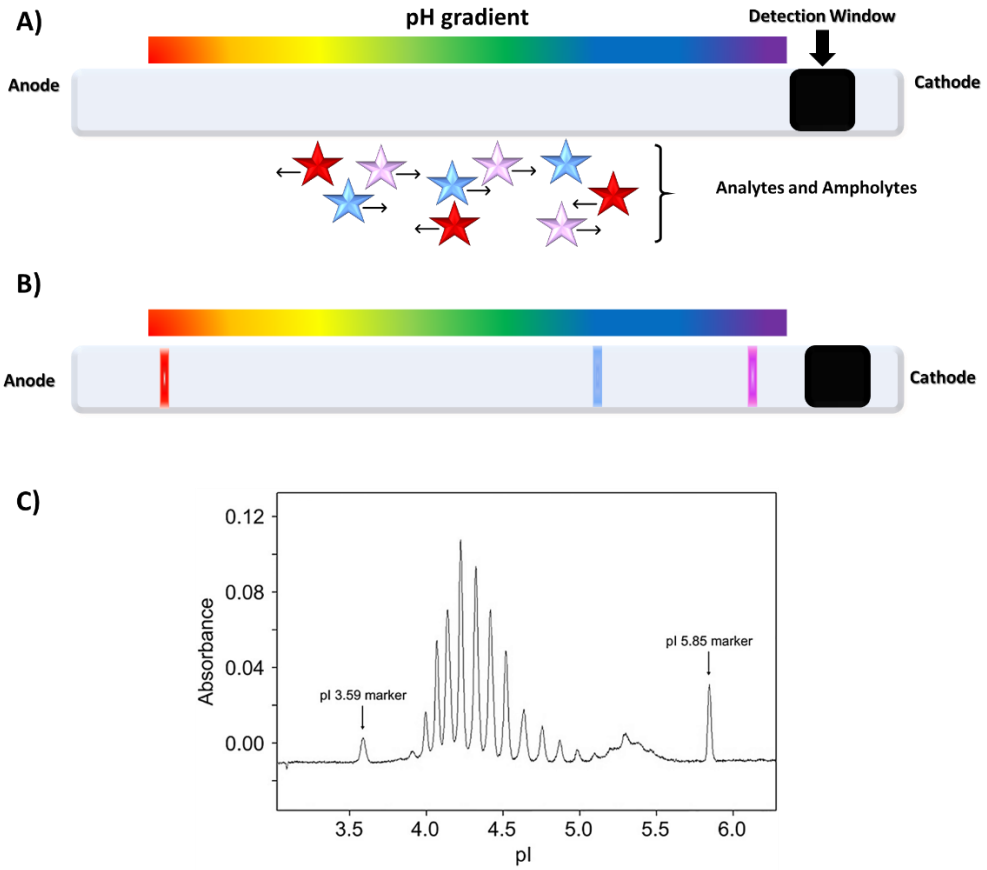

Figure 20: Illustration of the isoelectric focusing process on the capillary format. A) Electrophoretic movement of the analytes under an electric field. B) Focusing and mobilization of the analyte's concentrated bands. C: Example of an electropherogram for CIEF after protein separation and UV detection. Created by the author.

A noteworthy variant, Whole Column Imaging Detection (WCID), has been developed for capillary isoelectric focusing (CIEF) of proteins and peptides. WCID helps to overcome the limitations of single-point detection by eliminating the need for mobilization by dynamically detecting the entire capillary, offering rapid detection. This method also avoids the drawbacks of the mobilization process, such as pH gradient distortion and loss of resolution. (Goodridge et al., 2004; Mao & Pawliszyn, 1999a)

In 2005, Busnel et al. introduced a significant development in capillary isoelectric focusing (CIEF) using a glycerol-water mixture. This method leverages the unique properties of glycerol, which is commonly used in biochemistry to stabilize

proteins, maintain enzymatic activity, and solubilize hydrophobic proteins. The higher viscosity of glycerol compared to water slows fluid movement, enabling precise focusing of carrier ampholytes and proteins. Moreover, glycerol improves wettability, reduces evaporation, and minimizes heat generation. In this context, glycerol serves as an anticonvective medium in CIEF, reducing electroosmotic flow (EOF) and the electrophoretic mobility of proteins. This allows the use of bare silica capillaries instead of traditional gels. The authors observed that the glycerol-water system exhibited a lower and more stable current intensity than conventional aqueous gel systems (see Figure 21), reducing Joule heating despite slightly extending analysis time. This method's reduced conductivity and optimized focusing conditions were key advantages for capillary IEF, particularly for analyzing challenging protein samples. (Busnel et al., 2005a)

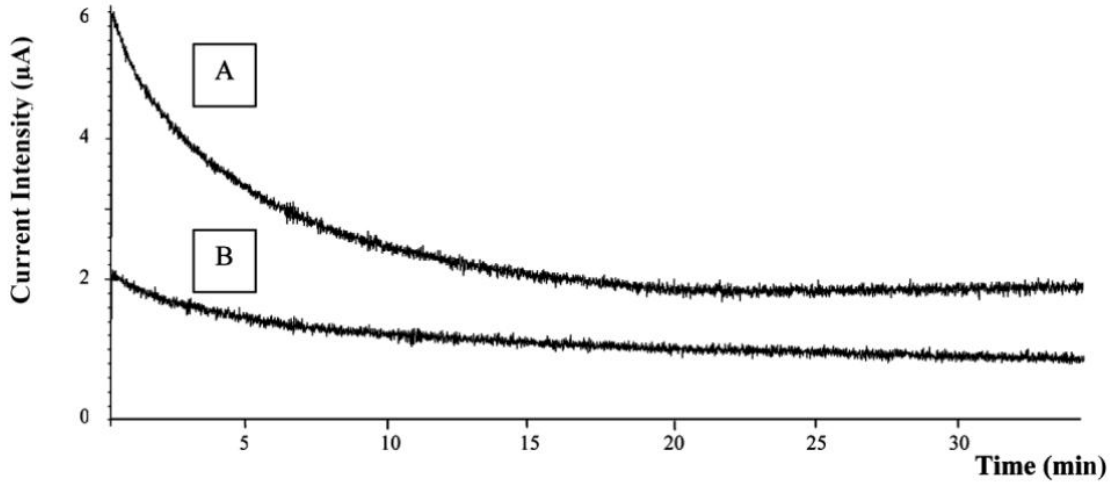

Figure 21: Current intensity profile during the focusing step for (A) the conventional aqueous gel CIEF system and (B) the glycerol-water CIEF system. (Busnel et al., 2005a)

Building on this foundation, Mokaddem et al. (2009) introduced an innovative approach for the online coupling of CIEF with electrospray ionization mass

spectrometry (ESI-MS). Using glycerol in the separation medium effectively maintained protein stability and focused precision while achieving compatibility with MS detection. The authors used a mixture of model proteins including ribonuclease A (Rnase, pI 9.45), α-chymotrypsinogen A type II (α-Tryp, pI 8.3), myoglobin (Myo, pI 6.3), carbonic anhydrase II (CA II, pI 5.9), β-lactoglobulin A (β-Lac, pI 5.1), and trypsin inhibitor (TI, pI 4.5) as outlined in Figure 22.

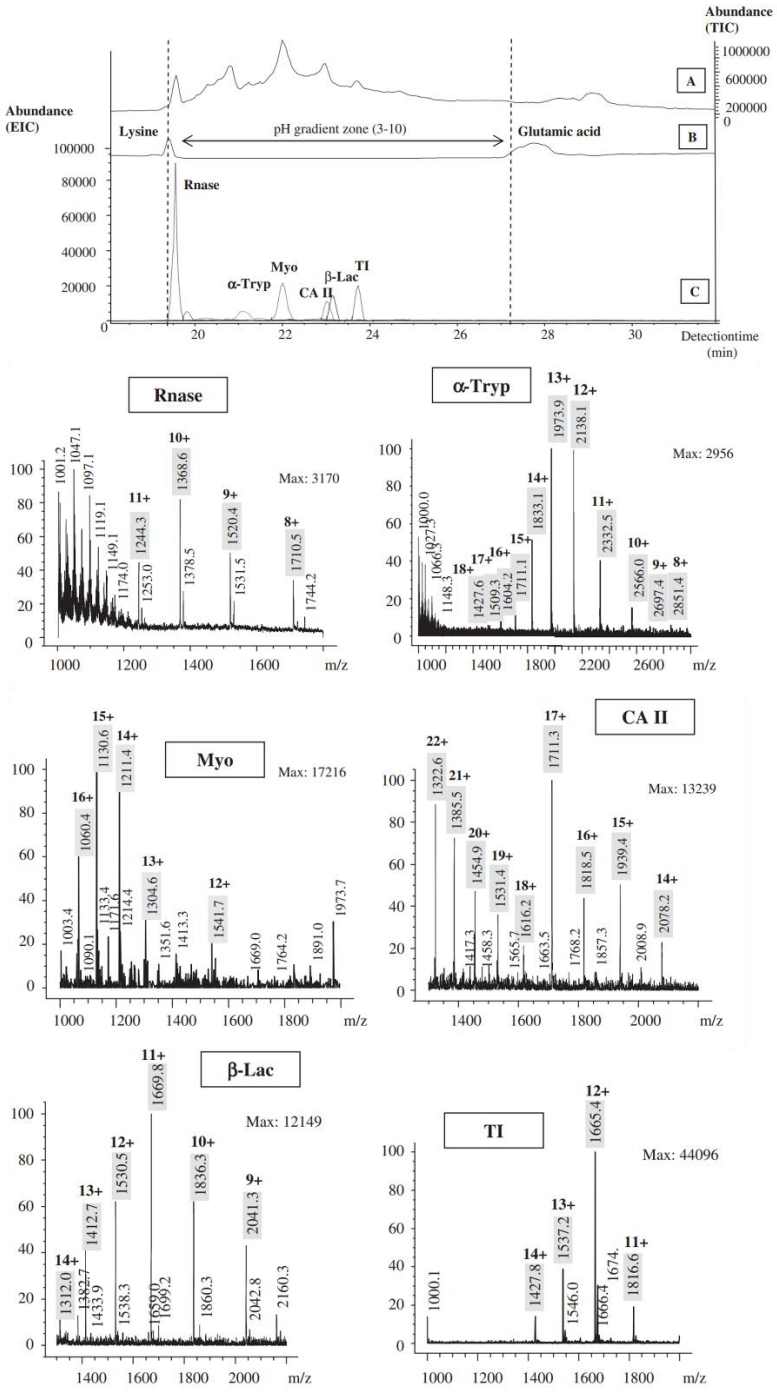

Figure 22: CIEF-ESI-MS analysis and extracted mass spectra of six model proteins reported by (Mokaddem et al., 2009). (A) Total ion current electropherogram within the m/z range of 1000–2500; (B) Selected ion monitoring electropherogram at m/z 148; (C) Extracted ion chromatogram electropherogram for six proteins: RNase (m/z 1369), α-Trypsin (m/z 2139), Myoglobin (m/z 1211), Carbonic Anhydrase II (m/z 1940), β-Lactoglobulin (m/z 2041), and Trypsin Inhibitor (m/z 1666). The mass spectra of these proteins were obtained by averaging the scans corresponding to the peaks observed in panel A. (Mokaddem et al., 2009)

Lecoeur et al. (2010) further expanded the application of this glycerol-water CIEF system, demonstrating its effectiveness in separating hydrophobic proteins under native conditions (see Figure 23). Their study, which focused on a 30:70 v/v glycerol-water medium using a bare silica capillary, showed a strong correlation between protein isoelectric points (pIs) and migration times, confirming the method's accuracy. This glycerol-based system emerged as a promising alternative to conventional aqueous gel CIEF, particularly for the analysis of complex protein mixtures, offering a robust solution for the characterization of hydrophobic proteins.

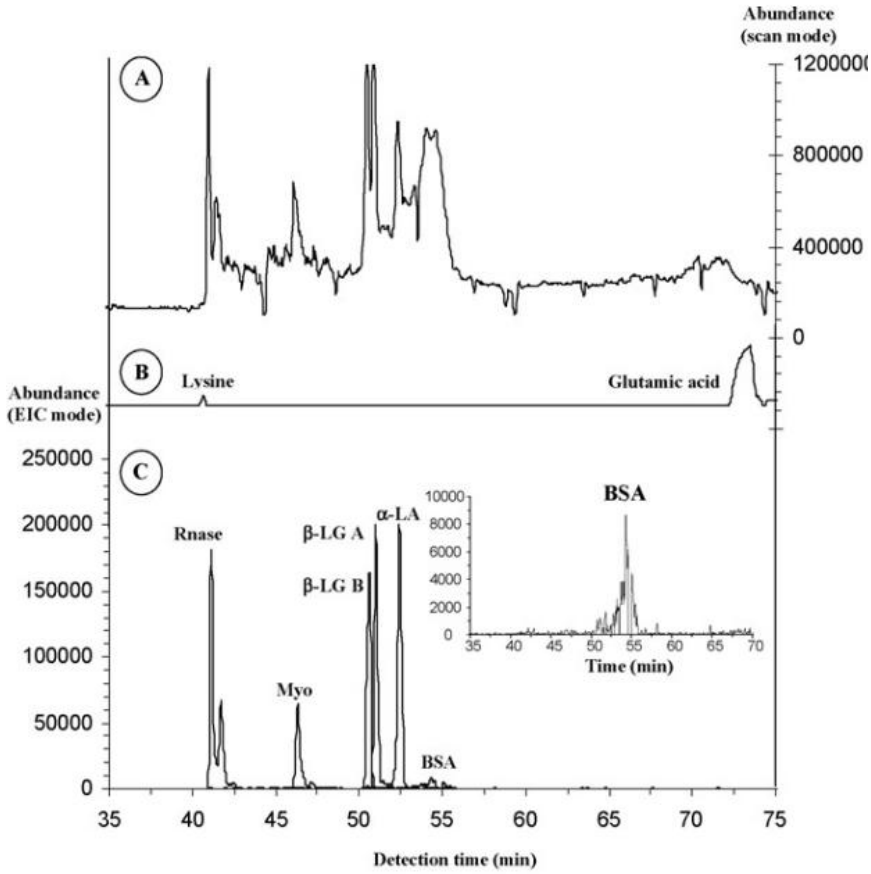

Figure 23: On-line CIEF–ESI/MS separation of standard whey protein mixture. (A) Electropherogram from scan mode; (B) Electropherogram of pH gradient markers; (C) Reconstructed extracted ion current electropherogram from each protein: Rnase, Myo, β-LG B, β-LG A, α-LA, BSA. (Lecoeur et al., 2010)

Online CIEF-MS can present an alternative to 2-D PAGE for rapid proteome analysis. It provides pI and Mr (relative molar mass) information with high-resolution capabilities and improved structural information, omitting the disadvantages of conventional gel electrophoresis, such as restrictions in sensitivity and tedious staining procedures. (Mokaddem et al., 2009) This online CIEF-MS represents a top-down strategy If we want to develop a bottom-up strategy, a digestion step should be included between IEF and MS, which is hardly possible in a capillary.

4.2: IEF in microchip format.

To address conventional scale issues, microchip isoelectric focusing was first reported in 1999. It involved creating microchannels into a quartz chip fabricated using photolithography and a chemical etching process (see Figure 24). The authors reported good reproducibility and resolution for linear polyacrylamide-coated channels in less than 10 minutes. (Mao & Pawliszyn, 1999b)

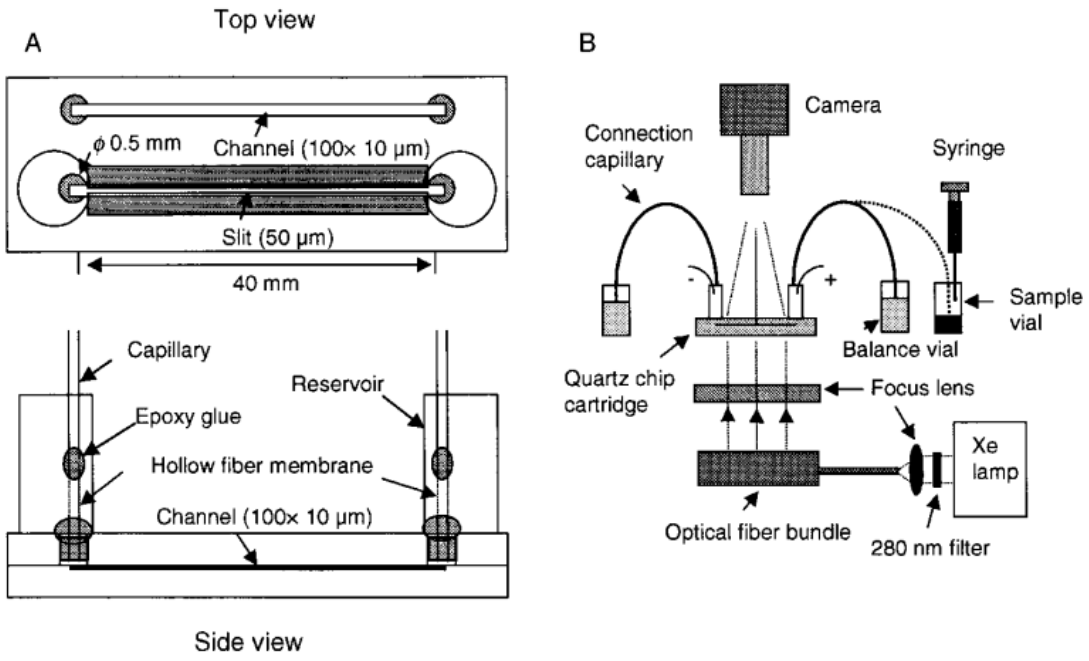

Figure 24: (A) Schematic illustration of the microchip IEF cartridge; (B) Representation of the instrument setup for chip IEF with absorption imaging detection. *(Mao & Pawliszyn, 1999b)*

In 2011, Shameli et al. developed a polydimethylsiloxane (PDMS)/modified PDMS membrane/SU-8/ quartz hybrid chip (see Figure 25) for protein separation using IEF coupled with the whole-channel imaging detection (WCID) method. The chip was tested by performing protein and pI marker separation, and it was more robust and had higher sensitivity than the ones reported before. (Shameli et al., 2011)

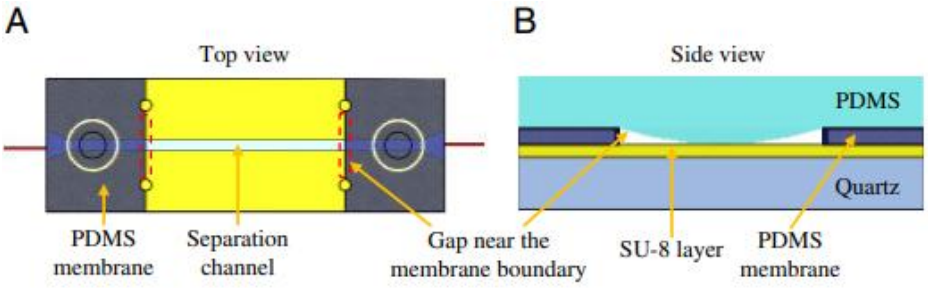

Figure 25: Illustration of the PDMS)/modified PDMS membrane/SU-8/ quartz hybrid chip. (A) Top view of the chip, (B) side view of the chip displaying the gap near the membrane edge. Adapted from (Shameli et al., 2011).

Zhao et al. introduced a SlipChip-based method for conducting microchip IEF in discrete droplets. This device comprised two micromilled plastic layers, each with wells, enabling the efficient compartmentalization of focused analyte bands into microdroplets in situ (see Figure 26). These sample droplets could be analyzed directly on-chip or collected for further examination using electrophoresis or MS. The proposed methodology prevents remixing, is scalable, and can potentially be integrated with other analytical techniques. (Y. Zhao et al., 2014)

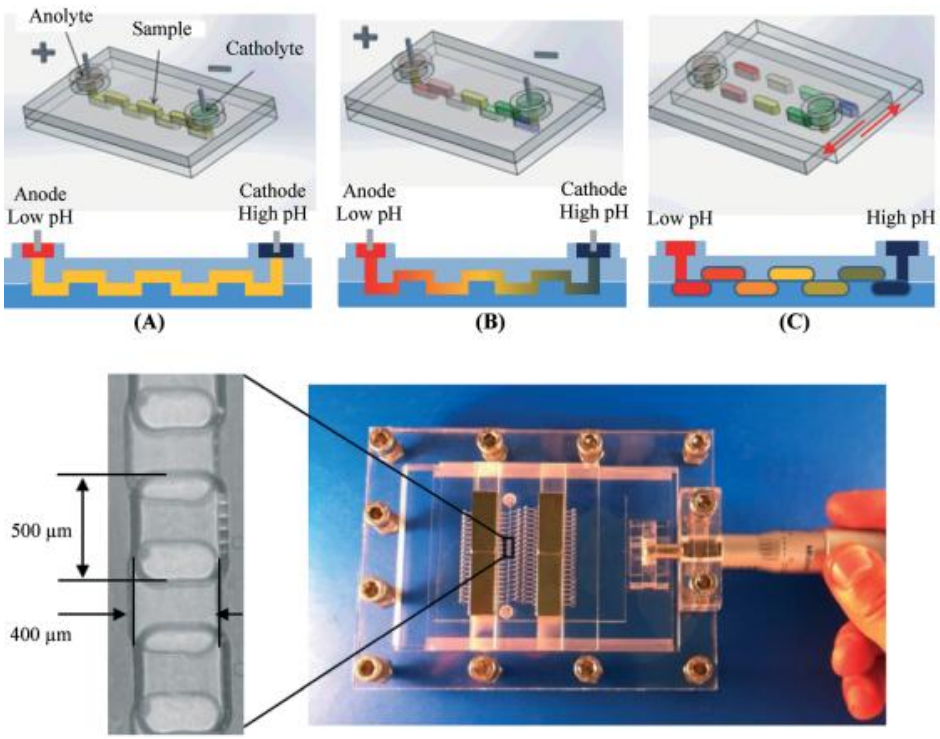

Figure 26: Diagram illustrating IEF separation and in situ compartmentalization in the proposed Slipchip. (A) Sample loading into a continuous "zig-zag" channel. (B) pH gradient formation and IEF process initiated after applying an electric field. (C) In situ compartmentalization following IEF separation. (D) The microdevice and platform made of PMMA, featuring a "zig-zag" channel. (Y. Zhao et al., 2014)

In 2019, Mack et al. detailed a microfluidic system to characterize and identify protein charge and mass isoforms within 15 minutes. Named iCIEF-MS, the system included a microchip, 280 nm absorbance imaging, and an on-chip electrospray

ionization (ESI) tip (see Figure 27). UV (ultraviolet) imaging across the separation channel provided a view of the focusing step. During mobilization, the imaged sample stacking demonstrated improved resolution, enhancing mass spectrometry analysis. This device characterized 33 molecular features in a single assay. The system reduced the time compared to offline methods. (Mack et al., 2019a)

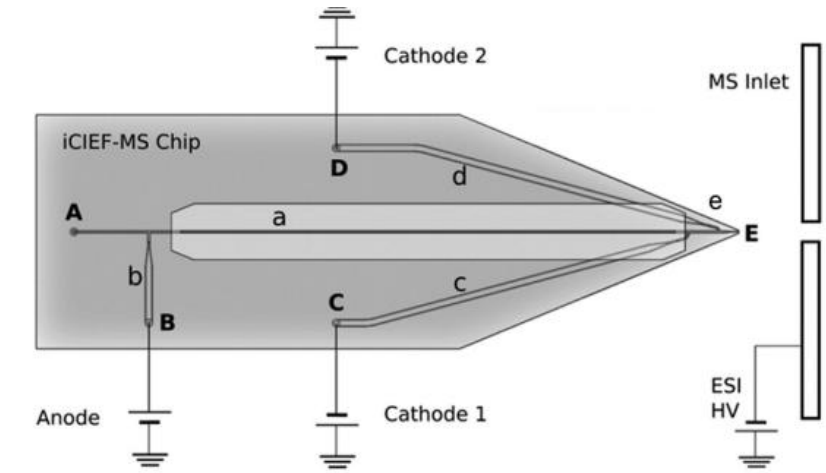

Features of the iCIEF-MS chip

A Sample port	a Sample channel
B Anolyte port	b Anolyte channel
C Catholyte port	c Catholyte channel
D Mobilizer port	d Mobilizer channel
E ESI tip	e ESI junction

Figure 27: Illustration of the iCIEF-MS microchip along with a multi-power supply high-voltage system.(Mack et al., 2019b)

In 2024, Fan et al. proposed improving the protein detection threshold by implementing micro-scale isoelectric focusing directly at the detection site on a protein sensor chip (see Figure 28). They found that this enhancement in the detection limit resulted from two key effects: the concentration of protein molecules and the reduction of diffusion-induced fluctuations. Their approach offered ultra-low-power all-electronic solutions for improving protein analysis detection limits. (X. Fan et al., 2024)

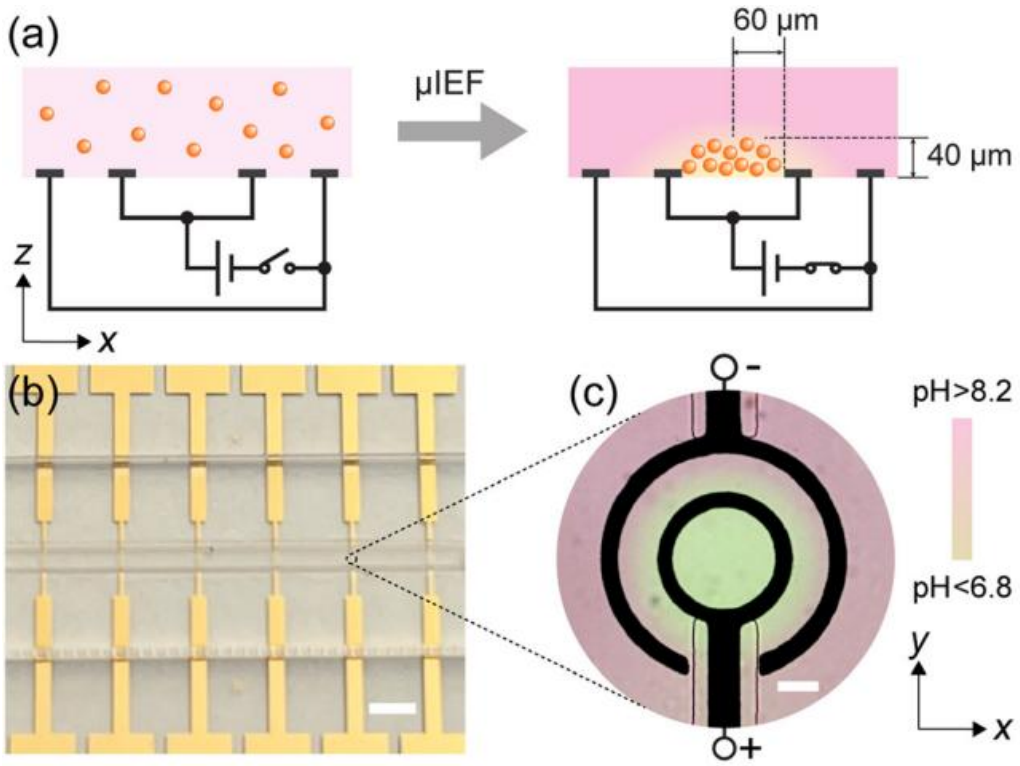

Figure 28: Protein focusing and sensing via pH-gradient formation between two concentric ring microelectrodes. (a) Diagram illustrating microscale isoelectric focusing (μIEF) with protein molecules shown as orange particles. (b) Optical image of the device with a scale bar of 1 mm. (c) Microscopic view showing the pH gradient visualized using phenol red. The scale bar is 50 μm. (X. Fan et al., 2024)

Despite technological advancements that have enhanced microfluidic IEF systems by increasing integration, sensitivity, detection limits, and robustness, up to our knowledge, no study in the scientific literature has yet presented a complete proteomic on-a-chip approach. Given the various steps involved in proteome analysis, paper substrates emerge as a strong candidate for integrating these steps due to their physicochemical properties, availability, and simplicity.

4.3. Paper-based IEF microfluidic systems

Different approaches have been employed to analyze protein samples, such as single protein assays or complex proteome profiling. These methods apply homemade and commercial microfluidic platforms to enhance analysis efficiency, reduce time, and improve detection limits, sensitivity, and total flow rate. (Lazar et al., 2020) Over the years, applications targeting specific goals or exploring diverse areas, including protein structure characterization and proteomic profiling of biological samples or processes, have been showcased. Allying paper substrate and microfluidic advantages, paper-based devices have emerged as a highly suitable substrate for microfluidic analytical devices aiming to integrate all steps of proteome analysis. (Kašička, 2024; Sena-Torralba et al., 2023; Skjærvø et al., 2019; Vitorino et al., 2021) However, few publications on paper-based analytical devices for protein separations using isoelectric focusing are available in the scientific literature.

Gaspar et al. showcased the separation and concentration of proteins through isoelectric focusing with an inkjet-printed silver electrode on a paper-based device. Additionally, they employed solid-ink technology to print hydrophobic wax barriers, fabricating paper microfluidic devices with integrated electrodes. The separation channel was reported as a paper strip with a wax barrier and absorbent PADs as the electrolyte reservoirs (see Figure 29). However, with no precision in positioning the reservoirs, it does not allow an ensemble of all the system's components to obtain a robust analytical system applicable in point-of-care tests, for example. (Gaspar et al., 2016)

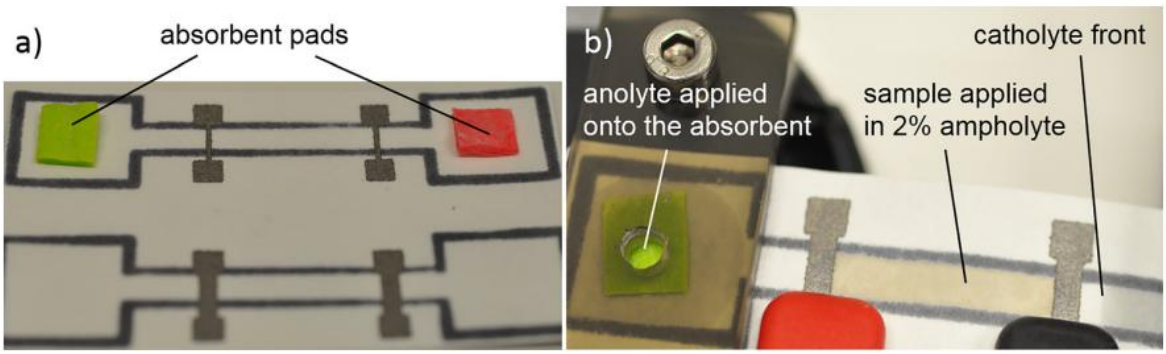

Figure 29: Paper-based IEF with silver-printed electrodes. (a) Two wax patterns featuring silver electrodes and absorbent pads for anolyte and catholyte. (b) Illustration of the filling step prior to IEF experiments.(Gaspar et al., 2016)

Xie et al. presented a proof of concept of a carrier ampholyte-free isoelectric focusing on a paper-based microfluidic device to separate color model proteins. The authors reported a separation of proteins along the paper strip separation channel, and the fractions from isoelectric focusing in the paper channel were directly cut and retrieved for subsequent analysis using sodium dodecyl sulfate-polyacrylamide gel electrophoresis and matrix-assisted laser desorption/ionization-time-of-flight mass spectrometry. The system developed in this study comprised a paper strip with the extremities dipped in the cap of plastic centrifuge tubes that served as reservoirs for the anolyte and catholyte (see Figure 30). What can be emphasized is that despite the authors report the efficient separation of the proteins, the system is rudimentary and has fragile precision. This is because the paper is handly dipped into the caps, leading to a lack of or reduced reproducibility and repeatability. (Xie et al., 2018)

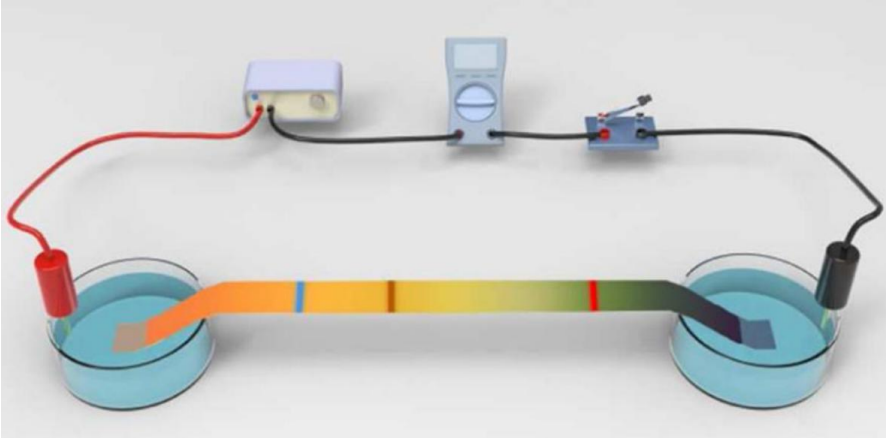

Figure 30: The system developed by Niu et al. and Xie et al., described as a paper strip with the extremities dipped in the caps of plastic tubes that served as reservoirs for the anolyte and catholyte. (J. C. Niu et al., 2018; Xie et al., 2018)

Niu et al. proposed an isoelectric focusing protein separation and concentration on a paper strip. The authors reported smartphone-based colorimetric detection of color model proteins and offline protein identification of the IEF fractions using matrix-assisted laser desorption ionization time-of-flight mass spectrometry (MALDI-TOF-MS). Here, the reservoirs were caps of microtubes (see Figure 30, the very same system as proposed by (Xie et al., 2018)); the paper strip separation channel was placed between the reservoirs, and the extremities were dipped into the caps with the anolyte and catholyte. As already discussed, even though the authors have documented the isolation of the proteins, the setup is basic and possesses delicate accuracy. Since the paper is manually immersed into the caps, resulting in deficient precision, reproducibility, and repeatability. (J. C. Niu et al., 2018)

Yu et al. published a scientific paper describing IEF for separating and enriching proteins into microfluidic paper-based analytical devices. For fabricating the µPADs, the authors reported an octadecyltrichlorosilane (OTS) silanization followed by selective plasma treatment in specific regions of the paper as shown in Figure 31 Besides other optimizations, polyvinylpyrrolidone (PVP) was evaluated to suppress

electroosmotic flow (EOF). The authors reported a parallel IEF across multiple channels to separate multiple protein samples on a single chip and compared their performance with the conventional gel-IEF system. (S. Yu et al., 2019)

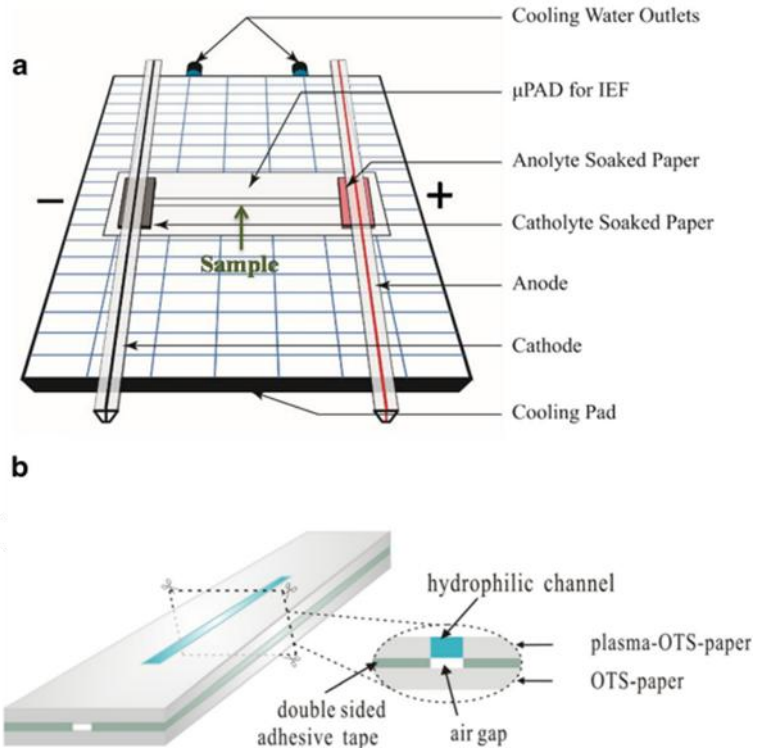

Figure 31 : Illustration of the paper-based IEF microfluidic chip. The μPAD for IEF was placed on a cooling pad. Two electrode wires were secured to the paper soaked with anolyte and catholyte. (b) Cross-section of the μPAD. Blue indicates the hydrophilic channel, gray represents the hydrophobic paper, and green denotes the double-sided adhesive tape. Adapted from (S. Yu et al., 2019)

Niu and coworkers proposed an isoelectric focusing apparatus featuring a 3D origami-paper-based device (see Figure 32) and a pair of chromatography paper reservoirs. With this setup, the researchers separated proteins within 35 minutes. The folded origami structure was unfolded for protein quantification, and the solution was applied onto the lateral flow strip sample pad. Allying low-voltage and easy target isolation for subsequent detection after pretreating samples and unfolding the origami-

paper-based devices can be integrated with various technologies to pretreat proteins and DNA samples, for example. (J. Niu et al., 2021)

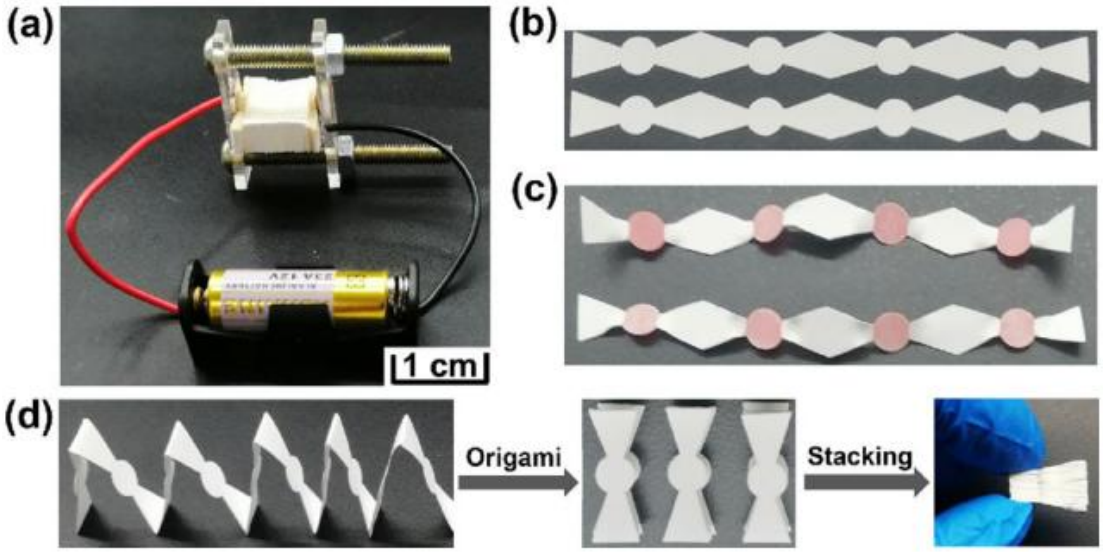

Figure 32: The proposed 3D paper-based IEF platform consists of (b) 2D cellulose acetate membrane channel designed by laser cutting, (c) 2D cellulose acetate membrane channel with hydrophobic pretreatment, and (d) an origami-stacked arrangement of cellulose acetate membranes. (J. Niu et al., 2021)

In 2023, Danchana and coworkers reported separating glutamic acid and histidine through IEF in an origami configuration of filter paper with channels defined by wax printing as shown in Figure 33. After 3 min at 30V, the separated peptides in each layer were extracted with water and quantified using high-performance liquid chromatography with pre-column derivatization employing dansyl chloride. Glutamic acid and histidine focused on different layers, corresponding to their isoelectric points. (Danchana et al., 2023)

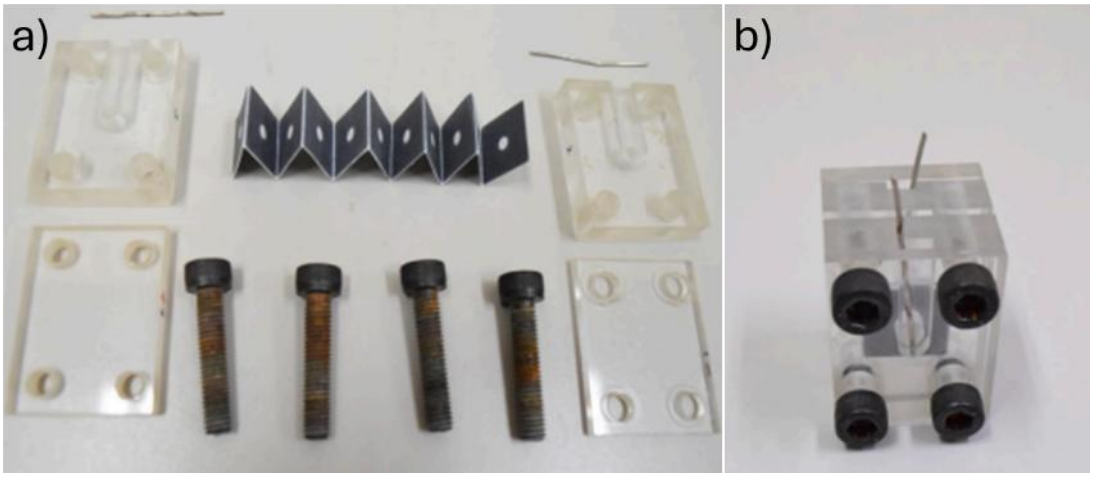

Figure 33: Origami-based IEF platform (oPADs): (a) Components of the oPADs; (b) assembled oPADs.(Danchana et al., 2023)

4.4. Conclusion

Proteome analysis involves various approaches, typically requiring protein separation and digestion into peptides. Integrating these steps remains a challenge on a conventional scale, making the shift toward miniaturization essential for advancing proteomics.

Few publications have utilized paper-based analytical devices for protein separations via isoelectric focusing. These studies highlight several limitations, including the lack of validated technology, precision issues, integration challenges, and a significant lack of system feasibility and robustness due to the absence of a holder. Additionally, all reported research on paper-based IEF has used water as the medium for protein separation. This approach restricts comprehensive proteome analysis, as it fails to adequately address both hydrophilic and hydrophobic proteins. Therefore, there is a pressing need for an integrated, proteome-compatible, and validated paper-based analytical device to overcome these limitations and enhance the effectiveness of proteome analysis.

5. General Conclusion

Despite advances in the field, both protein and viral analysis face challenges. Classical techniques such as PCR and immunoassays have been essential in diagnostics. However, emerging alternatives such as LAMP hold promise for rapid point-of-care testing, yet scientific publications remain scarce. Similarly, proteomic analysis, which involves many analytical steps, faces integration challenges on a conventional scale, highlighting the importance of miniaturization for progress. Regardless of the promise of paper-based microdevices in diagnostics and proteomics, their presence in the scientific literature must be increased.

Bibliography

Akyazi, T., Basabe-Desmonts, L., & Benito-Lopez, F. (2018). Review on microfluidic paper-based analytical devices towards commercialisation. In Analytica Chimica Acta (Vol. 1001, pp. 1–17). Elsevier B.V. https://doi.org/10.1016/j.aca.2017.11.010

Albar, J. P., & Monteoliva, L. (n.d.). Differential proteomics: An overview of gel and non-gel based approaches. https://academic.oup.com/bfg/article/3/3/220/295948

Albrecht, T. ; F. M. ; B. I. and. Rabson. A. S. (1996). Effects on Cells. In Baron S (Ed.), Medical Microbiology (4th ed.). Bookshelf.

Ali, Z., Jin, G., Hu, Z., Wang, Z., Khan, M. A., Dai, J., & Tang, Y. (2018). A Review on NanoPCR: History, Mechanism and Applications. Journal of Nanoscience and Nanotechnology, 18(12), 8029–8046. https://doi.org/10.1166/jnn.2018.16390

Anderson, N. L., & Anderson, N. G. (1998). Proteome and proteomics: New technologies, new concepts, and new words. In Electrophoresis (Vol. 19).

Aralekallu, S., Boddula, R., & Singh, V. (2023). Development of glass-based microfluidic devices: A review on its fabrication and biologic applications. In Materials and Design (Vol. 225). Elsevier Ltd. https://doi.org/10.1016/j.matdes.2022.111517

Arne Tiselius, B. (1937). A NEW APPARATUS FOR ELECTROPHORETIC ANALYSIS O F COLLOIDAL MIXTURES.

Baek, Y. H., Um, J., Antigua, K. J. C., Park, J. H., Kim, Y., Oh, S., Kim, Y. il, Choi, W. S., Kim, S. G., Jeong, J. H., Chin, B. S., Nicolas, H. D. G., Ahn, J. Y., Shin, K. S., Choi, Y. K., Park, J. S., & Song, M. S. (2020). Development of a reverse transcription-loop-mediated isothermal amplification as a rapid early-detection method for novel SARS-CoV-2. Emerging Microbes and Infections, 9(1), 998–1007. https://doi.org/10.1080/22221751.2020.1756698

Beer, N. R., Hindson, B. J., Wheeler, E. K., Hall, S. B., Rose, K. A., Kennedy, I. M., & Colston, B. W. (2007). On-chip, real-time, single-copy polymerase chain reaction in picoliter droplets. Analytical Chemistry, 79(22), 8471–8475. https://doi.org/10.1021/ac701809w

Beldarrain, L. R., Aldai, N., Picard, B., Sentandreu, E., Navarro, J. L., & Sentandreu, M. A. (2018). Use of liquid isoelectric focusing (OFFGEL) on the discovery of meat tenderness biomarkers. Journal of Proteomics, 183, 25–33. https://doi.org/10.1016/j.jprot.2018.05.005

Bhadra, S., Riedel, T. E., Lakhotia, S., Tran, N. D., & Ellington, A. D. (2021). High-Surety Isothermal Amplification and Detection of SARS-CoV-2. MSphere, 6(3). https://doi.org/10.1128/msphere.00911-20

Bohuslav Gas, Sttidrf, M., & Kenndle, E. (1997). Peak Broadening in Capillary Zone Electrophoresis. Elecrrophoresis, 18(12–13), 2123–2133.

Boobphahom, S., Ly, M. N., Soum, V., Pyun, N., Kwon, O. S., Rodthongkum, N., & Shin, K. (2020). Recent advances in microfluidic paper-based analytical devices toward high-throughput screening. In Molecules (Vol. 25, Issue 13). MDPI AG. https://doi.org/10.3390/molecules25132970

Bryan, A., Fink, S. L., Gattuso, M. A., Pepper, G., Chaudhary, A., Wener, M. H., Morishima, C., Jerome, K. R., Mathias, P. C., & Greninger, A. L. (2020). SARS-CoV-2 Viral Load on Admission Is Associated with 30-Day Mortality. Open Forum Infectious Diseases, 7(12). https://doi.org/10.1093/ofid/ofaa535

Bullard, J., Dust, K., Funk, D., Strong, J. E., Alexander, D., Garnett, L., Boodman, C., Bello, A., Hedley, A., Schiffman, Z., Doan, K., Bastien, N., Li, Y., van Caeseele, P. G., & Poliquin, G. (2020). Predicting infectious severe acute respiratory syndrome coronavirus 2 from diagnostic samples. Clinical Infectious Diseases, 71(10), 2663–2666. https://doi.org/10.1093/cid/ciaa638

Busnel, J. M., Varenne, A., Descroix, S., Peltre, G., Gohon, Y., & Gareil, P. (2005a). Evaluation of capillary isoelectric focusing in glycerol-water media with a view to hydrophobic protein applications. Electrophoresis, 26(17), 3369–3379. https://doi.org/10.1002/elps.200500252

Busnel, J. M., Varenne, A., Descroix, S., Peltre, G., Gohon, Y., & Gareil, P. (2005b). Evaluation of capillary isoelectric focusing in glycerol-water media with a view to hydrophobic protein applications. Electrophoresis, 26(17), 3369–3379. https://doi.org/10.1002/elps.200500252

Calvert, A. E., Biggerstaff, B. J., Tanner, N. A., Lauterbach, M., & Lanciotti, R. S. (2017). Rapid colorimetric detection of Zika virus from serum and urine specimens by reverse transcription loop-mediated isothermal amplification (RT-LAMP). PLoS ONE, 12(9). https://doi.org/10.1371/journal.pone.0185340

Candido, D. S., Claro, I. M., de Jesus, J. G., Souza, W. M., R Moreira, F. R., Dellicour, S., Mellan, T. A., du Plessis, L., M Pereira, R. H., S Sales, F. C., Manuli, E. R., Thézé, J., Almeida, L., Menezes, M. T., Voloch, C. M., Fumagalli, M. J., Coletti, T. M., M da Silva, C. A., Ramundo, M. S., … Rodrigues Faria, N. (2020). Evolution and epidemic spread of SARS-CoV-2 in Brazil. Science, 369, 1255–1260. https://www.science.org

Capriotti, A. L., Cavaliere, C., Foglia, P., Samperi, R., & Laganà, A. (2011). Intact protein separation by chromatographic and/or electrophoretic techniques for top-down proteomics. In Journal of Chromatography A (Vol. 1218, Issue 49, pp. 8760–8776). https://doi.org/10.1016/j.chroma.2011.05.094

Cassedy, A., Parle-McDermott, A., & O'Kennedy, R. (2021). Virus Detection: A Review of the Current and Emerging Molecular and Immunological Methods. In Frontiers in Molecular Biosciences (Vol. 8). Frontiers Media S.A. https://doi.org/10.3389/fmolb.2021.637559

Choi, G., Moehling, T. J., & Meagher, R. J. (2023). Advances in RT-LAMP for COVID-19 testing and diagnosis. In Expert Review of Molecular Diagnostics (Vol. 23, Issue 1, pp. 9–28). Taylor and Francis Ltd. https://doi.org/10.1080/14737159.2023.2169071

Choi, J. R., Tang, R., Wang, S. Q., Wan Abas, W. A. B., Pingguan-Murphy, B., & Xu, F. (2015). Paper-based sample-to-answer molecular diagnostic platform for point-of-care diagnostics. In Biosensors and Bioelectronics (Vol. 74, pp. 427–439). Elsevier Ltd. https://doi.org/10.1016/j.bios.2015.06.065

Chothia, C. (1984). Principles That Determine The Structure Of Proteins. Annual Review of Biochemistry, 53, 537–572. https://doi.org/10.1146/annurev.bi.53.070184.002541

Chow, F. W. N., Chan, T. T. Y., Tam, A. R., Zhao, S., Yao, W., Fung, J., Cheng, F. K. K., Lo, G. C. S., Chu, S., Aw-Yong, K. L., Tang, J. Y. M., Tsang, C. C., Luk, H. K. H., Wong, A. C. P., Li, K. S. M., Zhu, L., He, Z., Tam, E. W. T., Chung, T. W. H., … Lau, S. K. P. (2020). A rapid, simple, inexpensive, and mobile colorimetric assay covid-19-lamp for mass on-site screening of covid-19. International Journal of Molecular Sciences, 21(15), 1–10. https://doi.org/10.3390/ijms21155380

Chowdry, V. K., Luo, Y., Widén, F., Qiu, H. J., Shan, H., Belák, S., & Liu, L. (2014). Development of a loop-mediated isothermal amplification assay combined with a lateral flow dipstick for rapid and simple detection of classical swine fever virus in the field. Journal of Virological Methods, 197, 14–18. https://doi.org/10.1016/j.jviromet.2013.11.013

Chowdury, M. A., & Khalid, F. (2021). Application of microfluidic paper-based analytical device (μPAD) to detect COVID-19 in energy deprived countries. International Journal of Energy Research, 45(12), 18275–18280. https://doi.org/10.1002/er.6958

Chu, D. K. W., Pan, Y., Cheng, S. M. S., Hui, K. P. Y., Krishnan, P., Liu, Y., Ng, D. Y. M., Wan, C. K. C., Yang, P., Wang, Q., Peiris, M., & Poon, L. L. M. (2020). Molecular Diagnosis of a Novel Coronavirus (2019-nCoV) Causing an Outbreak of Pneumonia. Clinical Chemistry, 66(4), 549–555. https://doi.org/10.1093/clinchem/hvaa029

Cohn, E. J., & Mistry, C. (1925). THE PHYSICAL CHEMISTRY OF THE PROTEINS. www.physiology.org/journal/physrev

Conroy, P. J., Hearty, S., Leonard, P., & O'Kennedy, R. J. (2009). Antibody production, design and use for biosensor-based applications. In Seminars in Cell and Developmental Biology (Vol. 20, Issue 1, pp. 10–26). Elsevier Ltd. https://doi.org/10.1016/j.semcdb.2009.01.010

Creighton, T. (1989). Protein structure (T. E. Creighton, Ed.; 2nd ed.). A IRL Press .

Danchana, K., Yamashita, N., Umeda, M. I., & Kaneta, T. (2023). Separation and fractionation of glutamic acid and histidine via origami isoelectric focusing. Journal of Chromatography A, 1706. https://doi.org/10.1016/j.chroma.2023.464247

David Whitford. (2005). Proteins: Structure and Function. Wiley .

Davidson, J. L., Wang, J., Maruthamuthu, M. K., Dextre, A., Pascual-Garrigos, A., Mohan, S., Putikam, S. V. S., Osman, F. O. I., McChesney, D., Seville, J., & Verma, M. S. (2021). A paper-based colorimetric molecular test for SARS-CoV-2 in saliva. Biosensors and Bioelectronics: X, 9. https://doi.org/10.1016/j.biosx.2021.100076

de Oliveira, K. G., Borba, J. C., Bailão, A. M., de Almeida Soares, C. M., Carrilho, E., & Duarte, G. R. M. (2017). Loop-mediated isothermal amplification in disposable polyester-toner microdevices. Analytical Biochemistry, 534, 70–77. https://doi.org/10.1016/j.ab.2017.07.014

De Oliveira, K. G., Estrela, P. F. N., Mendes, G. D. M., Dos Santos, C. A., Silveira-Lacerda, E. D. P., & Duarte, G. R. M. (2021). Rapid molecular diagnostics of COVID-19 by RT-LAMP in a centrifugal polystyrene-Toner based microdevice with end-point visual detection. Analyst, 146(4), 1178–1187. https://doi.org/10.1039/d0an02066d

Dinh, V. P., & Lee, N. Y. (2022). Fabrication of a fully integrated paper microdevice for point-of-care testing of infectious disease using Safranin O dye coupled with loop-mediated isothermal amplification. Biosensors and Bioelectronics, 204. https://doi.org/10.1016/j.bios.2022.114080

Domingo, E. (2020). Introduction to virus origins and their role in biological evolution. In Virus as Populations (pp. 1–33). Elsevier. https://doi.org/10.1016/b978-0-12-816331-3.00001-5

Dorri, Y. (2019). Two-dimensional gel electrophoresis: Vertical isoelectric focusing. In Methods in Molecular Biology (Vol. 1855, pp. 291–302). Humana Press Inc. https://doi.org/10.1007/978-1-4939-8793-1_25

dos Santos, C. A., de Oliveira, K. G., Mendes, G. M., Silva, L. C., de Souza, M. N., Estrela, P. F. N., Guimarães, R. A., Silveira-Lacerda, E. P., & Duarte, G. R. M. (2021). Detection of SARS-CoV-2 in Saliva by RT-LAMP During a Screening of Workers in

Brazil, Including Pre-Symptomatic Carriers. Journal of the Brazilian Chemical Society, 32(11), 2071–2077. https://doi.org/10.21577/0103-5053.20210098

Duarte, G. R. M., Price, C. W., Augustine, B. H., Carrilho, E., & Landers, J. P. (2011). Dynamic solid phase DNA extraction and PCR amplification in polyester-toner based microchip. Analytical Chemistry, 83(13), 5182–5189. https://doi.org/10.1021/ac200292m

El Kennani, S., Crespo, M., Govin, J., & Pflieger, D. (2018). Proteomic analysis of histone variants and their PTMs: Strategies and pitfalls. In Proteomes (Vol. 6, Issue 3). MDPI AG. https://doi.org/10.3390/proteomes6030029

Emrich, C. A., Medintz, I. L., Chu, W. K., & Mathies, R. A. (2007). Microfabricated two-dimensional electrophoresis device for differential protein expression profiling. Analytical Chemistry, 79(19), 7360–7366. https://doi.org/10.1021/ac0711485

Engstrom-Melnyk, J., Rodriguez, P. L., Peraud, O., & Hein, R. C. (2015). Clinical applications of quantitative real-time PCR in virology. In Methods in Microbiology (Vol. 42, pp. 161–197). Academic Press Inc. https://doi.org/10.1016/bs.mim.2015.04.005

Faíco-Filho, K. S., Passarelli, V. C., & Bellei, N. (2020). Is higher viral load in SARS-CoV-2 associated with death? American Journal of Tropical Medicine and Hygiene, 103(5), 2019–2021. https://doi.org/10.4269/ajtmh.20-0954

Fajnzylber, J., Regan, J., Coxen, K., Corry, H., Wong, C., Rosenthal, A., Worrall, D., Giguel, F., Piechocka-Trocha, A., Atyeo, C., Fischinger, S., Chan, A., Flaherty, K. T., Hall, K., Dougan, M., Ryan, E. T., Gillespie, E., Chishti, R., Li, Y., … Zhu, A. (2020). SARS-CoV-2 viral load is associated with increased disease severity and mortality. Nature Communications, 11(1). https://doi.org/10.1038/s41467-020-19057-5

Falahi, S., & Kenarkoohi, A. (2020). Transmission routes for SARS-CoV-2 infection: review of evidence. In New Microbes and New Infections (Vol. 38). Elsevier Ltd. https://doi.org/10.1016/j.nmni.2020.100778

Fan, X., Zhang, X. ;, Bao, H. ;, Zhang, X. ;, & Ping J. (2024). On-chip microscale isoelectric focusing enhances protein detection limit Scilightfeatured. Applied Physics Letters, 124(10), 103701.

Fan, Y., Liu, S., He, J., Gao, K., & Zhang, Y. (2018). Rapid prototyping of flexible multilayer microfluidic devices using polyester sealing film. Microsystem Technologies, 24(6), 2847–2852. https://doi.org/10.1007/s00542-017-3630-3

Farmerie, L., Rustandi, R. R., Loughney, J. W., & Dawod, M. (2021). Recent advances in isoelectric focusing of proteins and peptides. In Journal of Chromatography A (Vol. 1651). Elsevier B.V. https://doi.org/10.1016/j.chroma.2021.462274

Fatima, S., Muzammal, M., Rehman, A., Ullah Shah, K., Kamran, M., Mashal, S., Ali Rustam, S., Waqar Sabir, M., & Nayab, A. (2020). Composition and function of Saliva: a review. WORLD JOURNAL OF PHARMACY AND PHARMACEUTICAL SCIENCES, 9(6). https://doi.org/10.20959/wjpps20206-16334

Fenner, F. , McAuslan, B. R. , Mims, C. A. , Sambrook, J. , & White, D. O. (1974). Cultivation, Assay, and Analysis of Viruses. In B. R. M. C. A. F. Fenner, J. Mims, Sambrook, & D. O. White (Eds.), The Biology of Animal Viruses (pp. 35–57). Academic Press.

Fenton, E. M., Mascarenas, M. R., López, G. P., & Sibbett, S. S. (2009). Multiplex lateral-flow test strips fabricated by two-dimensional shaping. ACS Applied Materials and Interfaces, 1(1), 124–129. https://doi.org/10.1021/am800043z

Fierabracci, A., Arena, A., & Rossi, P. (2020). COVID-19: A review on diagnosis, treatment, and prophylaxis. In International Journal of Molecular Sciences (Vol. 21, Issue 14, pp. 1–16). MDPI AG. https://doi.org/10.3390/ijms21145145

Fu, L. M., Liu, C. C., Yang, C. E., Wang, Y. N., & Ko, C. H. (2019). A PET/paper chip platform for high resolution sulphur dioxide detection in foods. Food Chemistry, 286, 316–321. https://doi.org/10.1016/j.foodchem.2019.02.032

Garcia, B. A. (2010). What Does the Future Hold for Top Down Mass Spectrometry? Journal of the American Society for Mass Spectrometry, 21(2), 193–202. https://doi.org/10.1016/j.jasms.2009.10.014

Garneret, P., Coz, E., Martin, E., Manuguerra, J. C., Brient-Litzler, E., Enouf, V., González Obando, D. F., Olivo-Marin, J. C., Monti, F., van der Werf, S., Vanhomwegen, J., & Tabeling, P. (2021). Performing point-of-care molecular testing for SARS-CoV-2 with RNA extraction and isothermal amplification. PLoS ONE, 16(1 January). https://doi.org/10.1371/journal.pone.0243712

Gaspar, C., Sikanen, T., Franssila, S., & Jokinen, V. (2016). Inkjet printed silver electrodes on macroporous paper for a paper-based isoelectric focusing device. Biomicrofluidics, 10(6). https://doi.org/10.1063/1.4973246

Ghosh, R., Gopalakrishnan, S., Savitha, R., Renganathan, T., & Pushpavanam, S. (2019). Fabrication of laser printed microfluidic paper-based analytical devices (LP-μPADs) for point-of-care applications. Scientific Reports, 9(1). https://doi.org/10.1038/s41598-019-44455-1

Gimenez, T. D., Bailão, A. M., De Almeida Soares, C. M., Fiaccadori, F. S., Borges De Lima Dias E Souza, M., & Duarte, G. R. M. (2017). Dynamic solid-phase RNA extraction from a biological sample in a polyester-toner based microchip. Analytical Methods, 9(13), 2116–2121. https://doi.org/10.1039/c6ay03481k

Gimpelev, M., Forrest, L. R., Murray, D., & Honig, B. (2004). Helical packing patterns in membrane and soluble proteins. Biophysical Journal, 87(6), 4075–4086. https://doi.org/10.1529/biophysj.104.049288

Goodridge, L., Goodridge, C., Wu, J., Griffiths, M., & Pawliszyn, J. (2004). Isoelectric Point Determination of Norovirus Virus-like Particles by Capillary Isoelectric Focusing with Whole Column Imaging Detection. Analytical Chemistry, 76(1), 48–52. https://doi.org/10.1021/ac034848s

Goto, M., Honda, E., Ogura, A., Nomoto, A., & Hanaki, K. I. (2009). Colorimetric detection of loop-mediated isothermal amplification reaction by using hydroxy naphthol blue. BioTechniques, 46(3), 167–172. https://doi.org/10.2144/000113072

Guo, Y., Cupp-Sutton, K. A., Zhao, Z., Anjum, S., & Wu, S. (2023). Multidimensional separations in top–down proteomics. In Analytical Science Advances (Vol. 4, Issues 5–6, pp. 181–203). John Wiley and Sons Inc. https://doi.org/10.1002/ansa.202300016

Guzman, J. M. C. C., Tayo, L. L., Liu, C. C., Wang, Y. N., & Fu, L. M. (2018). Rapid microfluidic paper-based platform for low concentration formaldehyde detection. Sensors and Actuators, B: Chemical, 255, 3623–3629. https://doi.org/10.1016/j.snb.2017.09.080

Han, S. Il, Lee, D., Kim, H., Yoo, Y. K., Kim, C., Lee, J., Kim, K. H., Kim, H., Lee, D., Hwang, K. S., Yoon, D. S., & Lee, J. H. (2019). Electrokinetic size-based spatial separation of micro/nanospheres using paper-based 3d origami preconcentrator. Analytical Chemistry, 91(16), 10744–10749. https://doi.org/10.1021/acs.analchem.9b02201

Han, T., Jin, Y., Geng, C., Aziz, A. ur R., Zhang, Y., Deng, S., Ren, H., & Liu, B. (2020). Microfluidic Paper-based Analytical Devices in Clinical Applications. In Chromatographia (Vol. 83, Issue 6, pp. 693–701). Springer. https://doi.org/10.1007/s10337-020-03892-1

Hasan, M. R., Mirza, F., Al-Hail, H., Sundararaju, S., Xaba, T., Iqbal, M., Alhussain, H., Yassine, H. M., Perez-Lopez, A., & Tang, P. (2020). Detection of SARS-CoV-2 RNA by direct RT-qPCR on nasopharyngeal specimens without extraction of viral RNA. PLoS ONE, 15(7 July). https://doi.org/10.1371/journal.pone.0236564

Hashimoto, M., Barany, F., & Soper, S. A. (2006). Polymerase chain reaction/ligase detection reaction/hybridization assays using flow-through microfluidic devices for the detection of low-abundant DNA point mutations. Biosensors and Bioelectronics, 21(10), 1915–1923. https://doi.org/10.1016/j.bios.2006.01.014

Hasöksüz, M., Kiliç, S., & Saraç, F. (2020). Coronaviruses and sars-cov-2. In Turkish Journal of Medical Sciences (Vol. 50, Issue SI-1, pp. 549–556). Turkiye Klinikleri. https://doi.org/10.3906/sag-2004-127

Hemmateenejad, B., Rafatmah, E., & Shojaeifard, Z. (2023). Microfluidic paper and thread-based separations: Chromatography and electrophoresis. In Journal of Chromatography A (Vol. 1704). Elsevier B.V. https://doi.org/10.1016/j.chroma.2023.464117

Hjertén S. (2003). Stellan Hjertén, Uppsala University. The Analyst, 128(11), 1307–1309. https://doi.org/10.1039/b307798p

Hu, J., Wang, S. Q., Wang, L., Li, F., Pingguan-Murphy, B., Lu, T. J., & Xu, F. (2014). Advances in paper-based point-of-care diagnostics. In Biosensors and Bioelectronics (Vol. 54, pp. 585–597). Elsevier Ltd. https://doi.org/10.1016/j.bios.2013.10.075

Iwamoto, T., Sonobe, T., & Hayashi, K. (2003). Loop-mediated isothermal amplification for direct detection of Mycobacterium tuberculosis complex, M. avium, and M.

intracellulare in sputum samples. Journal of Clinical Microbiology, 41(6), 2616–2622. https://doi.org/10.1128/JCM.41.6.2616-2622.2003

Janin, J., & Chotnia, C. (1985). Domains in Proteins: Definitions, Location, and Structural Principles. Analysis of Structure, 115(28), 420–430.

Jiang, F., Deng, L., Zhang, L., Cai, Y., Cheung, C. W., & Xia, Z. (2020). Review of the Clinical Characteristics of Coronavirus Disease 2019 (COVID-19). In Journal of General Internal Medicine (Vol. 35, Issue 5, pp. 1545–1549). Springer. https://doi.org/10.1007/s11606-020-05762-w

Jin, Y., Yi, Y., & Yeung, B. (2022). Mass spectrometric analysis of protein deamidation – A focus on top-down and middle-down mass spectrometry. In Methods (Vol. 200, pp. 58–66). Academic Press Inc. https://doi.org/10.1016/j.ymeth.2020.08.002

Juang, Y. J., Chen, P. S., & Wang, Y. (2019). Rapid fabrication of microfluidic paper-based analytical devices by microembossing. Sensors and Actuators, B: Chemical, 283, 87–92. https://doi.org/10.1016/j.snb.2018.12.004

Kašička, V. (2024). Recent developments in capillary and microchip electroseparations of peptides (2021–mid-2023). In Electrophoresis (Vol. 45, Issues 1–2, pp. 165–198). John Wiley and Sons Inc. https://doi.org/10.1002/elps.202300152

Keskin, O., Gursoy, A., Ma, B., & Nussinov, R. (2008). Principles of protein-protein interactions: What are the preferred ways for proteins to interact? In Chemical Reviews (Vol. 108, Issue 4, pp. 1225–1244). https://doi.org/10.1021/cr040409x

Kim, M. S., Pinto, S. M., Getnet, D., Nirujogi, R. S., Manda, S. S., Chaerkady, R., Madugundu, A. K., Kelkar, D. S., Isserlin, R., Jain, S., Thomas, J. K., Muthusamy, B., Leal-Rojas, P., Kumar, P., Sahasrabuddhe, N. A., Balakrishnan, L., Advani, J., George, B., Renuse, S., … Pandey, A. (2014). A draft map of the human proteome. Nature, 509(7502), 575–581. https://doi.org/10.1038/nature13302

Klein, S., Müller, T. G., Khalid, D., Sonntag-Buck, V., Heuser, A. M., Glass, B., Meurer, M., Morales, I., Schillak, A., Freistaedter, A., Ambiel, I., Winter, S. L., Zimmermann, L., Naumoska, T., Bubeck, F., Kirrmaier, D., Ullrich, S., Miranda, I. B., Anders, S., … Chlanda, P. (2020). SARS-CoV-2 RNA extraction using magnetic beads for rapid large-scale testing by RT-qPCR and RT-LAMP. Viruses, 12(8). https://doi.org/10.3390/v12080863

Kline, T. R., Runyon, M. K., Pothiawala, M., & Ismagilov, R. F. (2008). ABO, D blood typing and subtyping using plug-based microfluidics. Analytical Chemistry, 80(16), 6190–6197. https://doi.org/10.1021/ac800485q

Kolin, A. (1954). Separation and concentration of proteins in a pH field combined with an electric field. In The Journal of Chemical Physics (Vol. 22, Issue 9, pp. 1628–1629). https://doi.org/10.1063/1.1740497

Lalli, M. A., Langmade, J. S., Chen, X., Fronick, C. C., Sawyer, C. S., Burcea, L. C., Wilkinson, M. N., Fulton, R. S., Heinz, M., Buchser, W. J., Head, R. D., Mitra, R. D., & Milbrandt, J. (2021). Rapid and Extraction-Free Detection of SARS-CoV-2 from Saliva

by Colorimetric Reverse-Transcription Loop-Mediated Isothermal Amplification. Clinical Chemistry, 67(2), 415–424. https://doi.org/10.1093/clinchem/hvaa267

Lamb, L. E., Bartolone, S. N., Ward, E., & Chancellor, M. B. (2020). Rapid detection of novel coronavirus/Severe Acute Respiratory Syndrome Coronavirus 2 (SARS-CoV-2) by reverse transcription-loop-mediated isothermal amplification. PLoS ONE, 15(6). https://doi.org/10.1371/journal.pone.0234682

Lanciotti, R. S., Calisher, C. H., Gubler, D. J., Chang, G.-J., & Vorndamt, A. V. (1992). Rapid Detection and Typing of Dengue Viruses from Clinical Samples by Using Reverse Transcriptase-Polymerase Chain Reaction. In JOURNAL OF CLINICAL MICROBIOLOGY (Vol. 30, Issue 3). https://journals.asm.org/journal/jcm

Landers, J. P. (1997). Handbook of Capillary and Microchip Electrophoresis. In 3rd edition .

Lazar, I. M., Gulakowski, N. S., & Lazar, A. C. (2020). Protein and Proteome Measurements with Microfluidic Chips. In Analytical Chemistry (Vol. 92, Issue 1, pp. 169–182). American Chemical Society. https://doi.org/10.1021/acs.analchem.9b04711

Le, T. H., Nguyen, N. T. B., Truong, N. H., & Van De, N. (2012). Development of mitochondrial loop-mediated isothermal amplification for detection of the small liver fluke Opisthorchis viverrini (opisthorchiidae; trematoda; platyhelminthes). Journal of Clinical Microbiology, 50(4), 1178–1184. https://doi.org/10.1128/JCM.06277-11

Lecoeur, M., Gareil, P., & Varenne, A. (2010). Separation and quantitation of milk whey proteins of close isoelectric points by on-line capillary isoelectric focusing-Electrospray ionization mass spectrometry in glycerol-water media. Journal of Chromatography A, 1217(46), 7293–7301. https://doi.org/10.1016/j.chroma.2010.09.043

Lee, W. C., Ng, H. Y., Hou, C. Y., Lee, C. Te, & Fu, L. M. (2021). Recent advances in lab-on-paper diagnostic devices using blood samples. In Lab on a Chip (Vol. 21, Issue 8, pp. 1433–1453). Royal Society of Chemistry. https://doi.org/10.1039/d0lc01304h

Leland, D. S., & Ginocchio, C. C. (2007). Role of cell culture for virus detection in the age of technology. In Clinical Microbiology Reviews (Vol. 20, Issue 1, pp. 49–78). https://doi.org/10.1128/CMR.00002-06

Lenčo, J., Jadeja, S., Naplekov, D. K., Krokhin, O. V., Khalikova, M. A., Chocholouš, P., Urban, J., Broeckhoven, K., Nováková, L., & Švec, F. (2022a). Reversed-Phase Liquid Chromatography of Peptides for Bottom-Up Proteomics: A Tutorial. Journal of Proteome Research, 21(12), 2846–2892. https://doi.org/10.1021/acs.jproteome.2c00407

Lenčo, J., Jadeja, S., Naplekov, D. K., Krokhin, O. V., Khalikova, M. A., Chocholouš, P., Urban, J., Broeckhoven, K., Nováková, L., & Švec, F. (2022b). Reversed-Phase Liquid Chromatography of Peptides for Bottom-Up Proteomics: A Tutorial. Journal of Proteome Research, 21(12), 2846–2892. https://doi.org/10.1021/acs.jproteome.2c00407

Leon, A., & Pastor, O. (2021). Towards a Shared, Conceptual Model-Based Understanding of Proteins and Their Interactions. IEEE Access, 9, 73608–73623. https://doi.org/10.1109/ACCESS.2021.3080040

Li, A., Sowder, R. C., Henderson, L. E., Moore, S. P., Garfinkel, D. J., & Fisher, R. J. (2001). Chemical cleavage at aspartyl residues for protein identification. Analytical Chemistry, 73(22), 5395–5402. https://doi.org/10.1021/ac010619z

Li, J. J., Xiong, C., Liu, Y., Liang, J. S., & Zhou, X. W. (2016). Loop-mediated isothermal amplification (LAMP): Emergence as an alternative technology for herbal medicine identification. In Frontiers in Plant Science (Vol. 7, Issue DECEMBER2016). Frontiers Media S.A. https://doi.org/10.3389/fpls.2016.01956

Li, Q., An, Z., Sun, T., Ji, S., Wang, W., Peng, Y., Wang, Z., Salentijn, G. I. J., Gao, Z., & Han, D. (2023). Sensitive colorimetric detection of antibiotic resistant Staphylococcus aureus on dairy farms using LAMP with pH-responsive polydiacetylene. Biosensors and Bioelectronics, 219. https://doi.org/10.1016/j.bios.2022.114824

Li, X., Tian, J., & Shen, W. (2010). Thread as a versatile material for low-cost microfluidic diagnostics. ACS Applied Materials and Interfaces, 2(1), 1–6. https://doi.org/10.1021/am9006148

Lim, B., Ratcliff, J., Nawrot, D. A., Yu, Y., Sanghani, H. R., Hsu, C. C., Peto, L., Evans, S., Hodgson, S. H., Skeva, A., Adam, M., Panopoulou, M., Zois, C. E., Poncin, K., Vasudevan, S. R., Dai, S., Ren, S., Chang, H., Cui, Z., … Andersson, M. I. (2021). Clinical validation of optimised RT-LAMP for the diagnosis of SARS-CoV-2 infection. Scientific Reports, 11(1). https://doi.org/10.1038/s41598-021-95607-1

Lim, H., Jafry, A. T., & Lee, J. (2019). Fabrication, flow control, and applications of microfluidic paper-based analytical devices. In Molecules (Vol. 24, Issue 16). MDPI AG. https://doi.org/10.3390/molecules24162869

Lista, M. J., Matos, P. M., Maguire, T. J. A., Poulton, K., Ortiz-Zapater, E., Page, R., Sertkaya, H., Ortega-Prieto, A. M., Scourfield, E., O'Byrne, A. M., Bouton, C., Dickenson, R. E., Ficarelli, M., Jimenez-Guardeño, J. M., Howard, M., Betancor, G., Galao, R. P., Pickering, S., Signell, A. W., … Martinez-Nunez, R. T. (2021). Resilient SARS-CoV-2 diagnostics workflows including viral heat inactivation. PLoS ONE, 16(9 September). https://doi.org/10.1371/journal.pone.0256813

Liu, C. C., Wang, Y. N., Fu, L. M., & Yang, D. Y. (2017). Rapid integrated microfluidic paper-based system for sulfur dioxide detection. Chemical Engineering Journal, 316, 790–796. https://doi.org/10.1016/j.cej.2017.02.023

Liu, S., Li, Z., Yu, B., Wang, S., Shen, Y., & Cong, H. (2020). Recent advances on protein separation and purification methods. Advances in Colloid and Interface Science, 284(102254), 1–23. https://doi.org/10.1016/j.cis.2020.102254

Liu, Y. C., Kuo, R. L., & Shih, S. R. (2020). COVID-19: The first documented coronavirus pandemic in history. In Biomedical Journal (Vol. 43, Issue 4, pp. 328–333). Elsevier B.V. https://doi.org/10.1016/j.bj.2020.04.007

Loan Dao Thi, V., Herbst, K., Boerner, K., Meurer, M., Kremer, L. P., Kirrmaier, D., Freistaedter, A., Papagiannidis, D., Galmozzi, C., Stanifer, M. L., Boulant, S., Klein, S., Chlanda, P., Khalid, D., Barreto Miranda, I., Schnitzler, P., Kräusslich, H.-G., Knop, M., & Anders, S. (2020a). A colorimetric RT-LAMP assay and LAMP-sequencing for detecting SARS-CoV-2 RNA in clinical samples. In Sci. Transl. Med (Vol. 12). https://www.science.org

Loan Dao Thi, V., Herbst, K., Boerner, K., Meurer, M., Kremer, L. P., Kirrmaier, D., Freistaedter, A., Papagiannidis, D., Galmozzi, C., Stanifer, M. L., Boulant, S., Klein, S., Chlanda, P., Khalid, D., Barreto Miranda, I., Schnitzler, P., Kräusslich, H.-G., Knop, M., & Anders, S. (2020b). A colorimetric RT-LAMP assay and LAMP-sequencing for detecting SARS-CoV-2 RNA in clinical samples. In Sci. Transl. Med (Vol. 12). https://www.science.org

Lönnberg, M., & Carlsson, J. (2006). Lab-on-a-chip technology for determination of protein isoform profiles. Journal of Chromatography A, 1127(1–2), 175–182. https://doi.org/10.1016/j.chroma.2006.06.016

Lopes, L. C., Santos, A., & Bueno, P. R. (2022). An outlook on electrochemical approaches for molecular diagnostics assays and discussions on the limitations of miniaturized technologies for point-of-care devices. Sensors and Actuators Reports, 4. https://doi.org/10.1016/j.snr.2022.100087

Lopez-Ruiz, N., Curto, V. F., Erenas, M. M., Benito-Lopez, F., Diamond, D., Palma, A. J., & Capitan-Vallvey, L. F. (2014). Smartphone-based simultaneous pH and nitrite colorimetric determination for paper microfluidic devices. Analytical Chemistry, 86(19), 9554–9562. https://doi.org/10.1021/ac5019205

Lu, R., Wu, X., Wan, Z., Li, Y., Jin, X., & Zhang, C. (2020). A novel reverse transcription loop-mediated isothermal amplification method for rapid detection of sars-cov-2. International Journal of Molecular Sciences, 21(8). https://doi.org/10.3390/ijms21082826

Luo, L., Li, X., & Crooks, R. M. (2014). Low-voltage origami-paper-based electrophoretic device for rapid protein separation. Analytical Chemistry, 86(24), 12390–12397. https://doi.org/10.1021/ac503976c

Macgillivray, A. J., & Wood, D. R. (1974). The Heterogeneity of Mouse-Chromatin Nonhistone Proteins as Evidenced by Two-Dimensional Polyacrylamide-Gel Electrophoresis and Ion-Exchange Chromatography. European Journal of Biochemistry, 41(1), 181–190. https://doi.org/10.1111/j.1432-1033.1974.tb03258.x

Mack, S., Arnold, D., Bogdan, G., Bousse, L., Danan, L., Dolnik, V., Ducusin, M. A., Gwerder, E., Herring, C., Jensen, M., Ji, J., Lacy, S., Richter, C., Walton, I., & Gentalen, E. (2019a). A novel microchip-based imaged CIEF-MS system for comprehensive characterization and identification of biopharmaceutical charge variants. Electrophoresis, 40(23–24), 3084–3091. https://doi.org/10.1002/elps.201900325

Mack, S., Arnold, D., Bogdan, G., Bousse, L., Danan, L., Dolnik, V., Ducusin, M. A., Gwerder, E., Herring, C., Jensen, M., Ji, J., Lacy, S., Richter, C., Walton, I., & Gentalen, E. (2019b). A novel microchip-based imaged CIEF-MS system for comprehensive

characterization and identification of biopharmaceutical charge variants. Electrophoresis, 40(23–24), 3084–3091. https://doi.org/10.1002/elps.201900325

Magleby, R., Westblade, L. F., Trzebucki, A., Simon, M. S., Rajan, M., Park, J., Goyal, P., Safford, M. M., & Satlin, M. J. (2021). Impact of Severe Acute Respiratory Syndrome Coronavirus 2 Viral Load on Risk of Intubation and Mortality among Hospitalized Patients with Coronavirus Disease 2019. Clinical Infectious Diseases, 73(11), E4197–E4205. https://doi.org/10.1093/cid/ciaa851

Mahmud, M. A., Blondeel, E. J. M., Kaddoura, M., & MacDonald, B. D. (2016). Creating compact and microscale features in paper-based devices by laser cutting. Analyst, 141(23), 6449–6454. https://doi.org/10.1039/c6an02208a

Maier, H. J., Bickerton, E., & Britton, P. (2015). Coronaviruses Methods and Protocols Methods in Molecular Biology (1st ed., Vol. 1282). Springer New York Heidelberg Dordrecht London. https://doi.org/10.1007/978-1-4939-2438-7

Mali, S. B. (2015). Proteomics for early diagnostics. In Journal of Craniofacial Surgery (Vol. 26, Issue 4, pp. 1013–1014). Lippincott Williams and Wilkins. https://doi.org/10.1097/SCS.0000000000001705

Mansuy, J. M., Lhomme, S., Cazabat, M., Pasquier, C., Martin-Blondel, G., & Izopet, J. (2018). Detection of Zika, dengue and chikungunya viruses using single-reaction multiplex real-time RT-PCR. Diagnostic Microbiology and Infectious Disease, 92(4), 284–287. https://doi.org/10.1016/j.diagmicrobio.2018.06.019

Manz, A., Graber, N., & Widmer, H. M. (1990). Miniaturized Total Chemical Analysis Systems: a Novel Concept for Chemical Sensing. In Sensors and Actuators.

Mao, Q., & Pawliszyn, J. (1999a). Capillary isoelectric focusing with whole column imaging detection for analysis of proteins and peptides. In J. Biochem. Biophys. Methods (Vol. 39).

Mao, Q., & Pawliszyn, J. (1999b). Demonstration of isoelectric focusing on an etched quartz chip with UV absorption imaging detection †. Analyst, 124, 637–641.

Maráková, K., Opetová, M., & Tomašovský, R. (2023). Capillary electrophoresis-mass spectrometry for intact protein analysis: Pharmaceutical and biomedical applications (2018–March 2023). In Journal of Separation Science (Vol. 46, Issue 15). John Wiley and Sons Inc. https://doi.org/10.1002/jssc.202300244

Marin, M. J., Figuero, E., Herrera, D., & Sanz, M. (2017). Quantitative analysis of periodontal pathogens using real-time polymerase chain reaction (PCR). In Methods in Molecular Biology (Vol. 1537, pp. 191–202). Humana Press Inc. https://doi.org/10.1007/978-1-4939-6685-1_11

Mario Geysen, H., Bartelingt, S. J., & Meloent, R. H. (1985). Small peptides induce antibodies with a sequence and structural requirement for binding antigen comparable to antibodies raised against the native protein (peptide synthesis/antigenic determinant/foot-and-mouth disease virus/immune system) (Vol. 82). https://www.pnas.org

Martinez, A. W., Phillips, S. T., Butte, M. J., & Whitesides, G. M. (2007). Patterned Paper as a Platform for Inexpensive, Low-Volume, Portable Bioassays. Angewandte Chemie, 119(8), 1340–1342. https://doi.org/10.1002/ange.200603817

Martinez, A. W., Phillips, S. T., Whitesides, G. M., & Carrilho, E. (2010). Diagnostics for the developing world: Microfluidic paper-based analytical devices. Analytical Chemistry, 82(1), 3–10. https://doi.org/10.1021/ac9013989

Maurer, M. H. (2011). Proteomic definitions of mesenchymal stem cells. In Stem Cells International. https://doi.org/10.4061/2011/704256

Mayer, H. K., Lenz, K., & Halbauer, E. M. (2021). “A2 milk” authentication using isoelectric focusing and different PCR techniques. Food Research International, 147. https://doi.org/10.1016/j.foodres.2021.110523

McLeish, M. J., Fraile, A., & García-Arenal, F. (2019). Evolution of plant–virus interactions: host range and virus emergence. In Current Opinion in Virology (Vol. 34, pp. 50–55). Elsevier B.V. https://doi.org/10.1016/j.coviro.2018.12.003

Mendes, G. M., d’Orlye, F., Trapiella-Alfonso, L., Duarte, G. R. M., & Varenne, A. (2024). Streamlined integrated protein isoelectric focusing using microfluidic paper-based device. Journal of Chromatography A, 1732. https://doi.org/10.1016/j.chroma.2024.465222

Mendes, G. M., Oliveira, K. G., Borba, J. C., Oliveira, T. S., Fiaccadori, F. S., Nogueira, M. L., Bailão, A. M., Soares, C. M. A., Carrilho, E., & Duarte, G. R. M. (2019). Molecular diagnostics of dengue by reverse transcription-loop mediated isothermal amplification (RT-LAMP) in disposable polyester-toner microdevices. Journal of the Brazilian Chemical Society, 30(9), 1841–1849. https://doi.org/10.21577/0103-5053.20190092

Miller, R. M., & Smith, L. M. (2022). Overview and considerations in bottom-up proteomics. In Analyst (Vol. 148, Issue 3, pp. 475–486). Royal Society of Chemistry. https://doi.org/10.1039/d2an01246d

Millera, R. M., & Smith, L. M. (2023). Overview and considerations in bottom-up proteomics . Analyst, 148(3), 475–486.

Mokaddem, M., Gareil, P., & Varenne, A. (2009). Online CIEF-ESI-MS in glycerol-water media with a view to hydrophobic protein applications. Electrophoresis, 30(23), 4040–4048. https://doi.org/10.1002/elps.200900091

Mora, M. F., Garcia, C. D., Schaumburg, F., Kler, P. A., Berli, C. L. A., Hashimoto, M., & Carrilho, E. (2019). Patterning and Modeling Three-Dimensional Microfluidic Devices Fabricated on a Single Sheet of Paper. Analytical Chemistry, 91(13), 8298–8303. https://doi.org/10.1021/acs.analchem.9b01020

Mora-Cárdenas, E., & Marcello, A. (2017). Switch-on the LAMP to spot Zika. In Annals of Translational Medicine (Vol. 5, Issue 24). AME Publishing Company. https://doi.org/10.21037/atm.2017.10.19

Moradian, A., Kalli, A., Sweredoski, M. J., & Hess, S. (2014). The top-down, middle-down, and bottom-up mass spectrometry approaches for characterization of histone

variants and their post-translational modifications. In Proteomics (Vol. 14, Issues 4–5, pp. 489–497). Wiley-VCH Verlag. https://doi.org/10.1002/pmic.201300256

Morbioli, G. G., Mazzu-Nascimento, T., Stockton, A. M., & Carrilho, E. (2017). Technical aspects and challenges of colorimetric detection with microfluidic paper-based analytical devices (μPADs) - A review. In Analytica Chimica Acta (Vol. 970, pp. 1–22). Elsevier B.V. https://doi.org/10.1016/j.aca.2017.03.037

Mori, Y., Nagamine, K., Tomita, N., & Notomi, T. (2001). Detection of loop-mediated isothermal amplification reaction by turbidity derived from magnesium pyrophosphate formation. Biochemical and Biophysical Research Communications, 289(1), 150–154. https://doi.org/10.1006/bbrc.2001.5921

Mullis, K. B. (1990). The Unusual Origin of the Polymerase Chain Reaction. 262(4), 56–65. https://doi.org/10.2307/24996713

Musso, D., Roche, C., Robin, E., Nhan, T., Teissier, A., & Cao-Lormeau, V. M. (2015). Potential sexual transmission of zika virus. Emerging Infectious Diseases, 21(2), 359–361. https://doi.org/10.3201/eid2102.141363

Nawattanapaiboon, K., Pasomsub, E., Prombun, P., Wongbunmak, A., Jenjitwanich, A., Mahasupachai, P., Vetcho, P., Chayrach, C., Manatjaroenlap, N., Samphaongern, C., Watthanachockchai, T., Leedorkmai, P., Manopwisedjaroen, S., Akkarawongsapat, R., Thitithanyanont, A., Phanchana, M., Panbangred, W., Chauvatcharin, S., & Srikhirin, T. (2021). Colorimetric reverse transcription loop-mediated isothermal amplification (RT-LAMP) as a visual diagnostic platform for the detection of the emerging coronavirus SARS-CoV-2. Analyst, 146(2), 471–477. https://doi.org/10.1039/d0an01775b

Neuzil, P., Pipper, J., & Hsieh, T. M. (2006). Disposable real-time microPCR device: Lab-on-a-chip at a low cost. Molecular BioSystems, 2(6), 292–298. https://doi.org/10.1039/b605957k

Nge, P. N., Rogers, C. I., & Woolley, A. T. (2013). Advances in microfluidic materials, functions, integration, and applications. In Chemical Reviews (Vol. 113, Issue 4, pp. 2550–2583). https://doi.org/10.1021/cr300337x

Nie, Z., & Fung, Y. S. (2008). Microchip capillary electrophoresis for frontal analysis of free bilirubin and study of its interaction with human serum albumin. Electrophoresis, 29(9), 1924–1931. https://doi.org/10.1002/elps.200700596

Niu, J., Bao, Z., Wei, Z., Li, J. , X., Gao, B., Jiang, X., & Li, F. (2021). A three-dimensional paper-based isoelectric focusing device for direct analysis of proteins in physiological samples. Analytical Chemistry, 93(8), 3959–3967. https://doi.org/10.1021/acs.analchem.0c04883

Niu, J. C., Zhou, T., Niu, L. L., Xie, Z. S., Fang, F., Yang, F. Q., & Wu, Z. Y. (2018). Simultaneous pre-concentration and separation on simple paper-based analytical device for protein analysis. Analytical and Bioanalytical Chemistry, 410(6), 1689–1695. https://doi.org/10.1007/s00216-017-0809-5

Notomi, T., Mori, Y., Tomita, N., & Kanda, H. (2015). Loop-mediated isothermal amplification (LAMP): principle, features, and future prospects. In Journal of Microbiology (Vol. 53, Issue 1). Microbiological Society of Korea. https://doi.org/10.1007/s12275-015-4656-9

Notomi, T., Okayama, H., Masubuchi, H., Yonekawa, T., Watanabe, K., Amino, N., & Hase, T. (2000). Loop-mediated isothermal amplification of DNA. In Nucleic Acids Research (Vol. 28, Issue 12).

Nurul Najian, A. B., Engku Nur Syafirah, E. A. R., Ismail, N., Mohamed, M., & Yean, C. Y. (2016). Development of multiplex loop mediated isothermal amplification (m-LAMP) label-based gold nanoparticles lateral flow dipstick biosensor for detection of pathogenic Leptospira. Analytica Chimica Acta, 903, 142–148. https://doi.org/10.1016/j.aca.2015.11.015

Obubuafo, A., Balamurugan, S., Shadpour, H., Spivak, D., McCarley, R. L., & Soper, S. A. (2008). Poly(methyl methacrylate) microchip affinity capillary gel electrophoresis of aptamer-protein complexes for the analysis of thrombin in plasma. Electrophoresis, 29(16 SPEC. ISS.), 3436–3445. https://doi.org/10.1002/elps.200700854

O'farrells, P. H. (1975). High Resolution Two-Dimensional Electrophoresis of Proteins*. Journal of Biological Chemistry, 250(10), 400–4021.

O'Kennedy, R., Fitzgerald, S., & Murphy, C. (2017). Don't blame it all on antibodies – The need for exhaustive characterisation, appropriate handling, and addressing the issues that affect specificity. In TrAC - Trends in Analytical Chemistry (Vol. 89, pp. 53–59). Elsevier B.V. https://doi.org/10.1016/j.trac.2017.01.009

Paez-Espino, D., Eloe-Fadrosh, E. A., Pavlopoulos, G. A., Thomas, A. D., Huntemann, M., Mikhailova, N., Rubin, E., Ivanova, N. N., & Kyrpides, N. C. (2016). Uncovering Earth's virome. Nature, 536(7617), 425–430. https://doi.org/10.1038/nature19094

Pandeswari, P. B., & Sabareesh, V. (2019). Middle-down approach: a choice to sequence and characterize proteins/proteomes by mass spectrometry. In RSC Advances (Vol. 9, Issue 1, pp. 313–344). Royal Society of Chemistry. https://doi.org/10.1039/C8RA07200K

Pandey, C. M., Augustine, S., Kumar, S., Kumar, S., Nara, S., Srivastava, S., & Malhotra, B. D. (2018). Microfluidics Based Point-of-Care Diagnostics. In Biotechnology Journal (Vol. 13, Issue 1). Wiley-VCH Verlag. https://doi.org/10.1002/biot.201700047

Patterson, E. I., Prince, T., Anderson, E. R., Casas-Sanchez, A., Smith, S. L., Cansado-Utrilla, C., Solomon, T., Griffiths, M. J., Acosta-Serrano, Á., Turtle, L., & Hughes, G. L. (2020a). Methods of Inactivation of SARS-CoV-2 for Downstream Biological Assays. Journal of Infectious Diseases, 222(9), 1462–1467. https://doi.org/10.1093/infdis/jiaa507

Patterson, E. I., Prince, T., Anderson, E. R., Casas-Sanchez, A., Smith, S. L., Cansado-Utrilla, C., Solomon, T., Griffiths, M. J., Acosta-Serrano, Á., Turtle, L., & Hughes, G. L. (2020b). Methods of Inactivation of SARS-CoV-2 for Downstream

Biological Assays. Journal of Infectious Diseases, 222(9), 1462–1467. https://doi.org/10.1093/infdis/jiaa507

Perera, A. T. K., Pudasaini, S., Ahmed, S. S. U., Phan, D. T., Liu, Y., & Yang, C. (2020). Rapid pre-concentration of Escherichia coli in a microfluidic paper-based device using ion concentration polarization. Electrophoresis, 41(10–11), 867–874. https://doi.org/10.1002/elps.201900303

Pergande, M. R., & Cologna, S. M. (2017). Isoelectric point separations of peptides and proteins. In Proteomes (Vol. 5, Issue 1). MDPI AG. https://doi.org/10.3390/proteomes5010004

Permentier, H. P., & Bruins, A. P. (2004). Electrochemical oxidation and cleavage of proteins with on-line mass spectrometric detection: Development of an instrumental alternative to enzymatic protein digestion. Journal of the American Society for Mass Spectrometry, 15(12), 1707–1716. https://doi.org/10.1016/j.jasms.2004.09.003

Pujadas, E., Chaudhry, F., McBride, R., Richter, F., Zhao, S., Wajnberg, A., Nadkarni, G., Glicksberg, B. S., Houldsworth, J., & Cordon-Cardo, C. (2020). SARS-CoV-2 viral load predicts COVID-19 mortality. In The Lancet Respiratory Medicine (Vol. 8, Issue 9, p. e70). Lancet Publishing Group. https://doi.org/10.1016/S2213-2600(20)30354-4

Qin, L., Vermesh, O., Shi, Q., & Heath, J. R. (2009). Self-powered microfluidic chips for multiplexed protein assays from whole blood. Lab on a Chip, 9(14), 2016–2020. https://doi.org/10.1039/b821247c

Rabaan, A. A., Al-Ahmed, S. H., Al-Malkey, M. K., Alsubki, R. A., Ezzikouri, S., Hassan Al-Hababi, F., Sah, R., Al Mutair, A., Alhumaid, S., Al, J. A., Alshahrani, F., Bahadur Shrestha, D., Isaqali Karobari, M., & Arabia, S. (2021). Airborne transmission of SARS-CoV-2 is the dominant route of transmission: droplets and aerosols King Fahad Medical City. Le Infezioni in Medicina, 12(1), 10–19.

Rabilloud, T., Chevallet, M., Luche, S., & Lelong, C. (2010). Two-dimensional gel electrophoresis in proteomics: Past, present and future. In Journal of Proteomics (Vol. 73, Issue 11, pp. 2064–2077). https://doi.org/10.1016/j.jprot.2010.05.016

Rahman, M., Uddin, M., Sultana, R., Moue, A., & Setu, M. (2013). Polymerase Chain Reaction (PCR): A Short Review. Anwer Khan Modern Medical College Journal, 4(1), 30–36.

Ramalingam, A., Kudapa, H., Pazhamala, L. T., Weckwerth, W., & Varshney, R. K. (2015). Proteomics and metabolomics: Two emerging areas for legume improvement. In Frontiers in Plant Science (Vol. 6, Issue DEC). Frontiers Media S.A. https://doi.org/10.3389/fpls.2015.01116

Reddy, B. L., & Saier, M. H. (2020). The Causal Relationship between Eating Animals and Viral Epidemics. In Microbial Physiology (Vol. 30, Issue 6, pp. 2–8). S. Karger AG. https://doi.org/10.1159/000511192

Reyes, D. R., Iossifidis, D., Auroux, P. A., & Manz, A. (2002). Micro total analysis systems. 1. Introduction, theory, and technology. In Analytical Chemistry (Vol. 74, Issue 12, pp. 2623–2636). https://doi.org/10.1021/ac0202435

Righetti, P. G. (1984). ISOELECTRIC FOCUSING IN IMMOBILIZED pH GRADIENTS. In Journal of Chromatography (Vol. 300).

Righetti, P. G. (2004). Determination of the isoelectric point of proteins by capillary isoelectric focusing. Journal of Chromatography A, 1037(1–2), 491–499. https://doi.org/10.1016/j.chroma.2003.11.025

Righetti, P. G., & Bossi, A. (1997). Isoelectric focusing in immobilized pH gradients: an update. In Journal of Chromatography B (Vol. 699).

Righetti, P. G., Sebastiano, R., & Citterio, A. (2013). Capillary electrophoresis and isoelectric focusing in peptide and protein analysis. Proteomics, 13(2), 325–340. https://doi.org/10.1002/pmic.201200378

Ríos, Á., Zougagh, M., & Avila, M. (2012). Miniaturization through lab-on-a-chip: Utopia or reality for routine laboratories? A review. In Analytica Chimica Acta (Vol. 740, pp. 1–11). https://doi.org/10.1016/j.aca.2012.06.024

Rodriguez-Diaz, R., Wehr, T., Zhu, M., Rodriguez-Diaz', R., & Wehr', T. (1997). Capillary isoelectric focwsing. In Elecrrophorcsrs (Vol. 18).

Rosenfeld, T., & Bercovici, M. (2018). Amplification-free detection of DNA in a paper-based microfluidic device using electroosmotically balanced isotachophoresis. Lab on a Chip, 18(6), 861–868. https://doi.org/10.1039/c7lc01250k

Rudge, S. R., & Monnig, C. A. (2000). Electrophoresis techniques. Separation and Purification Methods, 29(1), 129–148. https://doi.org/10.1081/SPM-100100006

Sanchez, J.-Charles., Corthals, G. L., & Hochstrasser, D. F. (2004). Biomedical applications of proteomics. Wiley-VCH.

Sanjuán, R., & Domingo-Calap, P. (2016). Mechanisms of viral mutation. In Cellular and Molecular Life Sciences (Vol. 73, Issue 23, pp. 4433–4448). Birkhauser Verlag AG. https://doi.org/10.1007/s00018-016-2299-6

Schaumburg, F., Kler, P. A., Carrell, C. S., Berli, C. L. A., & Henry, C. S. (2020). USB powered microfluidic paper-based analytical devices. Electrophoresis, 41(7–8), 562–569. https://doi.org/10.1002/elps.201900273

Schräder, C. U., Lee, L., Rey, M., Sarpe, V., Man, P., Sharma, S., Zabrouskov, V., Larsen, B., & Schriemer, D. C. (2017). Neprosin, a Selective Prolyl Endoprotease for Bottom-up Proteomics and Histone Mapping* □ S. Molecular and Cellular Proteomics, 16, 1162–1171. https://doi.org/10.1074/mcp

Scott, A. T., Layne, T. R., O'Connell, K. C., Tanner, N. A., & Landers, J. P. (2020). Comparative Evaluation and Quantitative Analysis of Loop-Mediated Isothermal Amplification Indicators. Analytical Chemistry, 92(19), 13343–13353. https://doi.org/10.1021/acs.analchem.0c02666

See, I., Paul, P., Slayton, R. B., Steele, M. K., Stuckey, M. J., Duca, L., Srinivasan, A., Stone, N., Jernigan, J. A., & Reddy, S. C. (2021). Modeling Effectiveness of Testing Strategies to Prevent Coronavirus Disease 2019 (COVID-19) in Nursing Homes -

United States, 2020. Clinical Infectious Diseases, 73(3), E792–E798. https://doi.org/10.1093/cid/ciab110

Sena-Torralba, A., Banguera-Ordoñez, Y. D., Mira-Pascual, L., Maquieira, Á., & Morais, S. (2023). Exploring the potential of paper-based electrokinetic phenomena in PoC biosensing. In Trends in Biotechnology (Vol. 41, Issue 10, pp. 1299–1313). Elsevier Ltd. https://doi.org/10.1016/j.tibtech.2023.04.004

Shakeri, A., Khan, S., & Didar, T. F. (2021). Conventional and emerging strategies for the fabrication and functionalization of PDMS-based microfluidic devices. In Lab on a Chip (Vol. 21, Issue 16, pp. 3053–3075). Royal Society of Chemistry. https://doi.org/10.1039/d1lc00288k

Shameli, S. M., Elbuken, C., Ou, J., Ren, C. L., & Pawliszyn, J. (2011). Fully integrated PDMS/SU-8/quartz microfluidic chip with a novel macroporous poly dimethylsiloxane (PDMS) membrane for isoelectric focusing of proteins using whole-channel imaging detection. Electrophoresis, 32(3–4), 333–339. https://doi.org/10.1002/elps.201000643

Shen, X., Young, R., Canty, J. M., & Qu, J. (2014). Quantitative proteomics in cardiovascular research: Global and targeted strategies. In Proteomics - Clinical Applications (Vol. 8, Issues 7–8, pp. 488–505). Wiley-VCH Verlag. https://doi.org/10.1002/prca.201400014

Shortreed, M. R., Wenger, C. D., Frey, B. L., Sheynkman, G. M., Scalf, M., Keller, M. P., Attie, A. D., & Smith, L. M. (2015). Global identification of protein post-translational modifications in a single-pass database search. Journal of Proteome Research, 14(11), 4714–4720. https://doi.org/10.1021/acs.jproteome.5b00599

Shrivas, K., Monisha, Patel, S., Thakur, S. S., & Shankar, R. (2020). Food safety monitoring of the pesticide phenthoate using a smartphone-assisted paper-based sensor with bimetallic Cu@Ag core-shell nanoparticles. Lab on a Chip, 20(21), 3996–4006. https://doi.org/10.1039/d0lc00515k

Sidoli, S., Bhanu, N. V., Karch, K. R., Wang, X., & Garcia, B. A. (2016). Complete workflow for analysis of histone post-translational modifications using bottom-up mass spectrometry: From histone extraction to data analysis. Journal of Visualized Experiments, 2016(111). https://doi.org/10.3791/54112

Sidoli, S., & Garcia, B. A. (2017). Middle-down proteomics: a still unexploited resource for chromatin biology. In Expert Review of Proteomics (Vol. 14, Issue 7, pp. 617–626). Taylor and Francis Ltd. https://doi.org/10.1080/14789450.2017.1345632

Silva, L. D. C., Dos Santos, C. A., Mendes, G. D. M., Oliveira, K. G. De, De Souza Júnior, M. N., Estrela, P. F. N., Costa, S. H. N., Silveira-Lacerda, E. D. P., & Duarte, G. R. M. (2021). Can a field molecular diagnosis be accurate? A performance evaluation of colorimetric RT-LAMP for the detection of SARS-CoV-2 in a hospital setting. Analytical Methods, 13(26), 2898–2907. https://doi.org/10.1039/d1ay00481f

Silvertand, L. H. H., Toraño, J. S., van Bennekom, W. P., & de Jong, G. J. (2008). Recent developments in capillary isoelectric focusing. In Journal of Chromatography A (Vol. 1204, Issue 2, pp. 157–170). https://doi.org/10.1016/j.chroma.2008.05.057

Singh, R., Savargaonkar, D., Bhatt, R., & Valecha, N. (2013). Rapid detection of Plasmodium vivax in saliva and blood using loop mediated isothermal amplification (LAMP) assay. In Journal of Infection (Vol. 67, Issue 3, pp. 245–247). https://doi.org/10.1016/j.jinf.2013.04.016

Skjærvø, Ø., Halvorsen, T. G., & Reubsaet, L. (2019). All-in-one paper-based sampling chip for targeted protein analysis. Analytica Chimica Acta, 1089, 56–65. https://doi.org/10.1016/j.aca.2019.08.043

Snyder, S. A., Boban, M., Li, C., Vanepps, J. S., Mehta, G., & Tuteja, A. (2020). Lysis and direct detection of coliforms on printed paper-based microfluidic devices. Lab on a Chip, 20(23), 4413–4419. https://doi.org/10.1039/d0lc00665c

Sohn, Y., Jeong, S. J., Chung, W. S., Hyun, J. H., Baek, Y. J., Cho, Y., Kim, J. H., Ahn, J. Y., Choi, J. Y., & Yeom, J. S. (2020). Assessing viral shedding and infectivity of asymptomatic or mildly symptomatic patients with COVID-19 in a later phase. Journal of Clinical Medicine, 9(9), 1–9. https://doi.org/10.3390/jcm9092924

Song, J., El-Tholoth, M., Li, Y., Graham-Wooten, J., Liang, Y., Li, J., Li, W., Weiss, S. R., Collman, R. G., & Bau, H. H. (2021). Single- And Two-Stage, Closed-Tube, Point-of-Care, Molecular Detection of SARS-CoV-2. Analytical Chemistry, 93(38), 13063–13071. https://doi.org/10.1021/acs.analchem.1c03016

Štěpánová, S., & Kašička, V. (2022). Applications of capillary electromigration methods for separation and analysis of proteins (2017–mid 2021) – A review. In Analytica Chimica Acta (Vol. 1209). Elsevier B.V. https://doi.org/10.1016/j.aca.2022.339447

Štěpánová, S., & Kašička, V. (2023). Recent developments and applications of capillary and microchip electrophoresis in proteomics and peptidomics (mid-2018–2022). Journal of Separation Science, 46(12). https://doi.org/10.1002/jssc.202300043

Sue P. Humphrey, R. Mse. and R. T. W. Dmd. (2001). A review of saliva: Normal composition, flow, and function. In THE JOURNAL OF PROSTHETIC DENTISTRY (Vol. 85, Issue 9). https://doi.org/doi:10.1067/mpr.2001.113778

Tainturierd D., Braun J.P, Rico A.G., & Thouvenot J.P. (1984). Variations in blood composition in dairy cows during pregnancy and after calving. Research in Veterinary Science , 37, 129–131.

Tanner, N. A., Zhang, Y., & Evans, T. C. (2015). Visual detection of isothermal nucleic acid amplification using pH-sensitive dyes. BioTechniques, 58(2), 59–68. https://doi.org/10.2144/000114253

Tata Rao, L., Rewatkar, P., Dubey, S. K., Javed, A., & Goel, S. (2020). Performance optimization of microfluidic paper fuel-cell with varying cellulose fiber papers as absorbent pad. International Journal of Energy Research, 44(5), 3893–3904. https://doi.org/10.1002/er.5188

Teo, A. K. J., Choudhury, Y., Tan, I. B., Cher, C. Y., Chew, S. H., Wan, Z. Y., Cheng, L. T. E., Oon, L. L. E., Tan, M. H., Chan, K. S., & Hsu, L. Y. (2021). Saliva is more sensitive

than nasopharyngeal or nasal swabs for diagnosis of asymptomatic and mild COVID-19 infection. Scientific Reports, 11(1). https://doi.org/10.1038/s41598-021-82787-z

Terry, S. C., Jerman, J. H., & Angell, J. B. (1979). A Gas Chromatographic Air Analyzer Fabricated on a Silicon Wafer. IEEE Trans. Electron Dev., 26(12), 1880–1886.

Thompson, D., & Lei, Y. (2020). Mini review: Recent progress in RT-LAMP enabled COVID-19 detection. In Sensors and Actuators Reports (Vol. 2, Issue 1). Elsevier B.V. https://doi.org/10.1016/j.snr.2020.100017

Toby, T. K., Fornelli, L., & Kelleher, N. L. (2016). Progress in Top-Down Proteomics and the Analysis of Proteoforms. In Annual Review of Analytical Chemistry (Vol. 9, pp. 499–519). Annual Reviews Inc. https://doi.org/10.1146/annurev-anchem-071015-041550

Tom, M. R., & Mina, M. J. (2020). To Interpret the SARS-CoV-2 Test, Consider the Cycle Threshold Value. In Clinical Infectious Diseases (Vol. 71, Issue 16, pp. 2252–2254). Oxford University Press. https://doi.org/10.1093/cid/ciaa619

Tomita, N., Mori, Y., Kanda, H., & Notomi, T. (2008a). Loop-mediated isothermal amplification (LAMP) of gene sequences and simple visual detection of products. Nature Protocols, 3(5), 877–882. https://doi.org/10.1038/nprot.2008.57

Tomita, N., Mori, Y., Kanda, H., & Notomi, T. (2008b). Loop-mediated isothermal amplification (LAMP) of gene sequences and simple visual detection of products. Nature Protocols, 3(5), 877–882. https://doi.org/10.1038/nprot.2008.57

Trinh, K. T. L., Chae, W. R., & Lee, N. Y. (2022). Recent advances in the fabrication strategies of paper-based microfluidic devices for rapid detection of bacteria and viruses. In Microchemical Journal (Vol. 180). Elsevier Inc. https://doi.org/10.1016/j.microc.2022.107548

Uribe-Alvarez, C., Lam, Q., Baldwin, D. A., & Chernoff, J. (2021). Low saliva pH can yield false positives results in simple RT-LAMP-based SARS-CoV-2 diagnostic tests. PLoS ONE, 16(5 May). https://doi.org/10.1371/journal.pone.0250202

Van Anh, N., Van Trung, H., Tien, B. Q., Binh, N. H., Ha, C. H., Le Huy, N., Loc, N. T., Thu, V. T., & Lam, T. D. (2016). Development of a PMMA Electrochemical Microfluidic Device for Carcinoembryonic Antigen Detection. Journal of Electronic Materials, 45(5), 2455–2462. https://doi.org/10.1007/s11664-016-4372-1

Vilkner, T., Janasek, D., & Manz, A. (2004). Micro total analysis systems. Recent developments. In Analytical Chemistry (Vol. 76, Issue 12, pp. 3373–3386). https://doi.org/10.1021/ac040063q

Vitorino, R., Guedes, S., da Costa, J. P., & Kašička, V. (2021). Microfluidics for peptidomics, proteomics, and cell analysis. In Nanomaterials (Vol. 11, Issue 5). MDPI AG. https://doi.org/10.3390/nano11051118

Walgama, C., Nguyen, M. P., Boatner, L. M., Richards, I., & Crooks, R. M. (2020). Hybrid paper and 3D-printed microfluidic device for electrochemical detection of Ag

nanoparticle labels. Lab on a Chip, 20(9), 1648–1657. https://doi.org/10.1039/d0lc00276c

Wang, C. H., Lien, K. Y., Wang, T. Y., Chen, T. Y., & Lee, G. Bin. (2011). An integrated microfluidic loop-mediated-isothermal-amplification system for rapid sample pre-treatment and detection of viruses. Biosensors and Bioelectronics, 26(5), 2045–2052. https://doi.org/10.1016/j.bios.2010.08.083

Wastling, S. L., Picozzi, K., Kakembo, A. S. L., & Welburn, S. C. (2010). LAMP for human African trypanosomiasis: A comparative study of detection formats. PLoS Neglected Tropical Diseases, 4(11). https://doi.org/10.1371/journal.pntd.0000865

Watzinger, F., Ebner, K., & Lion, T. (2006). Detection and monitoring of virus infections by real-time PCR. In Molecular Aspects of Medicine (Vol. 27, Issues 2–3, pp. 254–298). https://doi.org/10.1016/j.mam.2005.12.001

Wilkins, M. R., Sanchez, J. C., Gooley, A. A., Appel, R. D., Humphery-Smith, I., Hochstrasser, D. F., & Williams, K. L. (1996). Progress with proteome projects: Why all proteins expressed by a genome should be identified and how to do it. Biotechnology and Genetic Engineering Reviews, 13(1), 19–50. https://doi.org/10.1080/02648725.1996.10647923

Wilkins1, M. R., Pasquali2, C., Appel2, R. D., Ou1, K., Golar, O., Sanchez2, J.-C., Yan1, J. X., Gooley1, A. A., Hughes, G., Humphery-Smith3, I., Wlliams, K. L., & Hochstrasser2, D. F. (1996). • From Proteins to Proteomes: Large Scale Protein Identification by Two-Dimensional Electrophoresis and Amino Acid Analysis 6-a. In BIOTECHNOLOGY (Vol. 14). http://www.nature.com/naturebiotechnology

Xie, S. F., Gao, H., Niu, L. L., Xie, Z. S., Fang, F., Wu, Z. Y., & Yang, F. Q. (2018). Carrier ampholyte-free isoelectric focusing on a paper-based analytical device for the fractionation of proteins. Journal of Separation Science, 41(9), 2085–2091. https://doi.org/10.1002/jssc.201701438

Xu, T., Han, L., George Thompson, A. M., & Sun, L. (2022). An improved capillary isoelectric focusing-mass spectrometry method for high-resolution characterization of monoclonal antibody charge variants. Analytical Methods, 14(4), 383–393. https://doi.org/10.1039/D1AY01556G

Xuan, X. (2022). Review of nonlinear electrokinetic flows in insulator-based dielectrophoresis: From induced charge to Joule heating effects. In Electrophoresis (Vol. 43, Issues 1–2, pp. 167–189). John Wiley and Sons Inc. https://doi.org/10.1002/elps.202100090

Yagoda, H. (1937). Applications of Confined Spot Tests in Analytical Chemistry. INDUSTRIAL AND ENGINEERING CHEMISTRY, 9(2), 79–82.

Yang, M., Zhang, W., Zheng, W., Cao, F., & Jiang, X. (2017). Inkjet-printed barcodes for a rapid and multiplexed paper-based assay compatible with mobile devices. Lab on a Chip, 17(22), 3874–3882. https://doi.org/10.1039/c7lc00780a

Yang, S. M., Lv, S., Zhang, W., & Cui, Y. (2022). Microfluidic Point-of-Care (POC) Devices in Early Diagnosis: A Review of Opportunities and Challenges. In Sensors (Vol. 22, Issue 4). MDPI. https://doi.org/10.3390/s22041620

Yu, P., Deng, M., Yang, Y., Nie, B., & Zhao, S. (2020). 3d microfluidic devices in a single piece of paper for the simultaneous determination of nitrite and thiocyanate. Sensors (Switzerland), 20(15), 1–15. https://doi.org/10.3390/s20154118

Yu, S., Yan, C., Hu, X., He, B., Jiang, Y., & He, Q. (2019). Isoelectric focusing on microfluidic paper-based chips. Analytical and Bioanalytical Chemistry, 411(21), 5415–5422. https://doi.org/10.1007/s00216-019-02008-5

Zha, G., Xiao, X., Tian, Y., Zhu, H., Chen, P., Zhang, Q., Yu, C., Li, H., Wang, Y., & Cao, C. (2023). An efficient isoelectric focusing of microcolumn array chip for screening of adult Beta-Thalassemia. Clinica Chimica Acta, 538, 124–130. https://doi.org/10.1016/j.cca.2022.10.021

Zhai, H. M., Zhou, T., Fang, F., & Wu, Z. Y. (2020). Colorimetric speciation of Cr on paper-based analytical devices based on field amplified stacking. Talanta, 210. https://doi.org/10.1016/j.talanta.2019.120635

Zhang, X. X., Liu, J. J., Cai, Y., Zhao, S., & Wu, Z. Y. (2019). A field amplification enhanced paper-based analytical device with a robust chemiluminescence detection module. Analyst, 144(2), 498–503. https://doi.org/10.1039/c8an01859f

Zhao, L., Seth-Pasricha, M., Dragos¸stemate, D. D., Crespo-Bellido, A., Gagnon, J., Draghi, J., Duffy, S., & Pfeiffer, J. K. (2019). Existing Host Range Mutations Constrain Further Emergence of RNA Viruses. Jvi.Asm.Org 1 Journal of Virology, 93, 1385–1403. https://doi.org/10.1128/JVI

Zhao, Y., Pereira, F., Demello, A. J., Morgan, H., & Niu, X. (2014). Droplet-based in situ compartmentalization of chemically separated components after isoelectric focusing in a Slipchip. Lab on a Chip, 14(3), 555–561. https://doi.org/10.1039/c3lc51067k

Zhu, J., Guo, J., Xu, Y., & Chen, X. (2020). Viral dynamics of SARS-CoV-2 in saliva from infected patients. In Journal of Infection (Vol. 81, Issue 3, pp. e48–e50). W.B. Saunders Ltd. https://doi.org/10.1016/j.jinf.2020.06.059

General Introduction

Back in 2020, when the World Health Organization declared COVID-19 a pandemic, our research group already had significant experience in developing disposable, cost-effective point-of-care diagnostic tests for arboviruses. This expertise was rooted in our pioneering work with the LAMP (Loop-Mediated Isothermal Amplification) technique. At the time of our first LAMP publication, only seven articles from Brazil had been published that year on the Web of Science platform. Since then, our group has continued to contribute to the field with several additional studies utilizing the LAMP assay.

So, as the pandemic spread around the world and the first infections occurred in Goiania, our group started the studies for the development of a simple, affordable, disposable, and applicable in that emergency. Unlike other techniques, such as PCR (the gold standard), LAMP is less affected by inhibitors, enabling the direct use of various biological samples—such as serum, whole blood, urine, oral fluid, and semen—without needing prior nucleic acid extraction. This made LAMP particularly suitable for the public health crisis we were facing.

During the pandemic in Brazil, as in many other countries, hospitals were overwhelmed. Among the contributing factors were significant delays between hospital admission, sample collection, and final diagnosis, which exacerbated the strain on healthcare facilities. Implementing point-of-care testing (POCT) could significantly reduce the time to results, providing an effective solution to improve patient flow. Given the urgency of the situation, we have developed a LAMP assay for COVID-19 diagnosis, as it offered a rapid, sensitive, and low-cost testing method suitable for

point-of-care use. Due to time constraints and the emergency nature of the pandemic, the LAMP method was developed and validated using polypropylene microtubes, with plans to later adapt the methodology to a microfluidic platform.

This chapter reports our study of a colorimetric pH-based RT-LAMP assay for detecting SARS-CoV-2 in a hospital setting. This approach was designed to rapidly guide treatment decisions for infected patients, minimize the risk of cross-infection among non-COVID-19 patients due to delayed diagnosis, and shorten the time between admission and diagnosis. The chapter corresponds to the publication of this study, which was titled “Can a field molecular diagnosis be accurate? A performance evaluation of colorimetric RT-LAMP for the detection of SARS-CoV-2 in a hospital setting,” and published (front cover) in 2021 in Analytical Methods (Silva et al., 2021).

Chapter II: Can a field molecular diagnosis be accurate? A performance evaluation of colorimetric RT-LAMP for the detection of SARS-CoV-2 in a hospital setting

ABSTRACT

SARS-CoV-2 currently represents a serious global public health problem. Non-pharmaceutical intervention measures (NPIs) have been widely adopted, and the testing strategy since the beginning of the infection is the most effective tool for tracking, isolating, and minimizing transmission. The high operating costs and the need for sophisticated instrumentation related to gold standard diagnostic for COVID-19, Reverse Transcription quantitative Polymerase Chain Reaction (RT-qPCR), have highlighted the urgency and importance of developing and applying new diagnostic techniques, especially in places with scarce resources. Thus, alternative molecular tests, such as Reverse Transcription Loop-Mediated Isothermal Amplification (RT-LAMP), based on isothermal amplification have been used to detect SARS-CoV-2 using different protocols. The potential for field application of RT-LAMP is due to the lower cost and time and not requiring high-cost instrumentation. Here, we evaluate the colorimetric RT-LAMP to detect SARSCoV-2 in a hospital environment and correlate its performance with tests performed in a reference laboratory. The analysis performed at the hospital showed high sensitivity (88.89%), specificity (98.55%), accuracy (95.83%), and a Cohen's kappa of 0.895. However, we achieved 100% of agreement when comparing the RT-LAMP results with the gold standard results for samples with Ct < 30 in the hospital-based test. In addition, a similar performance was found in the field compared to the reference laboratory, corroborating the proposal to apply the test directly at point-of-care.

Introduction

Since 2020, the world has experienced a serious public health crisis caused by the rapid spread of severe acute respiratory syndrome coronavirus 2 (SARS-CoV-2). Once infected with SARS-CoV-2, patients can develop COVID-19, a respiratory syndrome that is, in mild cases, characterized mainly by cough, fever, tiredness, and loss of taste or smell. In severe cases, symptoms can evolve to shortness of breath and pneumonia, and medical assistance is required.[1,2] Therefore, it is essential to correctly diagnose infected patients so that they can be isolated and properly monitored. This measure can decrease the infection rate, thus avoiding hospital overload and reducing the number of new infections and deaths.[3]

The current SARS-CoV-2 diagnostic tools available are based on the detection of human antibodies,[4] viral antigens,[5] and viral nucleic acid.[6] The tests based on the identification of viral nucleic acid, such as RT-qPCR, are considered the “gold standard” and offer a sensitive and early detection of SARS-CoV-2.[7] The RT-qPCR is able to quantify the viral load that is determined by the value of the cycle threshold (Ct). The Ct is a parameter that determines the start of the exponential amplification, when the signal of the samples differs from the NTC (no template control) signal. Thus, the higher the viral load, the faster the amplification will occur and, therefore, the lower the Ct value, allowing the amplification time to be correlated with the viral RNA quantity. Although a very sensitive technique, RT-qPCR requires high-cost instrumentation and highly trained personnel.[8] In developing countries, these requirements are fatal drawbacks for mass testing, as laboratories suitable for performing RT-qPCR are

usually located in larger cities. As a consequence of the lack of testing, there is underreporting in the number of cases, and the real scenario is unknown.[9]

Alternative protocols for fast, inexpensive, easy to implement, and reliable molecular diagnostics are a current need. Among the new proposals, isothermal amplification methods such as LAMP (loop-mediated isothermal amplification) have emerged as suitable options that overcome the difficulties found in performing RT-qPCR.[10] Mautner et al. (2020) described the detection of SARS-CoV-2 applicable in point-of-care situations using a RT-LAMP methodology.[11] The authors reported that their assay is 12 times faster and 10 times cheaper than routine reverse transcription real-time polymerase chain reaction, depending on the assay used. Rodriguez-Manzano and coworkers (2021) reported the Development of a diagnostic test applicable in the point of care, detecting SARS-CoV-2 RNA under 20 min using semiconductor technology.[12] Wei et al. (2021) recently described an RT-LAMP colorimetric test directly on clinical samples of nasopharyngeal swab in viral transport medium with 85% positive percentage agreement and 100% negative percentage agreement. The authors highlight the good cost-effectiveness and short time (30 min) without the need for specialized or proprietary equipment or reagents.[13]

Since it is not strongly affected by inhibitors, a variety of biological samples, such as serum,[14] whole blood,[15] urine,[16] oral fuid,[17] and semen,[18] can be used in the LAMP assay without the prior need for nucleic acid extraction. For these reasons, it can be applied in situations and places with scarce resources since it does not require sophisticated equipment or laborious stages of sample preparation.[19]

During the pandemic, due to the increase in demand that exceeded hospital capacity, significant delays between hospital admission, sample collection, and final diagnosis have been evidenced. This delay is likely influenced by the logistic difficulties in transporting patient samples to centralized laboratories for RT-qPCR testing. Point-of-care testing significantly lowers the time to result, and it is an interesting approach that improves patient flow.[20] A rapid, sensitive, and low-cost test to detect positive cases that is applicable at point-of-care could assist in improving the response measures to halt the spread of the virus. In addition, the test performed in a hospital setting would be able to quickly guide treatment for infected patients, ensure that non-COVID-19 patients are not infected within the hospital facilities due to delay in diagnosis, and shorten the time between admission and diagnosis.

Although several studies have demonstrated the potential applicability of the RT-LAMP technique in the field,[10,21,22] such application to SARS-CoV-2 field detection is still poorly documented. Thus, in this present study, we evaluate the performance of RT-LAMP applied in a reference laboratory and the hospital to detect SARS-CoV-2. The colorimetric RT-LAMP was evaluated against RT-qPCR by testing 206 clinical specimens provided by the Hospital do Policial Militar, Goias-Brazil. The successful performance of the colorimetric RT-LAMP for detecting SARS-CoV-2 in both environments demonstrated a great potential for point-of-care applications.

MATERIALS AND METHODS

Biological samples and thermal treatment after swab collection

Nasopharyngeal samples of 206 patients suspected of COVID-19 admitted at the “Hospital do Policial Militar” during December 2020 and January 2021 were collected using swabs and stored in a cryotube containing 1 mL 0.9% NaCl solution. To inactivate the virus and lyse some of the sample content, all samples were heat-treated in a thermoblock at 95 °C for 10 min before testing. A total of 110 samples were analyzed at the reference laboratory, and 96 samples were analyzed directly at the hospital.

The study was conducted after approval by the Research Ethics Committee of the Federal University of Goias, with protocol number no. 4.111.485. All experiments were performed in compliance with nationally required guidelines, following the resolutions CNS 466/12 and CNS 441/11, and in compliance with institutional guidelines. All patients agreed to participate in the study with a written statement, according to local regulations.

Colorimetric detection RT-LAMP for SARS-CoV-2 and RNase P

RT-LAMP was performed using the WarmStart Colorimetric LAMP 2 Master Mix (New England Biolabs, Hitchin, UK), according to the manufacturer’s instructions with minor modifications. The final reaction volume was 15 mL, consisting of 7.5 mL LAMP master mix, 1.5 mL 10 primer mix (2 mM of each outer primer [F3 and B3], 16 mM of each inner primer [FIP and BIP], and 8 mM of each loop primer [LF and LB]), 4.5 mL nuclease-free water [Sigma Aldrich, Missouri, EUA], and 1.5 mL of the heat-treated sample. The primers used to detect SARSCoV-2 (Table 1) were previously described by Lamb et al.[23] and correspond to the region of the open reading frame (ORF) 1Ab.

Table 1: Primer sequence used in this study.

	SARS-CoV-2 [23]	RNAseP [24]
	PrimersSequence (5' a 3')	PrimersSequence (5' a 3')
F3	TCCAGATGAGGATGAAGAAGA	TTGATGAGCTGGAGCCA
B3	AGTCTGAACAACTGGTGTAAG	CACCCTCAATGCAGAGTC
FIP	AGAGCAGCAGAAGTGGCACAGGTG ATTGTGAAGAAGAAGAG	GTGTGACCCTGAAGACTCGGTTTTAGCC ACTGACTCGGATC
BIP	TCAACCTGAAGAAGAGCAAGAACTG ATTGTCCTCACTGCC	CCTCCGTGATATGGCTCTTCGTTTTTTTC TTACATGGCTCTGGTC
LF	CTCATATTGAGTTGATGGCTCA	ATGTGGATGGCTGAGTTGTT
LB	ACAAACTGTTGGTCAACAAGAC	CATGCTGAGTACTGGACCTC

The RT-LAMP reactions for SARS-CoV-2 detection were incubated at 65 C for 30 min in a thermoblock (Kasvi, Parana, BR). The primers used to detect the human RNAse P gene as an internal control were described previously by Curtis et al.[24] The reactions for endogenous control were incubated at 60 C for 50 min. The temperatures for each test have been optimized and changes in the incubation temperature can result in reduced efficiency.

The primers were synthesized by Integrated DNA Technologies (IDT, Iowa, USA), and sequences are available in Table 1. At the end of the amplification time for each primer set, all tubes were removed from the thermoblock and placed over sheets of white paper for image acquisition using a smartphone camera (Redmi Note 8, Xiaomi). The samples' positivity was determined by observing the change in color from pink (negative sample) to yellow (positive sample). In all tests, negative (blank) and positive (SARS-CoV-2 synthetic target) controls were used.

Sensitivity of the SARS-CoV-2 RT-LAMP assay

To evaluate the limit of detection (LOD) of the colorimetric SARS-CoV-2 RT-LAMP, a synthetic DNA (gBlock) containing the target sequence was homogenized in RNA-free water and inserted in the master mixture to obtain dilutions of 10 000, 1000, 500, 250, 125, 100, and 75 copies per reaction. The LOD in matrix presence was determined considering eight independent replicates, and probit analysis was performed with gBlock spiked in negative swab samples to obtain dilutions of 10 000, 1000, 500, 250, 125, 100, and 75 copies per reaction. In the real samples, the

RT-LAMP assay successfully amplified the target directly in the nasopharyngeal swab sample without the RNA purification step. The cycle threshold (Ct) values of swab samples considered positive by the RT-qPCR assay (#40) were compared to the performance of RT-LAMP. The RT-LAMPamplified products were determined by visual observation and gel electrophoresis (2% agarose and 0.5% Tris–EDTA–borate (TEB) buffer), revealed with GelRed-Biotium® in a UV transilluminator coupled to a photo documentation system.

RT-qPCR assay

The RNA of all samples was extracted using a QuickExtract RNA Extraction Kit (Lucigem, Wisconsin, EUA) according to the manufacturer's instructions and analyzed by RT-qPCR using the GoTaq probe 1-step RT-qPCR system (Promega, Wisconsin, USA) performed in an AriaMx Real-Time PCR System (Agilent, California, EUA). The total reaction volume was 10 mL (5 mL GoTaq Probe qPCR Master Mix, 0.2 mL Go Script RT Mix for 1-Step RTqPCR, 1.55 mL nuclease-free water, 0.75 primers/probe, and 2.5 mL of RNA). The primers/probes used for detection targeted two coronavirus regions (N1 and N2) and human RNase P (internal control) were provided by Integrated DNA Technologies (IDT, Iowa, USA). The amplification program consisted of one cycle at 45 °C for 15 min for reverse transcription, one cycle at 95 °C for 2 min for reverse transcriptase denaturation and DNA polymerase activation, followed by 40 cycles at 95 °C for 3 s, and 55 °C for 30 s for denaturation and amplification.

RT-LAMP for the detection of SARS-CoV-2 in the hospital setting

The tests carried out in a hospital setting were performed with the support of a central laboratory, which was used to prepare the master mix. This mixture was then transported in a cooler support to the hospital facility. For the second stage, two different rooms were used inside the hospital. In the first room, one thermoblock was set at 95 °C for sample inactivation and release the RNA. After this processing, the samples were pipetted into both the SARS-CoV-2 and RNaseP RT-LAMP reagent mixtures. In the second room, one thermoblock was set at 65 °C for the SARS-CoV-2 reaction and the other was set at 60 °C for the RnaseP reaction.

Statistical validation

To calculate the limit of detection of RT-LAMP for SARS-CoV-2, we performed a probit regression using MedCalc software (Version 19.6.4, MedCalc Software, Ostend, Belgium). Eight independent replicates were performed for each RNA concentration, the data (concentration, number of replicates, number of positive results and hit rate) were input to the MedCalc software and the C95 value was obtained (concentration detectable 95% of the time), indicating the limit of detection.

To evaluate sensitivity, specificity, positive and negative predictive values, and test accuracy, the results obtained by RTLAMP were compared with the results obtained by RT-qPCR. For simplicity, we used a MedCalc's Diagnostic Test Evaluation Calculator (available online at https://www.medcalc.org/calc/) to

calculate specificity, sensitivity, negative predictive values, positive predictive values and accuracy. In addition, the mathematical equations are found in the ESI.† The four variables used for statistical analysis are (a) the number of samples positive by both RT-LAMP and RT-qPCR, therefore referred to as “True Positive”, (b) the number of samples that were negative by RT-LAMP and positive by RT-qPCR, therefore referred to as “False Negative”, (c) the number of samples that were positive by RT-LAMP and negative by RT-qPCR, therefore referred to as “False Positive” and (d) the number of samples that were negative by both methods, therefore referred to as “True Negative”. The sensitivity of the test is determined by: a/(a + b). Prevalence is the ratio between the number of samples positive by RT-qPCR (a + b) and the total number of samples (a + b + c + d). The specificity is determined by d/(c + d). Accuracy is calculated by: sensitivity prevalence + specificity (1 prevalence).

In order to assess the agreement between the two alternative techniques employed in this study, we calculated Cohen’s kappa and p values using RStudio version 3.4.4 and the IRR library (available at: https://www.R-project.org/).

Results

Protocol for RT-LAMP application under laboratory and field setup

In this study, we established guidelines executing RT-LAMP for the correct diagnosis. The schematic overview of the SARS-CoV2 RT-LAMP procedure is shown in Figure 1.

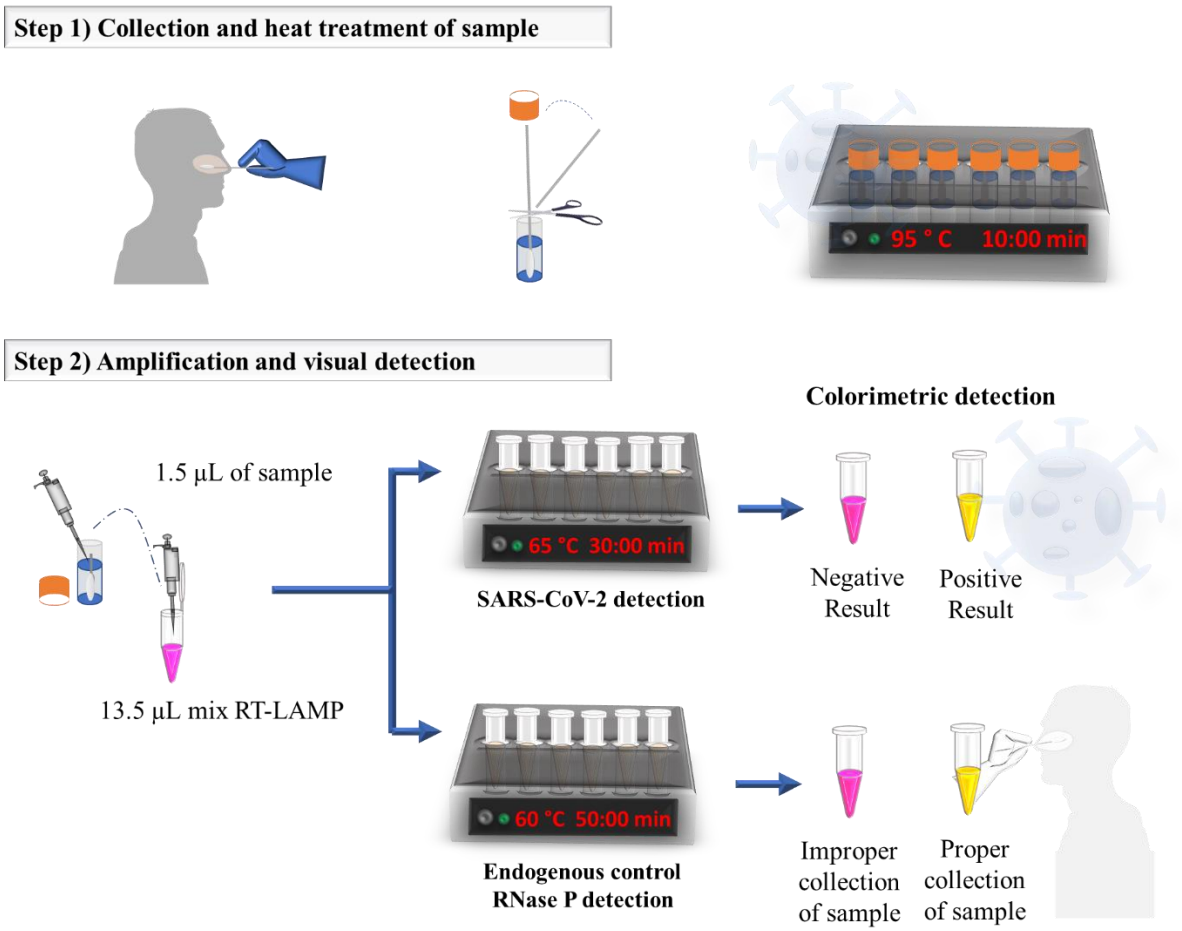

Figure 1: Schematic overview of the RT-LAMP procedure. Step 1: Swab collection and heat treatment of the samples. The nasopharyngeal sample was collected using a swab and stored in a cryotube in 1 mL 0.9% saline solution. The samples were submitted to 95 °C for 10 min for heat extraction and viral inactivation. Step 2: Amplification and visual detection; 1.5 µL of sample was added to two mixtures, each containing either the SARS-CoV-2 or RNAse P primers, water, and WarmStart Colorimetric LAMP 2X Master Mix and then incubated in two thermoblocks; one for 30 min at 65 °C for SARS-CoV-2 detection, and the other for 50 min at 60 °C for RNase P detection in collected samples. The positivity of the samples was determined by observing the change in color from pink (negative sample) to yellow (positive sample). Changes in incubation temperatures for the detection of RNase P and SARS-CoV-2 can result in low efficiency in amplification so they should be maintained as previously described.

For the laboratory tests, the RT-LAMP mix, sample processing, addition, and amplification were performed in different rooms. The access to the amplification room is limited, and individuals involved in the pre-amplification workfow did not access the area due to the high risk of carryover contamination of LAMP amplicons.

The room set up for the RT-LAMP application at the hospital was also optimized in two rooms. Since the mix was previously prepared in a laboratory, the first was destined for viral inactivation of the samples and addition of the target in the reaction, and the second room was used only for the amplification process. Even though the amplification of RT-LAMP products is done in a separate and closed room, the reaction tubes should never be opened. This was to help mitigate false-positive results in the target-free reactions due to carryover contamination. The RT-LAMP reagents were prepared on the day of the experiment in a support laboratory (the same laboratory used for carrying the tests in this validation study), placed in a cooler rack, and then taken to the hospital to perform the test.

It is important to note that all samples were subjected to the inactivation process for 10 min at 95 °C to ensure safety during manipulation. Other biosafety procedures, such as the use of masks, lab coats, hair caps, facial protectors, and the constant disinfection of countertops, were also implemented and considered essential steps in this study's execution.

To assess the integrity and presence of human genomic material in the swab samples, we assayed a LAMP reaction targeting the human RNase P gene as an endogenous control, and the positive diagnostic for COVID-19 was determined

using a combination of RNase P and SARS-CoV-2 detection. Failure to amplify the RNase P reaction in any circumstance would invalidate the test, and recollection would be advised. All 206 nasopharyngeal swab samples showed positive results for endogenous control, not rendering any of them useless.

Limit of detection of RT-LAMP for SARS-CoV-2 colorimetric detection

In reactions containing the SARS-CoV-2 synthetic target, the detection limit found by colorimetric RT-LAMP was 125 copies per reaction for visual detection, with the possibility of detecting up to 100 copies per reaction using the gel electrophoresis (Fig. 2). However, the additional step for gel electrophoresis detection is not worthwhile for rapid tests since both methods have very close detection limits of SARS-CoV-2 RNA.

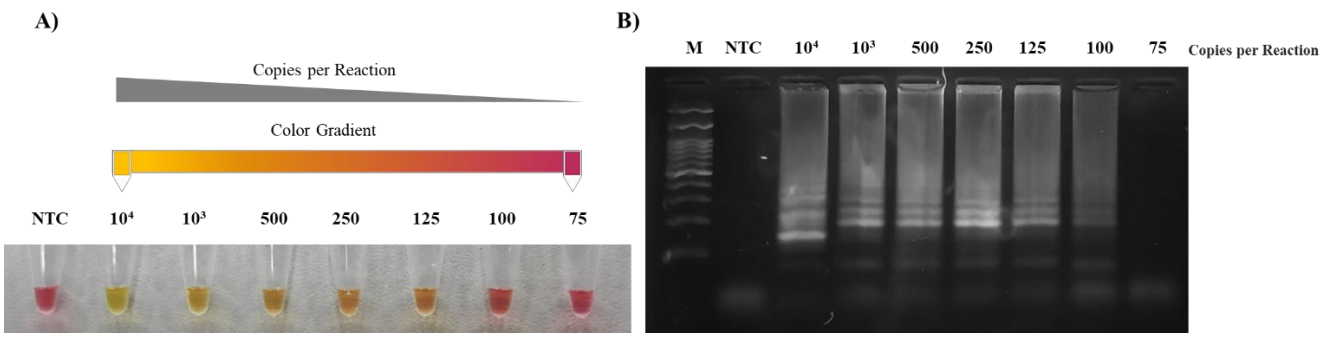

Figure 2: Analytical sensitivity of the RT-LAMP assay using a purified gene fragment. (A) Visual detection. (B) Amplified products separated on 2% agarose gel. M – marker and NTC – Negative Template Control.

The probit regression analysis (Fig. 3A) showed that the detection limit within 95% reliability was 255 copies per reaction of the SARS-CoV-2 RNA, with a

confidence interval of 221-338 copies per reaction (Fig. 3B). The detection rate in simulated infected clinical samples of nasopharyngeal swabs reduced to 50% success in samples with 200 copies per reaction in the presence of the biological matrix. However, a 100% detection rate was found when the reaction had an initial concentration of 250 copies per reaction, directly in the nasopharyngeal swab (Fig. 3C).

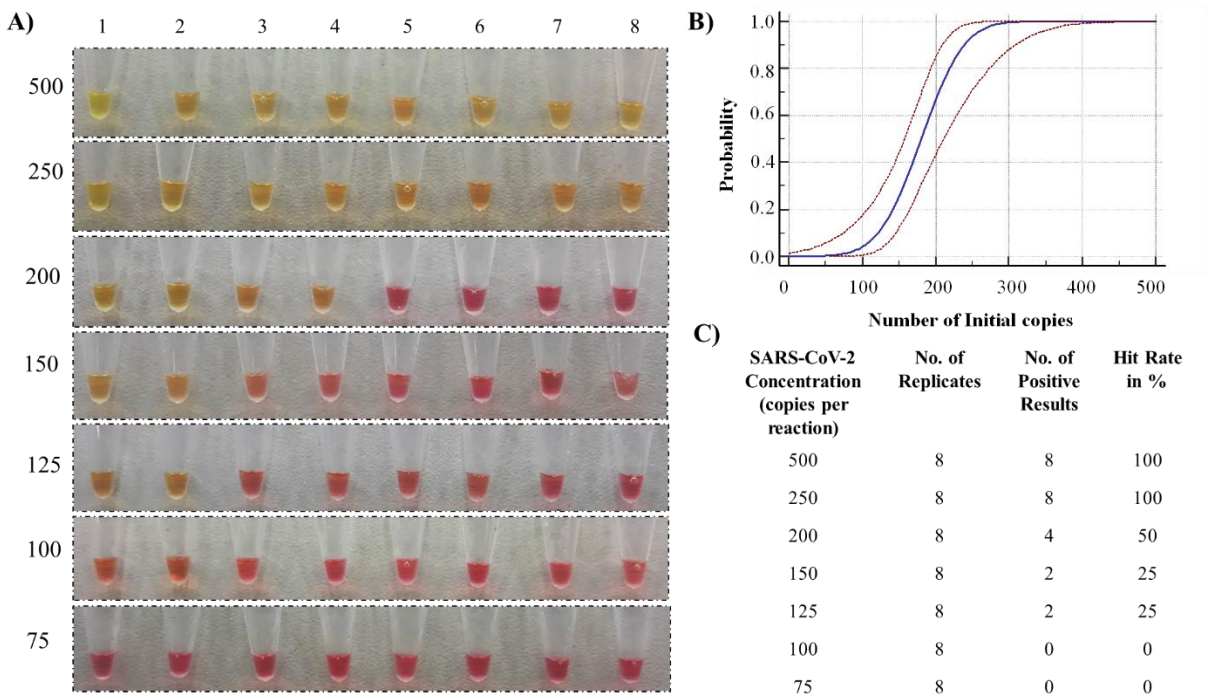

C)

SARS-CoV-2 Concentration (copies per reaction)	No. of Replicates	No. of Positive Results	Hit Rate in %
500	8	8	100
250	8	8	100
200	8	4	50
150	8	2	25
125	8	2	25
100	8	0	0
75	8	0	0

Figure 3: Limit of detection of the RT-LAMP assay for SARS-CoV-2 detection spiked in a biological sample. A) Sensitivity of colorimetric RT-LAMP assay for SARS-CoV-2 detection. B) Probit regression analysis curve considering eight independent replicates with different initial copies per reaction. C) Table with the hit rate (%) reached in all eight replication replicates.

We checked the correlation between the detection limit and Ct value of eight samples with different Sars-CoV-2 viral loads (no Cq and 18 # Ct # 32) previously confirmed by RT-qPCR. The detection of the human RNase P gene for all samples analyzed is shown in Fig. 4A. In the colorimetric RT-LAMP assay in real samples, all positive samples with a Ct < 30 (250 copies per reaction) changed the color of the reaction mixture (pink to yellow) within 30 min of the reaction (Fig. 4B), as confirmed by gel electrophoresis.

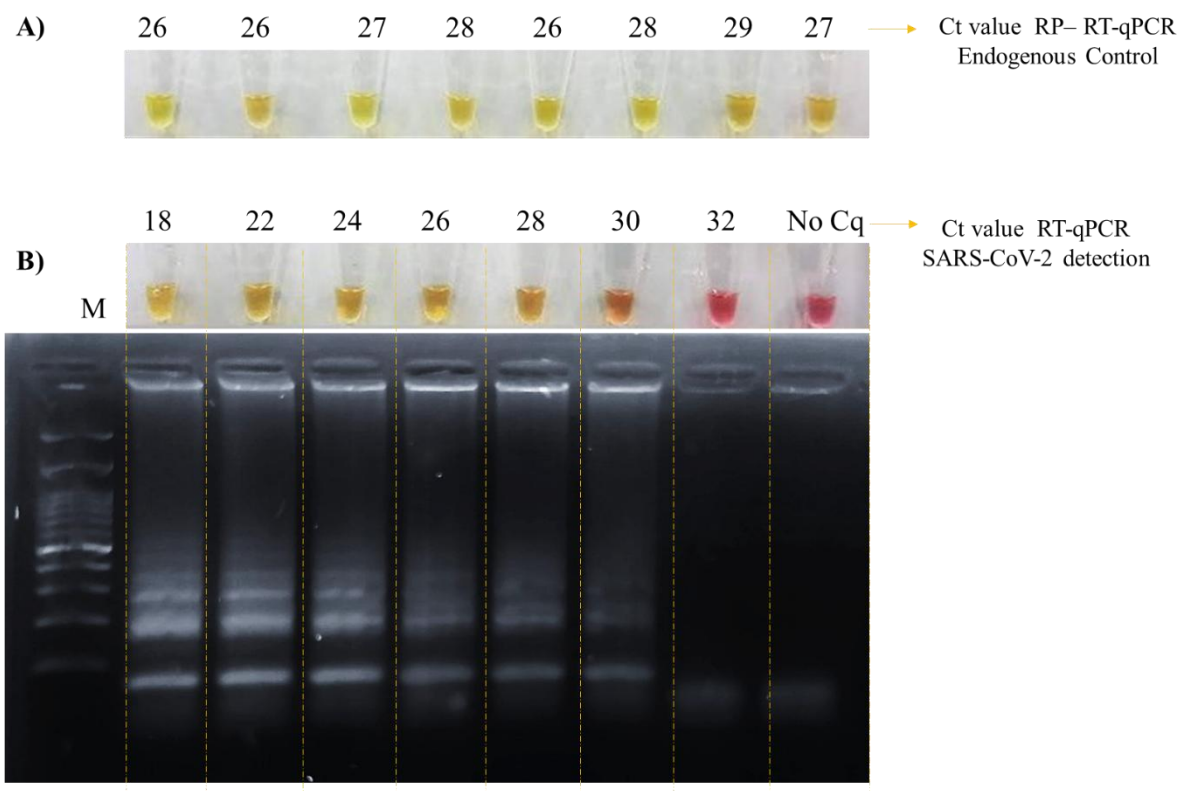

Figure 4: Detection of the RT-LAMP amplified product. (A) Evaluation of human RNase P (RP) endogenous control quality in swab samples; eight (8) positive samples by RT-qPCR. (B) Detection of SARS-CoV-2 RT-LAMP in eight (8) samples

with different viral loads visualized by visual detection and electrophoretic separation. No. Cq: no. cycle quantification.

Performance of the colorimetric RT-LAMP test for the detection of SARS-CoV-2

We performed an RT-LAMP-based molecular detection for SARS-CoV-2 in clinical samples at a laboratory with a total of 110 samples. Samples were also analyzed by RT-qPCR. Of these 110 samples, 27 were positive, and 83 were negative by RT-qPCR. Among the 27 positive samples by RT-qPCR, 23 were also positive by RT-LAMP, and among the 83 negative samples by RT-qPCR, 83 were also negative by RT-LAMP. Four false-negative results were observed. The Ct values, the number of SARS-CoV-2 RNA copies obtained by RT-qPCR, and the results of the RTLAMP assay for each sample are shown in Table S1.†

As shown in Table 2, the colorimetric RT-LAMP performed in the laboratory resulted in a sensitivity of 85.19% (95% CI: 66.27– 95.81%), a specificity of 100% (95% CI: 95.65–100%), a negative predictive value of 95.40% (95% CI: 89.36–98.09%), and a positive predictive value of 100.00% (95% CI: 77.34–99.41%), with an accuracy of 96.36% (95% CI: 89.67–98.85%). The RT-LAMP showed high concordance with RT-qPCR with a kappa coefficient of 0.897 (95% CI: 0.798–0.966) and p value < 0.05.

Since RT-LAMP has excellent reliability and accuracy in a controlled environment, such as a laboratory, we implemented the test in a hospital

environment to serve as proof of its potential application in the field. A total of 96 samples were analyzed (Table S1†). Among the 96 samples, 27 were positive, and 69 were negative by RT-qPCR. RT-LAMP identified 24 of 27 positive samples by RT-qPCR and 68 of 69 samples negative by RT-qPCR. Of all the samples analyzed in the hospital, only four had non-concordant results between the two tests; one false positive and three false negatives were associated with RT-LAMP. However, it is important to note that false-negative results are associated with the limit of the test itself.

RT-LAMP in the field presented a sensitivity of 88.89% (95% CI: 70.84–97.65%), a specificity of 98.55% (95% CI: 92.19– 99.96%), a negative predictive value of 95.77% (95% CI: 88.83– 98.51%), and a positive predictive value of 96% (95% CI: 77.34– 99.41%), with an accuracy of 95.83% (95% CI: 89.67–98.85%). The kappa value was 0.895 (95% CI: 0.794–0.995) (Table 2) with a p value < 0.05.

Table 2: Statistical evaluation of the RT-LAMP in the laboratory and hospital settinga.

Laboratory			Hospital		
Statistic	Value	95% CI	Statistic	Value	95% CI
Sensitivity	85.19%	66.27% to 95.81%	Sensitivity	88.89%	70.84% to 97.65%

Specificity	100.00%	95.65% to 100.00%	Specificity	98.55%	92.19% to 99.96%
Disease prevalence	24.55%	16.84% to 33.67%	Disease prevalence	28.12%	19.42% to 38.22%
Positive predictive value	100.00%	—	Positive predictive value	96.00%	77.34% to 99.41%
Negative predictive value	95.40%	89.36% to 98.09%	Negative predictive value	95.77%	89.67% to 98.85%
Accuracy	96.36%	90.95% to 99.00%	Accuracy	95.83%	89.67% to 98.85%
Cohen's kappa	0.897	0.798 to 0.996	Cohen's kappa	0.895	0.794 to 0.995

[a] CI-confidence interval.

Correlation between the percentage of hit rate of RT-LAMP and Ct values

The correlation between the hit rate of the RT-LAMP and Ct of the samples was analyzed. After separating the samples by Ct ranges (#19, 20–24, 25–29, and $30), we observed that the hit rate of RT-LAMP to samples analyzed in the laboratory with Ct values # 19, 20–24, and 25–29 was 100%. However, with Ct $ 30, the reaction did not show positivity (Fig. 5A). Among the four positive samples

determined to be false-negatives by RT-LAMP, three samples presented Ct values of Ct $ 30 and one presented Ct values in the range 25–29 (Fig. 5B).

This same correlation was observed for the samples analyzed at the hospital. The hit rate of RT-LAMP for samples with Ct # 19, 20-25, and 25–30 was 100% (Fig. 5C). The correlation of Ct values with RT-LAMP results showed that all false-negative samples presented Ct > 30 (Fig. 5D). These data demonstrate that the RT-LAMP assay was able to effectively identify SARSCoV-2 in samples up to Ct 30.4

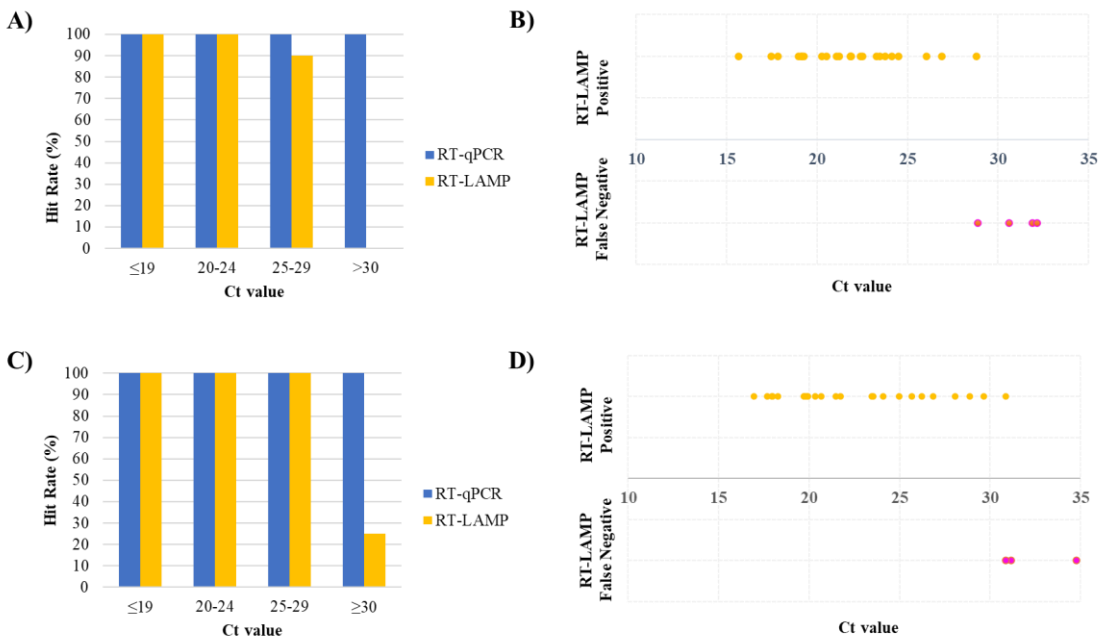

Figure 5: The performance of colorimetric RT-LAMP analyzing clinical samples previously quantified by RT-qPCR. (A) Hit rate of RT-LAMP and (B) correlation of Ct with positive and false-negative samples analyzed in the laboratory. (C) Hit rate of RT-LAMP and (D) correlation of Ct with positive and false-negative samples analyzed in the hospital.

Discussion

In places with limited resources, several challenges have been associated with PCR-based diagnostics, including the lack of infrastructure, trained personnel, and expensive equipment. In this context, the demand for instrumentally simpler tests ("rapid tests"), usually based on lateral low (LFA) detection, has emerged rapidly. Currently, lateral low tests are available for both antibody and antigen detection. Kruttgen and co-workers[25] developed a study to compare the Real Star SARS-CoV-2 RT-PCR kit and the SARS-CoV-2 Rapid antigen test (lateral low assay) using 75 swabs from patients previously tested positive and 75 swabs from patients previously tested negative by SARS-CoV-2 qPCR. The authors reported a specificity of 96% and a sensitivity according to different cycle threshold values. For Cts < 25, 25 – <30, 30 – <35, and $35 the sensitivity was 100%, 95%, 44.8% and 22.2% respectively. Although it is possible to read the final results of lateral low assays within 30 min, as well as the test developed in this manuscript, the lateral low still requires high-cost reagents such as antibodies and labels, as opposed to the detection method used here, based on the pH indicator. Regarding lateral low tests for antibody detection, these tests are serological tests (IgG and IgM detection), which perform an indirect detection, that is, the detection of the immune response of the host to the SARS-CoV-2 infection.[26] As well, serological tests are not suitable for diagnosing patients at the beginning of the infection, unlike molecular tests, which are able to detect the infection even in the early days of symptoms. On the other hand, it would be possible to use a molecular test such as

RT-LAMP and perform detection by lateral low, however, we do not recommend it, as (i) in addition to the increased cost, (ii) it would require a step of opening the tube after the amplification stage, increasing the probability of crossover contamination, thus compromising the reliability of the test.

During the Global Research and Innovation Forum, the World Health Organization warned about the need for research into diagnoses of point-of-care for use at the community level.[27] Several studies have proposed the use of the colorimetric RT-LAMP technique for the Development of simple tests with potential for application at the point-of-care. For this, simple extraction, amplification, and detection methodologies similar to those addressed in this paper were developed. Diego et al. (2021), with samples of RNA extracted from nasopharyngeal swab inactivated with lysis buffer, carried out a vast study between primers and enzymes for colorimetric RT-LAMP.[28] The authors reported that primers based on the ORF1ab and N region with the enzyme Bst 2.0 DNA Polymerase resulted in better performance in the detection of SARS-CoV-2 RNA (amplification times and analytical sensitivity). Yamazaki et al. (2021) described a simple method to extract RNA from saliva samples using semi-alkaline proteinase, compatible with colorimetric RT-LAMP in a 45 minute test with 82.6% diagnostic sensitivity (19/23) and a limit of 250 copies per reaction.[29] Bokelmann et al. combined RNA purification by hybridization capture with colorimetric LAMP, and were able to correctly identify 100% of positive samples with high viral loads with Ct < 24, when using primers in the Orf1a region.[30] Therefore, our manuscript brings clear advantages, performing

the detection of SARS-CoV-2 in 100% of the samples with Ct < 30 in the field, directly in nasopharyngeal swab samples employing only the heat treatment. The heat treatment of the sample, as described in our paper, is advantageous because in addition to being quick, it does not require steps to open sample tubes, corroborating biosafety in the performance of the tests. But in addition to the sample preparation process, in this paper, we use an endogenous control (RP), which determines the viability of the sample giving greater reliability to the test. Furthermore, in this study, we exceed the limits of "potential application of the method" for effective application in point-of-care (hospital environment) settings with good results in terms of rapid, accurate and sensitivity diagnosis which can contribute to the control of the pandemic, especially in environments with scarce resources.

Here, we evaluated the performance of RT-LAMP in a laboratory and hospital environment. The results showed that the performance of RT-LAMP is similar in both environments, even with the high possibility of contamination within a hospital, confirming its feasibility of application in the field. However, the major challenge when planning to use molecular diagnostic tests is the correct structuring of the working environment and protocol to be used. The extreme capacity of RT-LAMP amplification is also accompanied by its great sensitivity to cross-contamination or its own amplified products.[23,24,31] The configuration of rooms used to optimize tests in the laboratory and hospital proved to be sufficient to minimize problems with contamination by amplicons. In places with limited resources, several challenges

have been associated with PCR based diagnostics, including the lack of infrastructure, trained personnel, and expensive equipment.

SARS-CoV-2 is classified as a risk group 3 biological agent, and the correct compliance with the guidelines of laboratory safety procedures and sample handling is essential.[32] The protocol for viral inactivation by heat treatment is already well established[33,34] and shows advantages for field application and compatibility with the colorimetric kit used in this study. Studies have already shown that heating at 95 °C for five minutes could inactivate the virus.[35] Since we work with freshly collected samples, we decided to double the time to ensure safety in handling the samples.

Since the use of chemical reagents, such as lysis buffers, significantly changes the pH of the samples, making them unfeasible for testing using a pH-based colorimetric assay, the pre-heating protocol, besides promoting the inactivation process by denaturing proteins essential for attachment and replication of the virus in a host cell,[36–38] proved to be an ideal pretreatment of nasopharyngeal swabs to release RNA using heat excluding the need for nucleic acid extraction. This approach of pre-heating the samples was also used by Barza et al. as a strategy to expose the viral genome and denature possible inhibitors of the PCR reaction.[39]

In relation to the detection limit, our SARS-CoV-2 results feature a strong concordance with other studies that describe the decrease in sensitivity due to the presence of a biological matrix.[40] The performance of RT-LAMP reported in this

study is also in agreement with those previously described in the literature.[21,40,41] Nawattanapaiboon et al.,[40] using viral RNA extracted from 2120 clinical samples of nasopharyngeal and throat swabs collected in Thailand, obtained an accuracy of 95.8% using the same colorimetric master mix (WarmStart® Colorimetric LAMP 2 Master Mix) and time (30 min). The other statistical values demonstrate the potential of the test to be used as a screening for SARS-CoV-2, mainly in places with low laboratory resources.

The Ct values of the RT-qPCR reaction are inversely correlated with the viral load, high Ct values represent low viral load, and low Ct values represent high viral load.[42] Some studies have correlated the potential of infectivity and Ct values.[43] Magleby et al. correlated the Ct of patients with the disease severity, and Ct > 30 is related to lower mortality.[44] Thus, considering the detection limit found in our analyses and that it is according with the limit reported in others studies,[45] the assay proposed here can be useful for screening patients at the beginning of the infection with high viral load and consequently with a greater potential for viral spread and progression to severe clinical conditions due to infection of SARS-CoV-2. Therefore, although the RT-LAMP test described here has a lower sensitivity than RT-PCR, the detection of Ct < 30 is adequate to detect likely contagious individuals and aid in the implementation of isolation measures.

An important factor to be considered in the management of COVID-19 is the waiting time for current tests, which is difficult for decision making related to the immediate care of patients with major problems and their correct isolation. In this

context, decentralized tests, when compared to RT-PCR, are associated with a significant reduction in the time to release the results. Brendish et al.[20] showed that the application of point-of-care PCR reduced approximately 14 hours of waiting for results. In our study, we also observed an even greater reduction in time from the request of the test to the result, requiring less than 1 hour to perform all the RT-LAMP steps in the field. The nasopharyngeal sample collection step, using a swab, takes less than 5 minutes. Then, 10, 50 and 5 minutes are spent in the heat treatment, amplification and detection process, respectively. Counting the time needed to prepare the reaction mix, label and transporting the microtubes across the rooms, the total analysis time is less than 1.5 h. Thus, considering the simplicity of the test execution, the speed of results, the lowest aggregate cost, analyzing the scenario of overcrowding in emergency rooms due to the growing demand for care during the pandemic, and the need to isolate infected patients, the results presented here demonstrate that RT-LAMP has important clinical application, mainly in the hospital screening sector, to try to minimize the problem of overcrowding, allowing immediate care for the most urgent patients.

Conclusion

The colorimetric RT-LAMP assay applied in the hospital setting proved to be a powerful tool for detecting SARS-CoV-2 with a great cost-benefit in the context of point-of-care. The pre-heat treatment of samples is a simple strategy compatible

with pHbased tests that promotes safety in handling and performing tests. Besides, it also assisted in the detection of SARS-CoV-2 nucleic acid directly in unextracted swab samples. The results show that the methodology was able to deliver reliable and accurate results, both in the field and the laboratory. Results can be obtained in less than 1.5 h, as long as the proposed workflow is respected. It is of utmost importance to use the RT-LAMP endogenous control as it can help identify samples with low quantities of biological material due to failure in collection. Furthermore, the RT-LAMP carried out in the hospital exhibited a diagnostic performance comparable to RT-qPCR and the assay performed in the reference laboratory with high sensitivity (88.89%), specificity (94.20%), and a detection limit of 255 copies of RNA per reaction. Based on the data, the limitation of RT-LAMP in contrast to the gold standard is sensitivity. In a recently published study conducted by Alcoba-Florez and colleagues, a direct RT-qPCR assay performed on clinical samples for the detection of SARS-CoV-2 using a nasopharyngeal heat treatment swab yielded a sensitivity of 87.8%, 100% specificity and 99.9% accuracy. The detection limit found in this study is greater than that reported in the literature by Alcoba-Florez and collaborators who reached a detection limit of 120 copies of RNA per reaction with an average Ct value of 38.48 0.57.[46] In fact, the RT-LAMP is less sensitive than the RT-qPCR assay, however, the direct RT-LAMP technique is easier to perform, thus eliminating the need for complex equipment, which can help increasing the frequency of tests. Advantages, such as directly detecting the target in clinical swab samples without the need for RNA extraction, the use of low-cost equipment, and the easy reading and differentiation of positive and negative results by the naked

eye through the color change from pink to yellow, suggest that the RT-LAMP method can be broadly applied to many other kinds of places without great infrastructure. Our RT-LAMP assay has great potential to aid in on-field SARS-CoV-2 screening and enable rapid and accurate treatment of infected patients.

References

1 N. Chen, M. Zhou, X. Dong, J. Qu, F. Gong, Y. Han, Y. Qiu, J. Wang, Y. Liu, Y. Wei, J. Xia, T. Yu, X. Zhang and L. Zhang, The Lancet, 2020, 395, 507–513.

2 C. Huang, Y. Wang, X. Li, L. Ren, J. Zhao, Y. Hu, L. Zhang, G. Fan, J. Xu, X. Gu, Z. Cheng, T. Yu, J. Xia, Y. Wei, W. Wu, X. Xie, W. Yin, H. Li, M. Liu, Y. Xiao, H. Gao, L. Guo, J. Xie, G. Wang, R. Jiang, Z. Gao, Q. Jin, J. Wang and B. Cao, The Lancet, 2020, 395, 497–506.

3 A. J. Kucharski, P. Klepac, A. J. K. Conlan, S. M. Kissler, M. L. Tang, H. Fry, J. R. Gog, W. J. Edmunds, J. C. Emery, G. Medley, J. D. Munday, T. W. Russell, Q. J. Leclerc, C. Diamond, S. R. Procter, A. Gimma, F. Y. Sun, H. P. Gibbs, A. Rosello, K. van Zandvoort, S. Hu´e, S. R. Meakin, A. K. Deol, G. Knight, T. Jombart, A. M. Foss, N. I. Bosse, K. E. Atkins, B. J. Quilty, R. Lowe, K. Prem, S. Flasche, C. A. B. Pearson, R. M. G. J. Houben, E. S. Nightingale, A. Endo, D. C. Tully, Y. Liu, J. Villabona- Arenas, K. O'Reilly, S. Funk, R. M. Eggo, M. Jit, E. M. Rees, J. Hellewell, S. Clifford, C. I. Jarvis, S. Abbott, M. Auzenbergs, N. G. Davies and D. Simons, Lancet Infect. Dis., 2020, 20, 1151–1160.

4 J. J. Deeks, J. Dinnes, Y. Takwoingi, C. Davenport, R. Spijker, S. Taylor-Phillips, A. Adriano, S. Beese, J. Dretzke, L. Ferrante di Ruffano, I. M. Harris, M. J. Price, S. Dittrich, D. Emperador, L. Hoo□, M. M. Leeflang, A. Van den Bruel and Cochrane COVID-19 Diagnostic Test Accuracy Group, Cochrane Database Syst. Rev., 2020, 6, CD013652.

5 G. C. Mak, P. K. Cheng, S. S. Lau, K. K. Wong, C. S. Lau, E. T. Lam, R. C. Chan and D. N. Tsang, J. Clin. Virol., 2020, 129, 104500.

6 B. B. Chen, M. L. Liu and C. Z. Huang, J. Pharm. Anal., 2021, 11(2), 129–137.

7 V. M. Corman, O. Landt, M. Kaiser, R. Molenkamp, A. Meijer, D. K. Chu, T. Bleicker, S. Bru¨nink, J. Schneider, M. L. Schmidt, D. G. Mulders, B. L. Haagmans, B. van der Veer, S. van den Brink, L. Wijsman, G. Goderski, J.-L. Romette, J. Ellis, M. Zambon, M. Peiris, H. Goossens, C. Reusken, M. P. Koopmans and C. Drosten, Eurosurveillance, 2020, 25(3), 23–30.

8 W. Feng, A. M. Newbigging, C. Le, B. Pang, H. Peng, Y. Cao, J. Wu, G. Abbas, J. Song, D.-B. Wang, M. Cui, J. Tao, D. L. Tyrrell, X.-E. Zhang, H. Zhang and X. C. Le, Anal. Chem., 2020, 92, 10196–10209.

9 R. Li, S. Pei, B. Chen, Y. Song, T. Zhang, W. Yang and J. Shaman, Science, 2020, 368, 489–493.

10 K. G. de Oliveira, P. F. N. Estrela, G. de M. Mendes, C. A. dos Santos, E. de P. Silveira-Lacerda and G. R. M. Duarte, Analyst, 2021, 146(4), 1178–1187.

11 L. Mautner, C.-K. Baillie, H. M. Herold, W. Volkwein, P. Guertler, U. Eberle, N. Ackermann, A. Sing, M. Pavlovic, O. Goerlich, U. Busch, L. Wassill, I. Huber and A. Baiker, Virol. J., 2020, 17, 160.

12 J. Rodriguez-Manzano, K. Malpartida-Cardenas, N. Moser, I. Pennisi, M. Cavuto, L. Miglietta, A. Moniri, R. Penn, G. Satta, P. Randell, F. Davies, F. Bolt, W. Barclay, A. Holmes and P. Georgiou, ACS Cent. Sci., 2021, 7, 307–317. 13 S. Wei, E. Kohl, A. Djandji, S. Morgan, S. Whittier, M. Mansukhani, E. Hod, M. D'Alton, Y. Suh and Z. Williams, Sci. Rep., 2021, 11, 2402.

14 P. F. N. Estrela, G. de M. Mendes, K. G. de Oliveira, A. M. Bail˜ao, C. M. de A. Soares, N. A. Assunç˜ao and G. R. M. Duarte, J. Virol. Methods, 2019, 271, 113675.

15 K. Takehana, T. Kinjyo, M. Nemoto and K. Matsuno, J. Vet. Med. Sci., 2019, 81, 504–507.

16 A. E. Calvert, B. J. Biggerstaff, N. A. Tanner, M. Lauterbach and R. S. Lanciotti, PLoS One, 2017, 12, e0185340.

17 P. Asprino, F. Bettoni, A. Camargo, D. Coelho, G. Coppini, I. Correa, E. Freitas, L. Inoue, J. P. Kitajima, M. Kuroki, C. Masotti, T. Marques, A. Reis, L. F. Reis, B. Santos, E. dos Santos, D. Schlesinger, C. Sena, T. Spadaccini and L. Taniguti, A scalable saliva-based, extraction-free rt-lamp protocol for sars-cov-2 diagnosis, Infect. Dis., 2020, DOI: 10.1101/2020.10.27.20220541.

18 K. R. Jackson, T. Layne, D. A. Dent, A. Tsuei, J. Li, D. M. Haverstick and J. P. Landers, Forensic Sci. Int.: Genet., 2020, 45, 102195.

19 C. A. Herrada, M. A. Kabir, R. Altamirano and W. Asghar, J. Med. Device, 2018, 12, 0408021–4080211.

20 N. J. Brendish, S. Poole, V. V. Naidu, C. T. Mansbridge, N. J. Norton, H. Wheeler, L. Presland, S. Kidd, N. J. Cortes, F. Borca, H. Phan, G. Babbage, B. Visseaux, S. Ewings and T. W. Clark, Lancet Respir. Med., 2020, 8, 1192–1200.

21 F. W.-N. Chow, T. T.-Y. Chan, A. R. Tam, S. Zhao, W. Yao, J. Fung, F. K.-K. Cheng, G. C.-S. Lo, S. Chu, K. L. Aw-Yong, J. Y.-M. Tang, C.-C. Tsang, H. K.-H. Luk, A. C.-P. Wong, K. S.-M. Li, L. Zhu, Z. He, E. W. T. Tam, T. W.-H. Chung, S. C. Y. Wong, T.-L. Que, K. S.-C. Fung, D. C. Lung, A. K.-L. Wu, I. F.-N. Hung, P. C.-Y. Woo and S. K.-P. Lau, Int. J. Mol. Sci., 2020, 21, 5380.

22 C. Yan, J. Cui, L. Huang, B. Du, L. Chen, G. Xue, S. Li, W. Zhang, L. Zhao, Y. Sun, H. Yao, N. Li, H. Zhao, Y. Feng, S. Liu, Q. Zhang, D. Liu and J. Yuan, Clin. Microbiol. Infect., 2020, 26, 773–779.

23 L. E. Lamb, S. N. Bartolone, E. Ward and M. B. Chancellor, PLoS ONE, 2020, 15, e0234682.

24 K. A. Curtis, D. Morrison, D. L. Rudolph, A. Shankar, L. S. P. Bloomfield, W. M. Switzer and S. M. Owen, J. Virol. Methods, 2018, 255, 91–97.

25 A. Kru¨ttgen, C. G. Cornelissen, M. Dreher, M. W. Hornef, M. Im¨ohl and M. Kleines, J. Virol. Methods, 2021, 288, 114024.

26 T. Nicol, C. Lefeuvre, O. Serri, A. Pivert, F. Joubaud, V. Dub´ee, A Kouatchet, A. Ducancelle, F. Lunel-Fabiani and H. Le Guillou-Guillemette, J. Clin. Virol., 2020, 129, 104511.

27 World Health Organization's, COVID-19 Public Health Emergency of International Concern (PHEIC) Global research and innovation forum, https://www.who.int/publications/m/ item/covid-19-public-health-emergency-of-international- concern-(pheic)-global-research-and-innovation-forum, accessed February 9, 2021.

28 J. Garc´ıa-Bernalt Diego, P. Fern´andez-Soto, M. Dom´ınguez- Gil, M. Belhassen-Garc´ıa, J. L. M. Bellido and A. Muro, Diagnostics, 2021, 11, 438.

29 W. Yamazaki, Y. Matsumura, U. Thongchankaew-Seo, Y. Yamazaki and M. Nagao, J. Clin. Virol., 2021, 136, 104760. 30 L. Bokelmann, O. Nickel, T. Maricic, S. P¨a¨abo, M. Meyer, S. Borte and S. Riesenberg, Nat. Commun., 2021, 12, 1467. 31 N. Tomita, Y. Mori, H. Kanda and T. Notomi, Nat. Protoc., 2008, 3, 877–882.

32 A. M. Kaufer, T. Theis, K. A. Lau, J. L. Gray and W. D. Rawlinson, Pathology, 2020, 52, 790–795.

33 B. Pastorino, F. Touret, M. Gilles, X. de Lamballerie and R. N. Charrel, Viruses, 2020, 12(7), 1–8.

34 J. Burton, H. Love, K. Richards, C. Burton, S. Summers, J. Pitman, L. Easterbrook, K. Davies, P. Spencer, M. Killip, P. Cane, C. Bruce and A. D. G. Roberts, J. Virol. Methods, 2021, 290, 114087.

35 C. Bat´ejat, Q. Grassin, J.-C. Manuguerra and I. Leclercq, Journal of Biosafety and Biosecurity, 2021, 3, 1–3.

36 M. R. Hasan, F. Mirza, H. Al-Hail, S. Sundararaju, T. Xaba, M. Iqbal, H. Alhussain, H. M. Yassine, A. Perez-Lopez and P. Tang, PLoS ONE, 2020, 15, e0236564.

37 E. I. Patterson, T. Prince, E. R. Anderson, A. Casas-Sanchez, S. L. Smith, C. Cansado-Utrilla, T. Solomon, M. J. Griffiths, A´. Acosta-Serrano, L. Turtle and G. L. Hughes, J. Infect. Dis., 2020, 222, 1462–1467.

38 M. J. Lista, R. Page, H. Sertkaya, P. M. Matos, E. Ortiz- Zapater, T. J. A. Maguire, K. Poulton, A. M. O'Byrne, C. Bouton, R. E. Dickenson, M. Ficarelli, M. Howard, G. Betancor, R. P. Galao, S. Pickering, A. W. Signell, H. Wilson, P. Cliff, M. T. Kia Ik, A. Patel, E. MacMahon, E. Cunningham, M. Agromayor, J. Martin-Serrano, E. Perucha, H. E. Mischo, M. Shankar-Hari, R. Batra, J. Edgeworth, M. H. Malim, S. Neil and R. T. Martinez- Nunez, Resilient SARS-CoV-2 diagnostics workflows including viral heat inactivation, Health Systems and Quality Improvement, 2020, DOI: 10.1101/ 2020.04.22.20074351.

39 R. Barza, P. Patel, L. Sabatini and K. Singh, J. Clin. Virol., 2020, 132, 104587.

40 K. Nawattanapaiboon, E. Pasomsub, P. Prombun, A. Wongbunmak, A. Jenjitwanich, P. Mahasupachai, P. Vetcho, C. Chayrach, N. Manatjaroenlap,

C. Samphaongern, T. Watthanachockchai, P. Leedorkmai, S. Manopwisedjaroen, R. Akkarawongsapat, A. Thitithanyanont, M. Phanchana, W. Panbangred, S. Chauvatcharin and T. Srikhirin, Analyst, 2021, 146, 471–477.

41 S. Klein, T. G. Mu¨ller, D. Khalid, V. Sonntag-Buck, A.-M. Heuser, B. Glass, M. Meurer, I. Morales, A. Schillak, A. Freistaedter, I. Ambiel, S. L. Winter, L. Zimmermann, T. Naumoska, F. Bubeck, D. Kirrmaier, S. Ullrich, I. Barreto Miranda, S. Anders, D. Grimm, P. Schnitzler, M. Knop, H.-G. Kr¨ausslich, V. L. Dao Thi, K. B¨orner and P. Chlanda, Viruses, 2020, 12, 863.

42 M. R. Tom and M. J. Mina, Clin. Infect. Dis., 2020, 71, 2252– 2254.

43 J. Bullard, K. Dust, D. Funk, J. E. Strong, D. Alexander, L. Garnett, C. Boodman, A. Bello, A. Hedley, Z. Schiffman, K. Doan, N. Bastien, Y. Li, P. G. Van Caeseele and G. Poliquin, Clin. Infect. Dis., 2020, 71(10), 2663–2666.

44 R. Magleby, L. F. Westblade, A. Trzebucki, M. S. Simon, M. Rajan, J. Park, P. Goyal, M. M. Safford and M. J. Satlin, Clin. Infect. Dis., 2020, ciaa851.

45 V. L. Dao Thi, K. Herbst, K. Boerner, M. Meurer, L. P. Kremer, D. Kirrmaier, A. Freistaedter, D. Papagiannidis, C. Galmozzi, M. L. Stanifer, S. Boulant, S. Klein, P. Chlanda, D. Khalid, I. Barreto Miranda, P. Schnitzler, H.-G. Kr¨ausslich, M. Knop and S. Anders, Sci. Transl. Med., 2020, 12, eabc7075.

46 J. Alcoba-Florez, R. Gonz´alez-Montelongo, A. ´In˜igo-Campos, D. G.-M. de Artola, H. Gil-Campesino, The Microbiology Technical Support Team, L. Ciuffreda, A. Valenzuela- Fern´andez and C. Flores, Int. J. Infect. Dis., 2020, 97, 66–68.

SUPPLEMENTARY MATERIAL

Can a field molecular diagnosis be accurate A performance evaluation of colorimetric RT-LAMP for the detection of SARS-CoV-2 in a hospital setting

Table S1. Samples used for RT-LAMP and RT-PCR

Laboratory				Hospital			
ID Number	Ct* value	Equivalent in number of copies	Result of RT-LAMP	ID Number	Ct* value	Equivalent in number of copies	Result of RT-LAMP
1	15.68	3.01E+07	Positive	**111**	16.96	7.55E+06	Positive
2	17.45	4.57E+06	Positive	**112**	17.69	3.60E+06	Positive
3	17.84	3.10E+06	Positive	**113**	17.96	2.75E+06	Positive
4	18.98	1.04E+06	Positive	**114**	17.99	2.67E+06	Positive
5	19.15	8.90E+05	Positive	**115**	18.27	2.04E+06	Positive
6	19.27	7.97E+05	Positive	**116**	19.73	5.26E+05	Positive
7	19.13	9.07E+05	Positive	**117**	19.75	5.17E+05	Positive
8	20.25	3.33E+05	Positive	**118**	19.85	4.73E+05	Positive
9	20.53	2.61E+05	Positive	**119**	19.94	4.37E+05	Positive
10	21.09	1.63E+05	Positive	**120**	20.36	3.03E+05	Positive

11	21.23	1.45E+05	Positive	**121**	20.66	2.34E+05	Positive
12	21.84	8.80E+04	Positive	**122**	21.49	1.17E+05	Positive
13	21.86	8.66E+04	Positive	**123**	21.74	9.54E+04	Positive
14	21.90	8.39E+04	Positive	**124**	23.47	2.48E+04	Positive
15	22.42	5.55E+04	Positive	**125**	23.53	2.37E+04	Positive
16	22.51	5.01E+04	Positive	**126**	24.08	1.58E+04	Positive
17	23.27	2.30E+04	Positive	**127**	24.97	8.33E+03	Positive
18	23.46	2.50E+04	Positive	**128**	25.68	5.08E+03	Positive
19	23.76	2.00E+04	Positive	**129**	26.25	3.45E+03	Positive
20	24.15	1.50E+04	Positive	**130**	26.86	2.30E+03	Positive
21	24.52	1.15E+04	Positive	**131**	28.06	1.07E+03	Positive
22	26.05	3.95E+03	Positive	**132**	28.90	6.35E+02	Positive
23	26.90	2.24E+03	Positive	**133**	29.66	4.02E+02	Positive
24	28.80	6.75E+02	Negative	**134**	30.30	2.76E+02	Negative
25	30.60	2.32E+02	Negative	**135**	30.87	1.99E+02	Positive
26	31.92	1.10E+02	Negative	**136**	31.16	1.69E+02	Negative
27	32.15	9.73E+01	Negative	**137**	34.77	2.45E+01	Negative
28	No Cq	ND	Negative	**138**	No Cq	ND	Negative
29	No Cq	ND	Negative	**139**	No Cq	ND	Negative

30	No Cq	ND	Negative	**140**	No Cq	ND	Negative
31	No Cq	ND	Negative	**141**	No Cq	ND	Negative
32	No Cq	ND	Negative	**142**	No Cq	ND	Negative
33	No Cq	ND	Negative	**143**	No Cq	ND	Negative
34	No Cq	ND	Negative	**144**	No Cq	ND	Negative
35	No Cq	ND	Negative	**145**	No Cq	ND	Positive
36	No Cq	ND	Negative	**146**	No Cq	ND	Negative
37	No Cq	ND	Negative	**147**	No Cq	ND	Negative
38	No Cq	ND	Negative	**148**	No Cq	ND	Negative
39	No Cq	ND	Negative	**149**	No Cq	ND	Negative
40	No Cq	ND	Negative	**150**	No Cq	ND	Negative
41	No Cq	ND	Negative	**151**	No Cq	ND	Negative
42	No Cq	ND	Negative	**152**	No Cq	ND	Negative
43	No Cq	ND	Negative	**153**	No Cq	ND	Negative
44	No Cq	ND	Negative	**154**	No Cq	ND	Negative
45	No Cq	ND	Negative	**155**	No Cq	ND	Negative
46	No Cq	ND	Negative	**156**	No Cq	ND	Negative
47	No Cq	ND	Negative	**157**	No Cq	ND	Negative
48	No Cq	ND	Negative	**158**	No Cq	ND	Negative

49	No Cq	ND	Negative	**159**	No Cq	ND	Negative
50	No Cq	ND	Negative	**160**	No Cq	ND	Negative
51	No Cq	ND	Negative	**161**	No Cq	ND	Negative
52	No Cq	ND	Negative	**162**	No Cq	ND	Negative
53	No Cq	ND	Negative	**163**	No Cq	ND	Negative
54	No Cq	ND	Negative	**164**	No Cq	ND	Negative
55	No Cq	ND	Negative	**165**	No Cq	ND	Negative
56	No Cq	ND	Negative	**166**	No Cq	ND	Negative
57	No Cq	ND	Negative	**167**	No Cq	ND	Negative
58	No Cq	ND	Negative	**168**	No Cq	ND	Negative
59	No Cq	ND	Negative	**169**	No Cq	ND	Negative
60	No Cq	ND	Negative	**170**	No Cq	ND	Negative
61	No Cq	ND	Negative	**171**	No Cq	ND	Negative
62	No Cq	ND	Negative	**172**	No Cq	ND	Negative
63	No Cq	ND	Negative	**173**	No Cq	ND	Negative
64	No Cq	ND	Negative	**174**	No Cq	ND	Negative
65	No Cq	ND	Negative	**175**	No Cq	ND	Negative
66	No Cq	ND	Negative	**176**	No Cq	ND	Negative
67	No Cq	ND	Negative	**177**	No Cq	ND	Negative

68	No Cq	ND	Negative	**178**	No Cq	ND	Negative
69	No Cq	ND	Negative	**179**	No Cq	ND	Negative
70	No Cq	ND	Negative	**180**	No Cq	ND	Negative
71	No Cq	ND	Negative	**181**	No Cq	ND	Negative
72	No Cq	ND	Negative	**182**	No Cq	ND	Negative
73	No Cq	ND	Negative	**183**	No Cq	ND	Negative
74	No Cq	ND	Negative	**184**	No Cq	ND	Negative
75	No Cq	ND	Negative	**185**	No Cq	ND	Negative
76	No Cq	ND	Negative	**186**	No Cq	ND	Negative
77	No Cq	ND	Negative	**187**	No Cq	ND	Negative
78	No Cq	ND	Negative	**188**	No Cq	ND	Negative
79	No Cq	ND	Negative	**189**	No Cq	ND	Negative
80	No Cq	ND	Negative	**190**	No Cq	ND	Negative
81	No Cq	ND	Negative	**191**	No Cq	ND	Negative
82	No Cq	ND	Negative	**192**	No Cq	ND	Negative
83	No Cq	ND	Negative	**193**	No Cq	ND	Negative
84	No Cq	ND	Negative	**194**	No Cq	ND	Negative
85	No Cq	ND	Negative	**195**	No Cq	ND	Negative
86	No Cq	ND	Negative	**196**	No Cq	ND	Negative

87	No Cq	ND	Negative	**197**	No Cq	ND	Negative
88	No Cq	ND	Negative	**198**	No Cq	ND	Negative
89	No Cq	ND	Negative	**199**	No Cq	ND	Negative
90	No Cq	ND	Negative	**200**	No Cq	ND	Negative
91	No Cq	ND	Negative	**201**	No Cq	ND	Negative
92	No Cq	ND	Negative	**202**	No Cq	ND	Negative
93	No Cq	ND	Negative	**203**	No Cq	ND	Negative
94	No Cq	ND	Negative	**204**	No Cq	ND	Negative
95	No Cq	ND	Negative	**205**	No Cq	ND	Negative
96	No Cq	ND	Negative	**206**	No Cq	ND	Negative
97	No Cq	ND	Negative				
98	No Cq	ND	Negative				
99	No Cq	ND	Negative				
100	No Cq	ND	Negative				
101	No Cq	ND	Negative				
102	No Cq	ND	Negative				
103	No Cq	ND	Negative				
104	No Cq	ND	Negative				
105	No Cq	ND	Negative				

106	No Cq	ND	Negative
107	No Cq	ND	Negative
108	No Cq	ND	Negative
109	No Cq	ND	Negative
110	No Cq	ND	Negative

***** Mean CT (Cycle Threshold) determined for N1 and CT N2. ND (Not determinate). No Cq - No cycle quantification.

Statistical Analysis

In order to calculate the values for sensitivity, specificity, disease prevalence, positive and negative predictive values and accuracy, the following data was considered:

Laboratory:

RT-LAMP Results	RT-qPCR Results				
	Present	n	Absent	n	Total
Positive	True Positive (a)	23	False Positive (c)	0	a + c
Negative	False Negative (b)	4	True Negative (d)	83	b + d
Total		a + b		c + d	

Hospital:

RT-LAMP Results	RT-qPCR Results				
	Present	n	Absent	n	Total
Positive	True Positive (a)	24	False Positive (c)	1	a + c
Negative	False Negative (b)	3	True Negative (d)	68	b + d
Total		a + b		c + d	

Given that: true positive = a, false negative = b, false positive = c and true negative = d, the results were calculated considering the following:

$$Sensitivity = \frac{a}{(a+b)}$$

$$Specificity = \frac{d}{(c+d)}$$

$$PPV = \frac{sensitivity \times prevalence}{sensitivity \times prevalence + (1 - specificity) \times (1 - prevalence)}$$

$$NPV = \frac{specificity \times (1 - prevalence)}{(1 - sensitivity) \times prevalence + specificity \times (1 - prevalence)}$$

$$Accuracy = Sensitivity \times Prevalence + Specificity \times (1 - Prevalence)$$

Cohen's Kappa was calculated using the following. N = the total number of samples

$$\kappa = \frac{\Pr(\alpha) - \Pr(e)}{1 - \Pr(e)}$$

$$\Pr(\alpha) = \frac{a+d}{N}$$

$$\Pr(e) = \frac{\frac{(a+b) \times (a+c)}{N} + \frac{(c+d) \times (b+d)}{N}}{N}$$

General Introduction

In addition to our study on direct detection of SARS-CoV-2 in nasopharyngeal swab samples, we extended our research to explore the application of the LAMP technique using saliva as the testing matrix. The motivation behind this approach was to create a more accessible and non-invasive diagnostic tool, particularly suited for populations where frequent testing is needed, such as school children, individuals with some health challenges, or those who might find nasopharyngeal swabs uncomfortable or distressing.

This chapter corresponds to the development and validation of the RT-LAMP colorimetric assay designed specifically for screening large groups. The method proved effective in detecting SARS-CoV-2 in RNA extracted from saliva samples, offering a reliable option both for identifying symptomatic carriers and for identifying asymptomatic and pre-symptomatic carriers. The ability to use saliva not only simplified the sample collection process but also increased the feasibility of mass testing campaigns, which remains crucial for controlling viral spread in community settings. This chapter brings the publication of this study details of this study, which was published (front cover) in the Journal of Brazilian Chemistry Society, entitled “Detection of SARS-CoV-2 in Saliva by RT-LAMP During a Screening of Workers in Brazil, Including Pre-Symptomatic Carriers” (Santos et al., 2021).

Chapter III: Detection of SARS-CoV-2 in Saliva by RT-LAMP During a Screening of Workers in Brazil, Including Pre-Symptomatic Carriers

Abstract

The coronavirus pandemic has been causing damage to many nations, as public and private health systems deteriorate by the increasing demand. Some infected patients have culturable severe acute respiratory syndrome coronavirus-2 (SARS-CoV-2) even though not presenting any symptoms, and therefore, are probably able to transmit it. Correctly diagnosing and isolating infected patients is an important step towards preventing new infections. Current diagnostic methods rely mainly on reverse transcription quantitative polymerase chain reaction (RT-qPCR). Methods such as reverse transcription loop-mediated isothermal amplification (RT-LAMP) have risen as viable alternatives, as they are cheaper and require less infrastructure, they have the potential to be applied in low-resource scenarios and even at point-of-care. Here we report a colorimetric RT-LAMP assay capable of detecting SARS-CoV-2 in ribonucleic acid (RNA) from saliva. In some cases, the test was able to detect viral RNA before symptom onset and even in a self-reported asymptomatic carrier. It had a limit of detection of 300 copies *per* reaction and showed a sensitivity of 80%, a specificity of 100%, a general accuracy of 99.59%, and a Cohen's kappa of 0.887. The possibility of detecting positive cases even before the clinical manifestation shows great potential and can contribute to controlling the pandemic.

Keywords: screening, molecular diagnosis, isothermal amplification, COVID-19 test.

Introduction

In December 2019, a new coronavirus named severe acute respiratory syndrome coronavirus-2 (SARSCoV-2) was detected in Wuhan, Hubei province, China. Since then, the virus has spread rapidly around the world and the World Health Organization (WHO) has declared the disease caused by the new coronavirus 2019 (COVID-19) as a pandemic in March 2020.[1] The main route of transmission for SARS-CoV-2 is through respiratory droplets carrying infectious virus that might be released into the air when people cough, sneeze, breathe or speak,[2] therefore, presenting high transmissibility. The high number of SARS-CoV-2 infections is putting pressure on the healthcare system, in addition to leading to major health, social and economic consequences for countries.[3,4] As of 10 May 2021, there have been 157,973,438 confirmed cases of COVID-19, including 3,288,455 deaths.[5]

Patients infected with SARS-CoV-2 can develop coronavirus disease (COVID-19). It has a broad clinical spectrum, ranging from a mild disease characterized by symptoms such as fever, cough, sore throat, congestion or runny nose, muscle or body aches, ageusia and/or anosmia, to a severe disease characterized by severe respiratory failure, need for hospitalization, intensive care and invasive mechanical ventilation, which can lead to death.[6] Also, during the pandemic, asymptomatic cases have been reported and although these patients do not demonstrate clinical manifestation of the disease, recent researches have shown that they are responsible for about 17 to 20% of new infections.[7,8] The imposition of non-pharmaceutical interventions (NPIs), such as lockdowns, social

distancing, contact tracing, use of face masks and mass testing are key points for controlling COVID-19.[3,4,9]

Current diagnostic tests for SARS-CoV-2 detection rely mainly on reverse transcriptase quantitative polymerase chain reaction (RT-qPCR) as a gold-standard technique for nucleic acid amplification. This technique can detect SARS-CoV-2 with high sensitivity and specificity, and most primer sets can detect at least 100 viral copies.[10] However, the cost, complexity and facility requirements to use this test on a large scale are major drawbacks for its wide implementation in developing countries. Other nucleic acid amplification methods such as reverse transcription loop-mediated isothermal amplification (RT-LAMP) have been proposed as viable alternatives to RT-qPCR. In addition to being cheaper, there is no need for complex, expensive instrumentation to perform RT-LAMP.

In this study, we evaluated the use of the RT-LAMP assay using ribonucleic acid (RNA) extracted from saliva samples as a tool for screening symptomatic and asymptomatic workers. We obtained data regarding COVID-19 related symptoms through a questionnaire, and we correlated symptom onset to positivity, reporting the efficiency of the test in helping separate positive cases from others.

Experimental

Biological samples

Nasopharyngeal swabs of 485 essential workers that, although not in the front line, kept working even during lockdown periods were collected. Participants were also asked to self-collect approximately 1 mL of saliva. All samples were stored in a cryotube containing 1 mL 0.9% NaCl solution (LBS Laborasa, São Paulo, Brazil). To inactivate the virus, all samples were incubated at 65 ºC for 1 h

before analysis. Of the total 485 samples tested, 72 samples were from the public transportation company, 121 were from the town's garbage collection company, 78 were from Federal Highway Patrol officers, 174 were from bus drivers working in public transportation and 40 were from employees at the Federal University of Goiás. All workers were interviewed before sample collection and data related to COVID-related symptoms such as fever, dyspnea, sore throat, runny nose, nasal congestion, chest pain, abdominal pain, myalgia, arthralgia, fatigue, headache, loss of smell, loss of taste, diarrhea, nausea, vomiting, conjunctivitis or decreased urine output were collected (Supplementary Information section, Table S1). This study was approved by the Research Ethics Committee of the Federal University of Goiás, protocol number 4.111.485/2020. Furthermore, all workers agreed to participate in the study with a written statement.

RT-LAMP primer designing

We designed RT-LAMP primers for the detection of SARS-CoV-2 using the LAMP Designer Software,[11] targeting the S gene. The six specific primers were synthesized by Integrated DNA Technologies (Coralville, USA). Primer sequences are displayed in Table 1.

Table 3: Primers used in the RT-LAMP reaction.

Primer	Sequence 5'-3'
F3	TGTTAACTGCACAGAAGTCC
B3	TGATGGATTGACTAGCTACA
FIP	AGCCTGCACGTGTTTGAAATTTTGCTATTCATGCAGATCAACT
BIP	ATGAGTGTGACATACCCATTGGTTTTGAGGAGAATTAGTCTGAGTCT

LF	ACACGCCAAGTAGGAGTA
LB	GCAGGTATATGCGCTAGTTAT

F3: forward displacement primer; B3: backward displacement primer; FIP: forward inner primer, BIP: backward inner primer; LF: loop forward primer; LB: loop backward primer; A: adenine; C: cytosine; G: guanine; T: thymine.

Colorimetric detection RT-LAMP for SARS-CoV-2

RNA from saliva samples for the RT-LAMP test was extracted using the Viral RNA + DNA Preparation Kit (Cellco, São Carlos, Brazil), according to the manufacturer's instructions. RT-LAMP reactions were carried out using the WarmStart Colorimetric LAMP 2X Master Mix (New England Biolabs, Hitchin, UK). The final volume of the reaction was 15 µL, consisting of 7.5 µL of the colorimetric LAMP Master Mix, 1.5 µL of a 10X primer mix (2 µM of each F3 and B3, 16 µM of each FIP and BIP, and 8 µM of each LF and LB), 4.5 µL of nuclease-free water (Sigma-Aldrich, St. Louis, USA) and 1.5 µL of RNA sample. Reactions were then heated on a thermoblock (Kasvi, São José dos Pinhais, Brazil) for 30 min at 68 ºC. The results of the colorimetric RT-LAMP test were determined visually by the change of the color pink (negative) to yellow (positive).

RT-qPCR assay

To perform RT-qPCR, RNA from swab samples was extracted using the QIAmp Viral RNA Mini Kit (Qiagen, Hilden, Germany), according to the manufacturer's instructions. RT-qPCR was performed using the GoTaq Probe 1-Step RT-qPCR Kit (Promega, Charbonnières-lesBains, France) and 2019-nCoV RUO Kit (Integrated DNA Technologies, Coralville, USA). For each sample, three sets of primers were used targeting the N1, N2 regions of SARS-CoV-2 and RNase P as internal human control, according to the CDC 2019-nCoV Real-Time RT-PCR Diagnostic Panel.[12] RT-qPCR reactions were carried out in a final volume of 20 µL containing 3.1 µL of nucleasefree water (Sigma-Aldrich, St. Louis, USA), 1.5 µL of the primers and probes, 10 µL of GoTaq Probe qPCR Master Mix with dUTP, 0.4 µL of Go Script RT Mix for 1-Step RT-qPCR and 5 µL of the sample. The amplification was performed in a Step-One Real-Time PCR System (Thermofisher Scientific, Rockford, USA), consisting of one cycle of 15 min at 45 ºC for reverse transcription, followed by one cycle of 2 min at 95 ºC for enzyme activation, and then 45 cycles of 2 s at 95 ºC and 30 s at 55 ºC for amplification. Samples were considered positive when all the three regions amplified.

Limit of detection of the SARS-CoV-2 RT-LAMP assay

To assess the limit of detection of the RT-LAMP test, we used serial dilutions of a gBlock synthesized by IDT Technologies (Coralville, USA) containing the target sequence. The test was performed in triplicates. The gBlock is a double-stranded DNA with known molecular size and sequence, obtained by high-fidelity synthesis. The number of copies was quantified using the formula in equation 1.

$$N = C \times M \times (1 \times 10^{-15} \text{ mol fmol}^{-1}) \times (6{,}02214086 \times 10^{23} \text{ mol}^{-1}) \quad (1)$$

where N is the number of copies in μL^{-1}, C is the concentration in ng μL^{-1} and M is the molecular weight in fmol ng^{-1}. Both concentration and molecular weight are provided by the manufacturer. The gBlock was used instead of the RNA standard because it is more stable, simplifying storage. The RT-LAMP-amplified products were determined by visual observation and gel electrophoresis 2% agarose (GBTSciences, Brasília, Brazil) and 0.5% Tris-ethylenediaminetetraacetic acid (EDTA)-borate (TEB) buffer (GBTSciences, Brasília, Brazil), revealed with GelRed® (Biotium, Fremont, USA) in an Ultra Lum Omega 10 Molecular Imaging System (Ultra Lum Inc., Claremont, USA).

Statistical analysis

The sensitivity, specificity and prevalence were calculated using the platform SciStat.[13] The variables used for statistical analysis are (i) true positive samples (number of samples that are positive by both RT-LAMP and RT-qPCR); (ii) false negative samples (number of samples that were negative by RT-LAMP and positive by RT-qPCR); (iii) false positive samples (number of samples that were positive by RT-LAMP and negative by RT-qPCR) and (iv) true negative samples (number of samples that were negative by both methods). Cohen's Kappa value was calculated using the VassarStats platform.[14]

Results and Discussion

Even though nasopharyngeal swabs have been proposed as the ideal samples to detect SARS-CoV-2, it is an invasive method and can present some risk to health professionals collecting samples. So, to perform RT-LAMP, we decided to

use saliva samples since it would be a less invasive test. Furthermore, some studies have demonstrated the reliability of saliva as a good sample to detect SARS-CoV-2.[15-18] Untreated saliva samples are not ideal for working directly with the colorimetric RT-LAMP, given the natural and broad range of pH in which saliva can be collected. Acidic saliva samples would turn the pH indicator in the reaction yellow, even before the amplification step, resulting in an erroneous interpretation of the results.[19] Another possibility is to add alkalinizing solutions to the samples, increasing their pH before adding to the reaction.[20]

The limit of detection of the RT-LAMP test was 300 copies of viral RNA *per* reaction because it was the minimum number of copies that successfully led to a color change in all replicates, as shown in Figure 1a. The limit of detection found here is similar to that reported in other papers that detected SARS-CoV-2 by colorimetric RT-LAMP.21,22

To confirm that the change from pink to yellow was due to specific amplification of the target, electrophoresis in agarose gel was performed (Figure 1b). Gel electrophoresis demonstrated a limit of detection of 200 copies of the viral RNA *per* reaction. Even though reactions with up to 200 copies presented visible amplification in the agarose gel, it was not vigorous enough to bring the pH indicator to a turning point. That is because the RT-LAMP colorimetric assay uses phenol red as a detection system, a colorchanging pH indicator molecule. Phenol red is used to identify the pH change as a result of successful amplification of the target region. In general, the pH change begins in the polymerization step, in which the enzyme acting in the 5'→3' direction incorporates a deoxynucleotide triphosphate in the target region and promotes the release of two by-products: the pyrophosphate ion, and the hydrogen ion. The interaction between these hydrogen cations (H^+) and the

phenol red indicator yields a gradual color transition from pink to yellow, over the pH range 7.3 to 6.8. Based on the color change we considered the limit of detection to be 300 copies *per* reaction. Therefore, despite the occurrence of amplification in reactions containing up to 200 copies (as observed in the agarose gel), the generation of hydronium ion was insufficient to reach the transition interval of the indicator molecule. Even though the limit of detection was lower in the agarose gel when compared to the colorimetric detection, the instrumental ease, low time, no use of mutagenic substances and no manipulation of the reaction after amplification, demonstrate great potential to opt for the colorimetric detection.

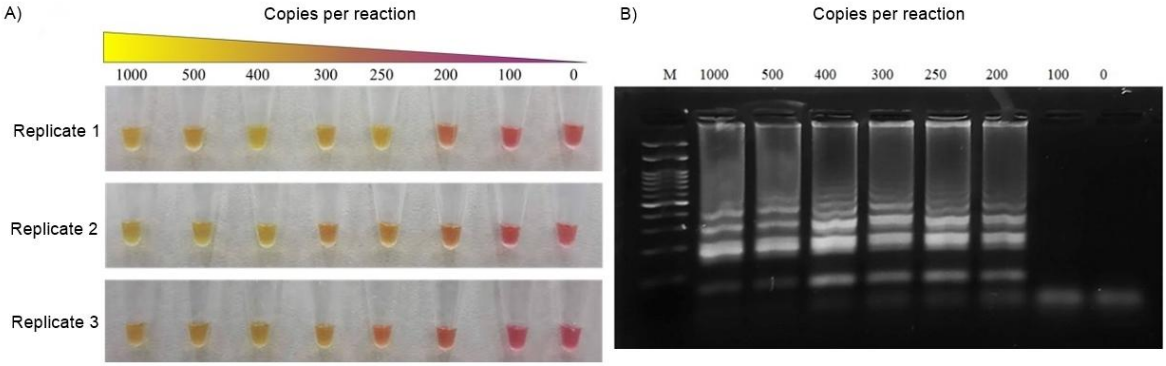

Figure 1: (a) Serial gBlock dilutions to assess the limit of detection of the test. Amplification successfully led to a color change from pink to yellow in the reactions containing at least 300 copies. (b) Agarose gel visualization of the products of the iamplification. M = 100 base pair molecular marker, 0 = no template control (nuclease-free water).

A total of 485 clinical samples were analyzed both by RT-qPCR and RT-LAMP. Of the total, 475 (97.9%) samples were negative and 10 (2.1%) were positive for SARS-CoV-2 by RT-qPCR. Of the 10 samples positive by RT-qPCR, 8 of them were positive by RT-LAMP, as summarized in Table 2.

Table 4: Comparison between the results of RT-LAMP and the results of RT-qPCR.

RT-LAMP	RT-qPCR		
	Positive	Negative	Total
Positive	8	0	8
Negative	2	475	477
Total	10	475	485

RT-LAMP: reverse transcription loop-mediated isothermal amplification; RT-qPCR: reverse transcription quantitative polymerase chain reaction.

Statistical analysis showed a sensitivity of 80% (95% confidence interval (CI) from 44.39 to 97.48%), a specificity of 100% (95% CI from 99.23 to 100.00%), a positive predictive value of 100%, a negative predictive value of 99.58% (95% CI from 98.57 to 99.88%) and overall accuracy of 99.59%. The calculated kappa value was 0.887 (95% CI from 0.731 to 1.0). All statistical results are summarized in Table 3.

Table 5: Statistical analysis results.

Statistic	Value	95% CI
Sensitivity	80.00%	44.39 to 97.48
Specificity	100.00%	99.23 to 100.00

Positive predictive value	100.00%	
Negative predictive value	99.58%	98.57 to 99.88
Accuracy	99.59%	98.52 to 99.95
Cohen's Kappa	0.887	0.731 to 1.0

CI: confidence interval.

All samples positive by RT-qPCR with low cycle of quantification (Cq) (Cq < 30) were positive by RT-LAMP, while higher Cq samples (Cq 32 and Cq 34) did not show amplification. This is due to the number of copies present in the sample, which are lower than the limit of detection of RT-LAMP, which would be a Cq of about 30 for real samples. Figure 2 shows the clinical samples that were positive by RT-qPCR with their respective Cq values and the comparison with RT-LAMP visual detection results.

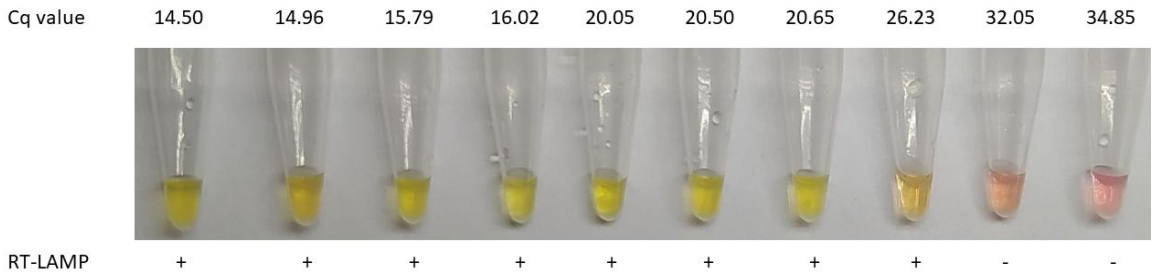

Figure 2: Clinical samples that were positive by RT-qPCR and the comparison with RT-LAMP results. Cq-Cycle quantification.

In Figure 3 we show the distribution of all positive samples by RT-qPCR (10) according to the Cq and the results of the RT-LAMP test. Of the 10 patients that were positive for SARS-CoV-2, 6 patients (patient numbers 80, 171, 233, 273, 295 and 395) reported feeling a medium of 5.17 (95% CI 4.57 to 5.77) symptoms on the day of collection and were, therefore, symptomatic for the disease. The other 4 did not report any symptoms at the time of collection. These potentially asymptomatic or presymptomatic patients were accompanied through telephone contact, and data regarding COVID-related symptoms was retrieved. Patients 53, 296 and 355 started showing COVID-related symptoms such as headache, cough, fever and muscle pain one day after collection. Patient 355 reported only feeling a mild headache, and patient number 132 claimed not having felt any symptom at all during the following 14 days after the testing, even though presenting a high viral load. All positive patients were informed of their results within 24 h from sample collection.

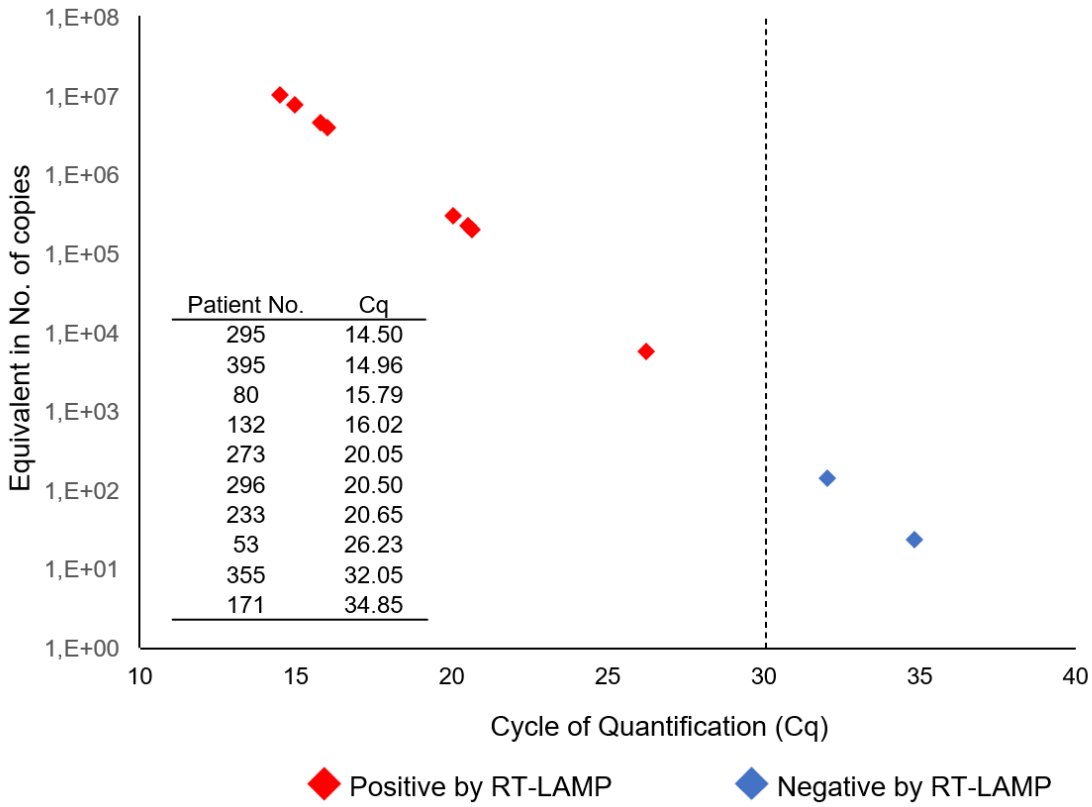

Patient No.	Cq
295	14.50
395	14.96
80	15.79
132	16.02
273	20.05
296	20.50
233	20.65
53	26.23
355	32.05
171	34.85

Figure 3: Comparison between RT-LAMP and RT-qPCR. Results of RT-qPCR are median of N1 and N2 Cqs. The number of copies was calculated based on the standard curve. Red diamonds represent samples positive by RT-LAMP and blue diamonds represent samples negative by RT-LAMP.

Of the 10 patients, 8 had detectable viral loads by both RTLAMP and RT-qPCR on the day of collection, and 2 patients (171 and 355) were negative by RT-LAMP and positive by RT-qPCR. The relatively low number of copies (Cqs 34.85 and 32.05, respectively) can be explained differently based on the patients' symptom onset (Figure 4). Patient 171 had been experiencing symptoms for 14 days when the test was done. It coincides with the shedding duration of the virus.[23] Therefore, we hypothesize the patient was in the final course of the infection. On the other hand, patient 355 was yet to experience symptoms on the day of collection and therefore was pre-symptomatic.

We hypothesize this patient was probably at the beginning of the exponential growth phase of the viral replication. Although the duration of this exponential growth is still not rigorously defined, models of SARS-CoV-2 transmission in ferrets project it to be on the order of a day.[24] Patients 53 and 296 were detected by RT-LAMP, as they presented Cqs lower than the limit of detection of the test. Due to the higher viral load when compared to patient 355, we hypothesize these patients were more advanced in the course of the disease.

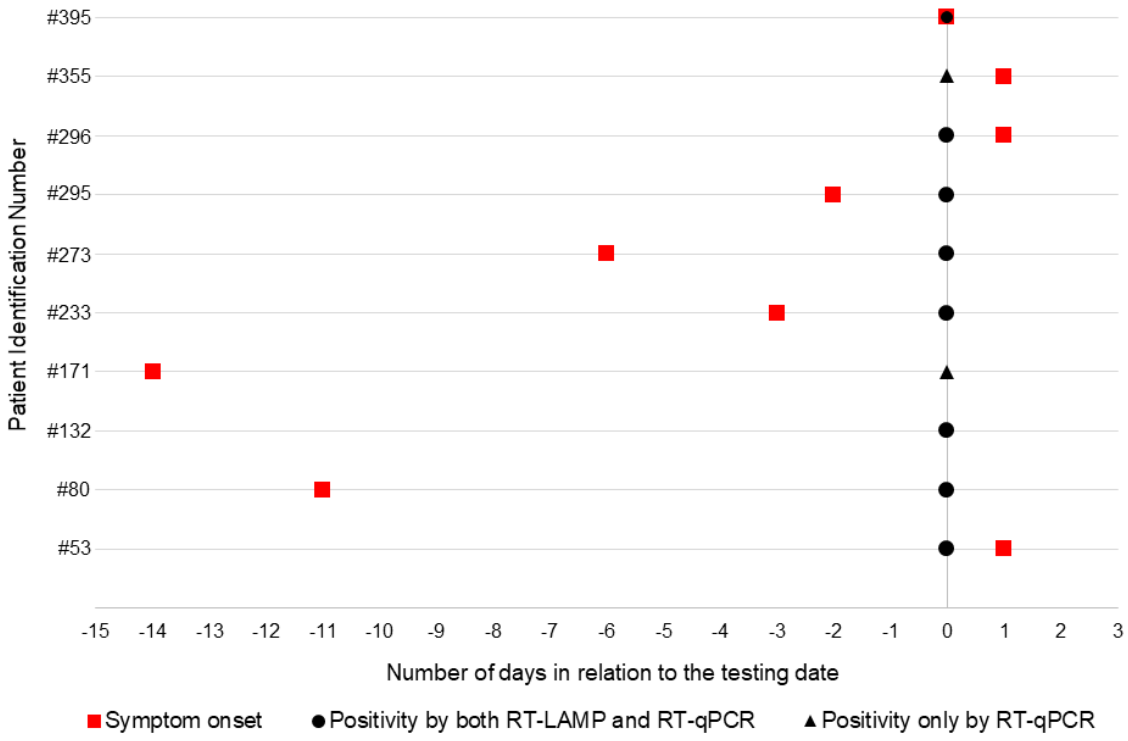

Figure 4: Relation between the number of days from symptom onset and the date of the positive result in a molecular test. Each line represents the course of the disease in one patient. Day 0 is regarded as the testing date. Negative numbers represent the number of days before testing, positive numbers represent the number of days after testing was done. Most patients experienced symptom onset prior to testing, while three patients (53, 296 and 355) presented a positive result

before symptom onset. Patient 395 reported symptom onset on the same day as the testing took place, and patient 132 claimed to never have presented symptoms.

As first pointed out by Larremore *et al*.[25] and Mina *et al*.,[26] it is necessary to rethink our SARS-CoV-2 testing strategy, shifting the focus from how well tests can detect lower quantities of copies to how well tests can detect patients in the infectious period. It is also important to take into account how fast results can be returned, as one of the most effective measures to lower infectivity rates is the isolation of symptomatic, pre-symptomatic and asymptomatic carriers. While developed countries such as the United States peaked at 5.0 tests *per* thousand people during the pandemic, available data shows that Brazil was hardly able to do 0.48 tests *per* thousand people.[27] There is therefore an urgent need to increase testing capacity in countries such as Brazil.

The RT-LAMP assay was able to correctly identify 8 of 10 positive cases, 3 of which did not have symptoms by the time of collection. Even though samples with a Cq > 30 did not present positive results in RT-LAMP, it is expected that these patients would have a lower probability of transmitting the virus.[28-30] In this particular study, RT-LAMP results were returned on the same day and positive cases were promptly isolated. We then propose that even not being able to detect these patients with low viral load, the test would still be of help in isolating positive cases, mainly if repeated frequently in a given population.[25]

Our data is limited to its size, and our test fails as it still needs RNA isolation to perform the test. Despite some tests that have shown promising results with a direct swab-to-lamp essay without the need for RNA extraction,[31] swabs can be difficult and painful to collect, especially for children or people of age. To increase

the effectiveness of a testing regimen and the chances of assaying a positive case, SARS-CoV-2 tests would ideally be done repeatedly in an individual on different occasions. Collecting swab samples weekly would have the potential to be a major drawback of testing, as many would probably refuse to have samples collected every couple of days. On the other hand, saliva is much easier to collect and could be collected easily and repeatedly from basically anyone. Therefore, there seems to be a tradeoff between the need for RNA extraction and the simplicity of collection.

To our knowledge, this is the first report that includes the detection of pre-symptomatic and asymptomatic cases of COVID-19 using RT-LAMP and correlates the positivity of the sample with a detailed symptom questionnaire. Although limited to its size, the questionnaire provides enough data to suggest that the test was able to diagnose 2/3 of the pre-symptomatic individuals and one asymptomatic individual. Giving a testing regimen that repeatedly tests individuals, we see the methodology described here as potentially helpful in isolating positive cases, helping in breaking the chain of infection.

Conclusions

We report an RT-LAMP colorimetric assay that can detect SARS-CoV-2 in RNA from saliva samples from workers at different stages of the infection, including pre-symptomatic carriers, with overall specificity of 100%, sensitivity of 80% and accuracy of 99.59%. In addition, the method takes less time than the gold standard method (RT-qPCR). Our results show that our colorimetric RT-LAMP assay is suitable for screening large groups, as the great majority of workers were correctly diagnosed based on this simple, fast and low-cost amplification test. Being able to correctly diagnose people carrying transmissible SARS-CoV-2 and quickly isolating

them is an important advantage that helps prevent the further spread of the virus, as the contact with others is severely reduced. Due to its low cost and simplicity compared to RT-qPCR, RT-LAMP could be used in countries that do not have the resources to perform RT-qPCR on a large scale, increasing testing capacity without necessarily increasing costs.

References

1. https://www.who.int/director-general/speeches/detail/whodirector-general-s-opening-remarks-at-the-media-briefing-oncovid-19---11-march-2020, accessed in June 2021.

2. Falahi, S.; Kenarkoohi, A.; New Microbes New Infect. 2020, 38, 100778.

3. Flaxman, S.; Mishra, S.; Gandy, A.; Unwin, H. J. T.; Mellan, T. A.; Coupland, H.; Whittaker, C.; Zhu, H.; Berah, T.; Eaton, J. W.; Monod, M.; Perez-Guzman, P. N.; Schmit, N.; Cilloni, L.; Ainslie, K. E. C.; Baguelin, M.; Boonyasiri, A.; Boyd, O.; Cattarino, L.; Cooper, L. V.; Cucunubá, Z.; Cuomo-Dannenburg, G.; Dighe,

4. A.; Djaafara, B.; Dorigatti, I.; van Elsland, S. L.; FitzJohn, R.

5. G.; Gaythorpe, K. A. M.; Geidelberg, L.; Grassly, N. C.; Green,

6. W. D.; Hallett, T.; Hamlet, A.; Hinsley, W.; Jeffrey, B.; Knock, E.; Laydon, D. J.; Nedjati-Gilani, G.; Nouvellet, P.; Parag, K. V.; Siveroni, I.; Thompson, H. A.; Verity, R.; Volz, E.; Walters, C. E.;

7. Wang, H.; Wang, Y.; Watson, O. J.; Winskill, P.; Xi, X.; Walker, P.

8. G. T.; Ghani, A. C.; Donnelly, C. A.; Riley, S.; Vollmer, M. A. C.; Ferguson, N. M.; Okell, L. C.; Bhatt, S.; Nature 2020, 584, 257.

9. See, I.; Paul, P.; Slayton, R. B.; Steele, M. K.; Stuckey, M. J.; Duca, L.; Srinivasan, A.; Stone, N.; Jernigan, J. A.; Reddy, S. C.; Clin. Infect. Dis., in press, DOI: 10.1093/cid/ciab110.

10. https://covid19.who.int/, accessed on May 10, 2021.

11. Guan, W.; Ni, Z.; Hu, Y.; Liang, W.; Ou, C.; He, J.; Liu, L.; Shan, H.; Lei, C.; Hui, D. S. C.; Du, B.; Li, L.; Zeng, G.; Yuen, K.-Y.; Chen, R.; Tang, C.; Wang, T.; Chen, P.; Xiang, J.; Li, S.; Wang, J.; Liang, Z.; Peng, Y.; Wei, L.; Liu, Y.; Hu, Y.;

Peng, P.; Wang, J.; Liu, J.; Chen, Z.; Li, G.; Zheng, Z.; Qiu, S.; Luo, J.; Ye, C.; Zhu, S.; Zhong, N.; N. Engl. J. Med. 2020, 382, 1708.

12. Buitrago-Garcia, D.; Egli-Gany, D.; Counotte, M. J.; Hossmann, S.; Imeri, H.; Ipekci, A. M.; Salanti, G.; Low, N.; PLoS Med. 2020, 17, e1003346.

13. Byambasuren, O.; Cardona, M.; Bell, K.; Clark, J.; McLaws, M. L.; Glasziou, P.; Off. J. Assoc. Med. Microbiol. Infect. Dis. Can. 2020, 5, 223.

14. Chu, D. K.; Akl, E. A.; Duda, S.; Solo, K.; Yaacoub, S.; Schünemann, H. J.; El-harakeh, A.; Bognanni, A.; Lotfi, T.; Loeb, M.; Hajizadeh, A.; Bak, A.; Izcovich, A.; Cuello-Garcia, C. A.; Chen, C.; Harris, D. J.; Borowiack, E.; Chamseddine, F.; Schünemann, F.; Morgano, G. P.; Muti Schünemann, G. E. U.; Chen, G.; Zhao, H.; Neumann, I.; Chan, J.; Khabsa, J.; Hneiny,

15. L.; Harrison, L.; Smith, M.; Rizk, N.; Giorgi Rossi, P.; AbiHanna, P.; El-khoury, R.; Stalteri, R.; Baldeh, T.; Piggott, T.; Zhang, Y.; Saad, Z.; Khamis, A.; Reinap, M.; Lancet 2020, 395, 1973.

16. Vogels, C. B. F.; Brito, A. F.; Wyllie, A. L.; Fauver, J. R.; Ott, M.; Kalinich, C. C.; Petrone, M. E.; Casanovas-Massana,

17. A.; Catherine Muenker, M.; Moore, A. J.; Klein, J.; Lu, P.; LuCulligan, A.; Jiang, X.; Kim, D. J.; Kudo, E.; Mao, T.; Moriyama,

18. M.; Oh, J. E.; Park, A.; Silva, J.; Song, E.; Takahashi, T.; Taura,

19. M.; Tokuyama, M.; Venkataraman, A.; El Weizman, O.; Wong,

20. P.; Yang, Y.; Cheemarla, N. R.; White, E. B.; Lapidus, S.; Earnest, R.; Geng, B.; Vijayakumar, P.; Odio, C.; Fournier, J.; Bermejo, S.; Farhadian, S.; Dela Cruz, C. S.; Iwasaki, A.; Ko, A. I.; Landry, M. L.; Foxman, E. F.; Grubaugh, N. D.; Nat. Microbiol. 2020, 5, 1299.

21. LAMP Designer, v.1.16; Premier Biosoft International, San Francisco, USA, 2011.

22. https://www.fda.gov/media/134922/download, accessed in June 2021.

23. https://www.scistat.com/statisticaltests/diagnostic_test.php, accessed in June 2021.

24. http://vassarstats.net/kappa.html, accessed in July 2021.

25. Yee, R.; Truong, T. T.; Pannaraj, P. S.; Eubanks, N.; Gai, E.;

26. Jumarang, J.; Turner, L.; Peralta, A.; Lee, Y.; Bard, J. D.; J. Clin. Microbiol. 2021, 59, e02686-20.

27. Sohn, Y.; Jeong, S. J.; Chung, W. S.; Hyun, J. H.; Baek, Y. J.; Cho, Y.; Kim, J. H.; Ahn, J. Y.; Choi, J. Y.; Yeom, J.-S.; J. Clin. Med. 2020, 9, 2924.

28. Teo, A. K. J.; Choudhury, Y.; Tan, I. B.; Cher, C. Y.; Chew, S.

29. H.; Wan, Z. Y.; Cheng, L. T. E.; Oon, L. L. E.; Tan, M. H.; Chan,

a. S.; Hsu, L. Y.; Sci. Rep. 2021, 11, 3134.

30. Zhu, J.; Guo, J.; Xu, Y.; Chen, X.; J. Infect. 2020, 81, e48.

31. Uribe-Alvarez, C.; Lam, Q.; Baldwin, D. A.; Chernoff, J.; PLoS One 2021, 16, e0250202.

32. Yang, Q.; Meyerson, N. R.; Clark, S. K.; Paige, C. L.; Fattor, W. T.; Gilchrist, A. R.; Barbachano-Guerrero, A.; Healy, B. G.; Worden-Sapper, E. R.; Wu, S. S.; Muhlrad, D.; Decker, C. J.; Saldi, T. K.; Lasda, E.; Gonzales, P. K.; Fink, M. R.; Tat, K. L.; Hager, C. R.; Davis, J. C.; Ozeroff, C. D.; Brisson, G. R.; McQueen, M. B.; Leinwand, L.; Parker, R.; Sawyer, S. L.; eLife 2021, 10, e65113.

33. Diego, J. G.-B.; Fernández-Soto, P.; Domínguez-Gil, M.; Belhassen-García, M.; Bellido, J. L. M.; Muro, A.; Diagnostics 2021, 11, 438.

34. Nawattanapaiboon, K.; Pasomsub, E.; Prombun, P.; Wongbunmak, A.; Jenjitwanich, A.; Mahasupachai, P.; Vetcho, P.; Chayrach, C.; Manatjaroenlap, N.; Samphaongern, C.; Watthanachockchai,

35. T.; Leedorkmai, P.; Manopwisedjaroen, S.; Akkarawongsapat, R.; Thitithanyanont, A.; Phanchana, M.; Panbangred, W.; Chauvatcharin, S.; Srikhirin, T.; Analyst 2021, 146, 471.

36. Cevik, M.; Tate, M.; Lloyd, O.; Maraolo, A. E.; Schafers, J.; Ho, A.; Lancet Microbe 2021, 2, e13.

37. Richard, M.; Kok, A.; de Meulder, D.; Bestebroer, T. M.; Lamers, M. M.; Okba, N. M. A.; van Vlissingen, M. F.; Rockx, B.; Haagmans, B. L.; Koopmans, M. P. G.; Fouchier, R. A. M.; Herfst, S.; Nat. Commun. 2020, 11, 3496.

38. Larremore, D. B.; Wilder, B.; Lester, E.; Shehata, S.; Burke, J. M.; Hay, J. A.; Tambe, M.; Mina, M. J.; Parker, R.; Sci. Adv. 2021, 7, eabd5393.

39. Mina, M. J.; Parker, R.; Larremore, D. B.; N. Engl. J. Med. 2020, 383, e120.

40. https://ourworldindata.org/coronavirus, accessed on April 10, 2021.

41. Kim, M.-C.; Cui, C.; Shin, K.-R.; Bae, J.-Y.; Kweon, O.-J.; Lee, M.-K.; Choi, S.-H.; Jung, S.-Y.; Park, M.-S.; Chung, J.-W.; N. Engl. J. Med. 2021, 384, 671.

42. Singanayagam, A.; Patel, M.; Charlett, A.; Bernal, J. L.; Saliba, V.; Ellis, J.; Ladhani, S.; Zambon, M.; Gopal, R.; Eurosurveillance 2020, 25, 2001483.

43. Walsh, K. A.; Spillane, S.; Comber, L.; Cardwell, K.; Harrington, P.; Connell, J.; Teljeur, C.; Broderick, N.; de Gascun, C. F.; Smith, S. M.; Ryan, M.; O'Neill, M.; J. Infect. 2020, 81, 847.

44. Dudley, D. M.; Newman, C. M.; Weiler, A. M.; Ramuta, M. D.; Shortreed, C. G.; Heffron, A. S.; Accola, M. A.; Rehrauer, W. M.; Friedrich, T. C.; O'Connor, D. H.; PLoS One 2020, 15, e0244882.

Chapter IV: Study of the application of RT-LAMP pH-based detection methodology on a paper platform, with a view to real-time monitoring

1. Introduction

Due to our intense efforts, we made it through 2020 and 2021 to study, develop, and apply a rapid and inexpensive molecular test. A colorimetric pH-based RT-LAMP assay that is a simple and cost-effective tool has proven to be a powerful method for detecting SARS-CoV-2 in a hospital setting, particularly in the context of point-of-care. (Silva et al., 2021) Also, we report an RT-LAMP colorimetric assay suitable for screening large groups that can detect SARS-CoV-2 in RNA from saliva samples, detecting asymptomatic and pre-symptomatic carriers. (dos Santos et al., 2021)

In the RT-LAMP pH-based detection assays developed and presented in this manuscript by our research group, and in many of the studies in the scientific literature, amplified products are detected using endpoint detection. (Bhadra et al., 2021; dos Santos et al., 2021; B. Lim et al., 2021; Silva et al., 2021; Song et al., 2021) This means that the only information obtained from the test is the final result, indicating the presence or absence of the nucleic acid: yellow indicates an infected patient, while pink indicates a healthy patient, when the phenol red indicator is used. Even though this information is vital during an outbreak or pandemic, it does not provide infected patients with details about the stage of infection or the viral load within the sample.

Quantifying the viral load in a patient's sample brings an understanding of the potential implications of their condition. Using the COVID-19 pandemic context as an example, viral load and other factors such as age, comorbidities, symptom severity, and hypoxia could help determine the need for hospital admission. Scientific evidence suggests that patients with older age and the presence of comorbidities also tend to

have higher SARS-CoV-2 viral loads upon hospital admission, which may contribute to their poorer outcomes. Patients with higher viral loads are more likely to develop complications such as myocardial infarction, congestive heart failure, and acute kidney increased hypoxia in heart and kidney tissues, or due to higher viral infection rates in these organs. (Bryan et al., 2020; Faíco-Filho et al., 2020; Fajnzylber et al., 2020; Magleby et al., 2021; Pujadas et al., 2020)

Patients admitted to the hospital with high SARS-CoV-2 viral loads, indicated by low Ct (cycle threshold) values from PCR tests of nasopharyngeal swab samples, were more likely to require intubation or succumb to the disease during their hospitalization, as shown in Figure 1. This association persisted even after adjusting for age, comorbidities, presenting symptoms, chest radiography findings, and the degree of hypoxia at presentation. The Ct value reflects the number of PCR cycles needed for the viral signal to become detectable; a lower Ct value means fewer cycles are needed, indicating a higher viral load, while a higher Ct value means more cycles are needed, indicating a lower viral load. (Magleby et al., 2021)

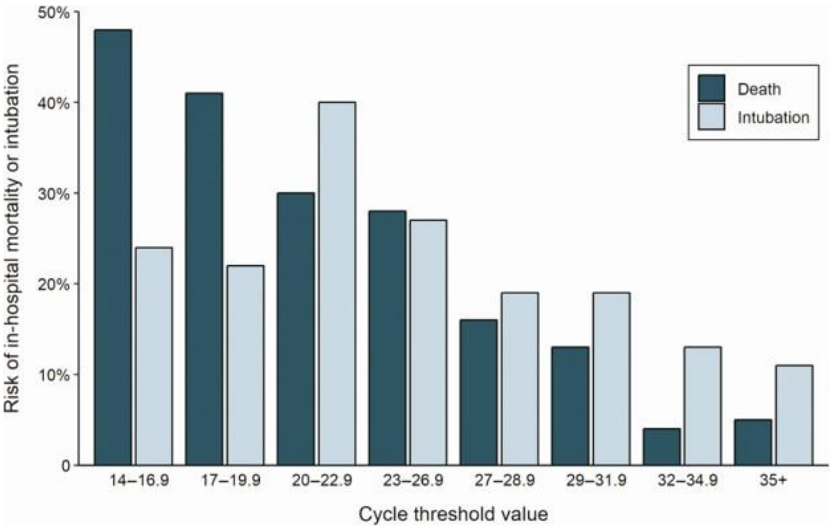

Figure 1: Cycle threshold values from nasopharyngeal swab samples upon admission and their association with the risk of intubation and mortality during hospitalization. (Magleby et al., 2021)

Therefore, even if further studies should be conducted, identifying the viral load upon admission has significant prognostic implications, as patients with high viral loads may benefit from prioritized therapeutic interventions such as antiviral agents. (Bryan et al., 2020; Faíco-Filho et al., 2020; Fajnzylber et al., 2020; Magleby et al., 2021; Pujadas et al., 2020)

Considering the importance of quantifying the sample's viral load, real-time detection is an alternative to endpoint detection. In real-time detection, the amplicon can be visualized/measured as the amplification progresses. The gold standard method for SARS-CoV-2 detection is real-time PCR, also known as quantitative PCR (qPCR). Three properties are uniquely associated with quantitative real-time PCR: quantification, standardization, and a lower detection limit. (Engstrom-Melnyk et al., 2015) Real-time PCR uses fluorescent signaling probes to measure DNA amplification at each PCR cycle during the point of exponential DNA accumulation. Due to the consistent changes in signal intensity during the exponential growth phase of PCR, it can provide quantitative reporting. (Engstrom-Melnyk et al., 2015; Watzinger et al., 2006) However, qPCR requires expensive reagents and equipment, time-consuming pretreatments, and elaborate protocols demanding highly trained professionals. These requirements make it difficult to adapt PCR to miniaturized and easy-to-use devices for point-of-care situations. (Lopes et al., 2022)

Portable and point-of-care (POC) devices for on-site monitoring are considered the future of rapid clinical diagnostics. (Lopes et al., 2022) Compromising portability, cost-effectiveness, and applicability at the point of care would contradict this goal. In this regard, it would be of interest to combine the advantages of real-time detection

with all the benefits of the pH-based RT-LAMP assay that we have developed and validated.

Microfluidic technologies have become increasingly important in developing point-of-care (POC) diagnostics due to their many advantages, including addressing global health challenges. (Hu et al., 2014; S. M. Yang et al., 2022) Many chip-based devices, often constructed from glass, (Aralekallu et al., 2023) polyester-toner (PeT), (De Oliveira et al., 2021) poly(methylmethacrylate) (PMMA), (Van Anh et al., 2016) and polydimethylsiloxane (PDMS), (Shakeri et al., 2021) incorporate integrated functional units like pumps and valves. However, these devices require complex fabrication and operation, limiting their practicality for POC applications. (Hu et al., 2014)

On the other hand, paper-based microfluidics offer significant potential for delivering POC diagnostics, particularly in resource-limited settings. They are affordable, sensitive, specific, user-friendly, rapid and robust, equipment-free, and deliverable to end-users (ASSURED criteria). The paper's inherent fluidic properties and white background provide an additional advantage in qualitative and quantitative analysis. (J. R. Choi et al., 2015; Hu et al., 2014; Pandey et al., 2018; S. M. Yang et al., 2022) These attributes make paper-based devices particularly well-suited for real-time monitoring of SARS-CoV-2 by LAMP.

Colorimetry is often considered the most appropriate detection method for integration with paper-based analytical devices due to its simplicity and compatibility with affordable reporting systems, such as smartphones, despite the potential for higher limits of detection (LOD). This approach allows for qualitative, semi-quantitative, and fully quantitative analysis of analytes. Various strategies can achieve

a colorimetric response in µPADs, including nanoparticles, dyes, redox reactions, and pH indicators. (Lopez-Ruiz et al., 2014; Morbioli et al., 2017) Building on our established RT-LAMP pH-based endpoint detection methodology, a pH-based quantitative colorimetric detection could be effectively implemented by adapting our LAMP assay to a paper-based platform.

Thus, this study aims to combine the advantages of our LAMP methodology by developing a paper-based microfluidic platform for the RT-LAMP pH-based detection test. With this approach, we aim to enable real-time control of the amplification process without sophisticated equipment. We intend to use a plug-in portable digital microscope that can connect to a computer or smartphone to monitor the amplification. Our goal involves keeping the three key properties of the gold standard method: quantification, standardization, and a low detection limit.

2. Materials and Methods

2.1 Materials and Chemicals

Glass Fiber Conjugate PAD, Ammonium sulfate ($(NH_4)_2SO_4$), potassium chloride (KCl), potassium hydroxide (KOH), cresol red pH indicator, ethylenediaminetetraacetic acid disodium salt dihydrate ($Na_2EDTA.{}_2H_2O$), trihydroxymethylaminomethane (TRIS), and water for molecular biology (DNase free, RNase free, and Protease free) were purchased from Sigma-Aldrich (St Louis, MO-USA). LAMP primers and the triphosphate deoxyribonucleotides (dNTPs) were purchased from Invitrogen/Life Technologies (Foster City, CA-USA). Magnesium sulfate (MgSO4), WarmStart RTx Reverse Transcriptase, and Bst DNA polymerase 2.0 were purchased from New England Biolabs (Ipswich, MA-USA). The thermoblock was purchased from KASVI (São José do Pinhais, PR-BR). A Silhouette Cameo 4

(Silhouette Cameo, Brazil) and a Kyocera Ecosys M2040dn/L Multifunctional printer were used to fabricate paper-based devices, and a Digital Microscope with a USB Cable 1000X Optical Zoom Professional HD 2.0MP Camera (CELLWORLD ®) was employed for reaction real-time monitoring.

2.2 RT-LAMP Protocol

The primer sequences used for RT-LAMP amplification are shown in Table 1.

Table 6: Primer sequences used for RT-LAMP amplification, designed by (Lamb et al., 2020)

Primers	Sequence 5' to 3'
F3	TCCAGATGAGGATGAAGAAGA
B3	AGTCTGAACAACTGGTGTAAG
FIP	AGAGCAGCAGAAGTGGCACAGGTGATTGTGAAGAAGAAGAG
BIP	TCAACCTGAAGAAGAGCAAGAACTGATTGTCCTCACTGCC
LF	CTCATATTGAGTTGATGGCTCA
LB	ACAAACTGTTGGTCAACAAGAC

First, the RT-LAMP master mixture was prepared in a tube and contained 0.2 µM of each outer primer (F3 and B3), 1.6 µM of each inner primer (FIP and BIP), 0.4 µM of each loop primer (LFP and LBP), 10 mM $MgSO_4$, 2.0 mM dNTP, 0.96 U µL−1 of Bst 2.0 polymerase, 0,6 U µL-1 of RTx reverse transcriptase, 10 mM of $(NH_4)_2SO_4$, 50 mM of KCl, 0,1X of TRIS-EDTA, 3.4 mM of KOH, 2 mM of cresol red pH indicator and varying amounts of RNA.

After preparing the master mixture, 10 µL of the RT-LAMP master mix was added to the paper-based microdevice. The hole that gives access to the reaction chamber was sealed with PCR adhesive films. The microdevice was then placed in a

thermoblock at 65 °C, and a portable microscope was used to monitor and record the color change of the reaction over 60 minutes (see Figure 2).

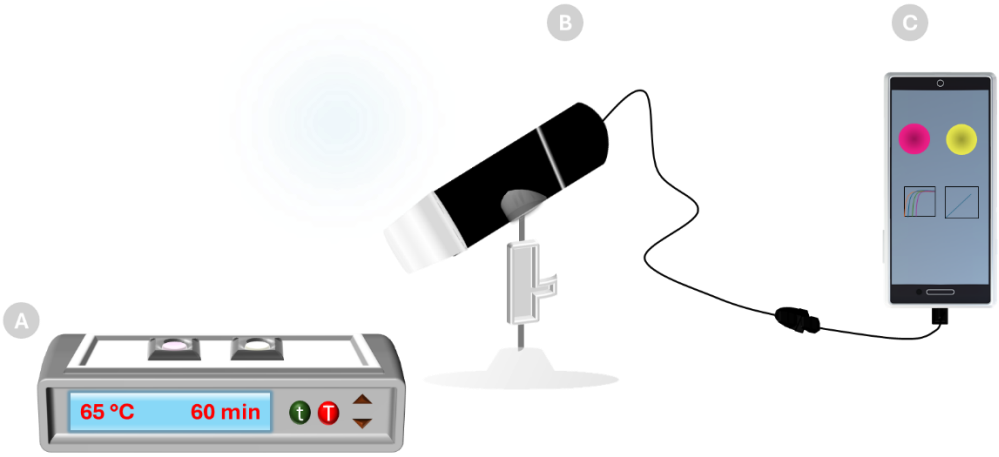

Figure 2: Schematic illustration of a paper-based RT-LAMP reaction (A) using a portable microscope (B) for real-time pH-based quantification(C). Created by the author.

This study aims to evaluate the relationship between the time of color change of RT-LAMP solution and the number of RNA copies. The goal is to correlate these two parameters—color change time and the number of copies—to establish a linear range of relationship. Consequently, this would allow us to correlate the amplification time/color change time with Ct values, thereby providing quantitative information based on the reaction's color change time.

2.3 Paper-based device Fabrication

A cutting plotter, Silhouette Cameo 4, was used to delineate physical boundaries and create a paper circle (⌀= 6mm) where the RT-LAMP reaction will proceed. A support was implemented to avoid evaporation, enable transport, and handle the paper microdevice. Some substrate materials for the support were

evaluated to ensure they preserved the paper's properties and did not interfere with the RT-LAMP mixture; the two most suitable candidates were polystyrene toner (PeT) and PCR adhesive tapes (Agilent 96-Well Plate Sealing Film Catalog #410150).

To produce polystyrene toner-based support, both sides of a polystyrene film (Filipaper InkJet Light, FP02603) were coated with 4 layers of toner using a laser printer (Kyocera Ecosys M2040dn/L Multifunctional printer) and then selectively cut according to the desired pattern using a cutting plotter (Silhouette Cameo 4). These intermediate polystyrene-toner films were then aligned on a polystyrene base (bottom layer) where a pre-cut circle to fit the paper was placed, and on an upper polystyrene layer. The top layer contained a hole to allow reagent access to the paper. Once aligned, the films were laminated, creating a ready-to-use microfluidic device (see Figure 3).

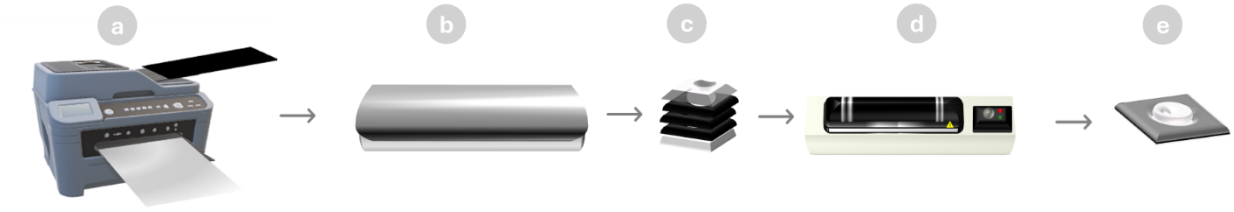

Figure 3: Schematic illustration of the production process for the polystyrene toner-based support for the paper: (a) toner printing on the polystyrene film; (b) cutting the desired design using a cutting plotter; (c) alignment of the polystyrene-toner layers; (d) lamination of the films; and (e) final device. Created by the author.

The second support material evaluated was the sealing film used for PCR tests (adhesive seals), typically composed of polyethylene. A Silhouette Cameo 4 cutter was used to cut the PCR sealing films into the desired configuration. The cut piece of paper was simply placed on the adhesive film without the protective layer, and then the top layer (with a hole cut out with a craft punch to allow paper access) was placed over

the paper. Gentle finger pressure finally bonded the layers using their own adhesive properties (see Figure 4).

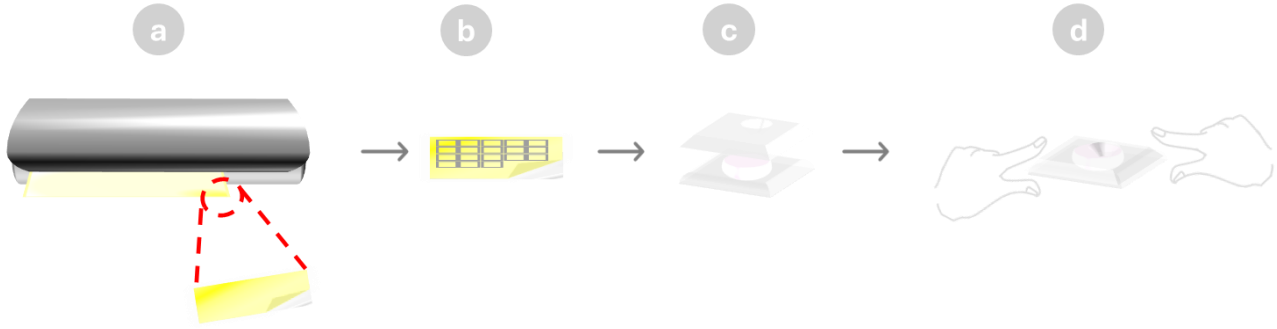

Figure 4: Schematic illustration of the fabrication process for the paper microfluidic device support using PCR sealing film: (a) cutting the adhesive film with a cutting plotter; (b) removing the protective backing from the adhesive films; (c) aligning the adhesive films with the paper; and (d) assembling the final device by applying gentle pressure to bond the layers. Created by the author.

2.4 Real-time Reaction Monitoring

A portable USB microscope (B07N2ZF88Q, CELLWORLD, Sonepur, India) was employed to record the reaction over one hour through amplification, capturing the real-time color change from pink to yellow with standardization light and position. The microscope has dedicated software that enables image and video capture once focus, zoom, and lighting conditions are ready. The recording can be initiated via a computer or smartphone.

3. Discussion

We aimed to apply RT-LAMP assays for screening in hospitals and clinical settings, particularly in underserved or remote regions where sophisticated equipment is unavailable. The advantages of our LAMP assay suggest that it can be enhanced for real-time analysis in situ, where access to a real-time PCR machine is not feasible.

We propose adapting the system into a microfluidic format to achieve this real-time detection capability, which offers quantification possibility. Precisely, a paper-based system aligns with our real-time detection objectives due to the optical properties, biocompatibility, cost-effectiveness, and simplicity of paper substrates, making them ideal for point-of-care applications. Here, we present the initial experiments and perspectives on the potential transposition of our methodology. Preliminary studies have been undertaken to conduct the assay using a Glass Fiber Conjugate PAD paper substrate. This paper substrate was selected based on the prior experience with the IEF protein separation on a paper device, where it demonstrated suitable performance and compatibility. (Mendes et al., 2024)

3.1 Device optimization

In this study, we applied a cutting plotter to precisely cut paper circles, delineating the reaction chamber for amplification. After the paper circles were prepared, the next step involved selecting a support platform to avoid evaporation and facilitate the transport and handling of the RT-LAMP paper. The focus is identifying simple, disposable, and cost-effective materials well-suited for low-resource settings.

Based on our group's previous experience, the first support material evaluated was a polystyrene-toner. (de Oliveira et al., 2017; De Oliveira et al., 2021; Gimenez et al., 2017; Mendes et al., 2019) Despite the simplicity of using polystyrene-toner as a support, several drawbacks were identified. First, the support material's composition (toner) interfered with the RT-LAMP solution's pH, causing the mixture to turn yellow even before the amplification process began, invalidating the result. Second, the polystyrene film used as the top layer lacked sufficient transparency and reflected the microscope light, making it challenging to accurately observe the color change in the

RT-LAMP mixture. Figure 5 shows the capture of the color change observed in a negative reaction (absence of target) immediately after incubation in the thermoblock. Further studies are required to elucidate this observation and validate our hypothesis that the toner used in the polystyrene film may alter the reaction pH and consequently affect the pH indicator's color.

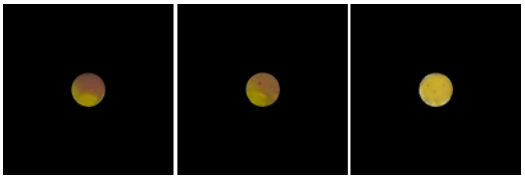

Figure 5: Images captured with a portable USB microscope showing the sequence of color changes in an RT-LAMP solution within less than 1 minute of incubation. The mixture of an RT-LAMP negative reaction (no template) was placed in a paper-based analytical device with a polystyrene toner support and incubated in a thermoblock.

The second support material evaluated was the sealing film used for PCR tests (adhesive seals), typically made of polyethylene. We used a Silhouette Cameo 4 cutter to cut the PCR sealing films into the desired configuration. The paper was easily positioned on the pre-cut adhesive films after removing the protective layer and secured by light finger pressure, using the films' self-adhesive properties. Our results indicated no interference with the reaction pH, and the fabrication process was both simple and practical (see Figure 6). The positive reaction turned yellow after 45 minutes of heating, and the negative reaction remained pink after the incubation period.

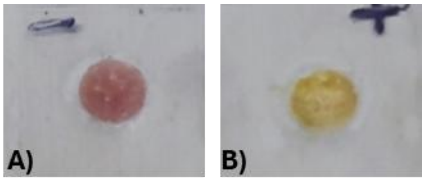

Figure 6: RT-LAMP reaction on a paper-based device using a polyethylene adhesive film as a support. A) Negative reaction: absence of target. B) Positive reaction: presence of target.

µPADs are usually fabricated by either creating hydrophobic zones within the hydrophilic paper or by cutting the paper to form physical barriers. The cutting approach enables the definition of channels or shapes without the need for hydrophobic materials. In this study, the PCR sealing film proved to be suitable as a base material for our paper microfluidic devices due to its excellent biocompatibility, a wide range of working temperatures, low cost, self-adhesive properties, and optical transmittance in the visible range. (Y. Fan et al., 2018)

By using tools like a knife plotter, CO2 laser, or craft punch, physical boundaries can be created to delineate channels and shapes. This method simplifies the fabrication process and reduces production costs. (Hu et al., 2014) By combining the use of a cutting plotter and polyethylene sealing films, the support's fabrication was straightforward, cost-effective, and practical. This makes it well-suited for low-resource settings, including remote regions, developing countries, or even developed ones during emergency situations such as the COVID-19 pandemic.

3.2 Optimizing Paper Design to Minimize Evaporation Loss

After optimizing the support, the paper circles were placed between polyethylene adhesive films, and the reactions were incubated in a thermoblock at 65

ºC. The color change was monitored using a microscope. However, an undesired phenomenon occurred: upon heating, bubbles formed, leading to the evaporation of the RT-LAMP solution. Figure 7 illustrates the described phenomenon. Photographs were captured at 10-minute intervals during the amplification process.

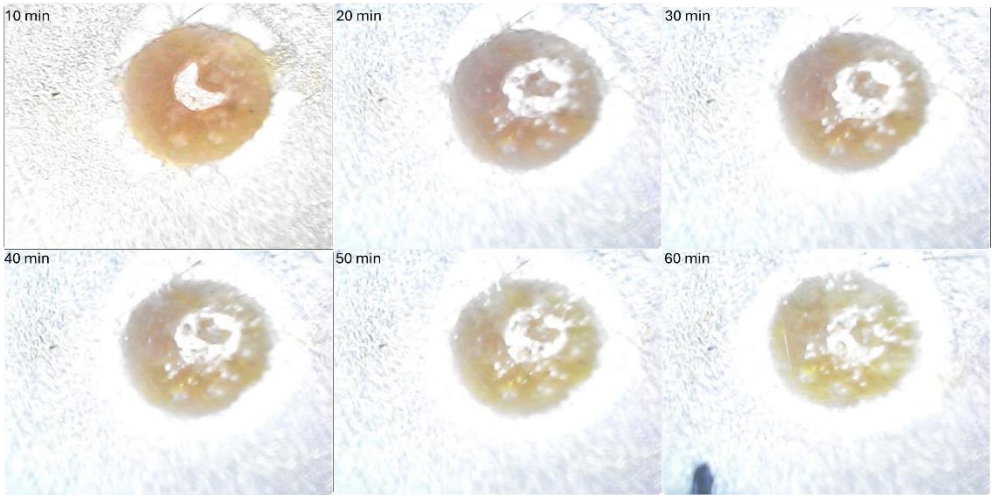

Figure 7: Evaporation phenomenon at 10-minute intervals during the RT-LAMP reaction. The image captures the evaporation of the RT-LAMP solution upon heating, leading to a disruption in the reaction.

We hypothesize that when the system is heated, bubbles form due to steam production, causing an increase in internal pressure. This pressure pushes the adhesive layer covering the reaction chamber upward (see Figure 8), eventually weakening the adhesion and leading to increased evaporation. In addition to the loss of the LAMP solution, this evaporation can cause cross-contamination between reactions, making it crucial to mitigate these effects.

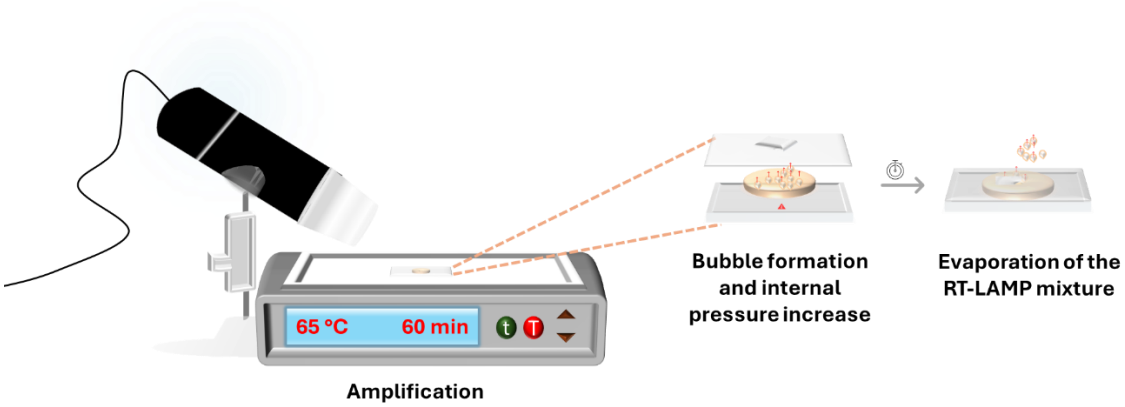

Figure 8: Schematic illustration of bubble formation and internal pressure increase causing the evaporation of the RT-LAMP solution.

To counteract the effects of system heating, the paper layout was refined to minimize evaporation throughout the process. In the previous design, the paper reaction chamber was accessed through a hole directly above it. As a result, when the system is heated and pressure increases, the sealing film receives this pressure directly and eventually loses adhesion. To address this issue, we redesigned the access points by removing them directly above the reaction chamber and creating two "branches" extending to the chamber (see Figure 9). This modification positioned the adhesive protective film away from the areas of highest pressure, relocating it to the extremities of the branches, thus preserving adhesion and reducing the risk of evaporation.

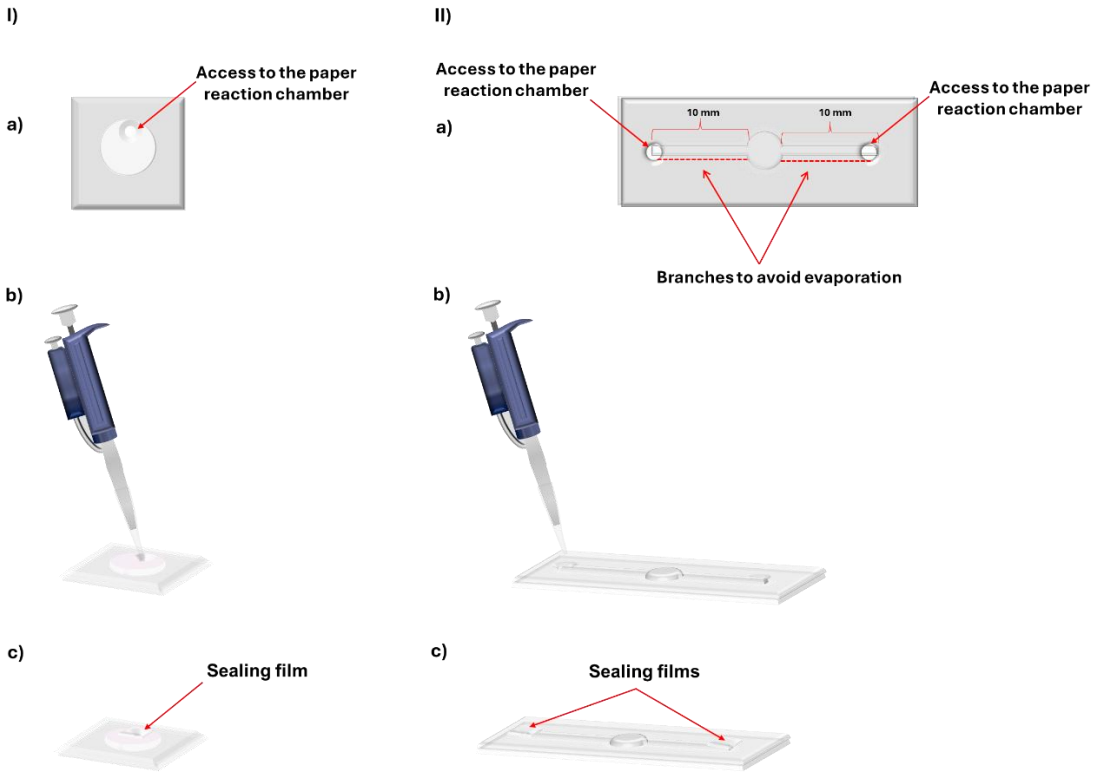

Figure 9: Illustration of paper design modifications to mitigate evaporation. (I) Original paper design; (II) Refined design with branch extensions. For both I and II: (a) Access to the paper reaction chamber, (b) Hole placement for pipetting the solution, (c) Adhesive film application.

Figure 10 depicts a series of images captured at 10-minute intervals during the RT-LAMP reaction using the new paper design. The images highlight the extended branches' effectiveness in reducing evaporation within the system, thereby improving the consistency of the reaction over time and minimizing the possibility of cross-contamination.

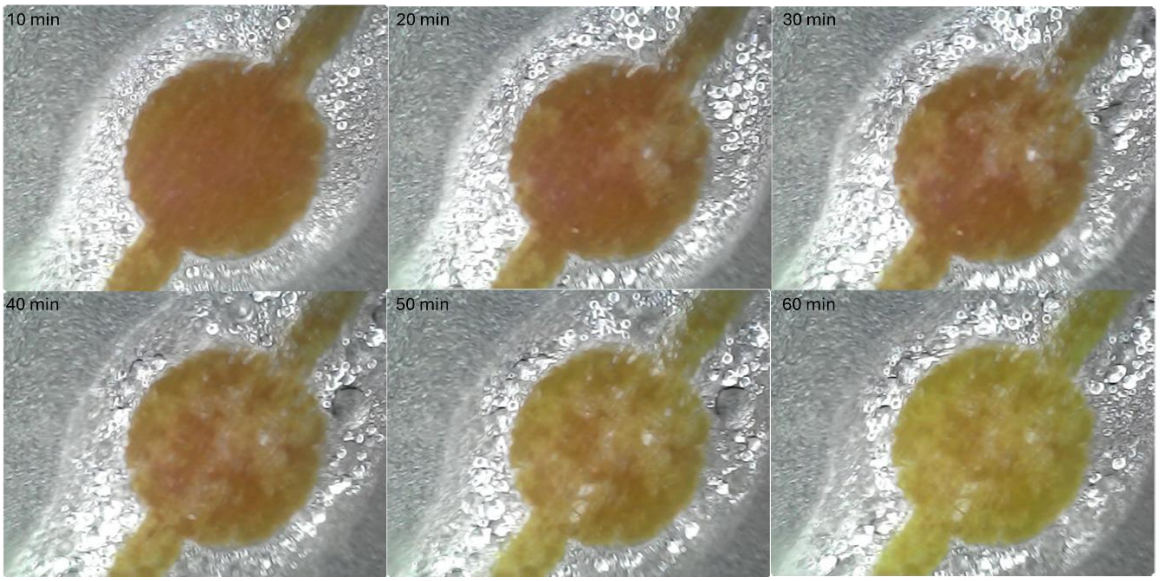

Figure 10: Images captured at 10-minute intervals during the RT-LAMP reaction using the new paper design with the extended branches.

As shown in Figure 10, the evaporation phenomenon was minimized. In addition to reducing evaporation, the new paper design significantly improved the homogeneity of the reaction color—a crucial factor for precise colorimetric quantification. Achieving consistent color homogeneity is essential for colorimetric readouts in µPADs, as it allows for more accurate measurements and enhances the analytical method's overall performance. (Morbioli et al., 2017)

4. Conclusions and Perspectives

This study paves the way to highlight the potential of our RT-LAMP assay when combined with the advantages of microfluidic paper platforms. Our primary objective is to correlate the time it takes for the reaction color to change from pink to yellow with the number of viral RNA copies and, consequently, with the cycle threshold value, allowing for a comparison with the gold standard. After that, the following steps will

include determining the figures of merit, evaluating and comparing the amplification time with Ct values, and applying the method to real samples.

The preliminary results of this exploratory study indicate the potential of combining the RT-LAMP assay with microfluidic paper-based analytical devices (µPADs) for real-time detection. We have designed a simple device using cut paper and adhesive films as a support. This device is feasible and cost-effective, requiring no sophisticated equipment or specialized training. It can be produced manually, making it suitable for use in remote or resource-limited settings. By optimizing the paper design to reduce evaporation and improve color homogeneity, we have enhanced the reliability of colorimetric quantification.

Our findings suggest that this method may be a viable alternative to more complex and expensive diagnostic systems, particularly for point-of-care. This chapter reports the exploratory nature of our study and the need for further research to fully realize its potential. This work lays the foundation for advancing our RT-LAMP assay by transposing it to a paper-based platform. This will provide a cost-effective, accessible, and reliable tool for real-time detection.

Bibliography

Aralekallu, S., Boddula, R., & Singh, V. (2023). Development of glass-based microfluidic devices: A review on its fabrication and biologic applications. In Materials and Design (Vol. 225). Elsevier Ltd. https://doi.org/10.1016/j.matdes.2022.111517

Bhadra, S., Riedel, T. E., Lakhotia, S., Tran, N. D., & Ellington, A. D. (2021). High-Surety Isothermal Amplification and Detection of SARS-CoV-2. MSphere, 6(3). https://doi.org/10.1128/msphere.00911-20

Bryan, A., Fink, S. L., Gattuso, M. A., Pepper, G., Chaudhary, A., Wener, M. H., Morishima, C., Jerome, K. R., Mathias, P. C., & Greninger, A. L. (2020). SARS-CoV-2 Viral Load on Admission Is Associated with 30-Day Mortality. Open Forum Infectious Diseases, 7(12). https://doi.org/10.1093/ofid/ofaa535

Choi, J. R., Tang, R., Wang, S. Q., Wan Abas, W. A. B., Pingguan-Murphy, B., & Xu, F. (2015). Paper-based sample-to-answer molecular diagnostic platform for point-of-care diagnostics. In Biosensors and Bioelectronics (Vol. 74, pp. 427–439). Elsevier Ltd. https://doi.org/10.1016/j.bios.2015.06.065

de Oliveira, K. G., Borba, J. C., Bailão, A. M., de Almeida Soares, C. M., Carrilho, E., & Duarte, G. R. M. (2017). Loop-mediated isothermal amplification in disposable polyester-toner microdevices. Analytical Biochemistry, 534, 70–77. https://doi.org/10.1016/j.ab.2017.07.014

De Oliveira, K. G., Estrela, P. F. N., Mendes, G. D. M., Dos Santos, C. A., Silveira-Lacerda, E. D. P., & Duarte, G. R. M. (2021). Rapid molecular diagnostics of COVID-19 by RT-LAMP in a centrifugal polystyrene-Toner based microdevice with end-point visual detection. Analyst, 146(4), 1178–1187. https://doi.org/10.1039/d0an02066d

dos Santos, C. A., de Oliveira, K. G., Mendes, G. M., Silva, L. C., de Souza, M. N., Estrela, P. F. N., Guimarães, R. A., Silveira-Lacerda, E. P., & Duarte, G. R. M. (2021). Detection of SARS-CoV-2 in Saliva by RT-LAMP During a Screening of Workers in Brazil, Including Pre-Symptomatic Carriers. Journal of the Brazilian Chemical Society, 32(11), 2071–2077. https://doi.org/10.21577/0103-5053.20210098

Engstrom-Melnyk, J., Rodriguez, P. L., Peraud, O., & Hein, R. C. (2015). Clinical applications of quantitative real-time PCR in virology. In Methods in Microbiology (Vol. 42, pp. 161–197). Academic Press Inc. https://doi.org/10.1016/bs.mim.2015.04.005

Faíco-Filho, K. S., Passarelli, V. C., & Bellei, N. (2020). Is higher viral load in SARS-CoV-2 associated with death? American Journal of Tropical Medicine and Hygiene, 103(5), 2019–2021. https://doi.org/10.4269/ajtmh.20-0954

Fajnzylber, J., Regan, J., Coxen, K., Corry, H., Wong, C., Rosenthal, A., Worrall, D., Giguel, F., Piechocka-Trocha, A., Atyeo, C., Fischinger, S., Chan, A., Flaherty, K. T., Hall, K., Dougan, M., Ryan, E. T., Gillespie, E., Chishti, R., Li, Y., … Zhu, A. (2020). SARS-CoV-2 viral load is associated with increased disease severity and mortality. Nature Communications, 11(1). https://doi.org/10.1038/s41467-020-19057-5

Fan, Y., Liu, S., He, J., Gao, K., & Zhang, Y. (2018). Rapid prototyping of flexible multilayer microfluidic devices using polyester sealing film. Microsystem Technologies, 24(6), 2847–2852. https://doi.org/10.1007/s00542-017-3630-3

Gimenez, T. D., Bailão, A. M., De Almeida Soares, C. M., Fiaccadori, F. S., Borges De Lima Dias E Souza, M., & Duarte, G. R. M. (2017). Dynamic solid-phase RNA extraction from a biological sample in a polyester-toner based microchip. Analytical Methods, 9(13), 2116–2121. https://doi.org/10.1039/c6ay03481k

Hu, J., Wang, S. Q., Wang, L., Li, F., Pingguan-Murphy, B., Lu, T. J., & Xu, F. (2014). Advances in paper-based point-of-care diagnostics. In Biosensors and Bioelectronics (Vol. 54, pp. 585–597). Elsevier Ltd. https://doi.org/10.1016/j.bios.2013.10.075

Lamb, L. E., Bartolone, S. N., Ward, E., & Chancellor, M. B. (2020). Rapid detection of novel coronavirus/Severe Acute Respiratory Syndrome Coronavirus 2 (SARS-CoV-2) by reverse transcription-loop-mediated isothermal amplification. PLoS ONE, 15(6). https://doi.org/10.1371/journal.pone.0234682

Lim, B., Ratcliff, J., Nawrot, D. A., Yu, Y., Sanghani, H. R., Hsu, C. C., Peto, L., Evans, S., Hodgson, S. H., Skeva, A., Adam, M., Panopoulou, M., Zois, C. E., Poncin, K., Vasudevan, S. R., Dai, S., Ren, S., Chang, H., Cui, Z., … Andersson, M. I. (2021). Clinical validation of optimised RT-LAMP for the diagnosis of SARS-CoV-2 infection. Scientific Reports, 11(1). https://doi.org/10.1038/s41598-021-95607-1

Lopes, L. C., Santos, A., & Bueno, P. R. (2022). An outlook on electrochemical approaches for molecular diagnostics assays and discussions on the limitations of miniaturized technologies for point-of-care devices. Sensors and Actuators Reports, 4. https://doi.org/10.1016/j.snr.2022.100087

Lopez-Ruiz, N., Curto, V. F., Erenas, M. M., Benito-Lopez, F., Diamond, D., Palma, A. J., & Capitan-Vallvey, L. F. (2014). Smartphone-based simultaneous pH and nitrite colorimetric determination for paper microfluidic devices. Analytical Chemistry, 86(19), 9554–9562. https://doi.org/10.1021/ac5019205

Magleby, R., Westblade, L. F., Trzebucki, A., Simon, M. S., Rajan, M., Park, J., Goyal, P., Safford, M. M., & Satlin, M. J. (2021). Impact of Severe Acute Respiratory Syndrome Coronavirus 2 Viral Load on Risk of Intubation and Mortality among Hospitalized Patients with Coronavirus Disease 2019. Clinical Infectious Diseases, 73(11), E4197–E4205. https://doi.org/10.1093/cid/ciaa851

Mendes, G. M., Oliveira, K. G., Borba, J. C., Oliveira, T. S., Fiaccadori, F. S., Nogueira, M. L., Bailão, A. M., Soares, C. M. A., Carrilho, E., & Duarte, G. R. M.

(2019). Molecular diagnostics of dengue by reverse transcription-loop mediated isothermal amplification (RT-LAMP) in disposable polyester-toner microdevices. Journal of the Brazilian Chemical Society, 30(9), 1841–1849. https://doi.org/10.21577/0103-5053.20190092

Morbioli, G. G., Mazzu-Nascimento, T., Stockton, A. M., & Carrilho, E. (2017). Technical aspects and challenges of colorimetric detection with microfluidic paper-based analytical devices (μPADs) - A review. In Analytica Chimica Acta (Vol. 970, pp. 1–22). Elsevier B.V. https://doi.org/10.1016/j.aca.2017.03.037

Pandey, C. M., Augustine, S., Kumar, S., Kumar, S., Nara, S., Srivastava, S., & Malhotra, B. D. (2018). Microfluidics Based Point-of-Care Diagnostics. In Biotechnology Journal (Vol. 13, Issue 1). Wiley-VCH Verlag. https://doi.org/10.1002/biot.201700047

Pujadas, E., Chaudhry, F., McBride, R., Richter, F., Zhao, S., Wajnberg, A., Nadkarni, G., Glicksberg, B. S., Houldsworth, J., & Cordon-Cardo, C. (2020). SARS-CoV-2 viral load predicts COVID-19 mortality. In The Lancet Respiratory Medicine (Vol. 8, Issue 9, p. e70). Lancet Publishing Group. https://doi.org/10.1016/S2213-2600(20)30354-4

Shakeri, A., Khan, S., & Didar, T. F. (2021). Conventional and emerging strategies for the fabrication and functionalization of PDMS-based microfluidic devices. In Lab on a Chip (Vol. 21, Issue 16, pp. 3053–3075). Royal Society of Chemistry. https://doi.org/10.1039/d1lc00288k

Silva, L. D. C., Dos Santos, C. A., Mendes, G. D. M., Oliveira, K. G. De, De Souza Júnior, M. N., Estrela, P. F. N., Costa, S. H. N., Silveira-Lacerda, E. D. P., & Duarte, G. R. M. (2021). Can a field molecular diagnosis be accurate? A performance evaluation of colorimetric RT-LAMP for the detection of SARS-CoV-2 in a hospital setting. Analytical Methods, 13(26), 2898–2907. https://doi.org/10.1039/d1ay00481f

Song, J., El-Tholoth, M., Li, Y., Graham-Wooten, J., Liang, Y., Li, J., Li, W., Weiss, S. R., Collman, R. G., & Bau, H. H. (2021). Single- And Two-Stage, Closed-Tube, Point-of-Care, Molecular Detection of SARS-CoV-2. Analytical Chemistry, 93(38), 13063–13071. https://doi.org/10.1021/acs.analchem.1c03016

Van Anh, N., Van Trung, H., Tien, B. Q., Binh, N. H., Ha, C. H., Le Huy, N., Loc, N. T., Thu, V. T., & Lam, T. D. (2016). Development of a PMMA Electrochemical Microfluidic Device for Carcinoembryonic Antigen Detection. Journal of Electronic Materials, 45(5), 2455–2462. https://doi.org/10.1007/s11664-016-4372-1

Watzinger, F., Ebner, K., & Lion, T. (2006). Detection and monitoring of virus infections by real-time PCR. In Molecular Aspects of Medicine (Vol. 27, Issues 2–3, pp. 254–298). https://doi.org/10.1016/j.mam.2005.12.001

Yang, S. M., Lv, S., Zhang, W., & Cui, Y. (2022). Microfluidic Point-of-Care (POC) Devices in Early Diagnosis: A Review of Opportunities and Challenges. In Sensors (Vol. 22, Issue 4). MDPI. https://doi.org/10.3390/s22041620

General Introduction

The research presented in this chapter results from the Cotutelle period exchange and is part of a larger project led by Professor Anne Varrene. Initially, the project explored the feasibility of using glycerol as a substitute for slab gels in capillary electrophoresis. This was followed by studies that successfully coupled capillary electrophoresis with mass spectrometry, introducing glycerol solutions as the separation medium.

The project's overarching goal is to integrate all the steps of proteome analysis into a single, streamlined process, something not feasible at conventional scales. Consequently, the research progressed to transposing the glycerol-based protein separation techniques to a microfluidic scale, with the ultimate aim of integrating protein separation and digestion into one unified device to go directly detect the peptides.

This chapter details the miniaturization of protein separation using isoelectric focusing within a microfluidic platform. All critical separation and technological parameters were optimized with a view to the integration of the digestion step, enabling direct MS detection. The chapter is the publication of the scientific article from this study, titled "Streamlined Integrated Protein Isoelectric Focusing Using Microfluidic Paper-Based Devices," published in the Journal of Chromatography A in 2024 (Mendes et al., 2024).

Chapter V: Streamlined Integrated Protein Isoelectric Focusing Using Microfluidic Paper-Based Device

ABSTRACT

An innovative integrated paper-based microdevice was developed for protein separation by isoelectric focusing (IEF), allowing for robust design thanks to a 3D-printed holder integrating separation channel, reservoirs, and electrodes. To reach robustness and precision, the optimization focused on the holder geometry, the paper nature, the reservoir design, the IEF medium, and various focusing parameters. A well-established and stable pH gradient was obtained on a glass-fiber paper substrate with simple sponge reservoirs, and the integration of the electrodes in the holder led to a straightforward system. The separation medium composed of water/glycerol (85/15, v/v) allowed for reducing medium evaporation while being an efficient medium for most hydrophobic and hydrophilic proteins, compatible with mass spectrometry detection for further proteomics developments. To our knowledge, this is the first report of the use of glycerol solutions as a separation medium in a paper-based microdevice. Analytical performances regarding pH gradient generation, pI determination, separation efficiency, and resolution were estimated while varying the IEF experimental parameters. The overall process led to an efficient separation within 25 minutes. Then, this methodology was applied to a sample composed of saliva doped with proteins. A minimal matrix effect was evidenced, underscoring the practical viability of our platform. This low-cost, versatile and robust paper-based IEF microdevice opens the way to various applications, ranging from sample pre-treatment to integration in an overall proteomic-on-a-chip device.

Keywords: Isoelectric focusing, Microfluidic paper-based, 3D-printed holder, Glycerol, Proteomics.

1. INTRODUCTION

Proteins are intricate and complex molecules, central in carrying out most tasks within the body's cells. They are indispensable for maintaining organ structure, operation, and control and overseeing their functionality. (Chothia, 1984; Janin & Chotnia, 1985; Leon & Pastor, 2021) Given proteins' vital role, they offer valuable insights into the underlying molecular aspects of health and disease. Consequently, in the context of proteomics, the capacity to describe, separate, and assess proteins analytically is essential for investigating their roles and functions. (Farmerie et al., 2021; Kim et al., 2014; Maurer, 2011)

Classically, protein characterization needs complex procedures. Two prominent strategies, bottom-up and top-down, are employed to analyze proteins. The top-down strategy involves the direct analysis of intact proteins by mass spectrometry (MS). Top-down strategy can mitigate certain limitations associated with bottom-up analysis by scrutinizing complete proteins. However, this approach remains less commonly used compared to bottom-up strategies. (Garcia, 2010; Guo et al., 2023; Lenčo et al., 2022a, 2022b; Maráková et al., 2023; Miller & Smith, 2022; Moradian et al., 2014; Štěpánová & Kašička, 2022, 2023) The bottom-up strategy involves the initial digestion of proteins into their peptides before subjecting them to separation and detection by MS. This strategy is widely utilized for protein sequence analysis due to the ease of separations at the peptide level, predictable fragmentation, and the extensive commercialization of hardware and software options. One notable challenge with this approach stems from the prevalence of specific peptides, impeding the precise identification of their respective proteins. Furthermore, the absence of complete sequences, the novelty of a protein not present in the database, or the existence of mutations or post-

translational modifications may lead to the omission of crucial information. (Shortreed et al., 2015) When dealing with a mixture of proteins, this strategy can be complemented by a first protein separation step for easier protein characterization.

In this context, technological evolutions have led to the development of various methodologies for protein separation, including isoelectric precipitation, organic solvent precipitation, dialysis, ultrafiltration, chromatography, electrophoresis, molecular imprinting, magnetic separation, reverse micelles, and crystallization, among others. (S. Liu et al., 2020) Concerning electrokinetic separations, isoelectric focusing (IEF) stands out as a powerful and highly resolutive approach for separating and enriching proteins and peptides. By establishing a pH gradient using a carrier ampholyte (C.A.) mixture, proteins are separated under an electric field according to their isoelectric point (pI), allowing then the coupling with detection methods. (Farmerie et al., 2021; Righetti et al., 2013)

A protocol was developed in our group to allow for direct coupling between IEF (in capillary format, CIEF) and mass spectrometry. A water/glycerol medium was employed to improve analytical performances. Indeed, by replacing classical gel media of IEF with more viscous water/glycerol media, efficient coupling to mass spectrometry could be directly performed while drastically lowering the electroosmotic flow for efficient IEF separations. Furthermore, this water/glycerol medium could allow for both hydrophilic and hydrophobic protein solubilization, providing a way for whole proteome analysis. (Busnel et al., 2005b; Mokaddem et al., 2009)

Given the objective of proteomic analysis, including successive protein separation, digestion into peptides, and peptide characterization by MS., the development of this CIEF should then be transferred into a microfluidic format. Indeed,

microfluidics emerges as a promising alternative for integrating these three steps into an automated process. Furthermore, miniaturization reduces analysis time and automation, preventing manual errors and cross-contamination. Additionally, microfluidic systems have the potential to reduce analysis costs and expand applications to low-resource settings. (X. Li et al., 2010; Martinez et al., 2007)

Over the past decade, the microfluidic paper-based analysis device (μPAD) has emerged as an innovative analytical microdevices and has garnered considerable interest. The μPADs offer several advantages, such as biocompatibility, low cost, low environmental impact, and the porous nature and chemical inertness of paper enable efficient immobilization and storage of reagents. Moreover, their lightweight and flexible properties simplify transportation. Regarding device manipulation, the most significant advantage arises from capillary action, eliminating the need for external pumps to drive liquid motion.(Hemmateenejad et al., 2023; Martinez et al., 2010)

Only a few publications employ paper-based analytical devices for protein separations via isoelectric focusing (IEF).(Gaspar et al., 2016; J. C. Niu et al., 2018; Xie et al., 2018; S. Yu et al., 2019) The studies thus far exhibit certain limitations, including the absence of a validated technology, issues related to precision, integration challenges, and a notable lack of system feasibility/robustness associated with the absence of a holder. As far as our knowledge extends, all the documented research on isoelectric focusing (IEF) in paper-based platforms has consistently employed water as the medium for protein separation. This practice, however, presents a limitation in conducting a comprehensive analysis of the complete proteome, as it encompasses both hydrophilic and hydrophobic proteins; besides, glycerol helps decrease the system's evaporation.

This work aims to develop a straightforward and robust IEF on a µPAD, which could then be directly coupled to protein digestion and MS. or be used as a pre-treatment protein sample. In this context, the main objective is to achieve an efficient focusing on the proteins rather than precisely determining their pI. Indeed, the focused protein bands would then be easily transferred to another µPAD by capillary effect for digestion and then transferred to MS. by paper-based interfaces, where the protein can be fully characterized. Therefore, a new µPAD with a specific 3D-printed holder was developed to overcome the actual issues. The 3D-printed holder design allowed to gain in automation, simplicity, and repeatability. For a matter of low-cost development, different paper-based materials were explored without any surface modification. Then the generation of pH gradient on the optimum paper strip was studied with the water/glycerol medium while optimizing the glycerol content and focusing time, to drastically diminish the electroosmotic flow and medium evaporation. The optimization of the IEF µPAD was performed with chromophore proteins (Cytochrome C, CytC, Phycocyanin and Myoglobin), allowing for a simple detection via smartphone image treatment. The proof of concept of this µPAD for IEF was performed with the chromophore proteins either diluted in the IEF medium or spiked in saliva.

2. MATERIALS AND METHODS

2.1. Materials and Chemicals

Whatman grade 1, Whatman 3MM, Glass Fiber Conjugate PAD, and glycerol (for molecular biology with 99% purity) were purchased from Sigma Aldrich (Darmstadt, Germany). The electrolyte reservoirs were simply multipurpose kitchen cleaning sponges (DANIHOME® Lingettes éponge), and their composition was 70%

cellulose and 30% cotton. The Bio-Lyte 40% (m/v) C.A. (pH 3-10), Bio-Lyte 40% (m/v) C.A. (pH 3-5), Bio-Lyte 40% (m/v) C.A. (pH 9-11), and IEF Standards (Phycocyanin pI 4.45, 4.65; 4.75; Mr 30 kDa; equine Myoglobin pI 6.8, 7.0; Mr 17.8 kDa; and Cytochrome C pI 9.6, Mr 11.7 kDa) were purchased from Bio-Rad (Hercules, USA). Phosphoric Acid (Density: 1.685 g/mL and 85% purity) and sodium hydroxide (20% m/v aqueous solution) were purchased from Alpha Aesar (Kandel, Germany). The solutions were prepared using PURELAB flex from ELGA VEOLIA (Lane End, U.K.). The platinum electrodes were purchased from LabSmith (Livermore, USA). A Silhouette Cameo 4 (Lindon, USA) was used to design and cut the paper strips. A Formlabs 2 SLA 3D printer (Somerville, USA) was used to print the bottom and the top of the 3D printed holder used in this work.

2.2. Saliva Samples

The saliva samples were provided by the authors of this work. The contributors voluntarily self-collected by passive drooling approximately 1 mL of saliva. Each participant diligently deposited their saliva sample into a designated tube.

2.3. Fabrication of the Holder

The holder to support the elements for the IEF was designed with the help of the Autodesk Fusion 360® (https://www.autodesk.com/products/fusion-360/overview) and printed on a stereolithography 3D printer with a commercial Formlabs Clear Resin (V4) as the printing material. This holder was explicitly created to facilitate the integration of the isoelectric focusing components, including the paper strip separation channel, the electrolyte reservoirs, and the electrodes, avoiding in such a way the mentioned issues of precision from previous µPAD devices. The holder has a bottom and a top part manufactured as outlined in Figure 1, following an optimization process

of all relevant printing parameters. The design incorporates specific features within the holder for precise positioning of components. The bottom section includes a fitting mechanism for the paper strip. Conversely, the top piece accommodates fit spaces for the electrolytes reservoirs and the platinum wires used as electrodes.

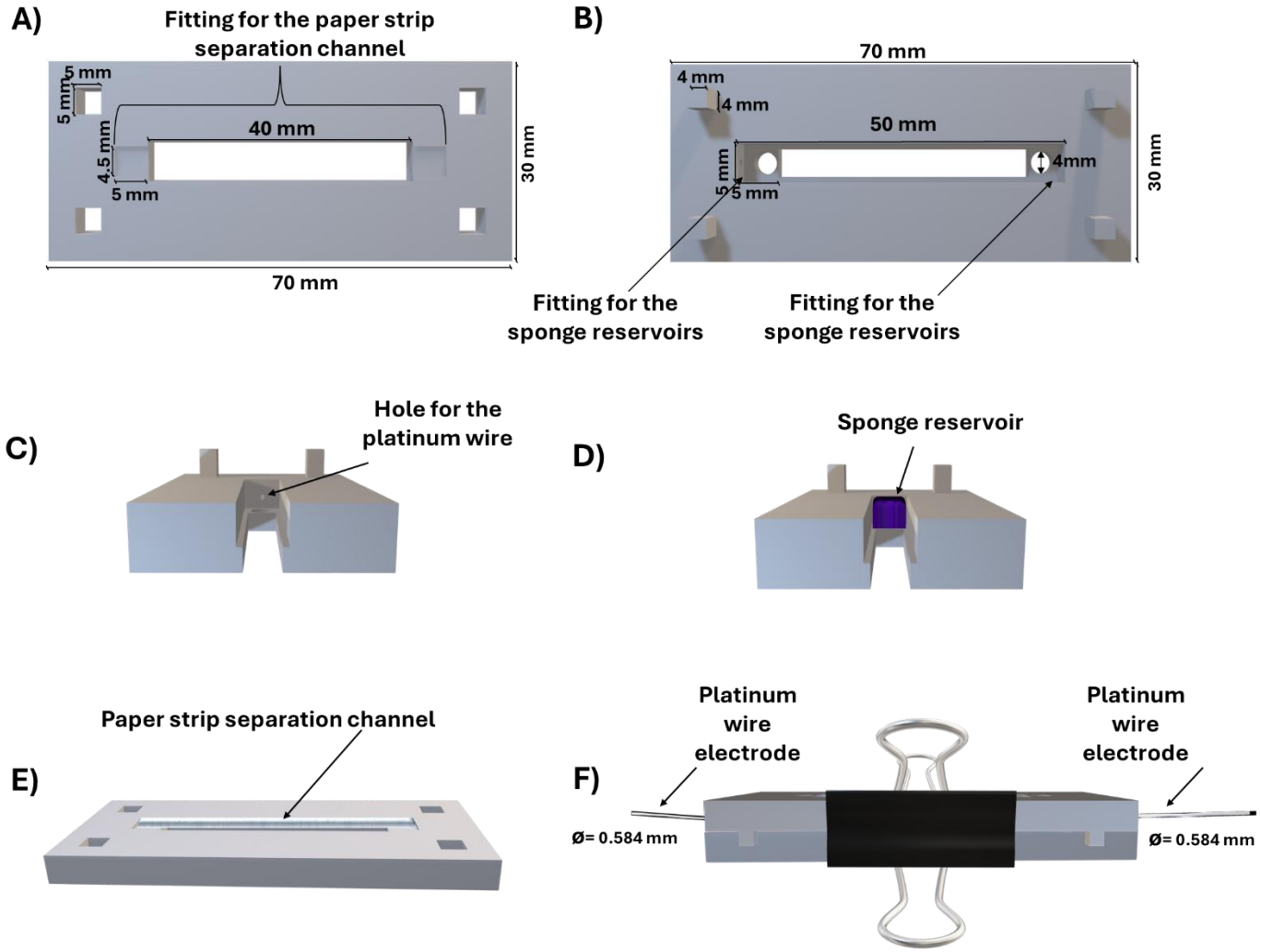

Figure 1: Scheme of the designed 3D printed holder: A) Bottom piece; B) Top piece; C) Cross-section of the top piece showing the hole for the platinum wire electrodes; D) Cross-section of the top piece showing the sponge reservoir; E) Bottom piece showing the paper strip separation channel fit; F) Holder assembled with a paper clip.

2.4. Experimental methodology

To fabricate the paper strip separation channel and reservoirs for the electrolyte's reservoirs, a Silhouette Cameo 4 was employed. The paper strip fluidic channel (50 mm x 4.5 mm) was placed within the lower section of the holder, while the reservoirs (5 mm length x 5 mm width x 5 mm height) were positioned in the upper section. Subsequently, the system assembly was achieved through a paper clip, effectively securing the parts in a fixed position and facilitating contact between the paper strip and the reservoirs, as shown in Figure 1.

Initially, it was simultaneously pipetted 60 µL of H_3PO_4 (pH 2) and 60 µL of NaOH (pH 13) into the anolyte and catholyte reservoirs, respectively. These liquids are then traversed by capillarity from the reservoirs to the paper strip. Subsequently, a 60 µL mixture of carrier ampholyte (C.A.) with varying pH gradients (pH 3-5 at 0.5%, pH 3-10 at 1%, and pH 9-11 at 0.5%) was pipetted at the center of the paper strip. Driven by capillary forces, the C.A. mixture diffused through the paper, reaching the paper strips' extremities and intermingled with the electrolyte solutions. Following a 1-minute duration to ensure the uniform dispersion of the solution, 8 µL of a $1 mg.mL^{-1}$ sample was applied at the center of the paper strip. Subsequently, a 200V voltage was applied with a Labsmith HVS488 High Voltage Sequencer, for 25 minutes.

After the electrophoretic process, an assessment of the establishment of the pH gradient and proteins separation was conducted, involving a systematic sequence of steps designed to evaluate the system's performance. Firstly, to verify the effectiveness of the separation, a photograph of the paper strip was captured using a Mi 10T M2007J3SY smartphone. Subsequently, a gray value curve was plotted against the channel length using the obtained image in the ImageJ software (http://imagej.net).

For the pH gradient assessment, a pH paper was deployed over the paper strip immediately following the image capture to gauge the establishment of the pH gradient along the separation paper. Subsequently, a correlation was established between the pH values (derived from the color patterns observed on the pH paper) and the migration distance, which yielded a correlation equation. The experimental isoelectric point (pI) of the analyzed proteins could be calculated using this equation.

The separation efficiency was evaluated by calculating the theoretical plate number (N_{plate}). The calculation was performed based on equation (1):

$$N = 5.55 \left(\frac{d}{W(\frac{1}{2})} \right)^2 \qquad (1)$$

Where N is the theoretical plate number, d is the protein migration distance (cm), w is the peak width at half-height (cm).

For quantitation studies and proof of concept in the saliva matrix, a calibration curve was obtained through serial dilutions of proteins in glycerol 15% solution. To evaluate the matrix effect, serial dilutions of proteins were spiked into saliva samples. The calibration curve for both cases correlated the average pixel values from the protein band in the image with the corresponding protein concentrations.

3. Results and Discussion

The primary goal of this study is to develop and optimize an isoelectric focusing-based pre-treatment device for subsequent protein digestion and generated peptides mass spectrometry detection. As discussed by Tata Rao et al. in 2020(Tata Rao et al., 2020), an analytical microdevice should possess several key attributes apart from high performance, including portability, automation, high throughput, versatile integration,

and cost-effectiveness. In this context, a paper-based Isoelectric Focusing (IEF) platform was designed to feature a 3D-printed holder with integrated platinum electrodes, electrolyte reservoirs, and a paper-based separation channel. The platform geometry (Figure 1) was optimized to allow for efficient, stable, and precise protein separations. The IEF separation channel was composed of a paper strip (50 mm x 4.5 mm) placed in the lower part of the platform, while the reservoirs composed of 70/30 % (m/m) cellulose/cotton sponges were positioned in the upper part. The paper channel and reservoirs were set in close contact in the 3D printed holder by closing and tweezing the two parts. The platinum electrodes were positioned within the upper part at the extremity of the holder, as pointed out in Figure 1.

To determine the paper-based IEF microdevice efficiency (calculated by the theoretical plate number, see 2.4), a series of procedural steps were delineated for each experimental result (Figure 2). First, concerning the experimental parameters to optimize, the IEF separation was followed by the evolution of the current, while applying the separation voltage. Then, the pH gradient on the paper strip was visualized thanks to portions of pH paper positioned on another strip, which was impregnated by capillarity from the paper strip (see Figure 2). This allowed to draw the pH versus distance on the paper strip, allowing for determining pH gradient efficiency and precision as well its width on the paper strip.

Chromophore model proteins were then separated, first allowing a visual coloration at different paper strip parts and then for a data treatment of the photography of the paper strip to generate electropherograms via the ImageJ software. The electropherograms were drawn before and after the separation voltage cut-off to evidence any dispersion of the protein bands; in this case, pH gradient determination was performed after the photography.

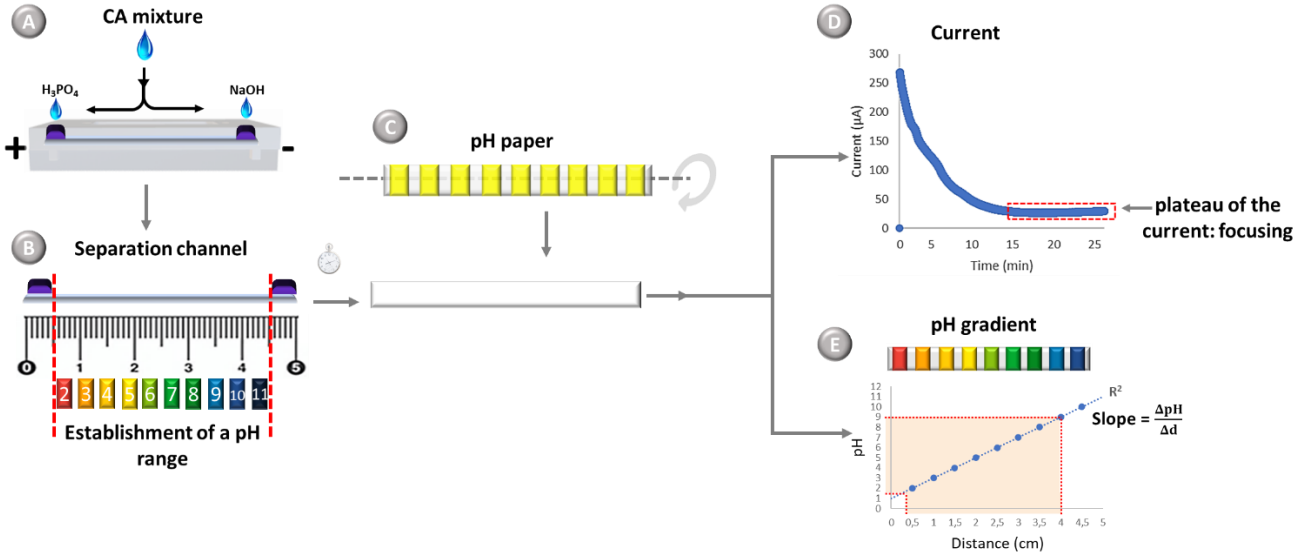

Figure 2: Comprehensive scheme for image processing and analysis of the results. A: Loading of the C.A. mixture into the system; B: establishment of the pH gradient along the paper strip; C: Placing the pH paper over the paper strip separation channel to assess the pH gradient; D: Current development over time obtained by the power supply; E: Plotting of the pH values (based on the obtained pH paper profile) over the paper strip distance.

Some experimental conditions were optimized in a preliminary step (results not shown). The separation voltage was optimized at 200V to obtain the largest pH gradient while avoiding high current and medium evaporation. The separation medium was composed of water/glycerol (85/15, v/v) as this medium avoids the addition of any gel that could impede then coupling to mass spectrometry for protein characterization and allows for the solubilization of the majority of hydrophobic and hydrophilic proteins(Busnel et al., 2005a; Lecoeur et al., 2010; Mokaddem et al., 2009), therefore compatible with the implementation of an integrated proteomic on-a-chip. The carrier ampholyte mixture was optimized with three pH ranges (pH 3-5 at 0.5%, pH 3-10 at 1%, and pH 9-11 at 0.5%), leading to a total of 2% C.A. mixture in the separation medium. Anolyte and catholyte were composed of H_3PO_4 (pH 2), and NaOH (pH 13), respectively.

3.1. Selection of the paper nature for the separation channel

Three paper substrates were assessed for the paper fluidic channel to establish a pH gradient along the paper strip and stabilize the current: Whatman® cellulose chromatography paper grade 1, Whatman® cellulose chromatography paper grade 3MM, and Glass Fiber Conjugate PAD. Both Whatman grade 1 and grade 3MM papers are composed of cellulose, differing only in thickness (0.18 mm and 0.34 mm, respectively). Glass Fiber Conjugate PADs are naturally composed of glass fiber and have a thickness of 0.43 mm.

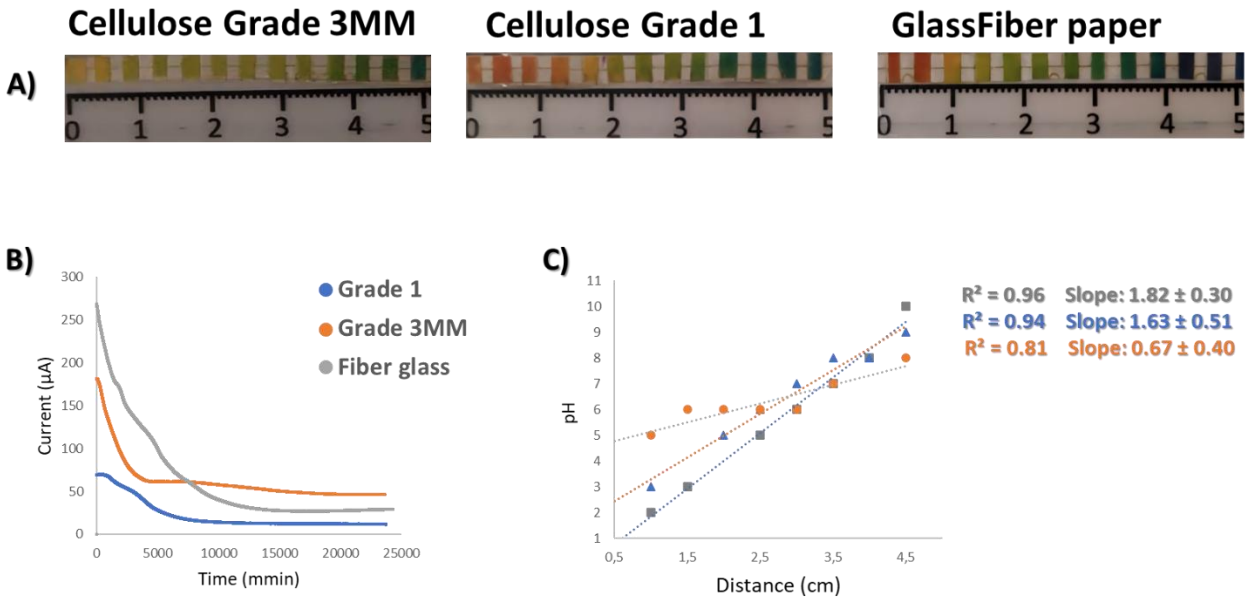

Figure 3: Selection of the paper nature for IEF: Cellulose Grade 3MM (orange), Cellulose Grade 1 (blue), Glass Fiber (grey). A) Identification of the pH gradient position on the paper strip, B) Current evolution over time (mmin stand for milliminutes), and C) Linear correlation of the pH with the electromigration distance on the paper strip. Experimental conditions: applied voltage, 200 V; separation medium, 2% C.A. (pH range 3-11) in glycerol/water 85/15, v:v); anolyte, H_3PO_4 (pH 2); catholyte, NaOH (pH13); focusing time,25 minutes.

The visualization of the pH gradient reveals a narrower range (5-8) for Cellulose Grade 3MM, while the larger pH gradient was reached with GlassFiber paper (2-10) (Figure 3-A). It is worth noting that the anticipated slope should be 2, considering a pH

range of 3 to 11 on a 4 cm paper separation channel, considering the 5 cm paper strip length and the 0.5 cm from each extremity reserved for the reservoirs. The current profiles (Figure 3-B) present a classical evolution, with focusing stabilization occurring when the current stabilizes around 10 min, with an initial higher current value for glass fiber paper. Subsequently, the correlation between pH and migration distance (Figure 3-C) was determined for all three types of papers, showing a broader pH gradient (2-10), a slope of 1.82 in closest alignment with the theoretical expectations, and a higher correlation coefficient for the glass fiber paper. Microscopic analyses (data not shown) revealed that glass fiber paper presents a less dense network of fibers, which could lead to higher porosity and then better fluid movement along the paper strip. This characteristic seems to contribute to the superior performance of glass fiber paper in establishing a well-defined pH gradient for the fluidic channel. Consequently, glass fiber paper was selected for the fluid separation channel in all subsequent experiments.

3.2. Optimization of the IEF medium

The efficient establishment of a pH gradient on the paper strip is essential for isoelectric focusing. As indicated above, the concentration and composition of the carrier ampholyte mixture, along with the pH of the anolyte and catholyte, were meticulously optimized by considering several parameters, such as initial and final current values, correlation coefficient, slope, and linear range.

So as to develop an IEF paper-based platform compatible with the whole proteome analysis, a water/glycerol medium was selected. Glycerol is widely used in biochemistry to stabilize proteins under their native form (Creighton, 1989). Glycerol's higher viscosity than water allows to slow down fluid movement within the

water/glycerol mixture, facilitating a more precise establishment of the focusing of carrier ampholytes and proteins. Furthermore, glycerol enhances the system's wettability, reducing evaporation and minimizing heat generation, as previously described. (Busnel et al., 2005a; Mokaddem et al., 2009)

The optimization of IEF was performed while varying the glycerol content (0%, 15%, and 20%, v/v) in water (Figure 4). First, current profiles (Figure 4A) and pH gradient establishments (Table 1) were determined and then a model protein (CytC, pI = 9.6) was employed to assess the separation efficiency in these three media (Figure 4B and Table 1). Glycerol did not interfere with the system's ability to establish a pH gradient and did not adversely affect any analytical parameter.

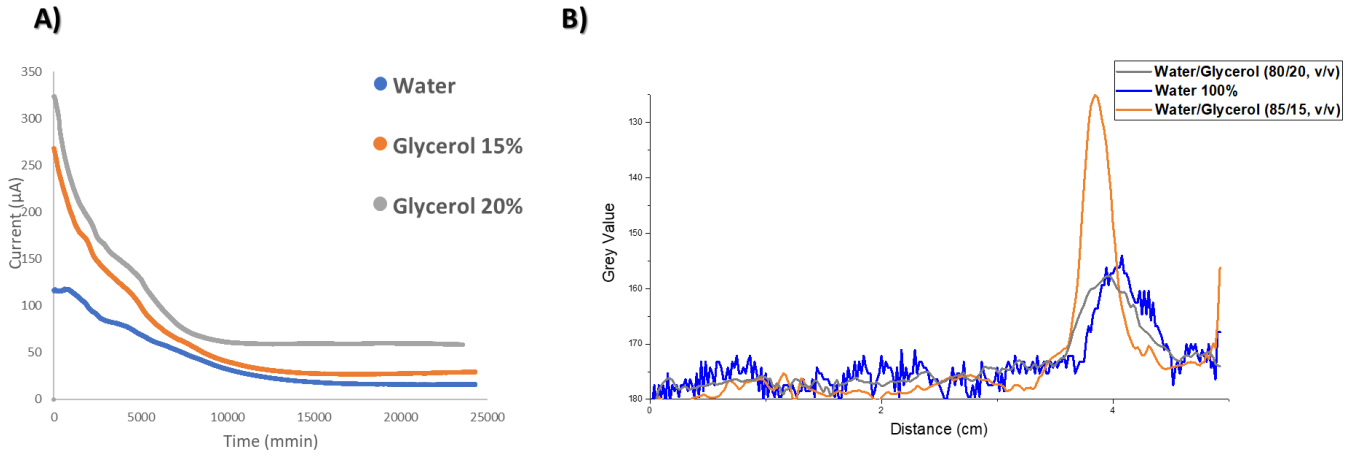

Figure 4: Influence of the separation medium composition on IEF: water 100% (in blue), water/glycerol (85/15, v/v, in orange), and water/glycerol (80/20, v/v, in grey). A) Current profile. B) Electropherogram of Cytochrome C. Experimental conditions: see Figure 3.

A 15% glycerol solution as the separation medium provided the highest slope (and therefore pH gradient range) with a higher correlation coefficient (see Figure 4). Furthermore, it allowed to focus CytC with a higher efficiency, a higher peak area and an experimental pI closer to the theoretical one.

Table 1: Analytical parameters and experimental pI values for the three different media

Separation Medium	Slope	Correlation Coeficient	Experimental pI Value	Efficiency
Water	1.40 ± 0.10	0.97± 0.02	8.8 ± 0.33	476.582
Glycerol 15%	1.70 ± 0.07	0.98± 0.02	9.2 ± 0.01	1050.530
Glycerol 20%	1.30 ± 0.03	0.97 ± 0.01	8.9 ± 0.08	452.293

These results can be correlated to the fact that glycerol, replacing gels in classical IEF, increases the viscosity of the IEF medium, and therefore reduces the electroosmotic flow (EOF) and the electrophoretic mobility of the proteins. Therefore an optimum in peak efficiency is attained at 15% glycerol, being a compromise between low EOF and sufficient mobility for efficient focusing.

3.3. Influence of focusing time and voltage continuity

During focusing, the evolution of the current is crucial to follow for estimating the optimal focusing time. Indeed, a focusing time that is too low could lead to a dispersion of the separation band, lowering separation efficiency and resolution. On the contrary, a prolonged focusing can introduce drawbacks, such as protein precipitation and liquid evaporation, especially in the case of an open-to-air paper microfluidic channel (Bohuslav Gas et al., 1997; Xuan, 2022). Furthermore, dispersion effect can arise when cutting the voltage after focusing, which could impact on resolution and subsequent coupling to other processes (such as digestion and /or protein characterization by mass spectrometry). To study these two parameters, CytC was separated with three focusing times of 10, 15, and 25 minutes, that is, at different times on the plateau of the current (as shown in Figure 2), and the CytC electropherograms were obtained while maintaining or cutting the voltage supply (Figure 5).

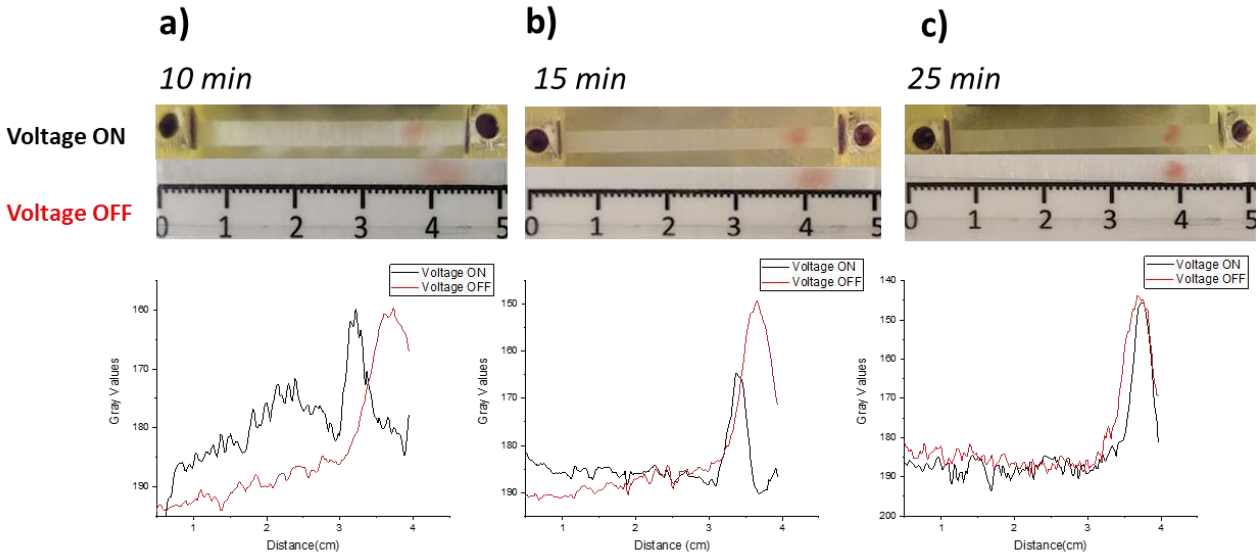

Figure 5: IEF Electropherogram of CytC showing the dispersion effect based on focusing time (a: 10 min, b: 15 min, c: 25 min) while maintaining (voltage ON / black) or discontinuing (voltage OFF / red) the voltage supply to the system. Experimental conditions are detailed in Figure 3.

For 10 and 15 minutes focusing, the protein peak tends to be broader when the voltage is cut at the end of the focusing process, with a modification of the peak apex. When the focusing time is extended to 25 minutes, a notable reduction in band dispersion is observed following the discontinuation of voltage, resulting in narrower bands, and peak apex is very slightly modified.

Table 2: Influence of focusing time and voltage continuity (on) or discontinuity (off) on the separation efficiency and experimental pI of CytC. Experimental conditions: see Figure 3

Focusing time (min)		Experimental pI (theoretical pI = 9.6)	Efficiency
10	on	7.3 ± 0.3	755
	off	8.4 ± 0.3	321
15	on	7.7 ± 0.2	844
	off	8.3 ± 0.3	938
25	on	8.4 ± 0.4	938
	off	8.4 ± 0.3	987

The pI values and pic efficiencies were computed for focusing times of 10 minutes, 15 minutes, and 25 minutes while maintaining or discontinuing the voltage (Table 2). Peak efficiency increases with focusing time (755, 844, and 938, for 10, 15, and 25 minutes, respectively) which aligns with the visualized decreased dispersion effect. When increasing the focusing time, the pI value gets closer to the theoretical one, and the values obtained with voltage continuity (on) or discontinuity (off) are more similar. It has to be noticed that the theoretical pI of CytC is the one determined in pure water, and not in the glycerol/water mixture of this study. As the main objective of this study is to provide an efficient protein focusing for coupling to further digestion in the context of proteomics, separation efficiency is a key parameter. Extending the focusing time to 25 minutes contributes therefore to improved efficiency by reducing dispersion, with a reduced effect of voltage cut-off. This investigation provides valuable insights into optimizing electrophoresis conditions for sharper sample bands. It underscores the crucial role of selecting an appropriate focusing time to minimize dispersion effects, thereby enhancing the efficiency and accuracy of experimental results.

3.4. Optimization of the reservoirs design

When developing paper-based electrophoretic microchips, one challenge concerns the design of reservoirs at the extremities of the paper strip. Gaspar et al. reported a paper-based microfluidic system for isoelectric focusing using paper PADs as reservoirs. However, this approach lacked robustness due to the absence of reported standardization in position and repeatability (Gaspar et al., 2016). Similarly, Niu et al. and Xie et al. proposed an isoelectric focusing system on a paper strip fluidic channel with caps from microtubes as electrolyte reservoirs (J. C. Niu et al., 2018; Xie

et al., 2018). The reproducibility of these systems was compromised due to the imprecise positioning of the paper separation channel, where the paper strip was dipped inside the reservoir without technical control.

The paper-based microdevice developed herein utilizes absorbent sponges as reservoirs for catholytes and anolytes, positioned at the upper part of the holder and in contact with the extremities of the paper strip. Similar scientific studies (Gaspar et al., 2016; S. Yu et al., 2019) utilize terms such as "absorbent PADS" and "soaked paper" to describe comparable reservoirs. However, no holder system with precise and optimized positions similar to the one presented here has been reported for analogous systems.

The 3D-printed holder developed here allows a good integration of the reservoirs and a good connection to the paper strip. Thus, to increase the performance of IEF separation, the design of the reservoirs was further optimized. Indeed, a potential source of errors arises from the manual stacking of the reservoirs within the holder, presenting a challenge in ensuring consistent stacking across different experiments. Furthermore, the "volume" of the reservoirs can impact the separation efficiency. Initially composed of 4 layers of sponges, the system stability and repeatability were studied while varying the number of sponge layers, therefore the height of the electrolyte reservoirs. For this purpose, the 3D-printed holder had to be redesigned in terms of reservoir height, to reach stability and repeatability in each case

Figure 6 illustrates the design of the holder according to the number of layers, that indicate the heights of the reservoir in the three configurations: Figure 6-A, with four layers of sponges (240 µL), Figure 6-B, with two layers of sponges (120 µL), and Figure 6-C, with a single layer of the sponge (60 µL). As the number of sponge layers

increases, the height of the fitting part located at the upper section proportionally rises. The precision of the pH gradient established in the paper strip was assessed by examining the current repeatability for each condition.

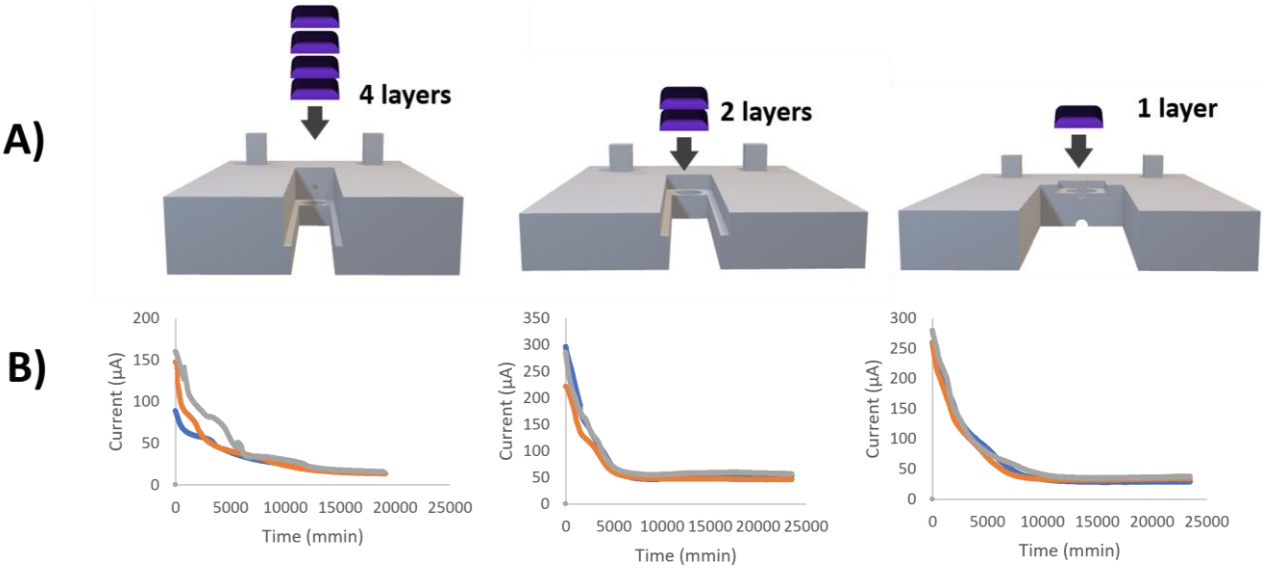

Figure 6: Influence of the reservoir design. A) Three geometries and the respective layers of reservoirs. B) Current profile in triplicates for each geometry. Experimental conditions: see Figure 3.

The reduction in the number of layers in both reservoirs exhibited a direct and proportional improvement in precision. Specifically, a single-layer reservoir provided the most favorable conditions for achieving consistent current. Table 3 presents the slope and correlation coefficient of the pH gradient generated for the three designs. The configuration with one sponge layer for the reservoir, associated with the corresponding modified holder, provided a higher slope, allowing for a higher separation performance. Furthermore, the manual introduction of different sponge layers could induce less repeatability in their positioning. This is likely attributed to introducing air into the system, diminishing electrical contact, and, subsequently, the system's performance. Utilizing a single layer enhances system performance, reduces solvent usage, and minimizes waste generation.

Table 3: Optimization of the reservoir design: influence of the number of layers for pH gradient establishment. Experimental conditions: see Figure 3

Number of layers	Slope	R^2
4	1.40 ± 0.40	0.986 ± 0.02
2	1.60 ± 0.20	0.985 ± 0.01
1	1.63 ± 0.07	0.980 ± 0.01

Integrating electrokinetic separation components with standardized positions, volumes, and geometries was facilitated using a 3D-printed holder. Our innovative design featured a straightforward paper strip and absorbent sponges serving as an electrolyte reservoir, creating a simplified and integrated paper-based platform. This platform effectively reduces the volumes of reagents and samples required, consequently reducing overall analysis costs, with an increased robustness.

3.5. A Proof of Concept with Saliva Sample Spiking

In a first step, the validity of the optimized methodology was determined by dissolving CytC in the medium employed for IEF separation (water/glycerol (85/15, v/v)) or spiking it in a saliva matrix. Saliva is a mildly acidic fluid, typically within a pH range of 6 to 7. It contains various elements, including oral bacteria, food particles, different types of cells, immunoglobulins, proteins, enzymes, and mucins. Additionally, it encompasses nitrogenous compounds like urea and ammonia, along with an array of electrolytes, such as sodium, potassium, calcium, magnesium, bicarbonate, and phosphates. (Sue P. Humphrey, 2001). Therefore, interference in the system performance is expected in the presence of saliva.

The calibration curve of CytC was performed either in the IEF medium or in two different salivas, using six independent replicates. In the IEF medium, a linear

response within the concentration range of 1.5 to 10.0 mg. mL^{-1} (R^2 of 0.9724) was obtained with a LOD and LOQ of 1.23 mg. mL^{-1} and 4.12 mg. mL^{-1}, respectively. In the two saliva (saliva 1 and saliva 2) tested, a linear response within the concentration range of 0.5 to 7.5 mg. mL^{-1} (R^2 of 0.954 and 0.955, respectively). The LOD and LOQ for saliva 1 were 1.26 mg. mL^{-1} and 4.21 mg. mL^{-1}, respectively, while the ones for saliva 2 were 1.87 mg. mL^{-1} and 6.24 mg. mL^{-1}, respectively.

Determining the limit of detection and quantification in analytical methods depends on the instrumentation used. This study developed a handmade, cost-effective system prioritizing satisfactory separation efficiency and resolution over strict optimization of LOD and LOQ parameters. Consequently, while the achieved LOD and LOQ results appear relatively high, it is pertinent to note that analogous investigations using paper-based isoelectric focusing (IEF) systems in the scientific literature(Gaspar et al., 2016; J. C. Niu et al., 2018; Xie et al., 2018; S. Yu et al., 2019) rarely provide explicit values for these parameters. Therefore, more comparative data is needed to assess the significance of the reported values. Regardless, it must be emphasized that the primary objective of this study is to achieve efficient protein focusing for subsequent analytical procedures.

Also, these results indicate a marginal sensitivity reduction attributable to matrix effects. This investigation underscores the method's suitability for real-world sample analysis and highlights the significance of considering matrix effects when assessing the performance of analytical procedures.

In a second step, the influence of saliva matrix was studied for a mixture of three chromophore proteins with different pIs and molecular masses (Phycocyanin (pI 4.62; Mr 30 kDa, providing a blue band), Myoglobin (pI 6.8–7.4; Mr 17.8 kDa, providing

a brown band), and Cytochrome C(pI 9.6; Mr 11.7 kDa, providing an orange band)) either dissolved in the IEF medium or spiked into saliva 1.

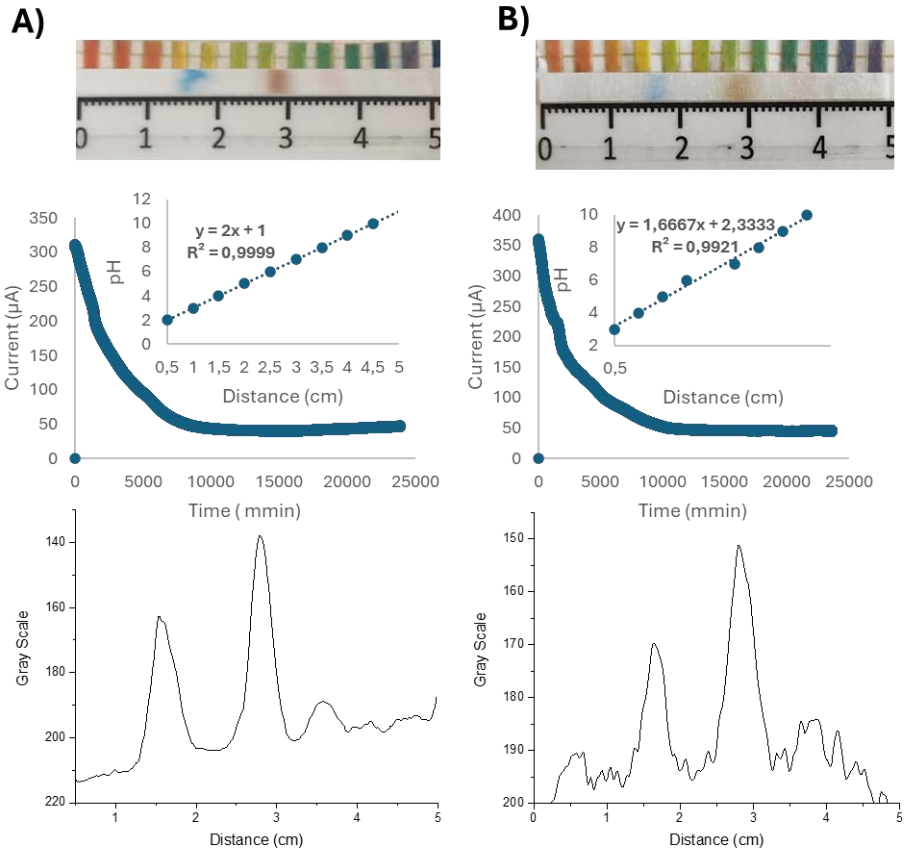

Figure 7: IEF of a mixture of Phycocyanin, Myoglobin and Cytochrome C, A) dissolved in the IEF medium and B) spiked within a saliva sample (2.0 $mgmL^{-1}$). Experimental conditions: see Figure 3.

As illustrated in Figure 7, the mixture of proteins, along with the presence of the matrix, do not noticeably impact on the establishment of the pH gradient within the paper separation channel, which allows for an effective separation of the proteins.

Table 4 provides the efficiency and resolution for the separation of this mixture of chromophore proteins, without or with saliva.

Table 4: Efficiency and resolution for the electrokinetic separation of a mixture of Phycocyanin, Myoglobin and Cytochrome C in the presence and absence of saliva. Experimental conditions: see Figure 3.

		Efficiency	Resolution	
Mixture of proteins	**Phycocyanin**	**163.5**	**4.74**	**2.46**
	Myoglobin	**643.7**		
	Cytochrome C	**580.0**		
Mixture of proteins in saliva	**Phycocyanin**	**163.84**	**4.2**	**2.7**
	Myoglobin	**538.24**		
	Cytochrome C	**576.0**		

Considering that the overarching goal is to achieve efficient focusing of the proteins for subsequent analytical steps, the system exhibited satisfactory separation resolution, whether in IEF medium or in saliva matrix. In light of the system's overall feasibility and practicality, in line with its cost-effectiveness and potential of integrating steps and application in low-resource settings, the matrix effect does not substantially compromise the integrity of the final analysis. This is particularly true considering that the separation of proteins represents a first step within the global analytical process for proteomics.

5. Conclusion

This study addresses key challenges related to designing a paper-based isoelectric focusing (IEF) microdevice. By designing and developing an efficient 3D-printed holder, all components of the IEF procedure were integrated to gain in analytical robustness. This versatile holder can adapt to different configurations, in terms of electrolyte reservoirs volumes and paper-based fluidic channel, and could be employed for other analytical processes. The holder functioned as a central hub, allowing for establishing a robust pH gradient, a linear correlation with electromigration and simplified data treatment. The optimization of the 3D printed holder design contributed to maintaining system integrity, offering advantages such as enhanced

precision, simplified handling, reduced errors, and potential for point-of-care applications. Whereas several studies have explored the use of chemical agents such as polyvinylpyrrolidone (PVP) (S. Yu et al., 2019) to prepare paper substrates for IEF, the paper-based microfluidic platform developed in this study demonstrated efficient protein separation without needing any pre-treatment within the paper fluidic channel. Notably, to our knowledge, this marks the first instance of glycerol/water being used as a separation medium in a paper-based analytical device. After optimization of focusing time and studying the effect of voltage cut-off, the proof of concept was performed in a saliva matrix, showing very low impact of the matrix upon the separation of three chromophore proteins, highlighting the practical viability of the platform.

This study represents a step forward in integrating a proteomic analysis within a paper-based microfluidic device. The outlined paper-based IEF platform offers an economically feasible and versatile solution for protein pre-treatment on paper, leveraging miniaturization and a simplified approach. It then opens the way for its further integration in a three-step proteomics-on-a-chip, with subsequent protein digestion and characterization of the generated peptides by MS.

Declaration of Generative A.I. in Scientific Writing

In preparing this paper, the authors used an in-house AI companion application (based on the GPT-4 version of Azure OpenAI) to rephrase certain passages and perform grammar checks. After using this application, the authors reviewed and edited the content as necessary and took full responsibility for the publication's content.

Conflicts of interest

There are no conflicts to declare.

CRediT authorship contribution statement

Geovana Mendes: Writing – review & editing, Writing – original draft, Visualization, Methodology, Investigation. **Fanny d'Orlye:** Visualization, Methodology, Supervision, Investigation, Conceptualization. **Laura Trapiella-Alfonso:** Visualization, Methodology, Supervision, Investigation, Conceptualization. **Gabriela Duarte:** Writing – review & editing, Supervision, Funding acquisition**. Anne Varenne:** Writing – review & editing, Writing – original draft, Supervision, Resources, Project administration, Investigation, Funding acquisition, Conceptualization.

Acknowledgments

We thank the CAPES-COFCUB project (grant number: 88887.192880/2018-00 ; Ph C 952/19) that supported this study.

References

Bohuslav Gas, Sttidrf, M., & Kenndle, E. (1997). Peak Broadening in Capillary Zone Electrophoresis. Elecrrophoresis, 18(12–13), 2123–2133.

Busnel, J. M., Varenne, A., Descroix, S., Peltre, G., Gohon, Y., & Gareil, P. (2005a). Evaluation of capillary isoelectric focusing in glycerol-water media with a

view to hydrophobic protein applications. Electrophoresis, 26(17), 3369–3379. https://doi.org/10.1002/elps.200500252

Busnel, J. M., Varenne, A., Descroix, S., Peltre, G., Gohon, Y., & Gareil, P. (2005b). Evaluation of capillary isoelectric focusing in glycerol-water media with a view to hydrophobic protein applications. Electrophoresis, 26(17), 3369–3379. https://doi.org/10.1002/elps.200500252

Chothia, C. (1984). Principles That Determine The Structure Of Proteins. Annual Review of Biochemistry, 53, 537–572. https://doi.org/10.1146/annurev.bi.53.070184.002541

Creighton, T. (1989). Protein structure (T. E. Creighton, Ed.; 2nd ed.). A IRL Press .

Farmerie, L., Rustandi, R. R., Loughney, J. W., & Dawod, M. (2021). Recent advances in isoelectric focusing of proteins and peptides. In Journal of Chromatography A (Vol. 1651). Elsevier B.V. https://doi.org/10.1016/j.chroma.2021.462274

Garcia, B. A. (2010). What Does the Future Hold for Top Down Mass Spectrometry? Journal of the American Society for Mass Spectrometry, 21(2), 193–202. https://doi.org/10.1016/j.jasms.2009.10.014

Gaspar, C., Sikanen, T., Franssila, S., & Jokinen, V. (2016). Inkjet printed silver electrodes on macroporous paper for a paper-based isoelectric focusing device. Biomicrofluidics, 10(6). https://doi.org/10.1063/1.4973246

Guo, Y., Cupp-Sutton, K. A., Zhao, Z., Anjum, S., & Wu, S. (2023). Multidimensional separations in top–down proteomics. In Analytical Science Advances (Vol. 4, Issues 5–6, pp. 181–203). John Wiley and Sons Inc. https://doi.org/10.1002/ansa.202300016

Hemmateenejad, B., Rafatmah, E., & Shojaeifard, Z. (2023). Microfluidic paper and thread-based separations: Chromatography and electrophoresis. In Journal of Chromatography A (Vol. 1704). Elsevier B.V. https://doi.org/10.1016/j.chroma.2023.464117

Janin, J., & Chotnia, C. (1985). Domains in Proteins: Definitions, Location, and Structural Principles. Analysis of Structure, 115(28), 420–430.

Kim, M. S., Pinto, S. M., Getnet, D., Nirujogi, R. S., Manda, S. S., Chaerkady, R., Madugundu, A. K., Kelkar, D. S., Isserlin, R., Jain, S., Thomas, J. K., Muthusamy, B., Leal-Rojas, P., Kumar, P., Sahasrabuddhe, N. A., Balakrishnan, L., Advani, J., George, B., Renuse, S., … Pandey, A. (2014). A draft map of the human proteome. Nature, 509(7502), 575–581. https://doi.org/10.1038/nature13302

Lecoeur, M., Gareil, P., & Varenne, A. (2010). Separation and quantitation of milk whey proteins of close isoelectric points by on-line capillary isoelectric focusing-Electrospray ionization mass spectrometry in glycerol-water media. Journal of Chromatography A, 1217(46), 7293–7301. https://doi.org/10.1016/j.chroma.2010.09.043

Lenčo, J., Jadeja, S., Naplekov, D. K., Krokhin, O. V., Khalikova, M. A., Chocholouš, P., Urban, J., Broeckhoven, K., Nováková, L., & Švec, F. (2022a). Reversed-Phase Liquid Chromatography of Peptides for Bottom-Up Proteomics: A Tutorial. Journal of Proteome Research, 21(12), 2846–2892. https://doi.org/10.1021/acs.jproteome.2c00407

Lenčo, J., Jadeja, S., Naplekov, D. K., Krokhin, O. V., Khalikova, M. A., Chocholouš, P., Urban, J., Broeckhoven, K., Nováková, L., & Švec, F. (2022b). Reversed-Phase Liquid Chromatography of Peptides for Bottom-Up Proteomics: A Tutorial. Journal of Proteome Research, 21(12), 2846–2892. https://doi.org/10.1021/acs.jproteome.2c00407

Leon, A., & Pastor, O. (2021). Towards a Shared, Conceptual Model-Based Understanding of Proteins and Their Interactions. IEEE Access, 9, 73608–73623. https://doi.org/10.1109/ACCESS.2021.3080040

Li, X., Tian, J., & Shen, W. (2010). Thread as a versatile material for low-cost microfluidic diagnostics. ACS Applied Materials and Interfaces, 2(1), 1–6. https://doi.org/10.1021/am9006148

Liu, S., Li, Z., Yu, B., Wang, S., Shen, Y., & Cong, H. (2020). Recent advances on protein separation and purification methods. Advances in Colloid and Interface Science, 284(102254), 1–23. https://doi.org/10.1016/j.cis.2020.102254

Maráková, K., Opetová, M., & Tomašovský, R. (2023). Capillary electrophoresis-mass spectrometry for intact protein analysis: Pharmaceutical and biomedical applications (2018–March 2023). In Journal of Separation Science (Vol. 46, Issue 15). John Wiley and Sons Inc. https://doi.org/10.1002/jssc.202300244

Martinez, A. W., Phillips, S. T., Butte, M. J., & Whitesides, G. M. (2007). Patterned Paper as a Platform for Inexpensive, Low-Volume, Portable Bioassays. Angewandte Chemie, 119(8), 1340–1342. https://doi.org/10.1002/ange.200603817

Martinez, A. W., Phillips, S. T., Whitesides, G. M., & Carrilho, E. (2010). Diagnostics for the developing world: Microfluidic paper-based analytical devices. Analytical Chemistry, 82(1), 3–10. https://doi.org/10.1021/ac9013989

Maurer, M. H. (2011). Proteomic definitions of mesenchymal stem cells. In Stem Cells International. https://doi.org/10.4061/2011/704256

Miller, R. M., & Smith, L. M. (2022). Overview and considerations in bottom-up proteomics. In Analyst (Vol. 148, Issue 3, pp. 475–486). Royal Society of Chemistry. https://doi.org/10.1039/d2an01246d

Mokaddem, M., Gareil, P., & Varenne, A. (2009). Online CIEF-ESI-MS in glycerol-water media with a view to hydrophobic protein applications. Electrophoresis, 30(23), 4040–4048. https://doi.org/10.1002/elps.200900091

Moradian, A., Kalli, A., Sweredoski, M. J., & Hess, S. (2014). The top-down, middle-down, and bottom-up mass spectrometry approaches for characterization of histone variants and their post-translational modifications. In Proteomics (Vol.

14, Issues 4–5, pp. 489–497). Wiley-VCH Verlag. https://doi.org/10.1002/pmic.201300256

Niu, J. C., Zhou, T., Niu, L. L., Xie, Z. S., Fang, F., Yang, F. Q., & Wu, Z. Y. (2018). Simultaneous pre-concentration and separation on simple paper-based analytical device for protein analysis. Analytical and Bioanalytical Chemistry, 410(6), 1689–1695. https://doi.org/10.1007/s00216-017-0809-5

Righetti, P. G., Sebastiano, R., & Citterio, A. (2013). Capillary electrophoresis and isoelectric focusing in peptide and protein analysis. Proteomics, 13(2), 325–340. https://doi.org/10.1002/pmic.201200378

Shortreed, M. R., Wenger, C. D., Frey, B. L., Sheynkman, G. M., Scalf, M., Keller, M. P., Attie, A. D., & Smith, L. M. (2015). Global identification of protein post-translational modifications in a single-pass database search. Journal of Proteome Research, 14(11), 4714–4720. https://doi.org/10.1021/acs.jproteome.5b00599

Štěpánová, S., & Kašička, V. (2022). Applications of capillary electromigration methods for separation and analysis of proteins (2017–mid 2021) – A review. In Analytica Chimica Acta (Vol. 1209). Elsevier B.V. https://doi.org/10.1016/j.aca.2022.339447

Štěpánová, S., & Kašička, V. (2023). Recent developments and applications of capillary and microchip electrophoresis in proteomics and peptidomics (mid-2018–2022). Journal of Separation Science, 46(12). https://doi.org/10.1002/jssc.202300043

Sue P. Humphrey, R. Mse. and R. T. W. Dmd. (2001). A review of saliva: Normal composition, flow, and function. In THE JOURNAL OF PROSTHETIC DENTISTRY (Vol. 85, Issue 9). https://doi.org/doi:10.1067/mpr.2001.113778

Tata Rao, L., Rewatkar, P., Dubey, S. K., Javed, A., & Goel, S. (2020). Performance optimization of microfluidic paper fuel-cell with varying cellulose fiber papers as absorbent pad. International Journal of Energy Research, 44(5), 3893–3904. https://doi.org/10.1002/er.5188

Xie, S. F., Gao, H., Niu, L. L., Xie, Z. S., Fang, F., Wu, Z. Y., & Yang, F. Q. (2018). Carrier ampholyte-free isoelectric focusing on a paper-based analytical device for the fractionation of proteins. Journal of Separation Science, 41(9), 2085–2091. https://doi.org/10.1002/jssc.201701438

Xuan, X. (2022). Review of nonlinear electrokinetic flows in insulator-based dielectrophoresis: From induced charge to Joule heating effects. In Electrophoresis (Vol. 43, Issues 1–2, pp. 167–189). John Wiley and Sons Inc. https://doi.org/10.1002/elps.202100090

Yu, S., Yan, C., Hu, X., He, B., Jiang, Y., & He, Q. (2019). Isoelectric focusing on microfluidic paper-based chips. Analytical and Bioanalytical Chemistry, 411(21), 5415–5422. https://doi.org/10.1007/s00216-019-02008-5

Conclusions and Perspectives

This research advanced the integration of isoelectric focusing within a paper-based microfluidic device, marking a significant step towards fully incorporating proteomic analysis into such platforms. By demonstrating the feasibility of IEF in this context, we have started the basis for more complex proteomics workflows on paper-based devices. The next phase will focus on directly integrating the protein digestion process within the microfluidic platform. Achieving this will simplify the proteomic workflow and allow for the direct analysis of digested proteins using mass spectrometry. This integration can enhance the efficiency, portability, and accessibility of proteomic analyses, particularly in resource-limited settings.

CURRICULUM

Identification

Name: Geovana de Melo Mendes

Formal Education

2020 Doctorate in Chemistry.

Universidade Federal de Goiás, UFG, Goiania, Brazil

(**Co-tutelle**) École Nationale Supérieure de Chimie de Paris - Chimie ParisTech (Advisor: Anne Varenne)

Advisor: Gabriela Rodrigues Mendes Duarte

Scholarship from : Coordenação de Aperfeiçoamento de Pessoal de Nível Superior, CAPES, Brazil.

2018 - 2020 Master's in Chemistry.

Universidade Federal de Goiás, UFG, Goiania, Brazil

Title: Testes moleculares baseados em amplificação isotérmica mediada por Loop para detecção de arbovírus em microdispositivos descartáveis, Year of degree: 2020

Advisor: Gabriela Rodrigues Mendes Duarte

Scholarship from : Conselho Nacional de Desenvolvimento Científico e Tecnológico, CNPq, Brazil.

2014 - 2017 Graduation in .Chemistry

Universidade Federal de Goiás, UFG, Goiania, Brazil

Title: DETECÇÃO DO VÍRUS DA DENGUE POR RT-LAMP EM DISPOSITIVOS DESCARTÁVEIS DE

POLIÉSTER-TONER Advisor: Gabriela Rodrigues Mendes Duarte

2018 - 2020 Graduation in Licenciatura em Formação Pedagógica.

Instituto Federal de Educação, Ciência e Tecnologia de Goiás, IFG, Goiania, Brazil

Awards

2022 IX Prêmio SBPC/GO de Popularização da ciência- Edição 2022, SBPC/GO

2021 Artigo na Capa do Periódico Analyst, 146(4):1178-1187. doi: 10.1039/d0an02066d, Analyst

2021 Artigo na Capa do Periódico Analytical Methods, https://doi.org/10.1039/D1AY00481F, Analytical Methods

2021 Artigo na Capa do Periódico Journal of the Brazilian Chemical Society- https://dx.doi.org/10.21577/0103- 5053.20210098, JBCS- Journal of the Brazilian Chemical Society

2021 Reconhecimento Consuni 2020 à Comenda Professor Colemar Natal e Silva, Consuni

2019 Artigo na Capa do Periódico Journal of the Brazilian Chemical Society, Vol. 30, No. 9, 1841-1849, 2019, Journal of the Brazilian Chemical Society (JBCS)

2019 Menção Honrosa ao Trabalho apresentado, III Workshop da Pós Graduação em Químcia

2018 Prêmio de melhor poster, premiação SBQ regional centro-oeste no 19° Encontro Nacional de Química Analítica, Secretaria Region

2016 Melhor painel (Química Analítica), 39ª Reunião da Sociedade Brasileira de Química

2013 Medalha de bronze na categoria Relevância Social da IV Feira de Ciências do IFG, Instituto Federal de Educação, Ciência e Tecnologia de Goiás

2013 Medalha de ouro na categoria Ciências Exatas e da Terra da IV Feira de Ciências do IFG, Instituto Federal de Educação, Ciência e Tecnologia de Goiás

2013 Medalha de prata na categoria Criatividade e Inovação da IV Feira de Ciências do IFG, Instituto Federal de Educação, Ciência e Tecnologia de Goiás

Articles Published in Scientific Journals

1. **MENDES, G. M.**; DORLYE, F.; TRAPIELLA-ALFONSO, L.; DUARTE, GABRIELA R.M.; VARENNE, A.. Streamlined integrated protein isoelectric focusing using microfluidic paper-based device. JOURNAL OF CHROMATOGRAPHY A. , v.1732, p.465222, 2024.

2. DOS SANTOS, CARLOS ABELARDO; SILVA, LÍVIA DO CARMO; SOUZA JÚNIOR, MARCIO NERES DE; **MENDES, GEOVANA DE MELO**; ESTRELA, PAULO FELIPE NEVES; DE OLIVEIRA, KÉZIA GOMES; DE CURCIO, JULIANA SANTANA; RESENDE, PAOLA CRISTINA; SIQUEIRA, MARILDA MENDONÇA; PAUVOLID-CORRÊA, ALEX; DUARTE, GABRIELA RODRIGUES MENDES; SILVEIRA- LACERDA, ELISÂNGELA DE PAULA. Detecting lineage-defining mutations in SARS-CoV-2 using

colorimetric RT-LAMP without probes or additional primers. Scientific Reports. , v.12, p.11500 - 9, 2022. **Citações:** 4 | 4

3. **MENDES, G. M.**; ESTRELA, PAULO FELIPE; DE SOUZA JR., MARCIO; BRITO, N. N.; ARRUDA, A.; AUGUSTO, M. R.; CLARO, I. C. M.; DURAN, A. F. A.; CABRA, A. D.; DE FREITAS BUENO, RODRIGO; DUARTE[1], G. R. M.. MONITORAMENTO DA CARGA VIRAL DE SARS-COV-2 EM ÁGUAS RESIDUAIS NA CIDADE DE GOIÂNIA: EPIDEMIOLOGIA BASEADA EM ESGOTO E UM SISTEMA DE ALERTA PRECOCE PARA COVID-19. QUÍMICA NOVA (ONLINE). , v.1, p.1 - 8, 2022. **Citações:** 1

4. DE FREITAS BUENO, RODRIGO; CLARO, IEDA CAROLINA MANTOVANI; AUGUSTO, MATHEUS RIBEIRO; DURAN, ADRIANA FELICIANO ALVES; CAMILLO, LÍVIA DE MORAES BOMEDIANO; CABRAL, ALINE DINIZ; SODRÉ, FERNANDO FABRIZ; BRANDÃO, CRISTINA CELIA SILVEIRA; VIZZOTTO, CARLA SIMONE; SILVEIRA, RAFAELLA; **DE MELO MENDES, GEOVANA**; ARRUDA, ANDREA FERNANDES; DE BRITO, NÚBIA NATÁLIA; MACHADO, BRUNA APARECIDA SOUZA; DUARTE, GABRIELA RODRIGUES MENDES; DE LOURDES AGUIAR-OLIVEIRA, MARIA. WASTEWATER-BASED EPIDEMIOLOGY: A BRAZILIAN SARS-COV-2 SURVEILLANCE EXPERIENCE. JOURNAL OF ENVIRONMENTAL CHEMICAL ENGINEERING. , v.108298, p.108298 - 36, 2022. **Citações:** 16 |13

5. SILVA, LÍVIA DO CARMO; DOS SANTOS, CARLOS ABELARDO; **MENDES, GEOVANA DE MELO**; DE OLIVEIRA, KÉZIA GOMES; SOUZA JÚNIOR, MARCIO NERES; ESTRELA, PAULO FELIPE NEVES; COSTA, SÉRGIO; SILVEIRA-LACERDA, ELISÂNGELA DE PAULA; DUARTE, GABRIELA R.M.. Can a field molecular diagnosis be accurate? A performance evaluation of colorimetric RT-LAMP for the detection of SARS-CoV-2 in a hospital setting. Analytical Methods. , v.10, p.1 - 26, 2021.

6. DOS SANTOS, CARLOS; DE OLIVEIRA, KÉZIA; **MENDES, GEOVANA**; SILVA, LÍVIA; DE SOUZA JR., MARCIO; ESTRELA, PAULO FELIPE; GUIMARÃES, RAFAEL; SILVEIRA-LACERDA, ELISÂNGELA; DUARTE, GABRIELA. Detection of SARS-CoV-2 in Saliva by RT-LAMP During a Screening of Workers in Brazil, Including Pre-Symptomatic Carriers. JOURNAL OF THE BRAZILIAN CHEMICAL SOCIETY. , v.1, p.1 - 7, 2021. **Citações:** 4 | 6

7. DE OLIVEIRA, KÉZIA GOMES; ESTRELA, PAULO FELIPE NEVES; **MENDES, GEOVANA DE MELO**; DOS SANTOS, CARLOS ABELARDO; SILVEIRA-LACERDA, ELISÂNGELA DE PAULA; DUARTE, GABRIELA

RODRIGUES MENDES. Rapid molecular diagnostics of COVID-19 by RT-LAMP in a centrifugal polystyrene-toner based microdevice with end-point visual detection. ANALYST. , v.4, p.1178 - 1187, 2021. **Citações:** 42 |44

8. **MENDES, GEOVANA**; OLIVEIRA, KÉZIA; BORBA, JULIANE; OLIVEIRA, THAIS; FIACCADORI, FABÍOLA; NOGUEIRA, MAURÍCIO; BAILÃO, ALEXANDRE; SOARES, CÉLIA MARIA; CARRILHO, EMANUEL; DUARTE, GABRIELA. Molecular Diagnostics of Dengue by Reverse Transcription-Loop Mediated Isothermal Amplification (RT-LAMP) in Disposable Polyester-Toner Microdevices. JOURNAL OF THE BRAZILIAN CHEMICAL SOCIETY. , v.30, p.1789 - 1998, 2019. **Citações:** 14 |13

9. ESTRELA, PAULO FELIPE NEVES; **MENDES, GEOVANA DE MELO**; DE OLIVEIRA, KÉZIA GOMES; BAILÃO, ALEXANDRE MELO; SOARES, CÉLIA MARIA DE ALMEIDA; ASSUNÇÃO, NILSON ANTÔNIO; DUARTE, GABRIELA RODRIGUES MENDES. Ten-minute direct detection of Zika virus in serum samples by RT-LAMP. JOURNAL OF VIROLOGICAL METHODS. , v.271, p.113675, 2019. **Citações:** 25 | 25

Presentations in Events

1. **MENDES, G. M.**; DORLYE, F.; TRAPIELLA-ALFONSO, L.; VARENNE, A.. Microfluidic Paper-based Device (µPAD) for protein IsoElectric Focusing (IEF) toward integrated proteomic analysis, 2023. (Congress,Presentations in Events)

2. **MENDES, G. M.**; DORLYE, F.; TRAPIELLA-ALFONSO, L.; VARENNE, A.. Microfluidic Paper-based Device (µPAD) for proteomic studies based on Isoelectric focusing (IEF), 2022. (Symposium,Presentations in Events)

3. **MENDES, G. M.**. Amplificação isotérmica mediada por Loop (LAMP): o futuro dos diagnósticos moleculares?, 2021. (Conference or lecture,Presentations in Events)

4. **MENDES, G. M.**. 'Na fronteira do conhecimento: O químico pode ter um papel importante no enfrentamento de uma crise sanitária?, 2021. (Other,Presentations in Events)

5. **MENDES, G. M.**. 'Na fronteira do conhecimento: O químico pode ter um papel importante no enfrentamento de uma crise sanitária?', 2021. (Conference or lecture,Presentations in Events)

6. ESTRELA, PAULO FELIPE NEVES; **MENDES, GEOVANA DE MELO**; DE OLIVEIRA, KÉZIA GOMES; ASSUNÇÃO, NILSON ANTÔNIO; DUARTE, GABRIELA. RÁPIDA DETECÇÃO MOLECULAR DE ZIKA VIRUS DIRETAMENTE EM AMOSTRAS COMPLEXAS POR RT-LAMP EM DISPOSITIVOS
MICROFLUIDICOS DESCARTÁVEIS DE PeT, 2021. (Congress,Presentations in Events)

7. **MENDES, G. M.**. Relato de Experiência na roda de conversa EXPERIÊNCIA DOS EGRESSOS DO CURSO TÉCNICO INTEGRADO EM QUÍMICA, 2021. (Seminar,Presentations in Events)

8. **MENDES, GEOVANA**; OLIVEIRA, K. G.; DUARTE[1], G. R. M.. Molecular Diagnostics of Dengue by Reverse Transcription-Loop mediated Isothermal Amplification (RT-LAMP) in Disposable Polyester-Toner Microdevices, 2019. (Other,Presentations in Events)

9. **MENDES, G. M.**. Molecular Diagnostics of Dengue by Reverse Transcription-Loop mediated Isothermal
Amplification (RT-LAMP) in Disposable Polyester-Toner Microdevices, 2019. (Other,Presentations in Events)

10. ESTRELA, PAULO FELIPE NEVES; **MENDES, G. M.**; OLIVEIRA, K. G.; BATISTA, R. P.; BAILAO, A. M.; BORBA, JULIANE; CARRILHO, EMANUEL; DUARTE, GABRIELA RODRIGUES MENDES. Detecção de zika vírus em 10 minutos por Amplificação Isotérmica de DNA em microchip de poliéster-toner, 2018. (Congress,Presentations in Events)

11. **MENDES, G. M.**; OLIVEIRA, K. G.; GIMENEZ, T. D.; BAILAO, A. M.; FIACCADORI, F. S.; BORBA,
JULIANE; CARRILHO, EMANUEL; DUARTE[1], G. R. M.. DETECÇÃO DO VÍRUS D'ENGUE POR RT- LAMP EM DISPOSITIVOS DESCARTÁVEIS DE POLIÉSTER-TONER (PET), 2018. (Other,Presentations in Events)

12. **MENDES, G. M.**; OLIVEIRA, K. G.; FIACCADORI, F. S.; BAILÃO, ALEXANDRE; BORBA, JULIANE;
CARRILHO, EMANUEL; DUARTE[1], G. R. M.. DIAGNÓSTICO MOLECULAR DA DENGUE POR
AMPLIFICAÇÃO ISOTÉRMICA MEDIADA POR LOOP PÓS TRANSCRIÇÃO REVERSA (RT-LAMP) EM
MICRODISPOSITIVOS DESCARTÁVEIS DE POLIÉSTER-TONER, 2018. (Congress,Presentations in Events)

13. **MENDES, G. M.**; OLIVEIRA, K. G.; GIMENEZ, T. D.; BAILAO, A. M.; FIACCADORI, F. S.; BORBA,
JULIANE; CARRILHO, EMANUEL; DUARTE[1], G. R. M.. Diagnóstico Molecular da Dengue por

Amplificação Isotérmica Mediada por “Loop” após Transcrição Reversa em Dispositivos Descartáveis de Poliéster-Tone, 2017. (Other,Presentations in Events)

14. **MENDES, G. M.**; OLIVEIRA, KÉZIA; BAILÃO, ALEXANDRE; FIACCADORI, FABÍOLA; DUARTE, GABRIELA. Detecção do vírus dengue por RT-LAMP em dispositivos descartáveis de poliéster-Toner (PeT), 2016. (Congress,Presentations in Events)

15. MENDES, G. M.; GIMENEZ, T. D.; BAILÃO, ALEXANDRE; FIACCADORI, F. S.; BORBA, JULIANE; CARRILHO, EMANUEL; DUARTE, GABRIELA RODRIGUES MENDES. Detecção Rápida do vírus da dengue por amplificação isotérmica mediada por loop após transcrição reversa em dispositivos descartáveis de poliéster-toner, 2016. (Congress,Presentations in Events)

RÉSUMÉ

Cette thèse a été efectuée dans le contexte d'une co-tutelle entre l'Université Fédérale de Goias (Goiania, Brésil) et Chimie ParisTech PSL. Elle a débuté au Brésil, au début de la pandémie, ce qui a très fortement orienté le travail dans le laboratoire brésilien. Loop mediated isothermal amplification a été utilisée pour créer un test simple et économique pendant la pandémie de COVID-19. Nous avons mis en œuvre ce test au point de soins dans un hôpital submergé par le nombre de patients, où les tests standards n'étaient pas réalisables. Notre test a fourni des diagnostics rapides et précis. De plus, nous avons proposé une méthode de dépistage non invasive basée sur l'ARN extrait de la salive des travailleurs essentiels durant la pandémie, qui s'est révélée à la fois pratique et efficace pour des tests fréquents. La transposition préliminaire de cette méthodologie à une plateforme en papier a montré des résultats prometteurs pour le suivi en temps réel des infections, en particulier celles du SARS-CoV-2, au point-of-care. Dans le cadre de la co-tutelle, des travaux ont été effectués ensuite dans le laboratoire français pour le développement et l'optimisation d'une plateforme papier pour la focalisation isoélectrique des protéines, en vue d'intégrer toutes les étapes de l'analyse protéomique dans un microdispositif. Dans ce travail, nous avons développé des systèmes de diagnostic pour les biomolécules appliqués ou applicables au point-of-care. Nous avons mis le focalisation isoélectrique sur une plateforme à base de papier, obtenant une séparation des protéines précise et reproductible, y compris dans des échantillons réels, avec une résolution et une efficacité acceptables. Ce système représente une étape supplémentaire dans un projet plus vaste visant à intégrer toutes les étapes protéomiques sur une seule puce. Le développement réussi de méthodes d'analyse des biomolécules, privilégiant l'économie, la rapidité et la simplicité, met en lumière le potentiel du papier en tant que plateforme pour ces tests diagnostiques. Le papier s'est avéré être une plateforme adaptée et accessible pour la réalisation de ces tests, soulignant son potentiel dans des contextes à ressources limitées.

MOTS CLÉS

Microfluidiques, biomolécules, IEF, protéomique, diagnostic moléculaire, diagnostic au chevet.

ABSTRACT

This thesis was conducted as part of a joint supervision between the Universidade Federal de Goiás (Goiânia, Brazil) and Chimie ParisTech PSL. Initiated in Brazil at the onset of the pandemic, the work developed during the Ph.D. at the Brazilian institution focused on developing LAMP-based methodologies for COVID-19 diagnosis. Loop-mediated isothermal amplification (RT-LAMP) was used to create a simple and low-cost test during the COVID-19 pandemic. This test was implemented at the point of care in an overwhelmed hospital where standard tests were not feasible, providing rapid and accurate diagnoses. Additionally, we proposed a non-invasive tracking method based on RNA extracted from the saliva of essential workers during the pandemic, which proved practical and effective for frequent testing. The preliminary transposition of this methodology to a paper-based platform showed promising results for real-time monitoring of infections, particularly SARS-CoV-2, at the point of care. Within the scope of the cotutella, subsequent work was carried out in the French laboratory to develop and optimize a paper-based platform for protein isoelectric focusing, aiming to integrate proteomic analysis steps into a microdevice. In this thesis, we developed diagnostic systems for biomolecules applied or applicable at the point of care. For protein analysis, isoelectric focusing on a paper-based platform allowed precise and reproducible protein separation, including in real samples, with acceptable resolution and efficiency. This system represents a significant step forward in a broader project aimed at integrating all proteomic steps into a single chip. The successful development of biomolecule analysis methods prioritizing cost-effectiveness, speed, and simplicity highlights the potential of paper as a platform for these diagnostic tests. Paper proved to be a suitable and accessible platform for conducting these tests, emphasizing its potential in resource-limited settings.

KEYWORDS

Microfluidic, biomolecules, IEF, proteomics, molecular diagnostic, point-of-care.